Role of orbital fibroblasts in tissue remodeling of Graves' orbitopathy – involvement of hypoxia dependent and independent pathways

Inaugural-Dissertation
zur
Erlangung des Doktorgrades
Dr. rer. nat.

der Fakultät für
Biologie
an der Universität Duisburg-Essen

vorgelegt von

M.Sc. Molekularbiologie
Gina-Eva Görtz

aus Hamburg
Februar 2017

Die der vorliegenden Arbeit zugrundeliegenden Experimente wurden in der Abteilung für Molekulare Ophthalmologie der Augenheilkunde des Universitätsklinikums Essen durchgeführt.

1. Gutachter: PD Dr. Utta Berchner-Pfannschmidt
2. Gutachter: Prof. Dr. Astrid Westendorf
3. Gutachter: Univ.-Prof. Dr. med. Matthias Schott

Vorsitzender des Prüfungsausschusses: Prof. Dr. Hynek Burda

Tag der mündlichen Prüfung: 12.05.2017

Publications

Görtz G-E, Horstmann M, Aniol B, Delos Reyes B, Fandrey J, Eckstein A, Berchner-Pfannschmidt U. Hypoxia-dependent HIF-1 activation impacts on tissue remodeling in Graves' ophthalmopathy – implications for smoking. J Clin Endocrinol Metab. 2016 Dec;101(12):4834-4842.

Görtz G-E, Moshkelgosha S, Jesenek C, Horstmann M, Edelmann B, Banga JP, Eckstein A, Berchner-Pfannschmidt U. Pathogenic phenotype of adipogenesis and hyaluronan in orbital fibroblasts from female Graves' orbitopathy mouse model. Endocrinology. 2016 Oct;157(10):3771-3778

Berchner-Pfannschmidt U, Moshkelgosha S, Diaz-Cano S, Edelmann B, Görtz G-E, Horstmann M, Noble A, Hansen W, Eckstein A, Banja JP. Comparative assessment of female mouse model of Graves‘ orbitopathy under different environments, accompanied by pro-inflammatory cytokine T cell responses to thyrotropin hormone receptor antigen. Endocrinology 2015, 157:1673-82

Brandau S, Bruderek K, Hestermann K, Görtz G-E, Horstmann M, Mattheis S, Lang S, Eckstein A, Berchner-Pfannschmidt U. Orbital fibroblasts from Graves‘ Orbitopathy patients share functional and immunophenotypic properties with mesenchymal stem/stromal cells. Invest Ophthalmol Vis Sci. 2015, 56:6549-5756

Awards

Görtz G-E, Horstmann M, Delos Reyes B, Fandrey J, Eckstein A, Berchner-Pfannschmidt U. (2015)
„Orbital fibroblast hypoxic response impacts tissue remodeling in Graves‘ Orbitopathy“
15th International Thyroid Congress 18-23.10.2015, Orlando, USA, Poster-Prize

Görtz G-E, Horstmann M, Delos Reyes B, Fandrey J, Eckstein A, Berchner-Pfannschmidt U. (2015)
„Orbitafibroblasten vermittelter Hypoxie-abhängiger Gewebeumbau bei Endokriner Orbitopathie“ 14. Tag der Forschung der Medizinischen Fakultät 20.11.2015, Universität Duisburg-Essen, Poster-Prize

Congress contributions

Görtz G-E, Moshkelgosha S, Jesenek C, Edelmann B, Horstmann M, Schlüter A, Banga J.P, Eckstein A, Berchner-Pfannschmidt U. (2016) Orbital fibroblasts from Graves‘ Orbitopathy mouse model show a pathogenic phenotype of adipogenesis and hyaluronan secretion. 15. Tag der Forschung der Medizinischen Fakultät 18.11.2016, Universität Duisburg-Essen, Poster

Görtz G-E, Horstmann M, Aniol B, Delos Reyes B, Fandrey J, Eckstein A, Berchner-Pfannschmidt U. (2016) Hypoxia-dependent HIF-1 activation impacts on tissue remodeling in Graves‘ Orbitopathy- implications for smoking. 39th Annual Meeting of the ETA 03-06.09.2016, Copenhagen, Denmark, Presentation

Görtz G-E, Horstmann M, Delos Reyes B, Fandrey J, Eckstein A, Berchner-Pfannschmidt U. (2016) Orbital fibroblast hypoxic response impacts tissue remodeling in Graves‘ Orbitopathy. D.A.CH.-Tagung der DEG, ÖGES und SGED 26-28.05.2016, Munich, Germany, Poster

Görtz G-E, Horstmann M, Delos Reyes B, Fandrey J, Eckstein A, Berchner-Pfannschmidt U. (2015) Hypoxia-dependent signaling in Graves‘ orbitopathy. Graduate School of Biomedical Science (Biome), Core: Cellular and Moleculare Immunology 30.11.2015, Presentation

Görtz G-E, Horstmann M, Delos Reyes B, Fandrey J, Eckstein A, Berchner-Pfannschmidt U. (2015) Orbitafibroblasten vermittelter Hypoxie-abhängiger Gewebeumbau bei Endokriner Orbitopathie. 14. Tag der Forschung der Medizinischen Fakultät 20.11.2015, Universität Duisburg-Essen, Poster

Görtz G-E, Horstmann, M., Delos Reyes B, Fandrey J, Eckstein A, Berchner-Pfannschmidt U. (2015) Orbital fibroblast hypoxic response impacts tissue remodeling in Graves‘ Orbitopathy. 15th International Thyroid Congress 18-23.10.2015, Orlando, USA, Poster and Presentation

Görtz G-E, Horstmann M, Delos Reyes B, Fandrey J, Eckstein A, Berchner-Pfannschmidt U. (2015) Orbital fibroblast hypoxic response impacts tissue remodeling

in Graves‘ Orbitopathy. 17. Jahrestagung der “Young active Research in Endocrinology (YARE)” 02-04.10.2015, Berlin, Germany, Presentation

Görtz G-E, Horstmann M, Delos Reyes B, Steuhl K-P, Fandrey J, Eckstein A, Berchner-Pfannschmidt U. (2015) Hypoxie-abhängige Vaskularisierung des retrobulbären Fettgewebes bei Endokriner Orbitopathie. 177. Versammlung des Verein Rheinisch-Westfälischer Augenärzte 30-31.01.2015, Dortmund, Germany, Presentation

Görtz G-E, Horstmann M, Delos Reyes B, Fandrey J, Eckstein A, Berchner-Pfannschmidt U. (2015) The role of HIF-1 dependent gene expression for the pathogenesis of Graves’ orbitopathy. Graduate School of Biomedical Science (Biome), Core: Cellular and Moleculare Immunology 26.01.2015, Presentation

Görtz G-E, Horstmann M, Delos Reyes B, Steuhl K-P, Fandrey J, Eckstein A, Berchner-Pfannschmidt U. (2014) Rolle der Orbitafibroblasten für die vermehrte Vaskularisierung des retrobulbären Fettgewebes bei Endokriner Orbitopathie. Deutsche Gesellschaft für Endokrinologie, Gemeinsame Jahrestagung der Sektion Schilddrüse 27.-29-11.2014, Marburg, Germany, Presentation

Görtz G-E, Horstmann M, Delos Reyes B, Fandrey J, Eckstein A, Berchner-Pfannschmidt U. (2014) Hypoxia-dependent signaling in Graves‘ orbitopathy. 13. Rorschungstag der Medizinischen Fakultät 21.11.2014, Universität Duisburg-Essen, Poster

Görtz G-E, Horstmann M, Delos Reyes B, Steuhl K-P, Fandrey J, Eckstein A, Berchner-Pfannschmidt U. (2014) Role of orbital fibroblasts for pathological vascularization in Graves‘ orbitopathy caused by induction of hypoxia-dependent signaling. 38th Annual Meeting of the European Thyroid Association 06.-10.09.2014, Santiago de Compostela, Spain, Poster

Görtz G-E, Horstmann M, Delos Reyes B, Steuhl K-P, Fandrey J, Eckstein A, Berchner-Pfannschmidt U. (2014) Rolle der Orbitafibroblasten für die vermehrte Vaskularisierung des retrobulbären Fettgewebes bei Endokriner Orbitopathie. Deutsche Ophthalmologische Gesellschaft, 112. DOG-Kongress 25.-28.09.2014, Leipzig, Germany, Presentation

Contents

1 Zusammenfassung/Summary

1.1 Zusammenfassung

Morbus Basedow (Graves‘ Disease) ist eine Schilddrüsenerkrankung, die durch Autoantikörper verursacht wird, die hauptsächlich gegen den Thyreotropin-stimulierenden Hormonrezeptor (TSHR) gerichtet sind und eine Hyperthyreose zur Folge haben. Endokrine Orbitopathie (Graves' Orbitopathie, GO) ist eine extrathyroidale Manifestation, die üblicherweise im Zusammenhang mit Morbus Basedow auftritt und durch Entzündung und Ausdehnung des retrookularen Bindegewebes und der extraokulären Muskeln (EOM) gekennzeichnet ist. Die Ausdehnung des orbitalen Gewebes in die räumlich begrenzte, knöcherne Orbita führt zu Proptosis, Muskeldysfunktion und in schweren Fällen zu einer Kompression des Sehnervs. Die Entzündung und Ausdehnung des orbitalen Gewebes kann eine Sauerstoffunterversorgung (Hypoxie) des Gewebes verursachen und somit zu einer Induktion von Hypoxie-induzierbarer Faktor 1 (HIF-1) abhängigen Signalwege führen. Die vorliegende Arbeit beschäftigt sich mit der Rolle orbitaler Fibroblasten (OF) und/oder mesenchymaler Stammzellen (MSC) in der Pathogenese von GO Patienten und im GO Mausmodell. Ziel war die Charakterisierung humaner und muriner OF und/oder MSC im Hinblick auf Hypoxie-abhängige und unabhängige pathophysiologische Prozesse der GO.

Orbitale Fibroblasten sind der zentrale Zelltyp im pathophysiologischen Prozess, und wurden entweder aus Fettbiopsien von GO Patienten/Kontrollpersonen oder aus orbitalem Gewebe eines GO Mausmodells/Kontrollmäuse gewonnen. Darüber hinaus identifizierten wir MSC im orbitalen Fettgewebe von GO Patienten und zeigten, dass OF alle biologischen Merkmale der MSC teilten: Sowohl OF als auch MSC exprimierten typische MSC Oberflächen-Marker, unterdrückten die T-Zellproliferation und sezernierten Zytokine. Des Weiteren produzierten sie Hyaluronsäure und waren in der Lage sowohl adipogen, osteogen und chondrogen als auch myogen und neuronal zu differenzieren. Dies zeigte, dass die OF Population undifferenzierte Vorläuferzellen beinhaltet, die für die gesteigerte Adipogenese und/oder Myogenese im Gewebe von GO Patienten verantwortlich sein könnten.

Um zu untersuchen, ob Hypoxie-abhängige Signalwege in den Gewebeumbau bei GO involviert sind, analysierten wir die Rolle von HIF-1 für die Angiogenese und Adipogenese unter hypoxischen Bedingungen. Als eine mögliche Folge der Hypoxiewirkung

fanden wir eine erhöhte Vaskularisierung und HIF-1α-positive Zellen im Binde-/Fettgewebe von GO Patienten. Die aus dem Fettgewebe der Patienten gezüchteten OF zeigten eine höhere HIF-1 Expression und sezernierten HIF-1 abhängig mehr VEGF. Des Weiteren wurde unter Hypoxie die adipogene Differenzierung der OF HIF-1 abhängig induziert. Die durch Hypoxie induzierte Adipogenese konnte durch Stimulation des TSHR unter Verwendung von TSH noch weiter gesteigert werden, was das ungünstige Zusammenwirken von Hypoxie und Effekten der Autoimmunität widerspiegelt. Rauchen ist der stärkste Risikofaktor für den Schweregrad einer GO und entfaltet seine Wirkung wahrscheinlich durch die Kombination von Rauchbestandteilen und Hypoxie. Interessanterweise konnten wir feststellen, dass OF von GO Rauchern im Vergleich zu GO Nichtrauchern höhere HIF-1α Mengen in Reaktion auf Zigarettenrauchextrakt und Hypoxie aufwiesen. Die erhöhte HIF-1α Expression bei GO Rauchern könnte die starke Gewebsexpansion, welche bei GO Rauchern beobachtet wird, begünstigen.

Um die pathologischen Veränderungen der OF im Verlauf einer GO untersuchen zu können, etablierten wir ein präklinisches GO Mausmodell, das durch genetische Immunisierung mit einem Plasmid, welches für die humane TSHR A-Untereinheit kodierte, induziert werden konnte. Die TSHR immunisierten Mäuse entwickelten alle Anzeichen von Morbus Basedow mit GO: Die Mäuse entwickelten TSHR-Antikörper mit unterschiedlichen Mengen an stimulierenden- und/oder blockierenden Antikörpern, eine TSHR-Antigen-spezifische Antwort von T-Zellen der Milz, Schilddrüsenfunktionsstörungen und Orbitopathie. Dabei entwickelten die Mäuse ähnlich wie GO Patienten im unterschiedlichen Maße eine Vergrößerung des orbitalen Fettgewebes und/oder eine Myopathie der EOM. Aus dem orbitalen Gewebe der Mäuse, welches überwiegend aus EOM und Fett bestand, isolierten und charakterisierten wir Fibroblasten. Ähnlich wie die OF von Patienten, exprimierten die Maus OF (mOF) typische MSC Marker, TSHR und Insulin Wachstumsfaktor-1-Rezeptor (IGF-1R). Ebenso zeigten mOF eine gesteigerte Adipogenese und vermehrte Hyaluronsäure Sekretion in Antwort auf TSHR und IGF-1R Aktivierung. Darüber hinaus, zeigten OF von GO Mäusen erhöhte HIF-1α Mengen unter hypoxischen Bedingungen, was darauf hindeutete, dass Hypoxie-abhängige Signalwege an der Pathogenese einer GO bei Mäusen beteiligt sein könnten. Somit zeigten die OF von GO Mäusen einen pathogenen Zelltyp, der den OF von GO Patienten ähnlich ist.

Zusammengefasst konnte gezeigt werden, dass OF und/oder MSC eine zentrale Zellpopulation in der Pathogenese von GO Patienten und GO Mausmodell darstellen. HIF-

1 abhängige Signalwege sind am Gewebeumbau und -expansion beteiligt. Das Verständnis, wie verschiedene orbitale Zellpopulationen am Gewebeumbau als Reaktion auf Hypoxie mitwirken, wird während des Verlaufs der Augenerkrankung im GO Mausmodell noch weiter untersucht. Darüber hinaus ist es von Interesse die Rolle von Hypoxie-abhängigen Signalwege im Entzündungsprozess im Kontext der Autoimmunität aufzuklären. Dies kann zu einem besseren Einblick in die Pathogenese der GO führen und ist von grundlegender Bedeutung für die Entwicklung neuer therapeutischer Ansätze.

1.2 Summary

Graves' disease (GD) is an autoimmune disease caused by autoantibodies directed mainly against the thyrotropin stimulating hormone receptor (TSHR) leading to hyperthyroidism. Graves' orbitopathy (GO) is the common extra-thyroidal manifestation of Graves' disease is characterized by inflammation and expansion of the retroocular connective/fat tissue and of the extraocular muscles (EOM). The expansion of the orbital tissue within the limited space of the bony orbit leads to proptosis, extraocular muscle dysfunction, and, in severe cases, to an optic nerve compression. Inflammation and enlargement of the orbital tissue can cause hypoxia and consequently induce hypoxia-inducible-factor 1 (HIF-1) pathways. The work presented in this thesis addressed the role of orbital fibroblast (OF) and/or mesenchymal stem cells (MSC) for pathogenesis of GO in patients and mouse model. We aimed to characterize human and mouse OF and/or MSC and involvement of hypoxia depending and independent pathways in the pathophysiological process leading to GO.

The central cell type in this pathophysiologic process are the orbital fibroblasts (OF) which we derived either from fat biopsies of GO patients/control persons or from orbital tissue of GO/control mouse model. Additionally, we identified MSC in the fat tissue of GO patients and showed that OF shared all biological characteristics of MSC: Both the OF and the MSC expressed a typical MSC surface marker set, suppressed T cell proliferation and secreted cytokines. Furthermore, the cells produced hyaluronan and were able to differentiate along adipogenic, osteogenic, chondrogenic, myogenic, and neuronal pathways. It appears that OF population comprises undifferentiated progenitor cells responsible for adipogensis and/or myogenesis in GO.

To analyze whether hypoxia dependent pathways are involved in tissue remodeling of GO we investigated the role of HIF-1 action for angiogenesis and adipogensis. Most likely as a consequence of hypoxia we found increased vascularization and HIF-1α positive cells in the connective/fat tissue of GO patients. OF derived thereof expressed higher HIF-1α levels and secreted elevated levels of VEGF in an HIF-1 dependent manner. Furthermore, hypoxia induced HIF-1 dependent adipogenic differentiation of OF which could be further increased by stimulation of TSHR using TSH indicating an unfavorable marriage between hypoxia and effects of autoimmunity. Smoking is the strongest risk factor for GO and develops it full effect most likely through smoke ingredients and hypoxia. Interestingly, we found that OF derived from GO smoker more

strongly induced HIF-1α levels in response to cigarette smoke extract and hypoxia compared to GO non-smoker. Increased HIF-1α expression can contribute to the strong tissue expansion observed GO smoker.

To investigate pathological changes in OF during the course of GO we established a preclinical mouse model of GO induced by genetic immunization of human TSHR A-subunit plasmid. The pathological features of GO in the experimental mouse model were similar in orbital pathology to those present in patients with GO; GO mice developed TSHR antibodies with different levels of stimulating and blocking activity as well as TSHR antigen specific response of splenic T cells. Furthermore GO mice just like GO patients developed thyroid dysfunction and orbital disease with mice showing either more enlargement of orbital adipose tissue or myopathy of EOM. We derived OF from tissue comprise of EOM and adipose of the immunized mice. Mouse OF (mOF) expressed MSC marker, elevated levels of TSHR and insulin-like growth factor 1 receptor (IGF-1R) similar to OF derived from GO patients. Likewise, mOF showed increased adipogenesis and enhanced hyaluronan secretion by activation of TSHR and IGF-1R. Moreover, in response to hypoxia OF derived from GO mice enhanced HIF-1α levels, suggesting that hypoxia dependent signaling is involved in orbital pathogenesis. Thus, OF derived from GO mice display a pathogenic cell type similar to OF derived from GO patients.

In conclusion, OF and MSC are central for GO pathogenesis in patients and mouse model. HIF-1 dependent pathways are involved in tissue remodeling and expansion during pathogenesis of GO. The understanding of the contribution of different orbital cell populations for tissue remodeling in response to hypoxia during the course of the eye disease will be further studied in the GO mouse model. In addition the role of hypoxia for inflammation in context of autoimmunity remains to be discovered. This will lead to a better insight of disease pathogenesis and is fundamental to develop potential novel therapeutic targets.

2 Introduction

2.1 Graves' disease

Graves' disease (GD) is an autoimmune disorder and the most common cause of insistent hyperthyroidism of the thyroid gland (Burch and Cooper, 2015). In 1840 Karl Adolph von Basedow reported a constellation of symptoms of goiter, exophthalmos and tachycardia, called the "Mersenburger Trias". In the same century Robert James Graves described a case of goiter with exophthalmos. Nowadays it is known as "Graves' disease" ("Morbus Basedow" in German speaking countries). Around 0.5-1% of the western population develops Graves' disease during their lifetime. Graves' disease is the most common cause of hyperthyroidism with an incidence of 20 to 30/100.000 cases each year. Women are with 3% more frequently affected than men with 0.5%. The disease typically occurs between 30 and 60 years of age, but all ages are concerned (Wiersinga and Bartalena, 2002; Burch and Cooper, 2015).

2.1.1 Clinical manifestations of Graves' disease

The disorder GD is caused by autoantibodies directed mainly against the thyrotropin stimulating hormone receptor (TSHR), which leads to stimulation of the thyroid gland. This leads to an increase in thyroid hormone levels and goiter of the thyroid gland (Ginsberg, 2003). The characteristic goiter is often accompanied with an infiltration of lymphocytes, which are the major source of autoantibodies (Weetman, 2000). Tremor, nervousness, emotional instability, insomnia and weight loss are typical signs of hyperthyroidism and chiefly traceable to the increased thyroid hormone levels (Weetman, 2000; Burch and Cooper, 2015). Approximately, 25% to 50% of GD patients also develop the extra-thyroidal manifestation Graves' orbitopathy (GO), also called Graves' ophthalmopathy. In addition, some patients develop rarely localized dermopathy and acropachy (Bahn, 2010; Wang and Smith, 2014). Over the last decades the number of patients with GD rose and reasons for this are changes in lifestyle and diet patterns. Also genetic and environmental factors as well as risk factors like smoking and diabetes can encourage the development of thyroidal and associated manifestations of the disease. A variety of genes encoding proteins with immune regulatory functions are associated with thyroid autoimmune diseases (e.g. HLA II, CTLA-4, PTPN22, CD40). Furthermore, thyroid specific proteins like TSHR and Thyroglobulin are also involved

in the pathogenic processes of GD and associated disorders (Eckstein et al., 2009; McLeod and Cooper, 2012; Rosenblum et al., 2015).

2.2 Characteristics of Graves' orbitopathy

Graves' orbitopathy (GO) is the common extra-thyroidal manifestation of Graves' disease and describes an eye disease of the orbital tissue that is characterized by inflammation as well as expansion of the retroocular connective fat tissue and fibrotic extraocular muscles. The expansion of the orbital tissue within the limited space of the bony orbit leads to proptosis, extraocular muscle dysfunction, and, in severe cases, to an optic nerve compression (Eckstein et al., 2009; Eckstein et al., 2016). GO patients show strong clinical variability of symptoms (Fig. 1).

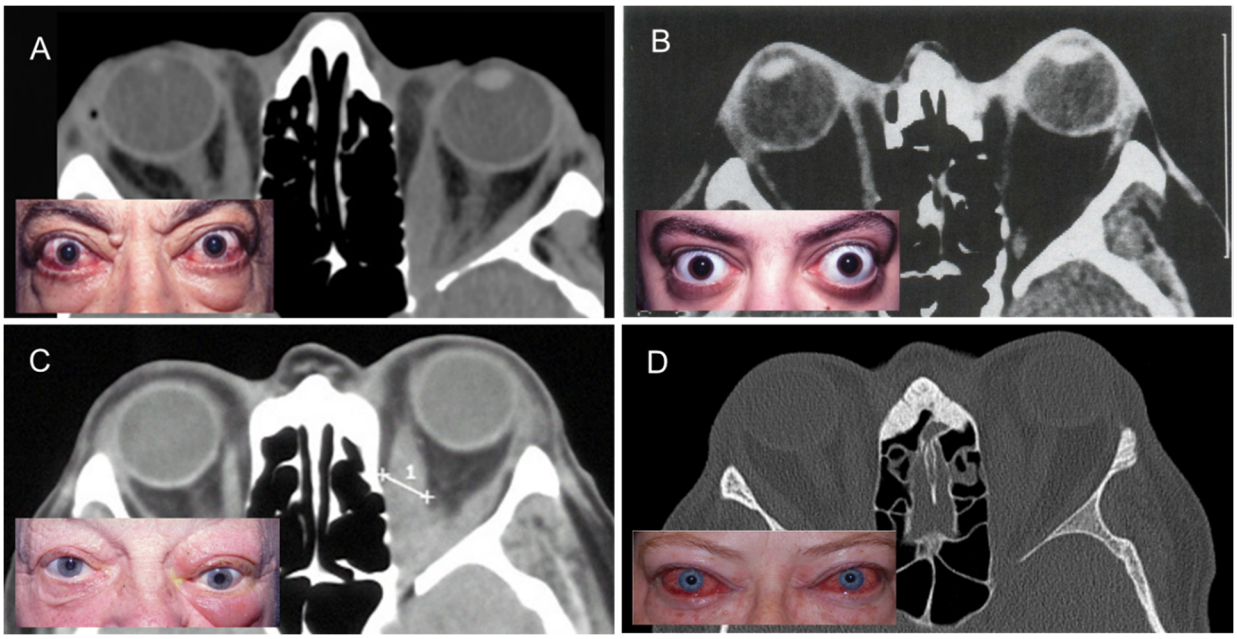

Figure 1. Patients with GO in different manifestations. Inflammation with swelling and redness (A), expansion of the retroorbital fat/connective tissue with extensive proptosis (B), enlargement of extraocular muscle volume with asymmetrical strabismus of the left eye (C), and impaired episcleral venous outflow with highly reddened eyes (D). Pictures show the manifestation in computer tomography and the outer appearance. Images were provided by Prof. Dr. med. Eckstein, University Eye Hospital Essen.

Most of the patients exhibit a combination of adipose tissue and orbital muscle expansion, but some patients appear to have a predominance for one of these processes or only symptoms for one eye. Children develop very rarely GO and inflammation symptoms and myopathy are almost always missing. Patients younger than 40 years create mostly a predominance for adipose tissue enlargement connected with inflammation.

Older patients develop more frequently a myopathy of the extraocular muscles (Fig. 1C) (Garrity and Bahn, 2006; Eckstein et al., 2009; Bahn, 2010; Eckstein et al., 2016).

Around 25-50% of GD patients develop GO in varying degrees (Fig. 2). For most of the patients a mild form occurs and can be treated with symptomatic treatment, but in around 3-5% of the cases the clinical course is severe and often orbital decompression surgery is necessary. It is largely unclear why some patients with GD develop a GO, unlike other patients show no symptoms or to a lesser extent (Eckstein et al., 2009; Wang and Smith, 2014; Banga et al., 2015). This is reflected in more or less active inflammation, fat and muscle expansion and fibrosis in the different patients. The clinical manifestation can also vary widely due to environmental influences and genetic background (Tomer and Davies, 2003). The strongest GO associated risk factor is cigarette smoking, which leads to higher prevalence of GO, a more severe course of the disease and a reduced response to anti-inflammatory treatment (Pfeilschifter and Ziegler, 1996; Eckstein et al., 2004; Cawood et al., 2006) . Further, the levels of stimulating TSHR antibodies affect the severity of GO (Eckstein et al., 2006).

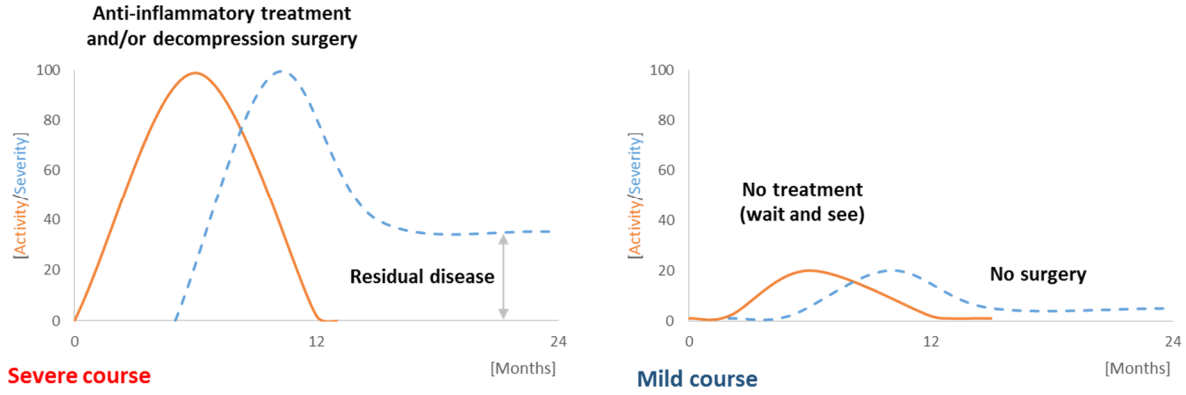

Figure 2. Rundle curve of activity and severity of GO. The graphs showing the activity (red line) and severity (blue line) of orbital manifestation in severe and mild course of GO patients as well as treatment and surgery methods. Adapted from Cawood et al., 2004.

The amount of activity is scored by the clinical activity score (CAS). This score is based on classical signs of inflammation (pain, swelling, and impaired function) and use a points system ranged from 0-10. In contrast the NOSPECS („no signs or symptoms“/„only signs or symptoms“/„soft tissue involvement”/ Proptosis/„extraocular muscle involvement“/„corneal involvement“/„sight loss“; EUGOGO) classifies severity according to occurrence and amount of lid retraction, lid lag, proptosis, restrictive extraocular myopathy and optic neuropathy (Mourits et al., 1997; Bartalena et al., 2016). Both scores are used for a standardized assessment and are required for treatment

decisions of the disease. The disease starts with an initial phase, called the active phase, which is characterized by inflammatory mediators and immigrant immunocompetent cells. This leads to fibrosis/myopathy of the affected regions and to a fat proliferation, which can caused the protrusion of the eyes. The following phase is the chronic inactive phase in which patients suffer from the permeant persistence of myopathy and proptosis (Eckstein et al., 2009; Bahn, 2010).

2.2.1 Stage dependent treatment of Graves' orbitopathy

The clinical presentation of Graves' orbitopathy is closely linked with the formation of hyperthyroidism and usually develops within 6 months together with thyroid dysfunction. For a successful therapy an early diagnosis is important, because immunosuppressive and modifying therapies are much better effective when GO is in a recent active stadium. Prerequisite for an effective treatment of GO is the successful treatment of thyroid dysfunction to restore the euthyroid status (Eckstein et al., 2007; Eckstein et al., 2016). Euthyriodism favors the immunosuppressive treatment of orbital symptoms and can be achieved primarily by thyrostatic therapy (Salvi and Campi, 2015). In cases of medication not being effective or having a relapse, the thyroids should be definitive treated either by radioiodine therapy or surgical removal. The treatment of GO depends on clinical activity and severity of eye disease and can be derived from the clinical activity score (CAS) and NOSPECS score of the GO patients (Mourits et al., 1997). To simplify treatment decision GO can be classified into mild, moderate to severe or sight-threatening disease (Fig. 3).

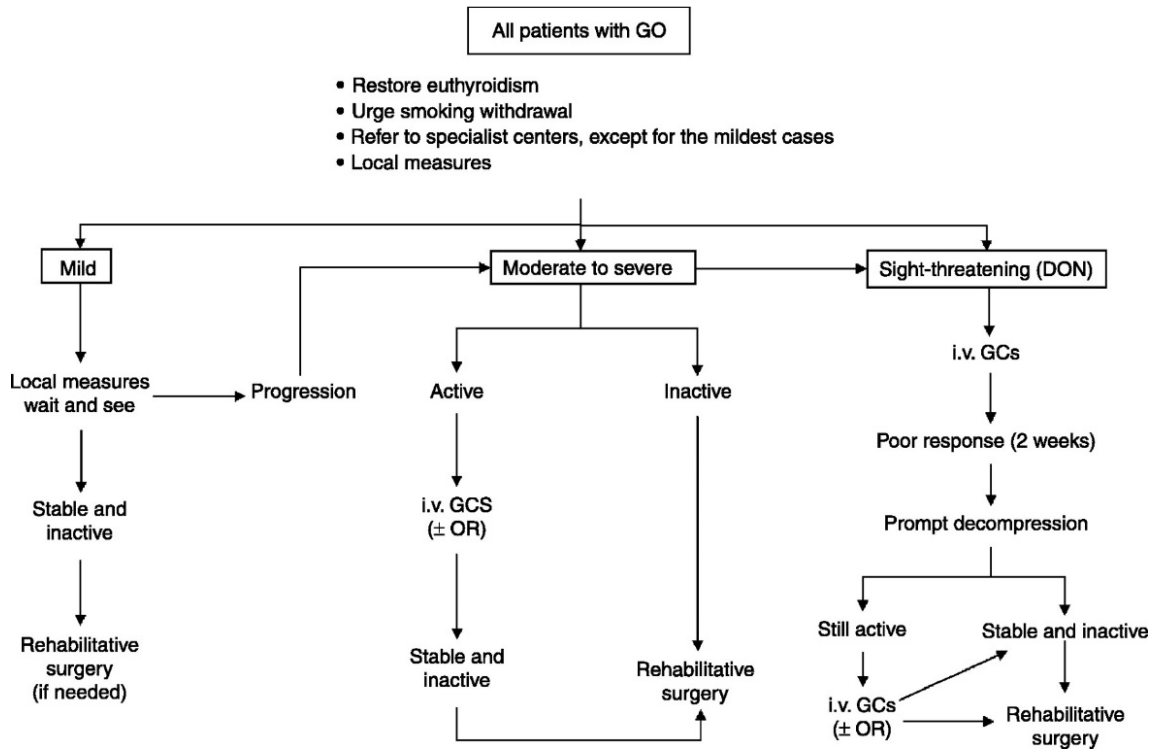

Figure 3. Therapy management of Graves' orbitopathy. Treatment strategy is based on severity/activity classification grouped in mild, moderate to severe and sight-threatening disease grades. Rehabilitative surgery includes orbital decompression, squint surgery, lid lengthening, and blepharoplasty. i.v. GCs, intravenous glucocorticoids; OR, orbital radiotherapy; DON, dysthyroid optic neuropathy. Diagram of therapy formulated from EUGOGO, 2008 (Bartalena et al., 2008; Bartalena et al., 2016).

In mild cases the general approach is a wait-and-see attitude, when patients have no suffering and a favorable risk profile. In situations the patient´s psychological strain require the treatment of mild cases selenium and/or glucocorticoids are reported to have positive effects (Bartalena et al., 2008; Bartalena et al., 2016). In patients with moderate-to-severe and sight-threatening GO an immunosuppressive therapy with glucocorticoid is indicated. The therapy with such drugs should lead to attenuation of the ongoing inflammation process. When patients are 6 month inactive and stable or when sight-threatening complications are present, an orbital decompression can/has to be performed. The aim of the bony orbital decompression is the treatment of the compartment syndrome within the bony orbit and the reduction of the exophthalmos (Bartalena et al., 2008; Salvi and Campi, 2015; Bartalena et al., 2016). Against the background of such serious consequence, it is to be considered that risk factors like smoking enhance not only the severity of the disease, but also increase the relapse rate. Further, the effectiveness of anti–inflammatory drugs is decreased in smokers.

Therefore, all patients should be actively encouraged to stop smoking (Hegedius et al., 2004).

In recent years several new treatment approaches have been found and studied. One is the immune modifying therapy with the $CD20^+$ B-cell attacking Rituximab which shows controversial data. A study by Salvi et al. 2015, which compared Rituximab with steroids, a promising therapeutic effect has been proved (Salvi et al., 2015). However, another Rituximab study could not show the same effect, but it can be assumed that a different timing of the treatment lead to divergent results (Stan et al., 2015). Only the really treatment is successful in such a disease where early fibrosis and adipogenesis is trigger by inflammatory stimuli. A potential novel therapeutic approach is the combined or single targeting of TSHR or IGF-1R. The TSHR can be targeted by either TSHR blocking antibodies like 5C9 and K1-70 (Sanders et al., 2010) or small TSHR blocking molecules, antagonists such as ANTAG2 and ANTAG3 (Neumann et al., 2011). Potential antibodies for IGF-1R blocking activities are Teprotumumab and the small molecule Linsitinib (Neumann et al., 2015). But all of these substances are not yet tested on patients (accept Teprotumumab – results of a randomized controlled trial (RCT) are on the way) and therefore the therapy of GO patients is still heavily based on corticosteroids, orbital irradiation and surgical decompression. Further profound studies and new treatment strategies need to be developed.

2.2.2 Pathogenesis of Graves' orbitopathy

The pathogenesis is very complex and multifaceted and local mechanisms for the development of GO are not fully understood. The interaction between various cells in the pathophysiological process of GO can support orbital inflammation and tissue expansion. In this process, immune cells like T-cells, B-cells, monocytes, macrophages and mast cells are involved while immigrating in the orbit. But most likely, the local orbital fibroblasts (OF) are the key players in the pathology of GO (Bahn, 2015; Smith and Hegedus, 2017). For a long time OF appeared as passive cells with more structural roles. Today OF are recognized as a heterogeneous cell population that fulfill complex functions in the normal and pathophysiological processes of tissue homeostasis. Orbital fibroblast were frequently derived from retro-bulbar connective/fat tissue of GO patients and *in vitro* studies thereof revealed that auto-antibodies against the TSH-

receptor (TRAK) and IGF-1R as well as cytokines and growth factors and interaction with immune cells activate the orbital fibroblasts (Bahn, 2010).

Role of orbital fibroblasts in Graves' orbitopathy

It could be shown that the interaction between autoimmunity and symptoms of GO are induced via TSHR, IGF-1R and CD40 activation (Fig. 4).

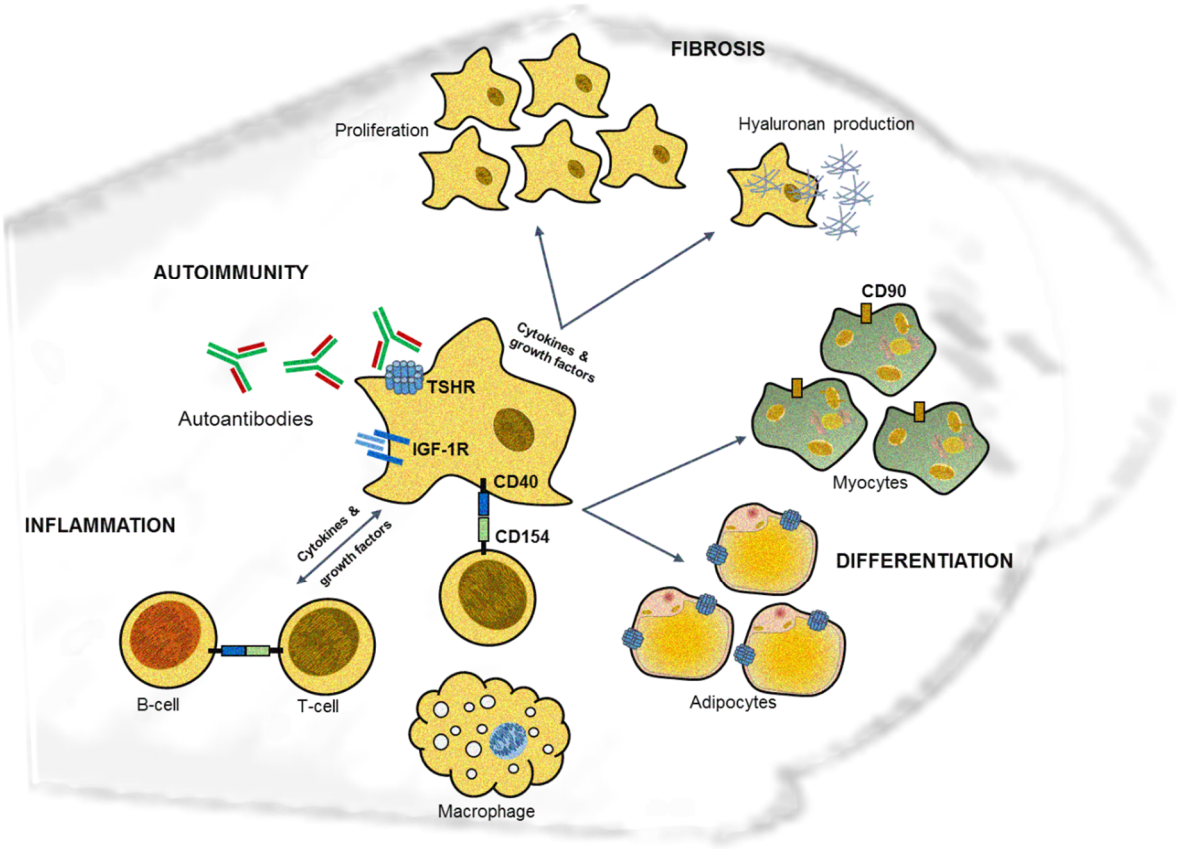

Figure 4. Pathophysiological processes in orbital tissue of GO patients. The orbital fibroblasts are the key players involved in four important mechanisms of GO pathophysiology: 1. Inflammation, 2. Autoimmunity, 3. Differentiation in adipocytes or/and myocytes and 4. Proliferation and hyaluronan production (fibrosis). These processes lead to expansion of the orbital connective/fat tissue and EOM as well as to continuous inflammation.

The orbital fibroblasts expressed TSHR, IGF-1R and CD40 more abundantly in GO patients than in controls (Bahn et al., 1998; Valyasevi et al., 1999; Kumar et al., 2004; Hwang et al., 2009; Bahn, 2010; Wang and Smith, 2014). The activation of these receptors elicits signaling cascades stimulating the production of glycosaminoglycan like hyaluronan, enhanced adipogenic differentiation, and leads to secretion of cytokines as well as inflammatory mediators (Bahn et al., 1987; Heufelder and Bahn, 1994; Bahn

et al., 1998; Iyer and Bahn, 2012). Interaction of T cells with OF via CD40-CD154 ligation enhances the proliferation and expression of cytokines in OF (Feldon et al., 2005; Hwang et al., 2009). Heterogeneity of OF population in the orbital tissue derived from GO patients can lead to different adipogenic or myogenic differentiation ability and secretion of inflammatory mediators. One reason might be based on surface expression of the glycoprotein CD90 (Thy1). CD90 is a glycophospharidylinositol (GPI)-anchored surface protein which plays immunological roles in T cell activation (Rege and Hagood, 2006) and non-immunological roles in cell-cell and cell-matrix interactions, apoptotic signaling, metastasis, inflammation and fibrosis (Khoo et al., 2008). CD90 negative OF are reported to differentiate to adipocytes and to produce higher levels of cytokines, such as IL-6. However, CD90 positive OF appeared to differentiate into myocytes in response to TGF-β stimulation (Koumas et al., 2002; Douglas et al., 2010; Smith, 2010). These findings suggest that CD90 negative cells are involved in orbital inflammation and adipogenesis whereas CD90 positive OF predominantly differentiate in myocytes and most likely play a role in EOM fibrosis. Relative portion of CD90 negative and/or positive OF, represent in the orbital tissue might explain why some GO patients developed more fat expansion whereas others show more muscle involvement or inflammation signs (Smith et al., 2002).

Inflammation and effects of autoantibodies in orbital fibroblasts

As described before, the expression of TSHR in GO tissue is increased compared to control (Ctrl) tissue (Bahn, 2010). Levels of TSHR autoantibodies (TRAbs) correlate positively with the clinical activity score (CAS) and the prevalence of GO (Khoo et al., 1999; Gerding et al., 2000). In sera of GO patients a mixture of stimulating (TSAbs), blocking (TSBAbs) and cleavage (neutral) TSHR autoantibodies, which bind on different regions in the TSH-receptor are found (Fig. 5) (Evans et al., 2010). While TSAbs mimic the actions of TSH and initiate the TSHR signaling cascade leading to hyperthyroidism, TSBAbs inhibit TSHR stimulation by TSH leading to a decrease of thyroid hormone secretion (Rees Smith et al., 1988; Jaume et al., 1997). Several assay exist to quantify TRAbs and TSAbs in sera of patients (Costagliola et al., 1999; Schott et al., 2009; Allelein et al., 2016). However, TBAbs can only be detected indirectly in a bioassay by measuring decreased production of cAMP in a cellular system (Diana et al., 2015). Stimulating antibodies partially bind to the leucine rich repeats (LRRs) and induce a structural change of the receptor which leads to signal transduction. However, blocking antibodies also bind to the LRRs but this binding cannot change the structure

of the receptor for signal transduction. Cleavage antibodies bind to the cleaved region and/or the N terminus of the TSHR ectodomain and this neither induce signal transduction nor block TSH binding (Davies et al., 2005). TSH or TSHR stimulating antibodies lead to an activation of the TSHR on the OF and induce the expression of cytokines and growth factors like ICAM1, HLA-DR, IL-6 and increased hyaluronan production (Kumar et al., 2011). Additionally the phosphatidyl inositol 3 (PI3) kinase pathway is involved which play a role for adipogenic differentiation of OF (Zhang et al., 2009; van Zeijl et al., 2011).

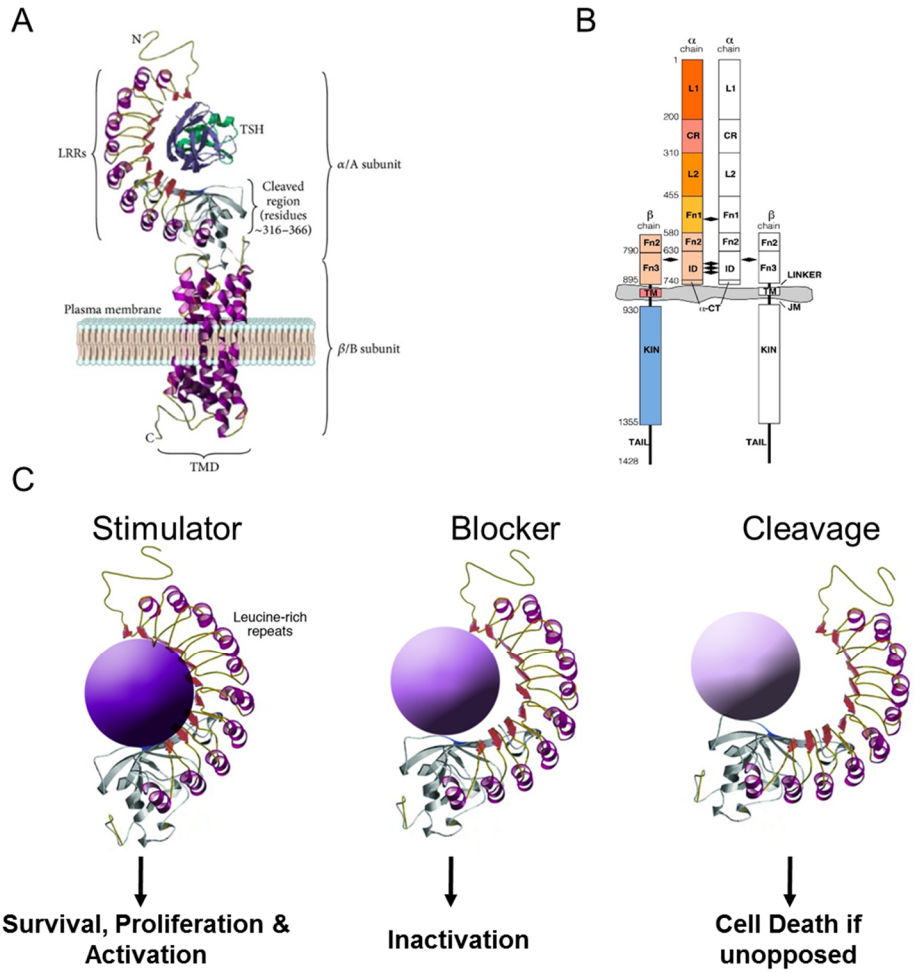

Figure 5. TSHR and IGF-1R as targets for autoantibodies. (A) Structure of G protein-coupled TSHR and (B) structure of tyrosine kinase IGF-1R. (C) A hypothetical model to explain the effect of structural changes in the TSH-binding site of the TSHR by stimulating, blocking or cleavage TSHR antibodies (Davies et al., 2005; Kavran et al., 2014). Binding of stimulatory (TSAbs), blocking (TSBAbs) or cleavage antibodies to the TSHR leads to different signal pathways and functional consequences, like stimulation, inactivation or cell death of thyrocytes. (Morshed and Davies, 2015). For example, TSAbs elevated hyaluronan production of OF that could be abolished by TSBAbs (Turcu et al., 2013). The action of cleavage TSHR antibodies in OF is currently unknown.

In thyrocytes TSHR blocking as well as neutral antibodies are also able to trigger signal pathways. TSHR blocking antibodies are involved in diverse multiple signaling cascades like, cell proliferation and increase Akt, CREB, c-Raf and ERK, which are important pathways for thyroid cell survival and proliferation. TSHR cleavage antibody action leads to apoptosis via mitochondrial ROS induction through suppressing PKA/CREB/AKT pathways (Morshed et al., 2010; Morshed et al., 2013; Morshed and Davies, 2015). The influence of these antibodies in GO-OF and in the pathological mechanisms of GO remains to be examined.

Furthermore, the IGF-1R is also a possible target for the autoantibodies in GO and is expressed at high levels on orbital fibroblasts (Khoo and Bahn, 2007). Studies found that sera from GD patients contained IGF-1R stimulatory antibodies that can induce the production of the T-cell chemoattractants IL-16, RANTES as well as hyaluronan in OF (Pritchard et al., 2003; Smith and Hoa, 2004). However, Minich et al. could not found anti-IGF-1 antibodies in sera of GO patients (Minich et al., 2013). It is also reported that there is a functional interaction between the TSHR and the IGF-1R in OF. Krieger and co-workers discovered that the activation of both TSHR and IGF-1R by monoclonal TSHR stimulatory antibody M22 leads to enhanced hyaluronan production of OF by using the dual-signaling cascade (Krieger et al., 2015). However, in this cross-talk model anti-IGF-1R antibodies were not implicated but instead stimulatory TSHR antibodies can activate TSHR and IGF-1R (Krieger et al., 2016). Apparently, around 30% of the TSHR mediated action happens via IGF-1R activation (Place et al., 2016).

Fibrosis and orbital fibroblasts

It could be shown that proliferation activity of OF derived from GO patients are higher than in control OF. The CD40-CD154 interaction between T-cells and OF but also cytokines and growth factors (e.g. IL-4, IGF-1 and TGF-β) lead to further enhancement of the proliferation rate (Heufelder and Bahn, 1994; Feldon et al., 2005). Additionally, OF are able to produce hydrophilic glycosaminglycans (GAGs), especially hyaluronan (Smith et al., 1991; Smith et al., 1995). Hyaluronan is essential in the orbital tissue as a component of the extracellular matrix. Hyaluronan is a main component of the expansion of the orbital tissue in GO patients. Three hyaluronan synthases (HAS1-3) control hyaluronan abundance but HAS2 is considered to represent the major contributor of hyaluronan overproduction in the orbit and may cause a greater expansion of the fat compartment in GO (Kaback and Smith, 1999, 1999). In addition, hyaluronan

secretion can also increase the size of muscle belly. Cytokines like IL-1β and CD40 ligand can cause an increase of hyaluronan production but also cellular interactions between OF and immune cells (mast cells and lymphocytes) are involved (Smith et al., 1991; Smith and Parikh, 1999). Tissue expansion and fibrosis are the major reason for myopathy and proptosis in GO and enhanced proliferation and hyaluronan overproduction of OF favor this pathological process.

Differentiation ability of orbital fibroblast

Differentiation ability is dependent on the phenotypical heterogeneity of OF. Two OF subpopulations depending on CD90 expression, CD90 negative and CD90 positive OF can be derived from orbital tissue of GO patients. Orbital fibroblasts which are CD90 negative have a high capacity to differentiate into adipocytes. The differentiation process into adipocytes increases the expression of adiponectin, leptin, PPAR-γ as well as enhanced TSHR presentation and cytokine production like IL-1β, IL-6 and IL-8 (Valyasevi et al., 1999; Koumas et al., 2002).

On the other hand, there is a pool of CD90 positive OF present in the orbital tissue. These OF are more abundant in the extra-ocular muscles and are not able to differentiate in adipocytes. However, in response to TGF-β the CD90 positive OF differentiate to myocytes (Koumas et al., 2003). It is described that the clinical manifestation of GO can be divided into two subtypes, which are characterized by either predominant fat expansion or EOM enlargement (Hiromatsu et al., 2000). A relative portion of either CD90 negative or positive OF in the orbital tissue might explain why some GO patients developed more fat expansion whereas others show more muscle involvement or inflammation signs (Smith et al., 2002). Recently, Kuriyan et al. demonstrated that two subtypes of clinical manifestations of GO patients showing either more fat expansion or EOM expansion corresponded to either enhanced adipogenesis or stronger proliferation rate of OF derived from the respective GO patients (Kuriyan et al., 2013). The interrelation of these cellular mechanisms causes an enormous increase in volume of the orbital tissue. Swelling and processes of inflammation in the limited bony orbit can encourage the long-term tissue hypoxia.

Smoking as a risk factor and effects on orbital fibroblasts

1987 Hagg and colleagues first described the association between smoking and Graves' orbitopathy (GO). Smoking is the strong risk factor and harmfully affects GO pathogenesis. A dose-dependent relation is known between the number of cigarettes

and development OF GO, with current smokers having a higher risk than past smokers (Hegedius et al., 2004). Disease development occurs more frequently and tend to be more severe in smokers than in non-smokers (Hagg and Asplund, 1987; Pfeilschifter and Ziegler, 1996). Studies could show that smoking can stimulate the generation of reactive oxygen species (ROS) and enhances proliferation and adipogenesis of the orbital tissue (Cawood et al., 2007; Yoon et al., 2013). The molecular process of fat expansion in the limited space of the body orbit is induced trough the differentiation potential of orbital fibroblasts and preadipocytes to mature adipocytes. Investigations with cigarette smoke extract showed a dose-dependent enhancement of OF adipogenesis. A relationship between orbital adipogenesis and ROS generation during cigarette consumption was shown (Yoon et al., 2013). Additionally, cigarette smoke stimulates the proliferation of OF. Hypoxic conditions as well as ROS have an additive effect on the proliferation and modulation of cytokine networks of OF (Cawood et al., 2007; Eckstein et al., 2009). The effect of smoking can be due to a combination of hypoxia, ROS and smoke ingredients.

2.3 Role of hypoxia

Energy generation of somatic cells is covered by the combustion of oxygen. Accordingly acute hypoxia leads to cell damage and can be trigger various serious diseases (Ziello et al., 2007). Oxygen concentration varies significantly in different tissues and range from 2.5% to 14% in highly perfused organs such as lung, kidney and heart. However, adipose tissue has low oxygen levels of 3% or less (Trayhurn, 2013). Hypoxia is a main factor in the pathophysiology of heart attack, stroke, when tissue expands by cancer or obese, in inflamed tissue and in many other disorders (Park et al., 2004). Further, it is possible that hypoxia is induced by smoking. The cells respond to the hypoxic microenvironment by adapting gene expression through the activation of Hypoxia-inducible factor 1 (HIF-1) (Semenza, 1998).

2.3.1 Transcriptional activator Hypoxia-inducible factor 1

Hypoxia-inducible factor 1 (HIF-1) is a transcription factor which controls the expression of most genes involved in adaption to hypoxic conditions (Semenza, 1998). HIF-1 is a heterodimeric transcription factor, composed of a α- and β-subunit (Fig. 6). Analysis found two HIF-1α homologues called HIF-2α and HIF-3α with structural similarity and interaction with HIF-1β. HIF-3α is the less related isoform and the regulation and

its transcriptional role under hypoxia is unclear (Carroll and Ashcroft, 2006). HIF-2α is closely related and binds to the same cDNA sequence as HIF-1. Both have similar post-translation, oxygen-sensitive modes of regulation but their expression patterns appears to be tissue specific (Ratcliffe, 2007). In contrast to HIF-1α which is ubiquitously expressed whereas HIF-2α is predominantly expressed in the lung, endothelium and carotid body (Ke and Costa, 2006). Studies in HIF-1α or HIF-2α knock-out mice demonstrate non redundant roles of HIF-1α and HIF-2α and result in different phenotypes of these mice (Ratcliffe, 2007; Lisy and Peet, 2008).

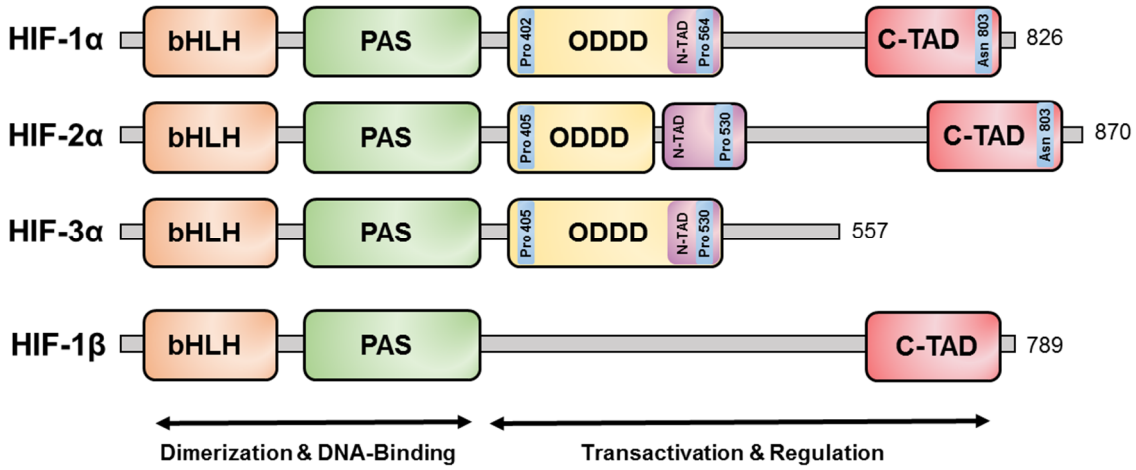

Figure 6. Schematic representation of α- and β- subunits of the transcription factor HIF. HIF is a heterodimeric transcription factor composed of an α-subunit and a ß-subunit. Three homologue α-subunits exist. The subunits have at its N-terminal end a helix-loop-helix (bHLH), as well as a Period/ARNT/single minded (PAS) domain. The function of bHLH is DNA binding, whereas the PAS domain mediated the dimerization between the both subunits. The α-subunits have an oxygen-dependent degradation domain (ODDD) with two hydroxylation sites (HIF-1α: Pro402; Pro564, HIF-2/3α: Pro405; Pro530) and a C-terminal transactivation domain (C-TAD), expect HIF-3α, with one further hydroxylation site (Asn803). The total number of amino acids of each subunit is marked at the end of the domain (Ke and Costa, 2006; Weidemann and Johnson, 2008; Lisy and Peet, 2008).

The 120 kDa α-subunit is strictly oxygen dependent, while the small β-subunit (94 kDa) is constitutively expressed (Stolze et al., 2002). Structures of both subunits show many homologies, which play a central role in the adaptation to hypoxia and for the regulation of HIF specific target genes. Both subunits possess a helix-loop-helix- (bHLH) on the amino terminal end as well as a PER-ARNT-SIM (PAS)-Domain. The bHLH domain mediates the DNA binding and the PAS domain's function is to dimerize between the both subunits. In contrast to HIF-1β, HIF-1/2α isoforms have additional functional protein domains (Weidemann and Johnson, 2008; Lisy and Peet, 2008; Berchner-

Pfannschmidt et al., 2010). These include the oxygen-dependent degradation domain (ODDD) as well as an N-terminal and C-terminal transactivation domain (N-TAD, C-TAD). The role of these transactivation domains is the interaction with cofactors, which are decisive for the complete activity of HIF. The oxygen-dependent hydroxylation of the ODDD domain serve the interaction with the von Hippel-Lindau tumor suppressor protein (pVHL) (Weidemann and Johnson, 2008; Berchner-Pfannschmidt et al., 2010).

2.3.2 Regulation of Hypoxia-inducible factor 1

HIF-1 is subject to a number of regulatory post-translational modifications, wherein the modification of the α-subunit is of particular interest (Fig. 7).

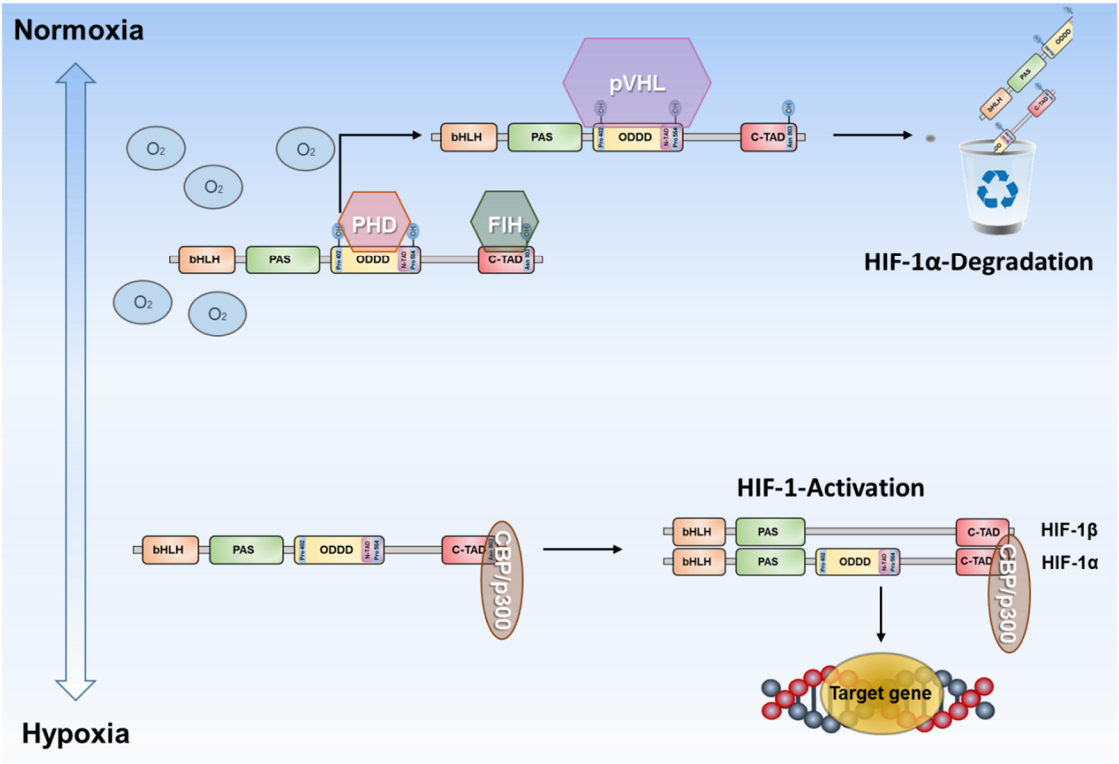

Figure 7. Oxygen dependent regulation of HIF-1α through post translational hydroxylation. Under high oxygen levels prolyl hydroxylases (PHD) hydroxylate two prolines residues existing in the ODDD domain of HIF-1α while factor inhibition HIF enzyme (FIH) hydroxylate a proline residues in the C-TAD domain. The pVHL protein detect the hydroxylated prolyl residues in the ODDD and initiates the ubiquitination and proteasomal degradation. The hydroxylated prolyl residue in the C-TAD domain prevents the interaction of HIF-1α with coactivator CBP/p300. Under Hypoxia, PHD and FIHs are inactive leading to stabilization of HIF-1α and dimerization of the HIF-1α/β transcription complex. Non-hydroxylation of the C-TAD domain allows CBP/p300 recruitment, resulting in activation of target gene expression (Weidemann and Johnson, 2008; Berchner-Pfannschmidt et al., 2010).

The fast degradation of HIF-1α under normoxia is mediated via hydroxylation processes. In the presence of O_2, HIF is targeted for degradation by an E3 ubiquitin ligase containing pVHL (Fig. 7). pVHL binds to HIF-1α when the proline residues are hydroxylated by the prolyl hydroxylases (PHD1-3) in the presence of O_2 under normoxia. VHL is part of the VCB-Cul2 E3 ligase complex that includes Elongin B, Elongin C, Cullin-2, Rbx-1. This complex, together with an ubiquitin-activating enzyme (E1), mediates the ubiquitination and proteasomal degradation of HIF-1α. In addition, the cofactor recruitment is prevented by asparagine hydroxylation at the C-TAD domain via factor inhibition HIF enzyme (FIH) under normoxia. The half-life period of HIF-1α is lesser than 5 minutes. In this short time period there a no possibilities to generate a functional transcription complex (Ke and Costa, 2006; Berchner-Pfannschmidt et al., 2007; Weidemann and Johnson, 2008).

However, if a critical oxygen concentration is undershot (Hypoxia), hydroxylation of HIF-1α is reduced and HIF-1α can stabilize and translocate in the nucleus where HIF-1α built a heterodimer with the constitutively expressed HIF-1β. The complete transcriptional activity of HIF-1 is regulated via the co-factor complex CBP/p300. HIF-1 activates more than 100 target genes via the hypoxia response element (HRE) (Chen et al., 2001; Ke and Costa, 2006; Weidemann and Johnson, 2008).

2.3.3 Hypoxia-inducible factor 1 target gene expression

Tissue and cells undersupplied with oxygen need to adapt to the hypoxic environment. The organism tries to recover the oxygen supply by various regulatory mechanisms which have to be activated. HIF-1 activates the expression of its target genes by binding to the hypoxia response element (HRE). Gene products of HIF-1 are involved in many cellular processes like erythropoiesis, glucose metabolisms, angiogenesis, cell proliferation, and adipogenesis (Ke and Costa, 2006) (Fig. 8).

One of the main oxygen-regulated glycoprotein is erythropoietin (EPO) which stimulates the proliferation, survival and differentiation of erythroid stem cells. Under heavy loss of blood or under hypoxic conditions expression of EPO can be increased up to 1000-fold. While hypoxia increases the expression of EPO, which is necessary for the formation of new red blood cells, the increased blood cell number enhances the delivery of oxygen supply. With this process the body adapts to regulate inadequate oxygen

conditions (Grimm et al., 2002; Arjamaa and Nikinmaa, 2006). Another important process to adapt on hypoxia is developing new blood vessels. A well-known growth factor for angiogenesis is the vascular endothelial growth factor (VEGF). VEGF stimulates the angiogenesis by recruiting endothelial cells into hypoxic and avascular areas and enhances their proliferation. HIF-1 induces the expression of genes involved in new formation and ingrowth of bold vessels in undersupplied areas (Ke and Costa, 2006; Arjamaa and Nikinmaa, 2006). Eukaryotic cells respond to low oxygen supply by switching to the oxygen-independent glucose metabolism (glycolysis). The switch from aerobic to anaerobic respiration is prerequisite for the adaption on hypoxic conditions. HIF-1 induces genes such as glycolytic enzymes and glycose transporter GLUT-1 and GLUT3. The enhanced expression of glycolytic enzymes and transporters allows an increased glycose uptake (Chen et al., 2001; Lu et al., 2002).

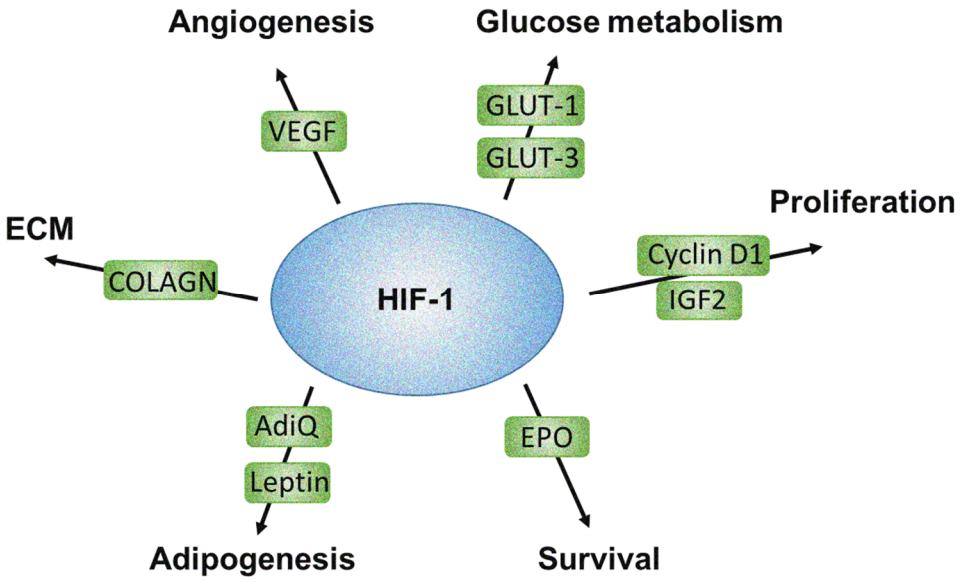

Figure 8. Involvement of HIF-1 gene products in cellular processes. Up to 100 target genes of HIF-1 are known (Chen et al., 2001; Ke and Costa, 2006; Weidemann and Johnson, 2008). Gene products of HIF-1 are involved in many cellular processes like erythropoiesis, glucose metabolisms, angiogenesis, cell proliferation, and adipogenesis. COLAGN, collagen, VEGF, vascular endothelial growth factor; GLUT-1/-3, glucose transporter 1/3; IGF2, insulin-like growth factor 2; EPO, Erythropoietin; AdiQ, adiponectin.

It has been reported that hypoxia is also involved in the expansion of adipose tissue for example in obese or cancer (Lu et al., 2002; Cawood et al., 2004). The expansion of adipose tissue is indicated in GO as well as enhanced levels of leptin, adiponectin, PPAR-γ, and CD90 (Lantz et al., 2005; Kumar et al., 2005; Khoo et al., 2008). The ability of orbital fibroblasts to differentiate in adipocytes leads to an increased adipogenesis of OF, with effects on enhanced TSHR expression and cytokine production

(Valyasevi et al., 1999; Kumar et al., 2005). In many pathophysiological states it has been reported that HIF-1 is involved as a mediator for the adaption to hypoxic conditions. However, no such information is available for hypoxic influences and HIF-1 dependent pathways in orbital tissue of GO patients. Therefore, it is important to investigate the role of HIF-1 and HIF-1 specific target genes signaling.

2.4 Animal models in Graves' orbitopathy

Animal models are indispensable for the understanding of the pathology and treatment options of autoimmune diseases. But at present there are none spontaneous models of GD including GO (Ludgate, 2000). The existing mouse models of GD depend mainly on genetic induction by using plasmids or adenovirus based methods (Wiesweg et al., 2013; Banga et al., 2016). A transgenic spontaneous model of GD has been developed recently (Rapoport et al., 2015; Rapoport et al., 2016). Unfortunately, all of this GD mouse models lacked signs of GO. For the understanding of the pathophysiological processes in GO, particularly for the examination of early states of GO and for the development of new treatments, it is necessary to develop other methods to induce GD with GO pathology in mice (Banga et al., 2016).

The first inducible mouse model was created in 1996 by Shimojo et al., and induced Graves hyperthyroidism in mice by immunization with TSHR receptor transfected fibroblasts. This approach leads to TSHR *in vivo* expression and production of TSHR antibodies expressing cells (Shimojo et al., 1996). The model showed an incidence of 10-15% with low hyperthyroidism and was reproducible with some improvements (Shimojo et al., 1996; Kita et al., 1999; McLachlan and Rapoport, 2004). Many other groups process different models with various methods. The methods include injection of TSHR expressing cells like the first described model, or genetic immunization via TSHR A-subunit plasmid or TSHR encoding adenovirus. But all of these models have proven not to be able to induce orbital signs or orbital symptoms were not reproducible. Only three studies reported mouse models with orbital complications but these models were not reproducible (McLachlan et al., 2005; Banga et al., 2015). Thus an important hallmark of animal models of GD is the ability to form orbital complications like inflammation, muscle enlargement, and expansion of the orbital connective tissue as well as eye signs such as lid swelling, redness, and edema (Banga et al., 2016; Ungerer et al., 2016).

In 2013 Moshkelgosha et al. established a promising new approach of genetic immunization of the human TSHR A-subunit encoding plasmid by electroporation of the leg muscles (Fig. 8). The human TSHR A-subunit immunized mice developed sustained levels of TSHR antibodies with varying degrees of stimulating and blocking antibodies leading to either hyperthyroidism or hypothyroidism of the mice. Moreover the immune mice showed orbital disease including inflammation of EOM, adipogenesis with expansion of retrobulbar adipose tissue and chemosis including dilated and congested orbital blood vessels (Moshkelgosha et al., 2013). To further study on disease pathology and novel therapeutics it has been important to initiate a comparative study to evaluate the model in two independent locations with different housing conditions and environmental factors.

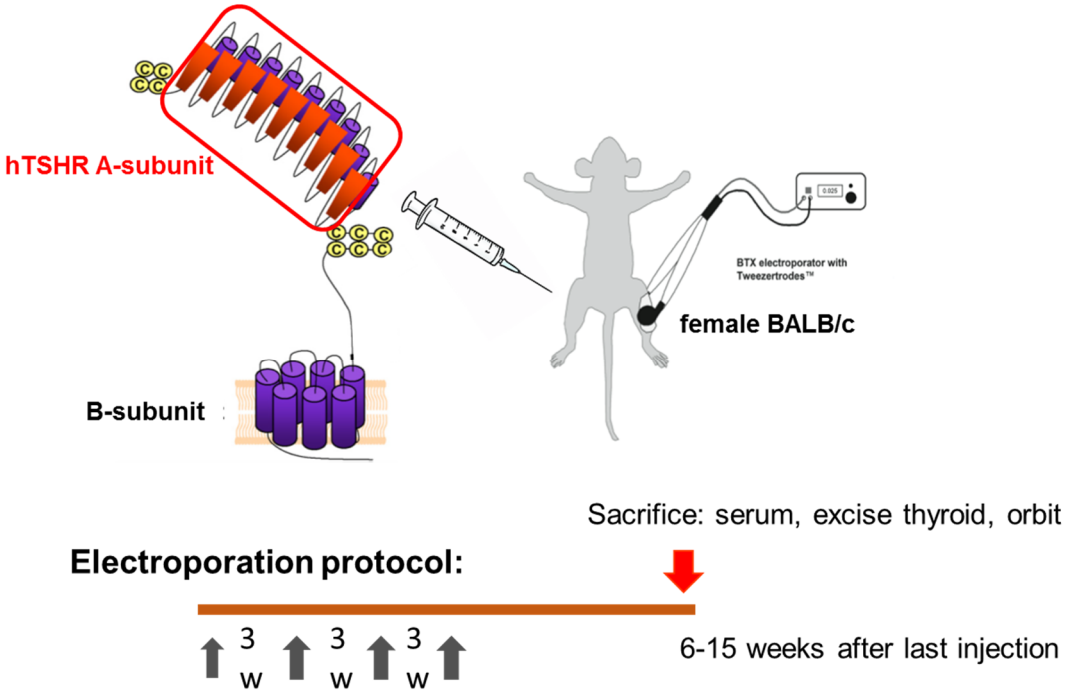

Figure 9. Induction of GO in mouse model by genetic immunization. Plasmids encoding for the human TSHR A-subunit or for ß-Galactosidase as a control plasmid were injected and electroporated in the big leg muscles of female BALB/c mice four times at 3-week intervals. Six to 15 weeks after the last immunization mice were sacrificed and serum, thyroids and orbits were investigated (adapted from Moshkelgosha et al., 2013; Rapoport and McLachlan, 2016).

2.5 Principal issues addressed in this thesis

Graves' orbitopathy (GO) leads to significant limitations in quality of life of patients, which may be symptomatic and physical strain. The medical treatments are not yet matured and molecular processes of the disease are incompletely understood. The studies which are included in this thesis aimed for a better understanding of molecular mechanisms and pathophysiological processes of tissue remodeling in GO. Although OF are considered to play an important role in tissue remodeling and inflammation, the orbital cell population of GO patients has been incomplete characterized. Differentiation of OF and resulting tissue expansion in conjunction with inflammation and the limited volume of the bony orbit can cause hypoxia. However the hypoxic response of OF has been unknown.
At the start of the thesis the recently described GO mouse model (2013), has not been reproduced and mouse OF were not available to study hypoxic and other pathways during the course of disease.

The aim of this thesis was the investigation of characteristics, immune modulation and differentiation ability of orbital cell populations derived from GO patients as well as GO mouse model. During the course of the thesis the GO mouse model should be established and reproduced to obtain and to characterize mouse OF. Furthermore, the role of hypoxia as a tissue remodeling driving factor has to be exploited. The understanding of the regulation and activation of orbital cell populations and role of hypoxia induced pathways in OF could be fundamental to develop potential novel therapeutic targets.

3 Publications

Publication 1

Orbital fibroblasts from Graves‘ Orbitopathy patients share functional and immunophenotypic properties with mesenchymal stem/stromal cells.

Brandau S, Bruderek K, Hestermann K, Görtz G-E, Horstmann M, Mattheis S, Lang S, Eckstein A, Berchner-Pfannschmidt U.

Invest Ophthalmol Vis Sci. 2015, 56:6549-5756

Contribution

Herein I performed cell culture experiments to analyze hyaluronan production like in Fig. 1 and neurogenic differentiation potential (Fig. 3) of OF and MSC derived from GO patients and control persons. I designed the experimental conditions and performed hyaluronan ELISA, neurogenic differentiation assay, staining of the cells and microscopy. I analyzed the obtained data and contributed to interpretation of the results. I was involved in writing methods and results of the publication.

Biochemistry and Molecular Biology

Orbital Fibroblasts From Graves' Orbitopathy Patients Share Functional and Immunophenotypic Properties With Mesenchymal Stem/Stromal Cells

Sven Brandau,[1] Kirsten Bruderek,[1] Khaleda Hestermann,[1,2] Gina-Eva Görtz,[2] Mareike Horstmann,[2] Stefan Mattheis,[1] Stephan Lang,[1] Anja Eckstein,[2] and Utta Berchner-Pfannschmidt[2]

[1]Department of Otorhinolaryngology, University of Duisburg-Essen, Essen, Germany
[2]Department of Ophthalmology, Molecular Ophthalmology Group, University of Duisburg-Essen, Essen, Germany

Correspondence: Utta Berchner-Pfannschmidt, Department of Ophthalmology, Molecular Ophthalmology Group, University Duisburg-Essen, 45147 Essen, Germany; utta.berchner-pfannschmidt@uk-essen.de.
Sven Brandau, Department of Otorhinolaryngology, University Duisburg-Essen, 45147 Essen, Germany; sven.brandau@uk-essen.de.

Submitted: February 4, 2015
Accepted: September 4, 2015

Citation: Brandau S, Bruderek K, Hestermann K, et al. Orbital fibroblasts from Graves' orbitopathy patients share functional and immunophenotypic properties with mesenchymal stem/stromal cells. *Invest Ophthalmol Vis Sci.* 2015;56:6549–6557. DOI:10.1167/iovs.15-16610

Purpose. In Graves' orbitopathy (GO), inflammation and expansion of the retrobulbar tissue are the result of a pathophysiologic process in which orbital fibroblasts (GO-Fs) are considered the central cell type. However, in a previous study we observed that GO-Fs expressed some of the consensus surface markers described for mesenchymal stem/stromal cells (MSC). In this study, we further elucidate the stem cell characteristics of GO-Fs by comparing them with orbital fat-derived mesenchymal stem cells.

Methods. We enriched primary human GO-MSCs and GO-Fs simultaneously from the same retrobulbar fat biopsies obtained during decompression surgery of GO patients. The biological characteristics of donor-matched GO-MSCs and -Fs were compared along criteria that define MSC: fibroblast-like growth, MSC surface marker profile, multilineage differentiation potential, and immunomodulatory functions.

Results. Application of a standardized isolation and expansion protocol yielded GO-MSCs, which showed plastic adherent fibroblast-like morphology and proliferated and produced hyaluronan similarly to GO-Fs. Both GO-MSCs and GO-Fs expressed orbital fat-derived stem cell surface markers CD29, CD44, CD71, CD73, CD90, CD105, and CD166 and were negative for CD31, CD34, CD45, CD146, and Stro-1 after ex vivo expansion. Further, GO-MSCs and GO-Fs displayed adipogenic, osteogenic, chondrogenic, myogenic, and neuronal differentiation, although GO-Fs with a lower capacity. In addition, when compared to GO-MSCs, the GO-Fs showed reduced T-cell suppression and secreted reduced amounts of IL-6, suggesting a lower immunosuppressive potential.

Conclusions. The in vitro data obtained in this study provide the first experimental evidence that orbital fibroblasts derived from retrobulbar fat of GO patients share biological characteristics with MSCs. These findings provide new insight into the biology of key cells in GO.

Keywords: mesenchymal stem/stromal cells, orbital fibroblasts, Graves' orbitopathy

Graves' orbitopathy (GO) is the most common extrathyroidal manifestation of Graves' disease.[1] Graves' orbitopathy is a fibroproliferative disease of autoimmune origin characterized by inflammation and by remodeling and expansion of the retro-ocular connective tissue.[2] Resident orbital fibroblasts (GO-Fs) are recognized as the central cell type mediating inflammation and tissue remodeling in GO. A series of observations made in vitro suggested that once GO-Fs were activated during the inflammatory process in response to anti–thyroid-stimulating hormone receptor (TSHR) autoantibodies, immigrated T cells and macrophages, inflammatory cytokines, or some combination of these, GO-Fs reacted with excessive proliferation and adipogenesis, as well as production of hyaluronan and proinflammatory cytokines.[3,4] However, GO-Fs were recognized as a heterogenous cell population containing subtypes exhibiting different adipogenic/myogenic differentiation ability, as well as production of inflammatory mediators, and thus may be differently involved in connective tissue remodeling and immune responses in GO.[5,6] In a previous study, we recognized that GO-Fs expressed some of the consensus surface markers described for mesenchymal stem cells (MSC); they were positive for CD73, CD90, and CD105 and negative for CD11b, CD19, CD31, CD45, and HLA-DR.[7] This surface marker set with the cells' ability to undergo adipogenic and myogenic differentiation[8] makes us wonder whether GO-Fs meet further characteristics of MSCs. Mesenchymal stem cells are fibroblast-like undifferentiated nonhematopoietic progenitor cells that are capable of differentiation into mesenchymal (fat, bone, cartilage, and muscle) and nonmesenchymal lineages (e.g., neuron).[9] Recent evidence suggests that MSCs play an important role in both tissue remodeling and immune response.[10] Because of their regenerative and immunoregulatory properties, MSCs are an attractive tool for the cellular treatment of inflammation and autoimmunity, which is reflected by an increasing number of clinical trials using allogenic MSCs in graft-versus-host disease, Crohn's disease, or multiple sclerosis.[9] Previously, we identified

Investigative Ophthalmology & Visual Science

MSCs from the head and neck region such as the nasal mucosa, parotid gland, and adipose tissue[11,12]; and recent studies have shown that mesenchymal progenitor cells can be isolated and expanded from orbital adipose tissue as well.[13,14] However, still little is known about tissue-resident mesenchymal progenitor cells in the deep retrobulbar connective/fat tissue of GO patients and about the interrelation of fibroblasts and MSCs in this tissue. In the present study we therefore isolated MSC from the retrobulbar fat tissue (GO-MSC) obtained during decompression surgery of GO patients and compared them with GO-Fs isolated from the same piece of fat tissue. Unexpectedly, we found that GO-Fs exhibit all of the characteristics that define MSC as well. On the other hand, we report some distinct differences in terms of differentiation capacity, T-cell suppression, and cytokine production, indicating that GO-MSCs and GO-Fs contain functionally different subsets of the resident mesenchymal progenitor cell population. Our data uncover stem cell characteristics of GO-Fs that will help to better understand the pathologic role of these cells in GO.

Methods

Patients

During orbital decompression procedures, surgical tissue explants of orbital adipose tissue were obtained from 12 patients with active, severe GO, as classified by the European Group on Graves' Orbitopathy. The mean clinical activity score (CAS) was 5.2 (range, 3–10), and the mean NOSPECS classification was 10.1 (range, 6–14). The mean duration time of GO was 10.5 (range, 6–108) months. The mean age of patients was 54.6 years, and 83.3% were female. Four patients receive anti-inflammatory treatment (steroids) immediately before decompression, and orbital irradiation was applied to four patients. Decompression was performed as primary therapy because of severe corneal exposure; intravenous steroids were given postoperatively. The study followed the tenets of the Declaration of Helsinki and was approved by the institutional ethics committees. All study participants gave written informed consent.

Isolation and Culture of Cells

After resection, orbital fat tissue samples or control samples from the mucosal tissue of the ethmoid from the same GO patients were collected aseptically in NaCl (0.9%; Fresenius Kabi, Bad Homburg, Germany). Subsequently, tissues were washed several times with PBS and cut into 1- to 2-mm pieces. Orbital fibroblasts were isolated in accordance with Bahn et al.[15] In brief, the orbital tissue pieces were placed directly in six-well culture plates in standard culture medium (Dulbecco's modified Eagle's medium [DMEM] supplement with 10 mM HEPES/pH 7.4, 10% fetal bovine serum, 1% penicillin/streptomycin, 1% sodium pyruvate, 100 mM nonessential amino acids) and grown in a humidified atmosphere of 5% CO_2 at 37°C. After 2 to 3 weeks the tissue pieces were removed, nonadherent cells were removed by washing with PBS, and the remaining cells were cultivated as described earlier.[7]

Potential mesenchymal stem cells from the orbital fat tissue (GO-MSC) were isolated in accordance with an isolation method for classical adipose-derived stem cells.[16] Briefly, the tissue pieces were digested in PBS/1%BSA solution containing 0.1% collagenase type I (Worthington Biochemical Corporation, Lakewood, NJ, USA) for 60 minutes at 37°C with gentle agitation. Tissues were centrifuged at 300*g* for 5 minutes. Tubes were vigorously shaken to release fat cells from the fibrous tissue. The cell suspension was then centrifuged again, and the supernatant was discarded. The pellet containing stromal cells was washed several times and resuspended in standard culture medium. Cells were transferred to 24-well dishes; nonadherent cells were removed by washing with PBS 72 hours later, and fresh culture medium was added over the remaining cells. Potential MSCs were isolated from control samples of the mucosal tissue of the ethmoid from GO patients (GO-EthC) with an MSC protocol as described earlier.[11,12]

Multiparameter Flow Cytometry

For immunophenotyping of GO-Fs and GO-MSCs, the following antibodies were used simultaneously in multiparameter multicolor flow cytometry, which included all markers within one staining procedure: CD29 PE (β1-integrin, clone MAR4; BD Bioscience, Heidelberg, Germany), CD31APC-eFluor 780 (PECAM-1, clone WM59; eBioscience, Frankfurt am Main, Germany), CD34 FITC (My10, clone 581, Class 3; Invitrogen, Karlsruhe, Germany), CD44 PE (clone 515; BD Bioscience), CD45 V500 (leukocyte common antigen, clone HI30; BD Bioscience), CD71APC (transferrin receptor, clone AD2; BD Bioscience), CD73 PerCP-eFluor 710 (ecto-5-NT, SH4; clone AD2; eBioscience), CD90 Brilliant Violet 421 (Thy-1, clone 5E10; BioLegend, Fell, Germany), CD105 PE-Cy7 (Endoglin/TGF1-b3 receptor, clone 43A3; BioLegend), CD146 Brilliant Violet 421 (MCAM, clone P1H12; BioLegend), CD166 PerCP-eFluor (ALCAM, clone 3A6; eBioscience), and Stro-1 Alexa Fluor 647 (clone Srto-1; BioLegend). To determine nonspecific signals, isotype controls were used at the same concentration as for the specific antibody. Analysis was performed using a BD FACSCanto II flow cytometer (BD Bioscience) with Diva Software 6.0.

Adipogenic Differentiation

For adipogenic differentiation, 6×10^4 cells were seeded on round glass slides in 24-well culture dishes and cultured in 1 mL standard culture medium until reaching 80% confluence. Adipogenic differentiation was induced with Mesenchymal Stem Cell Adipogenic Differentiation Medium (PromoCell, Heidelberg, Germany). In order to examine the generation of oil droplets in the cytoplasm after differentiation, cells were fixed with 10% formalin (Sigma-Aldrich Corp., St. Louis, MO, USA) and stained with Sudan III (Sigma-Aldrich Corp.) for 60 minutes at room temperature. In brief, cells were washed twice in PBS, and 0.03% Sudan III in 10 mL 70% ethanol was added. Hematoxylin was used to counterstain nuclei. Images were generated using an Axiocam MRc microscope camera and Axiovision AxioVS40 software (all Carl Zeiss MicroImaging, Göttingen, Germany).

Osteogenic Differentiation

For osteogenic differentiation, 6×10^4 cells were seeded on round glass slides in 24-well culture dishes; they were cultured in 1 mL standard culture medium until reaching 95% confluence and were fed every 3 to 4 days with Mesenchymal Stem Cell Osteogenic Differentiation Medium (PromoCell). As a marker for osteogenic differentiation, Alizarin red S staining was performed to detect microcrystalline or noncrystalline calcium phosphate salts. After fixation with formaldehyde, cells were stained with 1% Alizarin red S (Sigma-Aldrich Corp.).

Chondrogenic Differentiation

To induce chondrogenic differentiation, 2.5×10^6 cells were transferred into a 15-mL polypropylene tube and centrifuged at 300*g* for 5 minutes to form micromass pellets at the bottom of

the tube. After 48 hours of culture in standard medium, chondrogenic differentiation was induced with standard medium supplemented with dexamethasone: 1×10^{-3} M l-proline (Sigma-Aldrich Corp.), 10 ng/mL TGF-β3 (Peprotech, Hamburg, Germany), and 1% BD ITS Culture supplement (BD Bioscience). After 3 weeks of culture, micromass bodies were embedded in Tissue-Tek (Sakura Finetek, Staufen, Germany), cryosectioned at 5-μm thickness, and frozen at −80°C. To demonstrate the presence of glycosaminoglycans in specimens, we used Alcian blue 8X (Roth, Karlsruhe, Germany) staining, and Shandon Instant Hematoxylin (Thermo Scientific, Bonn, Germany) was used for counterstaining nuclei.

Myogenic Differentiation

Cells (6×10^4) were seeded on round glass slides in 24-well culture dishes overnight in standard medium. Myogenic differentiation was induced by adding 100 ng/mL TGF-β1 (Peprotech). Cells were immunostained for α-smooth muscle actin (α-SMA, 1:200, mouse monoclonal clone 1A4), secondary antibody goat anti-mouse IgG-fluorescein isothiocyanate (FITC) (1:100; Dianova, Hamburg, Germany), and 7-aminoactinomycin (7AAD).

Neuronal Differentiation

To induce neuronal differentiation, 5×10^4 cells were grown on glass slides in 24-well culture dishes and incubated with 40 μM neuronal inducer TCS 2210 (Tocris, Boston, MA, USA) in standard medium as described previously.[17] Neuronal differentiation was observed by detection of ß3-tubulin (1:200, rabbit monoclonal IgG; Cell Signaling Technology, Danvers, MA, USA) in combination with a secondary antibody goat anti-rabbit IgG-Alexa Fluor 594 (1:400; Invitrogen) and 4′,6-diamidino-2-phenylindol (DAPI) counterstaining of nuclei using immunofluorescence microscopy.[7]

T-Cell Suppression Assay

Responder T cell/monocytes were isolated by anti-CD3 and CD14 microbeads from peripheral blood of healthy volunteers according to the manufacturer's instructions (Miltenyi, Bergisch-Gladbach, Germany). Isolated responder cells were stained with 5 μM carboxyfluorescein diacetate succinimidyl ester (CFSE) (Invitrogen, Karlsruhe, Germany) and stimulated at 0.25×10^6 cells/mL with Dynabeads human T-Activator CD3/CD28/CD137 (Invitrogen; responder cell to beads ratio 1:10). GO-MSC or GO-F isolated from the same GO patient in the same passage was added to different amounts of T cells (40:1, 20:1, or 10:1 T-cell to GO-MSC/-F ratios). The CFSE dilution assays were analyzed after 7 days in a BD FACSCanto II flow cytometer, and the proliferation index was determined with ModFit LT 3.2 software (Verity Software House, Topsham, ME, USA).

Enzyme-Linked Immunosorbent Assay (ELISA) for Detection of Cytokines

Constitutive secretion of IL-6, IL-8, and MIF (macrophage migration inhibitory factor) was detected by DuoSet Human Immunoassay (R&D Systems, Wiesbaden, Germany) according to the manufacturer's protocol. Third-passage GO-MSCs or GO-Fs were washed three times with DMEM and cultured for 24 hours in standard medium at a concentration of 1×10^6 cells/mL. The supernatant was collected, further cleared from debris by centrifugation, and stored at −20°C until measurements.

Proliferation Assay

Proliferation of fourth-passage cells was measured with a chemiluminescent immunoassay for quantification of cell proliferation based on the measurement of bromodeoxyuridine (BrdU) incorporation during DNA synthesis (Roche, Mannheim, Germany) as described before.[7]

Measurement of Hyaluronan

For determination of hyaluronan production, 1×10^4 cells were grown for 48 hours in a 96-well plate in 200 μL DMEM supplemented as above. The medium was aspirated, and HA was measured with an enzyme-linked binding protein assay from Corgenix (Broomfield, CO, USA) according to the manufacturer's instructions as described before.[7]

Statistical Analysis

Statistical analysis was performed with 2-tailed Student's *t*-test with a confidence level greater than 95%. Data are presented as arithmetic means ± SD. Statistical significance was set at the level of $P \leq 0.05$.

Results

Isolation of Mesenchymal Stem Cells From Retrobulbar Fat Tissue of GO Patients

In the present study, we aimed to investigate the biological characteristics of orbital mesenchymal cells isolated from the diseased orbit along criteria that define MSC. To test whether orbital fat tissue can be a source of multipotent cells, retrobulbar-derived fibroblast-like cells from GO patients were isolated according to an isolation method for adipose tissue-derived stem cells.[16] To compare GO-MSCs with GO-Fs, which are key cells in GO pathology, we isolated GO-Fs simultaneously from the same piece of fat tissue of the respective GO patient with a standard method as described before.[7,15] As shown in Figure 1A, these putative orbital fat-derived GO-MSCs were of fibroblast-like morphology and expressed the mesenchymal marker protein vimentin and fibroblast surface protein 1 just as did the GO-Fs, indicating a similar morphology of the two cell populations. Because proliferation and hyaluronan production of GO-Fs are a hallmark of GO pathology, we tested hyaluronan secretion of GO-MSCs. We found that the putative GO-MSCs proliferated and produced hyaluronan to the same extent as the GO-Fs (Fig. 1B), implying that GO-MSCs can contribute to pathogenesis of GO.

Characterization of GO-MSCs and -Fs by Expression of Typical Surface Markers

To further characterize putative GO-MSCs and -Fs, we analyzed a set of surface markers with flow cytometry. As illustrated in Figure 2, after ex vivo selection and expansion into passage 3, both of the donor-matched cell lines were strongly positive for the consensus MSC markers CD29, CD44, CD71, CD73, CD90, CD105, and CD166 (Fig. 2A). In contrast, GO-MSCs and -Fs lacked expression of a known hematopoietic progenitor marker CD34, a leukocyte marker CD45, and the endothelial marker CD31, as well as the pericyte marker CD146 and Stro-1 (Fig. 2A). Additional analysis of early passage 1 cells revealed expression of CD31 and CD146 (Supplementary Fig. S1), which were downregulated after further expansion (Fig. 2A). Although the GO-MSCs and -Fs predominantly expressed CD90 to high levels

Investigative Ophthalmology & Visual Science

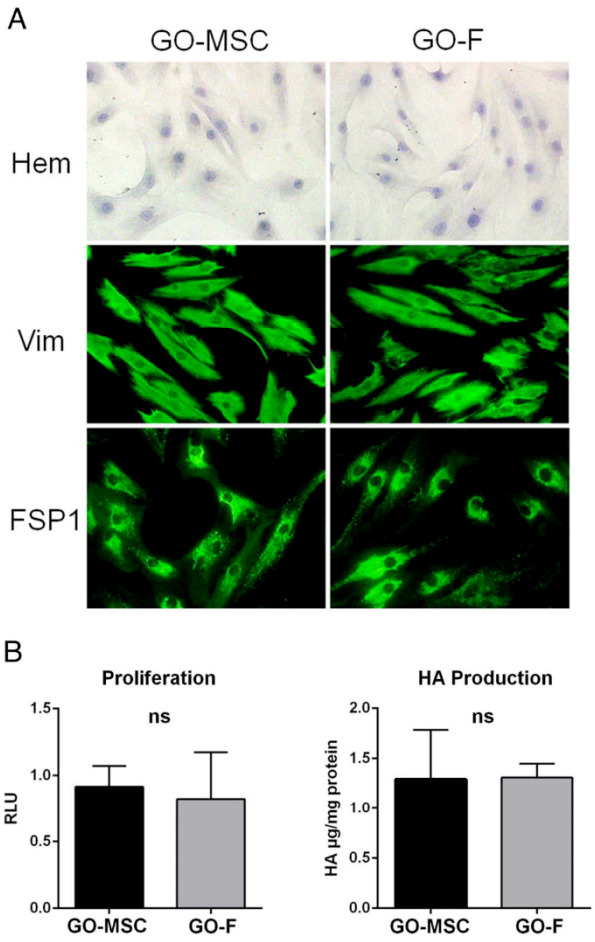

Figure 1. Morphology and synthetic capacity. GO-MSCs and GO-Fs were simultaneously isolated from retrobulbar fat tissue of GO patients. (**A**) The fibroblast-like morphology of plastic adherent cells was shown with hematoxylin (Hem) staining using light transmission microscopy (×200 magnification). The mesenchymal marker vimentin (Vim) and fibroblast surface protein 1 (FSP1) were detected in cells using immunofluorescence microscopy (×200 magnification) as described earlier.[13] Representative images are shown. (**B**) Proliferation and hyaluronan (HA) production of 4-6 GO-MSC/-F (third to sixth passage) was analyzed in duplicate 48 hours after seeding. Proliferation is shown as an average of three independent experiments. RLU, relative light units. Hyaluronan production was normalized to protein concentration, and a representative result from at least three independent experiments is shown.

(Figs. 2A, 2B, donor 1), some GO patients (two out of nine) exhibited subpopulations with low expression of CD90 (Fig. 2B, donor 2). Coexpression of MSC markers CD29/CD73/CD90/CD105 on the majority of cells was confirmed by multicolor flow cytometry (Fig. 2C). Notably, the GO-Fs expressed the identical set of surface antigens as the GO-MSCs (Fig. 2), suggesting GO-Fs to be orbital MSC-like cells as well.

Multilineage Differentiation Capacity of GO-MSC and GO-OF

To further analyze MSC characteristics of putative MSC types GO-MSCs and GO-Fs we investigated their multilineage differentiation capability. To examine whether these cells were able to undergo adipogenic, osteogenic, chondrogenic, myogenic, or neuronal differentiation, three to four independent cell cultures were subjected to the respective differentiation medium and compared to "nonorbital" fibroblastoid cells of adjacent mucosal ethmoid tissue (Fig. 3). After induction of differentiation with the respective induction medium, differentiation into multiple lineages was observed with standard staining methods indicating differentiation as described in Methods. GO-MSCs and GO-Fs were strongly stained positive for each of the stainings, indicating adipogenic, osteogenic, chondrogenic, myogenic, and neuronal differentiation capability (Fig. 3A). Control cells maintained in regular noninductive medium were negative or showed low staining. In contrast, GO-EthC isolated from samples of the ethmoid of the same GO patients showed only positive staining for αSMA, indicating differentiation into the myogenic lineage (Fig. 3A). Quantification of differentiation samples revealed that both GO-MSCs and GO-Fs exhibited multilineage differentiation capability, although GO-MSCs with a clearly higher differentiation capacity in terms of adipogenesis, osteogenesis, and myogenesis than GO-Fs (Fig. 3B). The in vitro differentiation data obtained here support the notion that GO-Fs, similar to the GO-MSC population, contain mesenchymal stem cells.

Orbital MSCs and -Fs Are Immunologically Active and Responsive

In the first part of our study we demonstrated that both GO-MSCs and GO-Fs fulfilled the minimal MSC definition criteria of plastic adherence and fibroblast-like growth (Fig. 1), distinct set of surface markers (Fig. 2), and multilineage differentiation (Fig. 3). In the second part of our study we further aimed to investigate typical immunomodulatory function of MSC. As suppression of T-cell proliferation is a functional hallmark of MSCs, we performed polyclonal stimulation of responder T cells in the presence of autologous monocytes. Donor-matched GO-MSCs and GO-Fs were added, and their suppressive potential on T-cell proliferation was compared. As illustrated in Figure 4A, T-cell proliferation is increasingly inhibited by both mesenchymal cell types depending on the T cell to GO-MSC/-F ratios. Notably, GO-MSCs exhibited a significant enhanced capacity to suppress polyclonal T-cell activation when compared to GO-Fs at a 40:1 ratio (Figs. 4A, 4B). The obtained data provide evidence that GO-Fs have an immunosuppressive potential, although with lower capacity compared to GO-MSCs.

Further, secretion of cytokines has previously been shown to mediate immunosuppressive ability of tissue-resident MSCs. Therefore, constitutive secretion of IL-6, IL-8, and MIF was determined by ELISA and compared for GO-MSCs and GO-Fs. Both mesenchymal cell lines produced low amounts of IL-8 (<1 ng/mL) and high amounts of MIF (>1 ng/mL). In contrast, GO-MSCs secreted higher levels ($P = 0.022$) of the inflammatory cytokine IL-6 that easily exceeded 1 ng/mL under standard culture conditions (Fig. 5). The data indicate that GO-MSCs and GO-Fs by secreting inflammatory cytokines could exert an immunomodulatory function in the orbit.

Discussion

In the present study, we successfully identified for the first time MSCs in adipose retobulbar tissue of patients with GO (GO-MSCs) using standard protocols for adipose tissue-derived stem cell isolation and expansion. We use the term mesenchymal stem/stromal cells (MSCs) because we could demonstrate that orbital fat-derived MSCs fulfill the minimal criteria for defining multipotent MSCs together with immunoregulatory function, in agreement with MSC phenotype definition of the Interna-

Investigative Ophthalmology & Visual Science

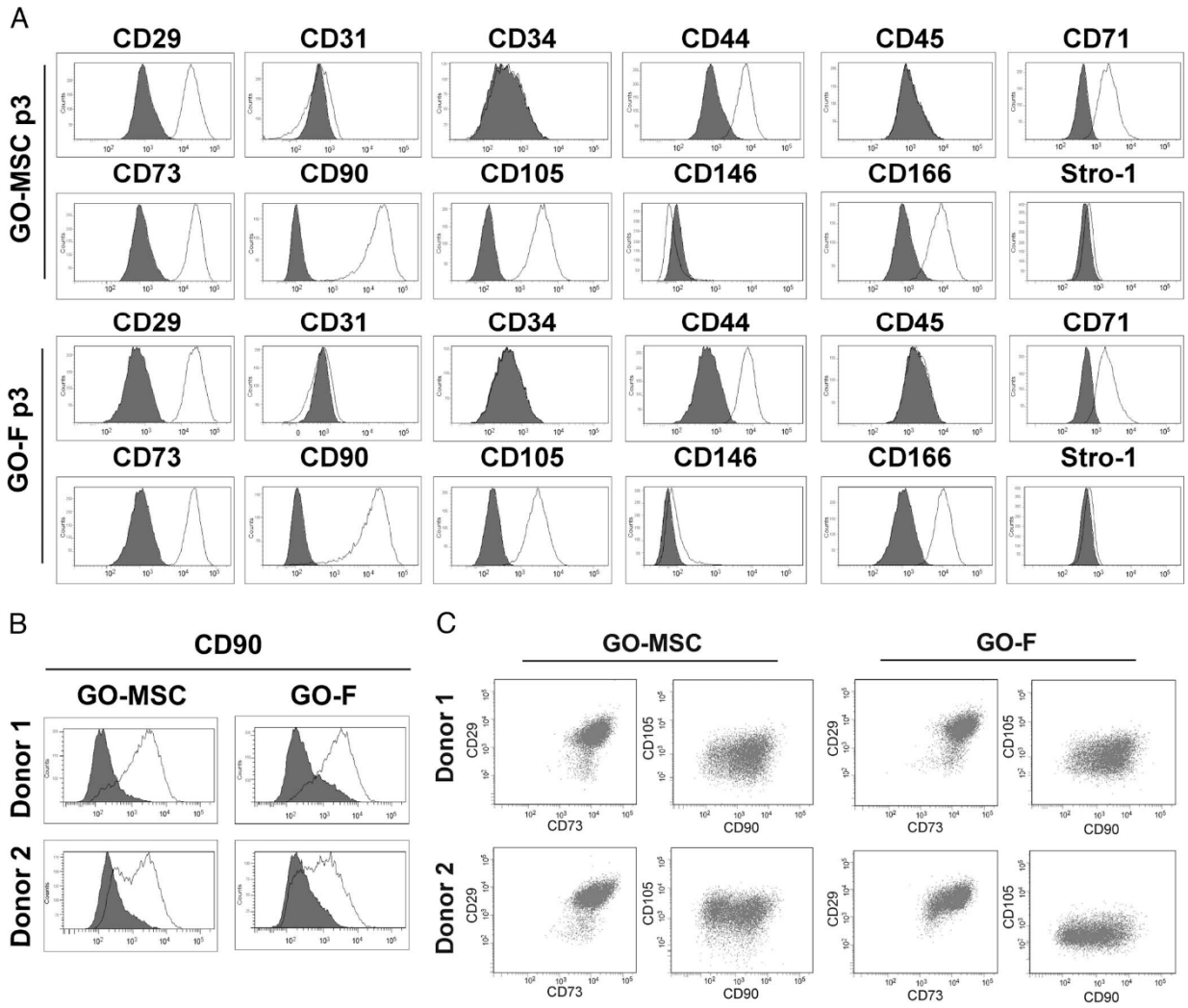

Figure 2. Comparative immunophenotypic characterization. Multiple surface antigens of GO-MSCs and GO-Fs isolated simultaneously from orbital fat tissue of nine GO patients (first to third passages) were analyzed using multiparameter flow cytometry based on multicolor staining. Data are shown as an overlay histogram: isotype control (*gray*) and specific cell surface markers (*white*). (**A**) A representative surface marker set of donor-matched GO-MSCs and GO-Fs in the third passage (p3) is shown. (**B**) Heterogeneity of CD90 expression. The histograms of two representative GO patients (donor 1 and donor 2) are shown. (**C**) Multiparameter analysis of CD29/CD73/CD90/CD105 of donor 1 and donor 2. *Dot blots* visualize the heterogeneity of the surface marker expression within the respective cell population.

tional Society for Cellular Therapy.[18] Importantly, we could demonstrate for the first time that GO-Fs, an accepted in vitro cell model of GO since their first isolation by Bahn and coworkers,[11] exhibit the same morphologic features, as well as a surface marker set and multilineage differentiation potential similar to GO-MSCs (Figs. 1, 2, 3). Interestingly, the GO-MSCs and -Fs expressed the same surface marker as orbital fat-derived stem cells obtained from fat tissue of the intraorbital cavity during blepharoplastic surgery.[19] In addition, the observed reduction of the surface markers CD31 and CD146 during the early passages (Fig. 2A, Supplementary Fig. S1) was found to be a characteristic of mesenchymal progenitor cells derived from orbital adipose tissue.[20] Taken together, the observed surface marker profile supports the notion that GO-MSCs and -Fs isolated from the retrobulbar tissue during decompression procedure of GO patients represent orbital fat-derived stem cell populations. Indeed, GO-MSCs and GO-Fs shared the most important characteristic of orbital adipose tissue-derived stem cells, namely, the potential to differentiate into adipocytes, chondrocytes, and osteoblasts, and in addition into myogenic and neuronal precursors.[13] These findings demonstrate that our isolation procedure effectively yields the generation of MSCs from retrobulbar fat tissue. In contrast, GO-EthC fibroblasts showed no multilineage differentiation capacity and therefore could not be considered as containing MSC populations although isolated with a MSC protocol. Similarly, fibroblasts isolated from the eyelid skin during blepharoplastic surgeries did not differentiate toward the adipogenic or osteogenic lineage, and they showed less pronounced signs of chondrogenic differentiation even though they expressed a similar set of surface markers as the orbital fat-derived stem cells.[14] Several working groups previously reported differentiation of GO-Fs into adipocytes or myocytes.[19–21] However, we found that GO-Fs were also able to differentiate along the osteocytic, chondrocytic, and neuronal lineages (Fig. 3), hence shared characteristics of classical adipose tissue-derived stem

Investigative Ophthalmology & Visual Science

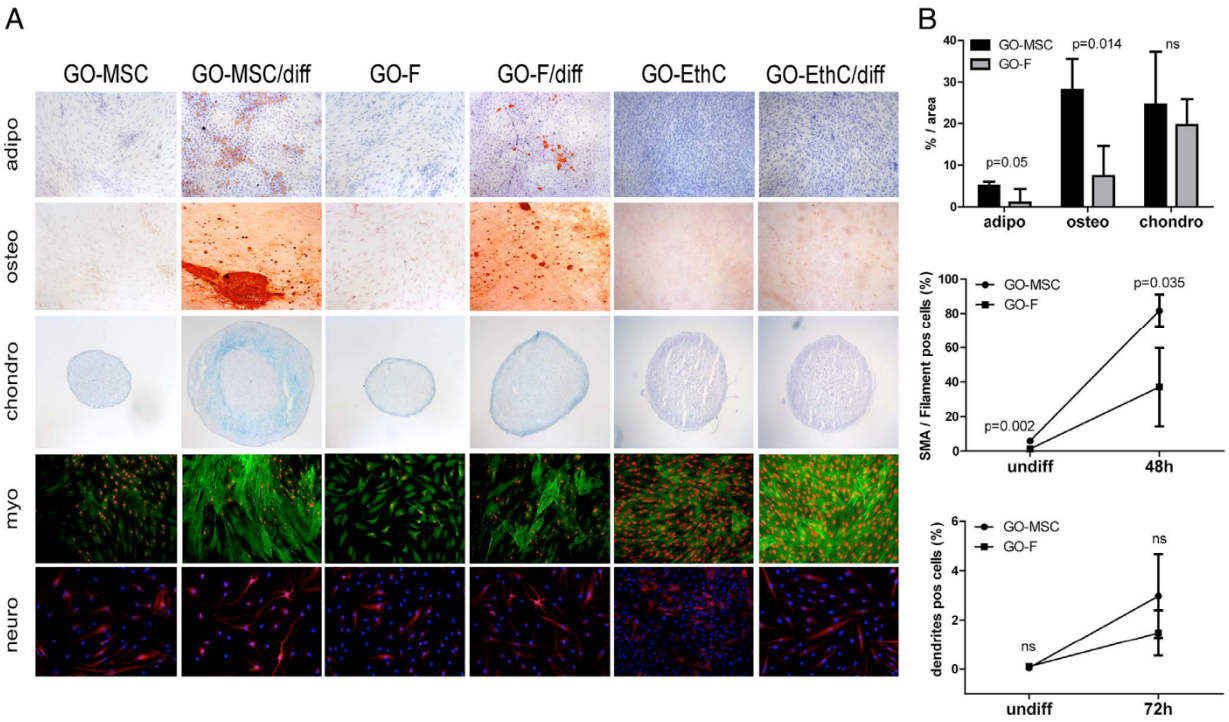

Figure 3. Multilineage differentiation studies. GO-MSCs/-Fs and GO-EthC isolated from three or four GO patients were subjected (first to third passages) to the respective differentiation medium (diff) to induce adipogenic (adipo), osteogenic (osteo), chondrogenic (chondro), myogenic (myo), or neuronal (neuro) lineages. After 2 weeks of incubation, the adipogenic differentiation was observed by staining fatty vacuoles with Sudan III. We demonstrated osteogenic differentiation by Alizarin red S staining of microcrystalline or noncrystalline calcium phosphate salts after 3 weeks of incubation. The chondrogenic differentiation with Alcian blue 8GX staining of glycosaminoglycans was observed after 4 weeks. The myogenic differentiation was analyzed after 48 hours by staining of α-SMA, and neuronal differentiation was observed by staining of ß3-tubulin after 72-hour incubation. (**A**) Representative images obtained with light transmission microscopy from three or four GO-MSC/-Fs or GO-EthCs (adipo, osteo, and chondro at ×100 magnification) or with fluorescence microscopy (α-SMA at ×100 magnification and β3-tubulin at ×200 magnification) are shown. (**B**) Semiquantitative analysis of differentiation was carried out using ImageJ (http://imagej.nih.gov/ij/; provided in the public domain by the National Institutes of Health, Bethesda, MD, USA) either by determining the colored stained area (%) (adipo, osteo, chondro) or by counting stained cells with changed morphology (myo: cells with α-SMA positive filaments; neuro: cells with β3-tubulin positive dendrites) from three to four fields of view at ×100 magnification of three or four GO-MSCs/-Fs, respectively.

cells that reside in the vascular stroma of adipose tissue as well as in the bone marrow.[22] Because adipose cells are mesodermal in origin, the differentiation of adipogenic stem cells into neural tissue of ectodermal origin seemed to be very unlikely. However, they can take on a neuronal morphology when exposed to different induction agents.[23] While MSCs, adipose-derived stem cells, and most tissue fibroblasts are of mesenchymal origin, the GO-Fs have been hypothesized to be derived from the neuroectodermal origin.[24] Although ocular and orbital components have been shown to be derived from a combination of mesodermal and neural crest cells,[25] the origin of the retrobulbar connective/fat tissue and derived cells remains unclear. Interestingly, it has been reported that in the cephalic region a subset of adipocytes arises from the neural crest.[26] Further, a subpopulation of adipogenic progenitors derived from the neural crest has been identified in adipose stromal cells.[27] Because our in vitro data provide the first experimental evidence that the GO-F population contains progenitors with neuronal differentiation potential, it appears possible that GO-Fs contain neural crest–derived progenitors. However, we found that GO-Fs differentiate and showed multilineage potency, indicating that mesenchymal multipotent progenitor cells were effectively present in the GO-F population. In comparison to GO-Fs, the GO-MSCs showed better cell differentiation ability in terms of adipogenesis, osteogenesis, and myogenesis. These data may suggest that GO-Fs, in contrast to GO-MSCs, represent a more heterogeneous population of fibroblastoid cells containing more mature differentiated cells and a minority of MSC-like multipotent progenitor cells. Further studies are needed to fully elucidate the functional heterogeneity of orbital progenitor cells.

While CD90 (Thy-1) is consistently expressed on the cell surface of adipose stem cells,[28] we found that GO-MSC and GO-F populations of some GO patients (two out of nine patients) contained considerable amounts of subtypes expressing low levels of CD90 (Fig. 2B). It was reported earlier that the degree of CD90 expression on GO-Fs influences their differentiation capacity. While $CD90^{+}$ subtypes differentiate into myocytes, $CD90^{-}$ subtypes differentiate into adipocytes.[5,8] However, it was shown recently that in GO-Fs expressing a high level of CD90, adipogenesis can also be induced in three-dimensional culture and under pressure stress as might occur in the diseased orbit.[29] In contrast, GO-MSCs clearly exhibited overall higher adipogenic and myogenic differentiation capacity than the GO-Fs (Fig. 3B), although CD90 expression level of the two populations was very similar (Fig. 2). This indicates that factors other than CD90 expression additionally impact differentiation capacity of GO-F-like/mesenchymal stem cells. However, constitutive proliferation capacity and hyaluronan production did not differ between undifferentiated GO-MSCs and GO-Fs (Fig. 1). It remains to be investigated whether under stimulation conditions as occur in the diseased orbit, GO-

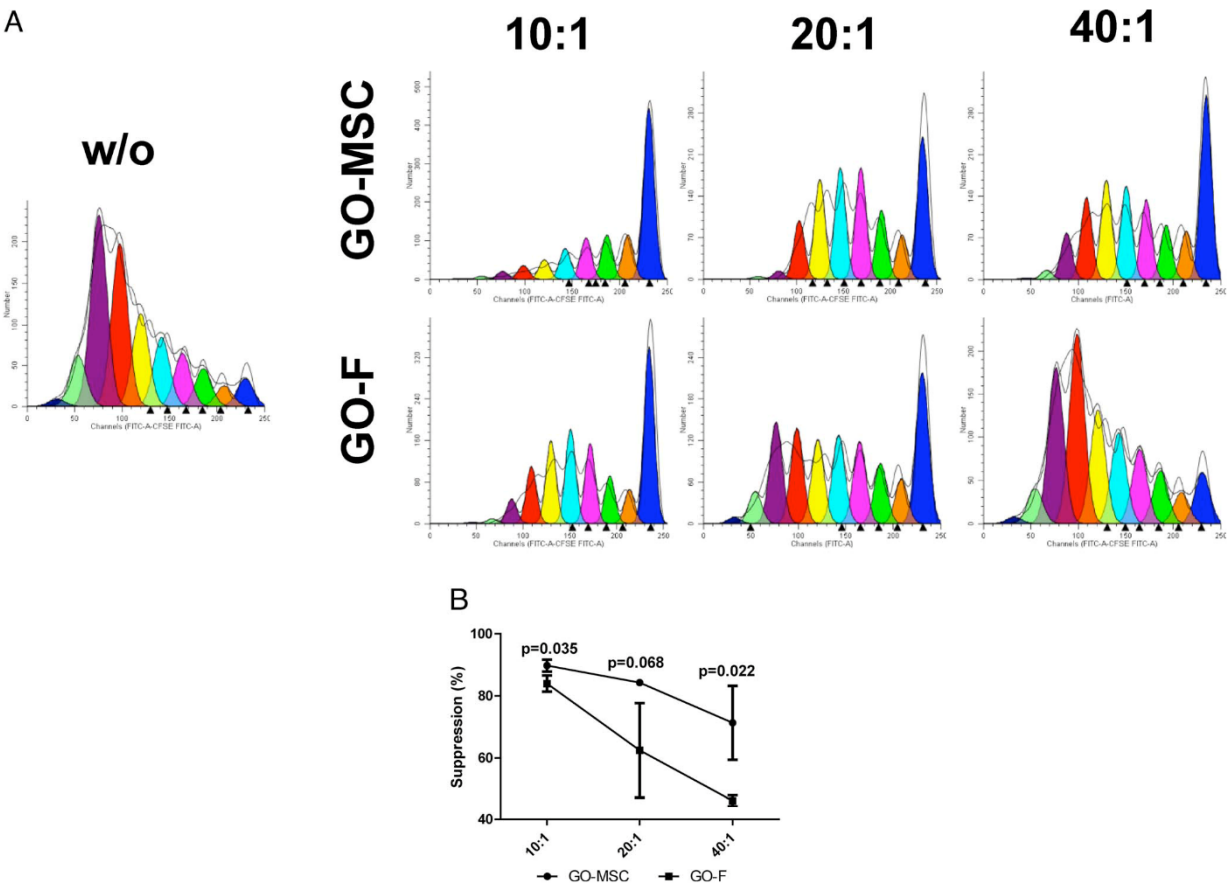

Figure 4. Comparative T-cell proliferation suppression studies. Activated heterologous $CD3^+/CD14^+$ cells were cocultivated with GO-MSCs or GO-Fs in 10:1, 20:1, 40:1 T-cell to GO-MSC/-F ratios or were left without GO-MSCs/-Fs (w/o). Carboxyfluorescein diacetate succinimidyl ester dilution in labeled T cells was analyzed by flow cytometry at day 7. (**A**) Illustration of a representative experiment. Histograms show changes in cell number of 10 successive T-cell generations from *right* (generation 1) to *left* (generation 10) in different colors. Each peak represents one T-cell generation. (**B**) Suppression (%) of T-cell proliferation is shown as an average from three independent experiments. Inhibition of T-cell proliferation by GO-MSCs and -Fs is shown as % suppression of the proliferation of T cells without GO-MSC/GO-F.

MSCs and GO-Fs were stimulated to different degrees in terms of proliferation, hyaluronan production, and adipogenic/myogenic differentiation and may differently contribute to pathologic volume enlargement of the orbit in GO. Beyond that, it is completely unknown whether osteocytic, chondrocytic, or neuronal differentiation pathways could be involved in GO. Hence comparative studies including MSCs/Fs derived from retrobulbar tissue of control healthy persons are needed to fully elucidate the role of the fat-derived stem cell population for tissue remodeling and expansion in GO.

An emerging body of evidence shows that in addition to their regenerative properties, MSCs also possess broad immunoregulatory abilities.[10] Recent studies have shown that MSCs can influence both the adaptive and the innate immune cells. Because MSCs release proinflammatory as well as immunosuppressive effects, they are considered to act as sensors and switchers of inflammation.[30] As GO-Fs are recognized as potent regulators of immune cell recruitment and activation,[31,32] the GO-MSC subtype may represent a thus far underestimated player in local immune regulation. To evaluate the potential role of GO-MSCs in orbital immunology, we tested key features of immunologic cell–cell interactions such as suppression of T-cell proliferation and secretion of inflammatory cytokines. When compared to GO-Fs, the GO-MSCs were more effective in suppression of T-cell proliferation (Fig. 4) and constitutively secreted higher amounts of IL-6 (Fig. 5). A current model of MSC–T-cell/monocyte interaction suggests that constitutively produced IL-6 by MSCs balances the polarization of monocytes into anti-inflammatory M2 macrophages and favors the emergence of regulatory T cells—while in the absence of IL-6, MSCs induce monocyte polarization into proinflammatory M1 macrophages and promote T-cell activation.[30] In accordance with this model, we propose that GO-MSCs represent an anti-inflammatory MSC subtype that could dampen inflammation. Regarding this, it has been shown that topical administration of allogenic orbital fat-derived stem cells inhibits inflammation during cornea injury.[19] Investigation of the immunosuppressive potential of GO-MSCs and control MSCs obtained from healthy persons in response to an inflammatory microenvironment (as occurs in the diseased orbit) could lead to a promising therapeutic approach for GO.

In summary, our data show for the first time the presence of mesenchymal progenitor cells (GO-MSCs) in the retrobulbar fat tissue of GO patients. Importantly, we discovered that GO-Fs share all biological characteristics with orbital MSCs. However, differentiation potential, T-cell suppression, and cytokine release suggest some distinct functional differences between

Investigative Ophthalmology & Visual Science

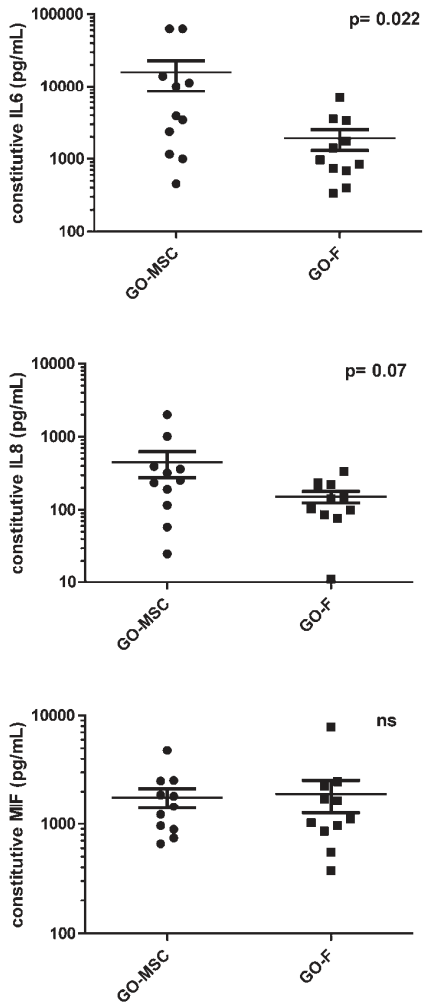

Figure 5. Analysis of cytokine secretion. Constitutive secretion of IL-6, IL-8, and MIF of GO-MSCs and GO-Fs (third passages) obtained from the same 11 GO patients was quantified as described in Methods.

GO-Fs and GO-MSCs. Further studies including orbital MSCs isolated from healthy control persons are needed to better define mesenchymal progenitor cell populations and their relative contribution to disease pathology in GO.

Acknowledgments

The authors thank all patients for their participation in this study.

Supported by Deutsche Forschungsgemeinschaft (DFG) Grants BE 3177/2-1 (UB-P), EC 379/3-1 (AE), BR 2278/3-1 (SB), a grant from Bartling-Stiftung (SB, SL), and an Interne Forschungsförderung Essen (IFORES) grant (KH).

Disclosure: **S. Brandau**, None; **K. Bruderek**, None; **K. Hestermann**, None; **G.-E. Görtz**, None; **M. Horstmann**, None; **S. Mattheis**, None; **S. Lang**, None; **A. Eckstein**, None; **U. Berchner-Pfannschmidt**, None

References

1. Bahn RS. Graves' ophthalmopathy. *New Engl J Med*. 2010;362:726–738.
2. Piantanida E, Tanda ML, Lai A, Sassi L, Bartalena L. Prevalence and natural history of Graves' orbitopathy in the XXI century. *J Endocrinol Invest*. 2013;36:444–449.
3. Eckstein AK, Johnson KT, Thanos M, Esser J, Ludgate M. Current insights into the pathogenesis of Graves' orbitopathy. *Horm Metab Res*. 2009;41:456–464.
4. Eckstein A, Esser J, Mann K, Schott M. Clinical value of TSH receptor antibodies measurement in patients with Graves' orbitopathy. *Pediatr Endocrinol Rev*. 2010;7(suppl 2):198–203.
5. Koumas L, Smith TJ, Phipps RP. Fibroblast subsets in the human orbit: Thy-1+ and Thy-1- subpopulations exhibit distinct phenotypes. *Eur J Immunol*. 2002;32:477–485.
6. Douglas RS, Afifiyan NF, Hwang CJ, et al. Increased generation of fibrocytes in thyroid-associated ophthalmopathy. *J Clin Endocrinol Metab*. 2010;95:430–438.
7. Meyer zu Horste M, Stroher E, Berchner-Pfannschmidt U, et al. A novel mechanism involved in the pathogenesis of Graves ophthalmopathy (GO): clathrin is a possible targeting molecule for inhibiting local immune response in the orbit. *J Clin Endocrinol Metab*. 2011;96:E1727–E1736.
8. Koumas L, Smith TJ, Feldon S, Blumberg N, Phipps RP. Thy-1 expression in human fibroblast subsets defines myofibroblastic or lipofibroblastic phenotypes. *Am J Pathol*. 2003;163:1291–1300.
9. Le Blanc K, Mougiakakos D. Multipotent mesenchymal stromal cells and the innate immune system. *Nat Rev Immunol*. 2012;12:383–396.
10. Uccelli A, Moretta L, Pistoia V. Mesenchymal stem cells in health and disease. *Nat Rev Immunol*. 2008;8:726–736.
11. Brandau S, Jakob M, Hemeda H, et al. Tissue-resident mesenchymal stem cells attract peripheral blood neutrophils and enhance their inflammatory activity in response to microbial challenge. *J Leukoc Biol*. 2010;88:1005–1015.
12. Dumitru CA, Hemeda H, Jakob M, Lang S, Brandau S. Stimulation of mesenchymal stromal cells (MSCs) via TLR3 reveals a novel mechanism of autocrine priming. *FASEB J*. 2014;28:856–866.
13. Korn BS, Kikkawa DO, Hicok KC. Identification and characterization of adult stem cells from human orbital adipose tissue. *Ophthal Plast Reconstr Surg*. 2009;25:27–32.
14. Martins TM, dc Paula AC, Gomcs DA, Gocs AM. Alkalinc phosphatase expression/activity and multilineage differentiation potential are the differences between fibroblasts and orbital fat-derived stem cells - a study in animal serum-free culture conditions. *Stem Cell Rev*. 2014;10:697–711.
15. Bahn RS, Gorman CA, Woloschak GE, David CS, Johnson PM, Johnson CM. Human retroocular fibroblasts in vitro: a model for the study of Graves' ophthalmopathy. *J Clin Endocrinol Metab*. 1987;65:665–670.
16. Estes BT, Diekman BO, Gimble JM, Guilak F. Isolation of adipose-derived stem cells and their induction to a chondrogenic phenotype. *Nat Protoc*. 2010;5:1294–1311.
17. Kim NR, Kang SK, Ahn HH, et al. Discovery of a new and efficient small molecule for neuronal differentiation from mesenchymal stem cell. *J Med Chem*. 2009;52:7931–7933.
18. Dominici M, Le Blanc K, Mueller I, et al. Minimal criteria for defining multipotent mesenchymal stromal cells. The International Society for Cellular Therapy position statement. *Cytotherapy*. 2006;8:315–317.
19. Lin KJ, Loi MX, Lien GS, et al. Topical administration of orbital fat-derived stem cells promotes corneal tissue regeneration. *Stem Cell Res Ther*. 2013;4:72.
20. Chen SY, Mahabole M, Horesh E, Wester S, Goldberg JL, Tseng SC. Isolation and characterization of mesenchymal progenitor cells from human orbital adipose tissue. *Invest Ophthalmol Vis Sci*. 2014;55:4842–4852.

21. Valyasevi RW, Erickson DZ, Harteneck DA, et al. Differentiation of human orbital preadipocyte fibroblasts induces expression of functional thyrotropin receptor. *J Clin Endocrinol Metab*. 1999;84:2557–2562.
22. Tang QQ, Lane MD. Adipogenesis: from stem cell to adipocyte. *Annu Rev Biochem*. 2012;81:715–736.
23. Safford KM, Rice HE. Stem cell therapy for neurologic disorders: therapeutic potential of adipose-derived stem cells. *Curr Drug Targets*. 2005;6:57–62.
24. Kazim M, Goldberg RA, Smith TJ. Insights into the pathogenesis of thyroid-associated orbitopathy: evolving rationale for therapy. *Arch Ophthalmol*. 2002;120:380–386.
25. Gage PJ, Rhoades W, Prucka SK, Hjalt T. Fate maps of neural crest and mesoderm in the mammalian eye. *Invest Ophthalmol Vis Sci*. 2005;46:4200–4208.
26. Billon N, Iannarelli P, Monteiro MC, et al. The generation of adipocytes by the neural crest. *Development*. 2007;134:2283–2292.
27. Sowa Y, Imura T, Numajiri T, et al. Adipose stromal cells contain phenotypically distinct adipogenic progenitors derived from neural crest. *PLoS One*. 2013;8:e84206.
28. Locke M, Windsor J, Dunbar PR. Human adipose-derived stem cells: isolation, characterization and applications in surgery. *ANZ J Surg*. 2009;79:235–244.
29. Li H, Fitchett C, Kozdon K, et al. Independent adipogenic and contractile properties of fibroblasts in Graves' orbitopathy: an in vitro model for the evaluation of treatments. *PLoS One*. 2014;9:e95586.
30. Bernardo ME, Fibbe WE. Mesenchymal stromal cells: sensors and switchers of inflammation. *Cell Stem Cell*. 2013;13:392–402.
31. Cao HJ, Wang HS, Zhang Y, Lin HY, Phipps RP, Smith TJ. Activation of human orbital fibroblasts through CD40 engagement results in a dramatic induction of hyaluronan synthesis and prostaglandin endoperoxide H synthase-2 expression. Insights into potential pathogenic mechanisms of thyroid-associated ophthalmopathy. *J Biol Chem*. 1998;273:29615–29625.
32. Hwang CJ, Afifiyan N, Sand D, et al. Orbital fibroblasts from patients with thyroid-associated ophthalmopathy overexpress CD40: CD154 hyperinduces IL-6, IL-8, and MCP-1. *Invest Ophthalmol Vis Sci*. 2009;50:2262–2268.

Investigative Ophthalmology & Visual Science

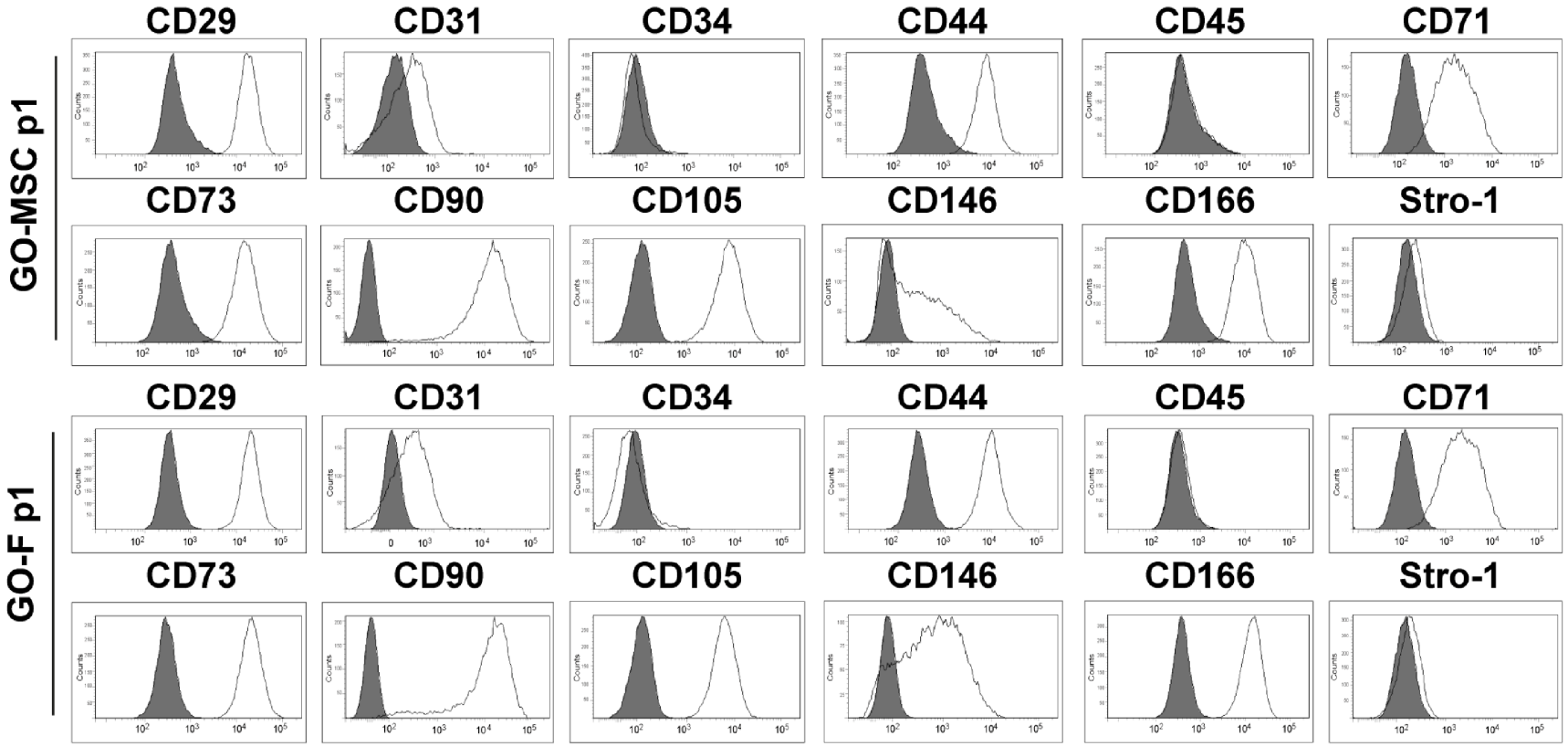

Supplementary FIGURE S1. Comparative immunophenotypic characterization. Multiple surface antigens of GO-MSCs and GO-Fs isolated simultaneously from orbital fat-tissue of 9 GO patients (first-third passages) were analyzed using multi-parameter flow cytometry based on multi-color staining. Data are shown as an

overlay histogram: isotype control (gray) and specific cell surface markers (white). A representative surface marker set of donor-matched GO-MSCs and GO-Fs in the first passage (p1) is shown.

Publication 2

Hypoxia-dependent HIF-1 activation impacts on tissue remodeling in Graves' ophthalmopathy- Implications for smoking.

Görtz G-E, Horstmann M, Anol B, Delos Reyes B, Fandrey J, Eckstein A, Berchner-Pfannschmidt U.

J Clin Endocrinol Metab. 2016, 101(12):4834-4842

Contribution

In this study I isolated OF from orbital fat tissue of GO patients and control persons. I performed cell culture experiments under hypoxia and analyzed HIF-1α and HIF-1 target gene expression by using western-blot, immunofluorescence microscopy, as well as real time PCR and ELISA like in Fig. 1-3, 5 and 6. I was involved in immuno-histology and microscopy of orbital biopsies and conducted quantification of CD31 staining (Fig. 4, supplementary Fig. 1). I established adipogenesis assay and quantified adipogenic differentiation of cells in response to hypoxia, TSH and HIF-1 inhibitor (Fig. 5, supplementary Fig. 2). I designed experiments and was centrally involved in discussing and analyzing data. I contributed to writing of abstract, introduction, methods, results and discussion of the publication.

ORIGINAL ARTICLE

Hypoxia-Dependent HIF-1 Activation Impacts on Tissue Remodeling in Graves' Ophthalmopathy—Implications for Smoking

Gina-Eva Görtz, Mareike Horstmann, Barbara Aniol, Buena Delos Reyes, Joachim Fandrey, Anja Eckstein, and Utta Berchner-Pfannschmidt

Molecular Ophthalmology (G.-E.G., M.H., B.A., A.E., U.B.-P.), Department of Ophthalmology, University of Duisburg-Essen, 45147 Essen, Germany; and Institute of Physiology (B.D.R., J.F.), University of Duisburg-Essen, 45147 Essen, Germany

Context: In Graves' ophthalmopathy (GO), inflammation with tissue expansion in a closed compartment like the bony orbit and smoking may cause tissue hypoxia.

Objectives: In this study, we investigated whether hypoxia-inducible factor-1 (HIF-1) action impacts on tissue remodeling in GO with the aim to identify possible new therapeutic targets.

Design/Setting/Participants: Orbital fibroblasts (OFs) were derived from GO patients and control (Ctrl) persons. We analyzed HIF-1α levels in response to hypoxia and cigarette smoke extract, as well as HIF-1-dependent vascular endothelial growth factor (VEGF) release and adipogenic differentiation, by using HIF-1α small interfering RNA, or HIF-1 inhibitor BAY 87–2243.

Main Outcome Measures: Western blot, real-time PCR, ELISA, and immunohistochemistry were used to analyze HIF-1α, VEGF, CD31, and adiponectin. Adipogenic differentiation was measured with Nile red assay.

Results: Higher HIF-1α levels in OFs were correlated with the clinical activity score of GO patients. Cigarette smoke extract elevated HIF-1α levels. HIF-1-dependent VEGF secretion was enhanced in GO-OF compared to Ctrl-OF, and as an in vivo consequence, we found a higher vessel density in GO tissue than in Ctrl tissue. Hypoxia strongly stimulated HIF-1-dependent adipogenesis and adiponectin release of GO-OF and enhanced TSH receptor-mediated adipogenesis.

Conclusions: Hypoxia impacts on tissue remodeling in GO by stimulating angiogenesis and adipogenesis through activation of HIF-1-dependent pathways in OFs. Our results offer a molecular mechanism for the detrimental influence of smoking on GO and an explanation as to why decompression can improve the outcome of patients. Drug-targeted inhibition of HIF-1/VEGF may provide a therapeutic option to control tissue expansion in GO. (***J Clin Endocrinol Metab*** **101: 4834–4842, 2016)**

Graves' disease of the thyroid is a form of hyperthyroidism caused by autoantibodies that are mainly directed against the TSH receptor (TSHR). In the context of the disease Graves' ophthalmopathy (GO), an inflammatory eye disease can occur (1). Typical characteristics of GO are inflammation, remodeling, and expansion of the retroocular connective tissue. Because of the limited space within the bony orbit, these increases in volume can lead to proptosis and, in severe cases, to exposure keratopathy and optic nerve compression (2). The pathophysiological mechanisms for the development of GO are complex and remain to be clarified. Local orbital fibroblasts (OFs) are

ISSN Print 0021-972X ISSN Online 1945-7197
Printed in USA

Received February 1, 2016. Accepted September 2, 2016.
First Published Online September 9, 2016

Abbreviations: CAS, clinical activity score; CSE, cigarette smoke extract; Ctrl, control; GLUT1, glucose transporter 1; GO, Graves' ophthalmopathy; HIF-1, hypoxia-inducible factor-1; OF, orbital fibroblast; siRNA, small interfering RNA; TSHR, TSH receptor; VEGF, vascular endothelial growth factor.

doi: 10.1210/jc.2016-1279 press.endocrine.org/journal/jcem 4835

predominantly involved in inflammation and tissue remodeling in GO and are regarded as the central cell type in the pathology of GO. OFs are activated in response to autoantibodies, cytokines, and growth factors as well as through interaction with immune cells. Once activated, OFs react with excessive proliferation and adipogenesis, as well as the production of hydrophilic hyaluronic acid and proinflammatory cytokines (3). An expansion of the OF compartment is an essential element in the mass-to-volume mismatch typical of GO.

In humans, oxygen concentration varies between 2 and 14% in different tissues depending on the perfusion (such as in lung, kidneys, and heart). Importantly, oxygen concentrations are typically 5% or lower in adipose tissue (4). Furthermore, microenvironment conditions found in inflamed tissues are characterized by metabolically highly active inflammatory cells, resulting in low levels of oxygen and glucose. Consequently, low oxygen tension could be an important component of the OF microenvironment during GO. When orbital fat growth outpaces vascularization, hypoxic areas will develop in the fat because the oxygen diffusion distances between the capillaries and the cells become too long (4). Moreover, smoking is a strong risk factor for development of GO (5, 6), and hypoxia induced by smoking was implicated as a contributor to the adverse effects of smoking (7, 8). Indeed, in vitro studies have shown that severely hypoxic OFs increased the production of glycosaminoglycan and stimulated adipogenesis (7, 8), both of which may contribute differently to tissue enlargement in smoker with GO (9). However, the underlying molecular mechanisms of hypoxia involved in GO are unknown.

Cells respond to hypoxia largely by adapting gene expression through the activation of hypoxia-inducible factor-1 (HIF-1). HIF-1 has been recognized as the "master regulator of oxygen homeostasis" both in physiology and pathophysiology (10). HIF-1 is composed of an oxygen-regulated α-subunit and a constitutively expressed nuclear β-subunit. Two of the tissue-specific isoforms of the hypoxia-inducible α subunit, HIF-1α and HIF-2α, can dimerize with HIF-1β to form the active HIF-1/-2 complex. Under well-oxygenated conditions (normoxia), the α-subunit is not detectable because it is post-translationally hydroxylated by oxygen-dependent prolyl hydroxylases (PHD1–3), which instantaneously leads to ubiquitin-proteasome-dependent degradation of the α-subunit (11). An oxygen-dependent asparagine hydroxylase (factor inhibiting HIF-1) limits the activity of the HIF complexes in normoxia (12). In contrast, under hypoxia the oxygen-dependent modifications of HIF-1/2α are inhibited due to the limited oxygen availability, and HIF-1α and/or HIF-2α accumulate in the nucleus to form the active HIF-1 or HIF-2 transcription factors.

HIF-1 controls the hypoxia-inducible expression of angiogenic factors such as vascular endothelial growth factor (VEGF) and coordinates tissue vascularization during cell growth and tissue remodeling (13). For metabolic adaptation to hypoxia, HIF-1 increases the expression of glucose transporters (eg, glucose transporter 1 [GLUT1]) and glycolytic enzymes for anaerobic ATP generation; moreover, HIF-1 induces regulatory proteins that reduce oxygen consumption under hypoxia. Many other HIF-1-dependent genes are involved in a wide range of cellular functions, including cell proliferation, matrix formation, adipogenesis, and inflammation (14). For many tumors, the detection of elevated HIF-1 levels is associated with a highly malignant phenotype, and HIF is understood to be an independent prognostic factor in many malignancies. Thus, understanding the regulation of HIF-1 activation in the orbital tissue might be fundamental to GO, and modulating HIF-1 activation in OFs could be a novel therapeutic avenue for GO treatment. Therefore, we investigated whether HIF-1-dependent gene expression is affected in the OFs of GO patients compared to healthy control persons. We demonstrate that the hypoxic response is induced in GO-derived OF, leading to increased expression of HIF-1 targets VEGF and GLUT1. VEGF secretion by GO-derived OFs can contribute to increasing vascularization during adipose tissue expansion caused by hypoxia- and/or smoking-induced HIF-1 activation.

Patients and Methods

Patients and cell cultures

During orbital decompression procedures, surgical tissue explants of orbital adipose tissue were obtained from 15 patients with severe GO, as classified by the European Group on Graves' Orbitopathy (6). The mean NOSPECS classification was 9.7 (range, 5–14), and the mean clinical activity score (CAS) was 5.7 (range, 1–10). Most of the experiments were performed with tissue samples from active patients, except the correlation study. The mean age of the patients at the time of surgery was 54.3 years; 80% of the patients were female and 80% were smokers. Orbital fat biopsies obtained during orbital surgery for other reasons (conditions not affecting the soft tissues of the orbita, noninflammatory conditions, blepharoplasty) were obtained from seven healthy control persons (mean age, 59.3 years; 71% female; 27% smokers). The study was approved by the institutional ethics committees, and all study participants gave written informed consent.

OFs were obtained from an orbital fat biopsy with an outgrow protocol and culture conditions as described before (15). All experiments were performed with OFs between passages 2 and 10 after culture initiation. The renal clear carcinoma cell line ccRCC 786-O served as HIF-2α-positive control cells (16). For cell culture experiments, cells were exposed to normoxia (5%

CO_2 in air); or placed in a hypoxic incubator with 3% O_2, 92% N_2, and 5% CO_2 at 37°C (Heraeus incubator); or placed in a hypoxic workstation (Invivo2 400; Ruskinn) for variable periods of time. Cigarette smoke extract (CSE) was produced as described before (6). To generate control extract, air was led through the medium instead of cigarette smoke.

Immunohistology and immunofluorescence

Sections (1 μm) of paraffinized fat biopsies were deparaffinized and rehydrated. Antigen retrieval was performed by boiling the sections in low-pH citrate buffer for 15 minutes. The sections were incubated overnight at 4°C with mouse anti-CD31 (PECAM-1) antibody (diluted 1:25; Cell Signaling) or mouse anti-HIF-1α antibody (diluted 1:50; Transduction Laboratories). The biotin-coupled secondary antibody (biotin goat-antimouse, 1: 10 000; Santa Cruz Biotech Inc.) was visualized using commercially available ABC and DAB Kits (Vectastain ABC/DA; Vector Labs). Endogenous peroxidase activity was inhibited with 3% H_2O_2. Slides were counterstained with hematoxylin. HIF-1α-positive cells or CD31-positive vessels were imaged using an Olympus BX51 microscope. CD31-positive vessels were counted in sections from fat biopsies of 18 healthy control persons and 21 GO patients.

For detection of HIF-1α in OF, immunofluorescence microscopy was conducted as described before (17). Cells were grown on coverslips overnight and stained with a mouse anti-HIF-1α antibody (diluted 1:250; Transduction Laboratories) and a secondary antibody an Alexa-568 conjugated goat antimouse IgG (diluted 1:400; Molecular Probes).

Western-blot analysis

OFs were grown overnight in six-well dishes at a density of 3×10^5 cells per dish. Whole-cell lysate was prepared, and 70 μg protein was subjected to Western-blot analysis as described before (17). As primary antibodies, a mouse anti-HIF-1α (diluted 1:750; Transduction Laboratories), a rabbit polyclonal HIF-2α (diluted 1:1000; Novus Biologicals), a rabbit polyclonal adiponectin antibody (diluted 1:2000; Abcam), a mouse monoclonal anti-α tubulin (diluted 1:1000; Santa Cruz Biotechnology), and a mouse monoclonal β-actin (diluted 1:10 000; MP Biomedicals) were used. Western blots were reprobed with antitubulin or antiactin antibodies as a loading control. Quantification of Western-blot signals was achieved with Image J software. HIF-1α signals were normalized to tubulin or actin signals and expressed as relative HIF-1α protein.

Real-time PCR

Total RNA was extracted using the guanidinium isothiocyanate method from six-well dishes as described before (17). Total RNA (1 μg) was reverse transcribed, and HIF-1α, VEGF, GLUT1 cDNAs and the cDNA of the housekeeping gene β-actin was quantified by real-time PCR as described (17). The primers used were as follows: HIF-1α— forward, GCT GGC CCC AGC CGC TGG AG; and reverse, GAG TGC AGG GTC AGC ACT AC; GLUT1—forward, GGG CAT GTG CTT CCA GTA TG; and reverse, GCG ATC TCA TCG AAG GTC CG; VEGF—forward, GCA AGA CAA GAA AAT CCC TGT GGG CC; and reverse, CCG CCT CGG CTT GTC ACA; and β-actin—forward, TCA CCC ACA CTG TGC CCA TCT ACG A; and reverse, CAG CGG AAC CGC TCA TTG CCA ATG G. The PCR amplification profile was as follows: 10 minutes at 95°C, followed by 30 cycles of 15 seconds at 95°C and 1 minute at 60°C. Ten-fold dilutions of purified PCR products starting at 1 pg to 0.1 fg were used as standards. The quantified cDNA were normalized to cDNA of the β-actin and expressed as normalized mRNA level.

RNA interference

For small interfering RNA (siRNA) experiments, OFs at 30–50% confluence were transfected with siRNA (final concentration, 20 nM) using Oligofectamine (Invitrogen) according to the manufacturer's instructions. siRNA designed to suppress expression of HIF-1α and a siControl nontargeting siRNA were purchased from Dharmacon. After transfection, cells were grown for 24 hours and then exposed to normoxic or hypoxic atmosphere for 24 hours.

ELISA

For determination of VEGF release of OFs, 1×10^5 cells were grown for 24 hours in a 12-well plate in 500 μL medium and incubated for another 24 hours at normoxic or hypoxic conditions. VEGF protein in cell culture supernatants was measured by ELISA (R&D Systems) according to the manufacturer's recommendations.

Adipogenic differentiation

OFs were seeded at a density of 1×10^5 cells per well in 96-well black clear bottom culture plates in standard culture medium until reaching 80–90% confluence. Adipocyte differentiation medium was used as described before (18). Control cells were maintained in standard medium (15). The medium with or without 10 mU/mL bovine TSH (Sigma-Aldrich Corp.) or hypoxia-induced HIF-1 activation inhibitor BAY 87–2243 (Hycultec) (19) was exchanged every 3–4 days during a 10-day differentiation period. To analyze the accumulation of lipid droplets in the cytoplasm after differentiation, cells were stained with a Lipid Droplets Fluorescence Assay Kit (Cayman Chemicals). Fluorescence intensity of Nile red-stained lipid droplets was read with a fluorescence plate reader (FLUOstar Omega; BMG LABTECH) using an excitation at 485 nm and an emission at 520 nm. To analyze adiponectin secretion, 100 μL of the supernatants was precipitated, and the pellets were dissolved in 100 μL extraction buffer. Protein concentration was determined, and 30 μg was subjected to Western-blot analysis.

Statistical analysis

Statistical analysis was performed with two-tailed Student's *t* tests with a confidence level greater than 95%. To analyze the difference in the hypoxic response of control (Ctrl)-OF vs GO-OF, a grouped analysis with two-way ANOVA was performed. Data are presented as arithmetic means ± SEM (see figures for specific information on statistical significance).

Results

HIF-1α expression is induced in OFs derived from GO patients

To investigate the general hypoxic response of GO-derived OFs in comparison to Ctrl-OF, we investigated the

doi: 10.1210/jc.2016-1279 press.endocrine.org/journal/jcem 4837

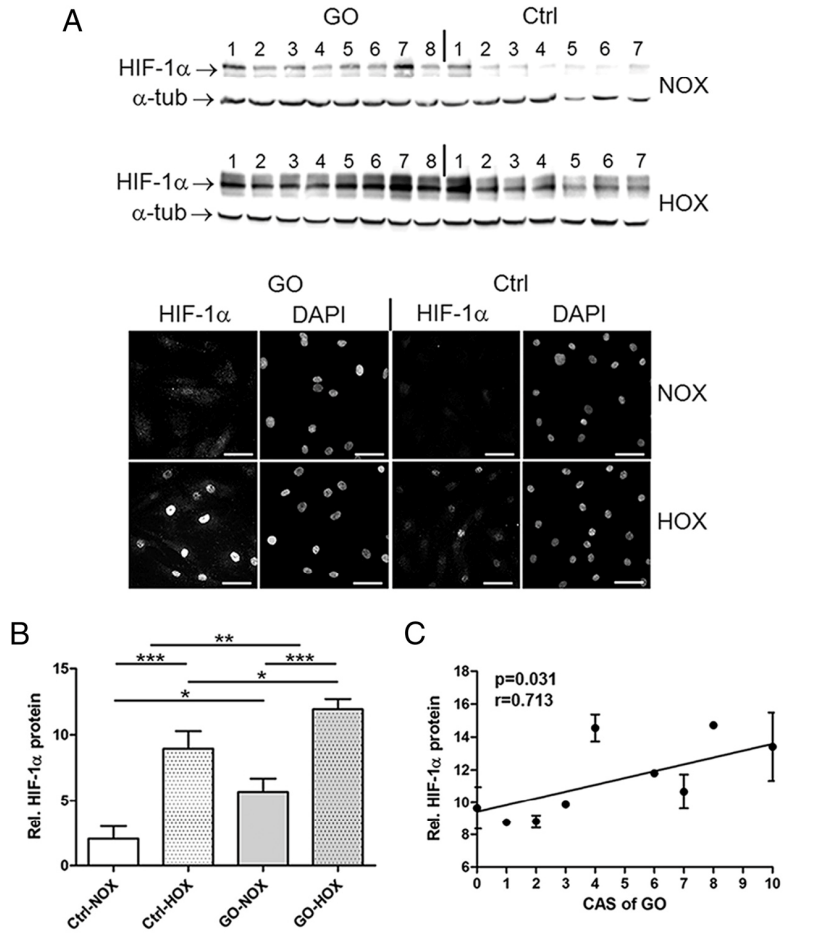

Figure 1. GO-derived OFs express more HIF-1α under normoxia and hypoxia than Ctrl-OF. OFs were subjected to normoxic (NOX) or hypoxic (HOX) conditions for 24 hours. A, Whole-cell lysates were obtained and subjected to Western-blot analysis for detection of HIF-1α and α-tubulin (α-tub) as a loading Ctrl. Representative Western blots are shown. In addition, OFs were grown on coverslips, and HIF-1α was detected by immunofluorescence microscopy. Cell nuclei were counterstained with DAPI. Images were captured at 200× magnification and shown in gray level. Bars represent 100 μm. Representative images are shown. B, Western blots shown in panel A are representative for at least three separate experiments. Western-blot signals of 15 GO-OF and seven Ctrl-OF were quantified by densitometry of immunoblots. The HIF-1α signal was normalized to the α-tubulin signal and expressed as relative HIF-1α protein. C, Relationship between CAS (1–10) of GO patients and hypoxia-induced HIF-1α ($P = .03$; r = 0.71). *$P \leq .05$; **$P < .01$; ***$P < .001$.

accumulation of the oxygen-labile HIF-1α under normoxic and hypoxic conditions by Western-blot analysis and immunofluorescence microscopy (Figure 1). In comparison to Ctrl-OF, the GO-derived OFs showed a higher basic level of HIF-1α under normoxia and a stronger induction of HIF-1α protein in response to hypoxia. Immunofluorescence microscopy of OFs revealed that HIF-1α was translocated to the cell nuclei in response to hypoxic incubation, suggesting HIF-1α in its active state. Although not all GO-derived OFs contained more HIF-1α than Ctrl-OF under the respective condition (Figure 1A), statistical analysis of Western-blot signals revealed that the observed differences in the hypoxic response between GO patients and healthy persons were significant (Figure 1B). More striking, the level of hypoxia-induced HIF-1α was positively correlated ($P < .05$) with the degree of disease activity of GO as determined by the CAS of the respective GO patients (CAS 1–10) (Figure 1C). Because the CAS reflects the level of orbital inflammation, these findings strongly suggest that hypoxic HIF-1α signaling is most likely involved in the inflammatory pathogenesis of GO.

HIF-1α mRNA expression is induced in OFs derived from GO patients

HIF-1α protein accumulation in the absence of hypoxia suggests that in addition to oxygen deprivation, other mechanisms are involved in the HIF-1α induction in OFs from GO patients. To get insight into the synthesis of HIF-1α, we analyzed HIF-1α mRNA expression by real-time PCR. We found that the HIF-1α mRNA was induced in GO-derived OFs when compared to OFs from Ctrls independently from oxygen concentration (Figure 2A). Enhanced HIF-1α mRNA expression is likely to be responsible for the observed normoxic HIF-1α basic level and the enhanced hypoxic accumulation in GO-OF (Figure 1). These findings indicate that besides hypoxia, additional signal pathways may impact on HIF-1α synthesis in GO patients.

Hypoxia-inducible gene expression is changed in OFs derived from GO patients

To test for consequences of the pronounced HIF-1 activity in OF, we analyzed the expression of HIF-1 target genes GLUT1 and VEGF using quantitative real-time PCR. GLUT1 and VEGF were induced by hypoxia at different degrees (Figure 2, B and C). Under normoxia, HIF-1 target gene expression was not significantly different in GO-OF compared to Ctrl-OF, whereas hypoxic induction of VEGF (Figure 2B) and GLUT1 (Figure 2C) was significantly higher in GO-OF than in controls. The data indicate that hypoxia-induced gene expression is substantially affected in GO-OF, which could have consequences for metabolism as well as angiogenesis.

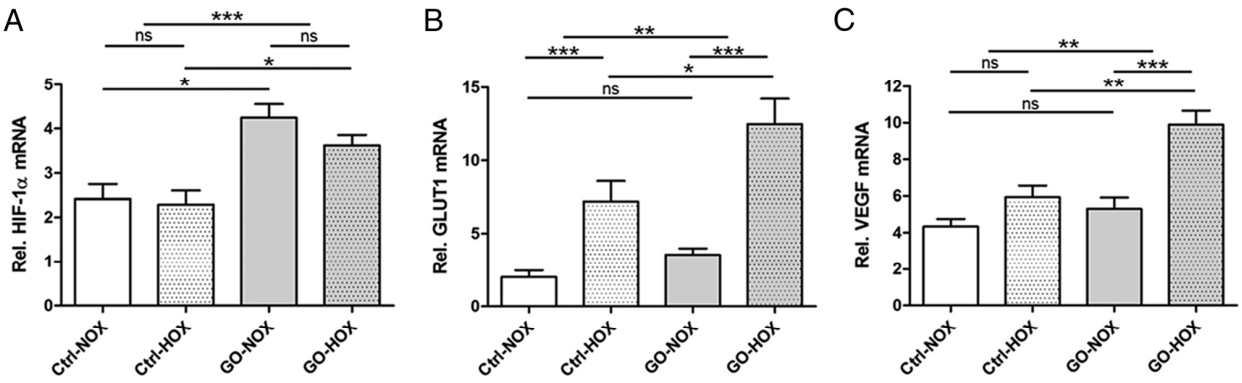

Figure 2. Expressions of HIF-1α gene and HIF-1 target genes were changed in GO-derived OFs. OFs from six GO patients and six healthy Ctrl persons were incubated under normoxia (NOX) or hypoxia (HOX) for 24 hours. Total mRNA was extracted and reversed transcribed. Real-time PCR was performed for HIF-1α cDNA (A), GLUT1 cDNA (B), and VEGF cDNA (C). The quantified cDNAs were normalized to the cDNA of β-actin and expressed as relative levels of HIF-1α, GLUT1, or VEGF mRNA. All data represent the mean ± SEM of experiments done in triplicate. *$P \leq .05$; **$P < .01$; ***$P < .001$; ns = $P > .5$. ns, not significant.

VEGF protein release is increased in GO-derived OFs under hypoxia

To analyze for HIF-1-dependent gene expression and the potential role of OFs for angiogenesis, we analyzed VEGF secretion by ELISA. VEGF protein in the culture supernatant was significantly increased under hypoxic conditions in GO-OFs compared to controls (Figure 3A). To prove that increased HIF-1α was responsible for the higher VEGF release under hypoxia, we suppressed HIF-1α expression in OFs by using the siRNA approach. Hypoxic VEGF release was blocked to basic levels after siRNA treatment (Figure 3B), indicating that higher HIF-1α was responsible for the induction of VEGF mRNA and released protein. Western-blot analysis of siRNA-treated OFs confirmed that HIF-1α was successfully suppressed by HIF-1α-specific siRNA treatment. Of note, the increased hypoxic VEGF response was solely due to HIF-1α because OFs did not express HIF-2α; the renal cancer cell line 786-O served as a positive control (16) (Figure 3C). Thus, HIF-1α-dependent VEGF secretion can contribute to increased angiogenesis in the retrobulbar fat of GO patients.

Vascularization is increased in orbital tissue from GO patients

To analyze vascularization of orbital fat biopsies from GO patients and healthy controls, CD31 was used as an endothelial marker protein. When the orbital tissues were immunohistochemically stained for CD31, we found more positively stained vessels and single cells (endothelial cells or immune cells like macrophages and T cells) in GO fat biopsies (Figure 4A and Supplemental Figure 1). In addition, CD31 staining was much stronger in the wall of vessels of GO fat than weak CD31 staining of Ctrl vessels. The results suggest that neovascularization is increased in orbital tissue most likely as an adaptive mechanism toward hypoxia during enlargement of orbital tissue volume in GO. In support of this, we identified HIF-1α-positive,

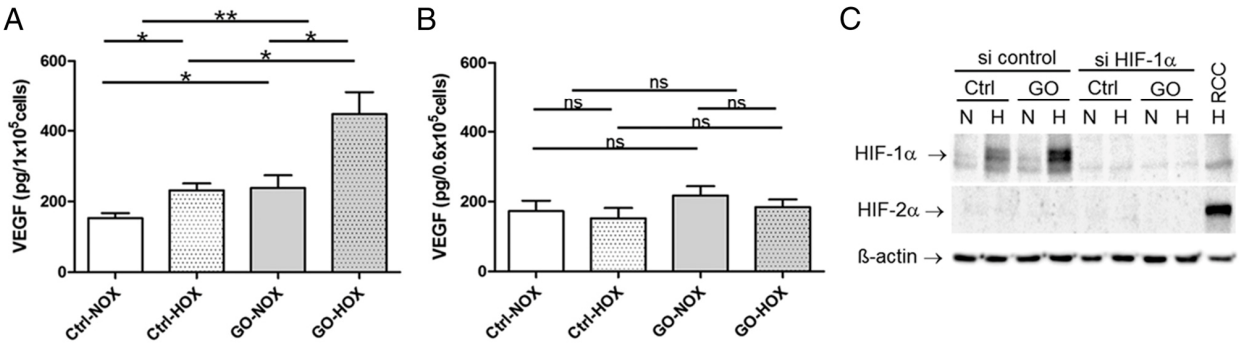

Figure 3. Pronounced hypoxia-induced VEGF secretion is HIF-1α dependent. OFs from six GO patients and six healthy Ctrl persons were incubated in duplicate under normoxia (NOX) or hypoxia (HOX) for 24 hours. A, VEGF secretion was measured in supernatants in response to normoxic and hypoxic incubation. B, VEGF secretion was measured in supernatants after knock-down of HIF-1α expression using HIF-1α-specific siRNA. Data represent the mean ± SEM of experiments representative for at least two separate experiments. C, Ctrl-OF and GO-OF were transfected with HIF-1α-specific siRNA or control siRNA. HIF-1α, HIF-2α, and β-actin levels were analyzed in Ctrl-OF and GO-OF and in a HIF-2α-positive renal carcinoma cell line under normoxia (N) and hypoxia (H). Western blot shown is representative for at least two separate experiments. *$P \leq .05$; **$P < .01$; ns = $P > .5$. ns, not significant.

doi: 10.1210/jc.2016-1279 press.endocrine.org/journal/jcem 4839

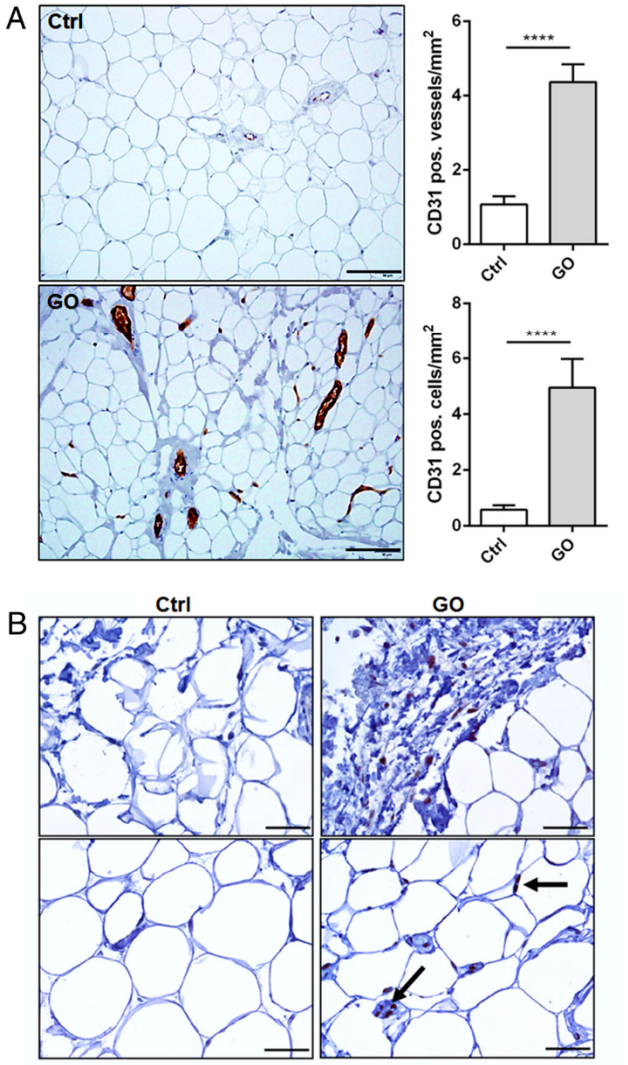

Figure 4. Vascularization is increased in fat biopsies from GO patients. Surgical tissue explants of orbital adipose tissue were obtained from 18 healthy Ctrl persons (mean age, 60 years; 83% female; 26% smokers) and 21 patients with severe GO (mean NOSPECS, 9.4; mean CAS, 4.7; mean age, 50 years; 67% female; 83% smokers). A, Orbital fat tissues from healthy Ctrl persons and GO patients were stained for CD31. Positive staining of CD31 (brown staining) was found in endothelial cells of vessels and in single cells. CD31-positive vessels and cells were counted separately in one section of each 18 Ctrl persons and 21 GO patients. Numbers of vessels and cells were normalized to total area of the sections (mean total section area: Ctrl, 22.02 mm^2; GO, 29.02 mm^2). Images were captured at 200× magnification. Bars represent 100 μm. Representative images are shown. B, Orbital fat tissues from healthy Ctrl persons and GO patients were stained for HIF-1α. Positive staining of HIF-1α (brown staining) was found in spindle-shaped fibroblast-like cells present in the connective (upper image) and fat tissue (lower image) of GO patients. HIF-1α-positive cells were localized close to adipocytes and their capillary network (marked by arrow). Images were captured at 400× magnification. Bars represent 50 μm. Representative images are shown. ****$P < .0001$.

spindle-shaped fibroblast-like cells present in the GO connective/fat tissue close to adipocytes and their capillary network (Figure 4B).

Adipogenesis of GO-OF is induced in response to hypoxia

Increased adipogenesis is a main feature of tissue volume enlargement in GO. To investigate whether hypoxia results in tissue enlargement, we investigated adipogenesis of OFs in vitro. Adipogenesis of GO-OF was induced in response to hypoxia, whereas Ctrl-OF were much less responsive (Figure 5A and Supplemental Figure 2). However, additional TSHR stimulation using TSH increased adipogenesis of GO-OF and significantly induced adipogenesis of Ctrl-OF. As a further marker of adipogenesis, we investigated adiponectin release during adipogenic differentiation. Hypoxia stimulated adiponectin release of GO-OF, whereas Ctrl-OF remained unaffected (Figure 5B). To investigate whether HIF-1 activation is involved in the induction of adipogenesis in response to hypoxia, we applied HIF-1 activation inhibitor BAY 87–2243 during adipogenic differentiation of GO-OF. By using BAY 87–2243, the hypoxic induction of adipogenesis was blocked (Figure 5C). The data strongly indicate that hypoxia stimulates adipogenesis of GO-OF in an HIF-1-dependent manner.

CSE elevated HIF-1α accumulation in OFs derived from GO smokers

Because smoking adversely affects the course and severity of GO, we investigated whether HIF-1α accumulation is related to smoking. We analyzed HIF-1α induction in OFs derived from nonsmokers and smokers separately in response to CSE under hypoxic conditions (Figure 6). Induction of HIF-1α was similar in nonsmokers and smokers, indicating that hypoxia-induced HIF-1α is not related to smoking alone. In contrast, CSE elevated HIF-1α accumulation significantly in OFs derived from GO smokers (Figure 6). The data suggest that smoking can strongly impact HIF-1 pathways.

Discussion

In the present study, we studied how hypoxia-dependent and hypoxia-independent HIF-1 signaling may contribute to tissue remodeling in GO. OFs, which are recognized as key cells in tissue activity and remodeling of GO, responded more sensitively toward hypoxia than Ctrl-OF. They show an increased induction of HIF-1α (Figure 1) followed by enhanced HIF-1 transcriptional action (Figures 2, 3, and 5), which in consequence impacts on angiogenesis (Figures 3 and 4) and adipogenesis (Figure 5). Moreover, we found that smoking appears to amplify this elevated HIF-1α response (Figure 6). Interestingly, hypoxic accumulation of HIF-1α was correlated with the

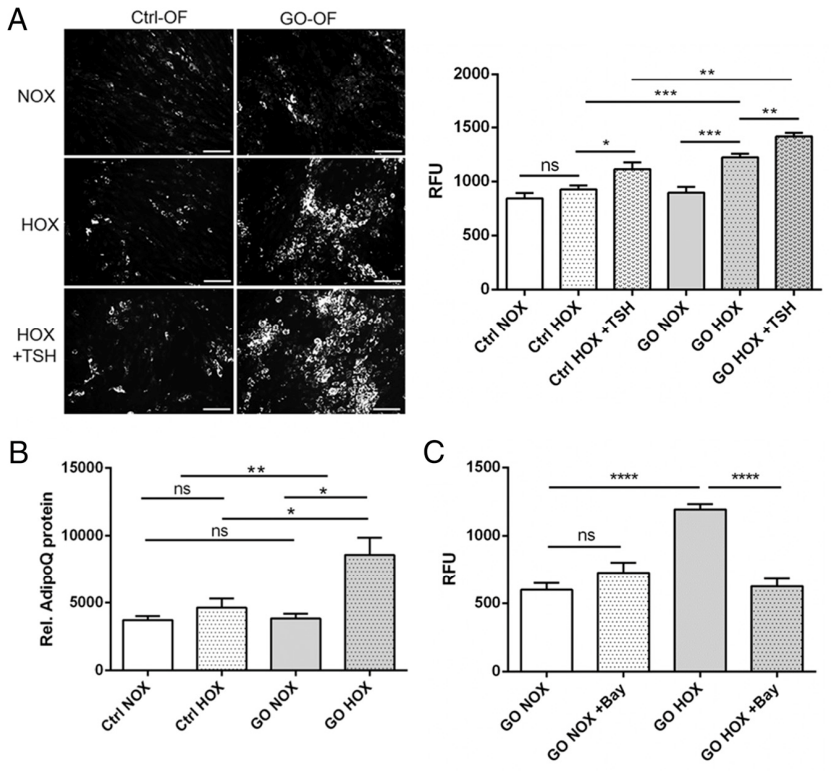

Figure 5. Hypoxia-induced adipogenic differentiation of GO-OF. To induce adipogenic differentiation, OFs from six healthy Ctrl persons and six GO patients were cultured on coverslips or in a 96-well plate with or without adipogenic differentiation media for 10 days. Cell cultivation was carried out under normoxia (NOX) and hypoxia (HOX). A, Lipid droplet accumulation in OFs was analyzed with a lipid droplet fluorescence assay after 10 days of cultivation with or without 10 mU/mL bovine TSH. Representative images were captured at 100× magnification and shown in gray level. Bars represent 200 μm. Fluorescence intensity was read with a fluorescence plate reader. Fluorescence intensity of nondifferentiated cells cultivated under normoxia or hypoxia with or without bovine TSH was subtracted from fluorescence intensity of the respective differentiated cells and expressed as relative fluorescence units (RFU). B, Adiponectin was quantified in the supernatants of the cells during adipogenic differentiation at day 4 and is given as relative AdipoQ protein. C, Lipid droplet accumulation in adipogenic differentiated OFs was analyzed after 10 days of cultivation with and without 100 nM hypoxia-induced HIF-1 activation inhibitor BAY 87–2243 (BAY). Fluorescence intensity of nondifferentiated cells cultivated under hypoxia with or without BAY 87–2243 was subtracted from fluorescence intensity of the respective differentiated cells and expressed as relative fluorescence units (RFU). All data represent the mean ± SEM of an experiment representative of at least three separate experiments. $*P \leq .05$; $**P < .01$; $***P < .001$; $****P < .0001$; ns = $P > .5$. ns, not significant.

CAS of GO patients, implicating crosstalk between hypoxia and inflammation and/or immunity. The pronounced hypoxic response of GO-derived OFs is most likely due to the enhanced basal expression of HIF-1α mRNA (Figure 2A), which might "prepare" the cells to efficiently respond to and function in a hypoxic microenvironment. We and others have previously reported that HIF-1α synthesis can be stimulated by signaling pathways activated by inflammation and immunity, particularly with NF-κB being a transcriptional activator of HIF-1α expression (20, 21). OFs respond to inflammatory mediators like IL-1β or to CD40 ligand with activation of NF-κB and MAPK pathways (22, 23), and these pathways in turn can impact on HIF-1α levels and HIF-1 activity (24). On the other hand, hypoxia can activate NF-κB (25), which could lead to an HIF-1/NF-κB-activating loop during inflammatory hypoxia. However, the role of NF-κB for pathogenesis of GO and crosstalk with HIF-1 clearly needs further investigation.

As a direct consequence of HIF-1 activation, we found an induction in VEGF expression and release by OFs (Figure 3). VEGF is a key mediator of developmental angiogenesis but is also identified as one of the critical mediators of pathological neovascularization in eye diseases, cancer formation, and chronic inflammatory disorders such as rheumatoid arthritis, psoriasis, and periodontitis (26, 27). Indeed, we found CD31-positive vessels substantially increased in GO-derived fat/connective tissue, indicating that neovascularization had occurred during adipose tissue development. This could be the result of an adaption toward hypoxia because we could identify HIF-1α-positive cells in connective/fat tissues of GO patients (Figure 4). In this respect, it is of interest that the application of the HIF-1 inhibitor YC-1 reduced VEGF expression, decreased vessel immunoreactivity for CD31, and reduced vessel density in the retina (28). Provided that adipose tissue enlargement in GO requires continuous remodeling of the vasculature, targeting of HIF-1/VEGF could be a potential therapeutic option in GO.

Increased adipose tissue volume in GO is due to de novo adipogenesis maintained by adipogenic differentiation of OFs, which are therefore also described as preadipocytes (29) or adipose tissue-derived mesenchymal stromal/stem cells (30). Adipogenic differentiation of OFs is stimulated in vitro either by activating anti-TSHR antibodies and TSH or various growth factors and cytokines (18, 31–33). However, in this study we show that adipogenic differentiation is induced in response to hypoxia in an HIF-1-dependent manner in GO-derived OFs, whereas Ctrl-OF remained less responsive (Figure 5). Likewise, in response to hypoxia, GO-OF released adiponectin during adipo-

doi: 10.1210/jc.2016-1279 press.endocrine.org/journal/jcem 4841

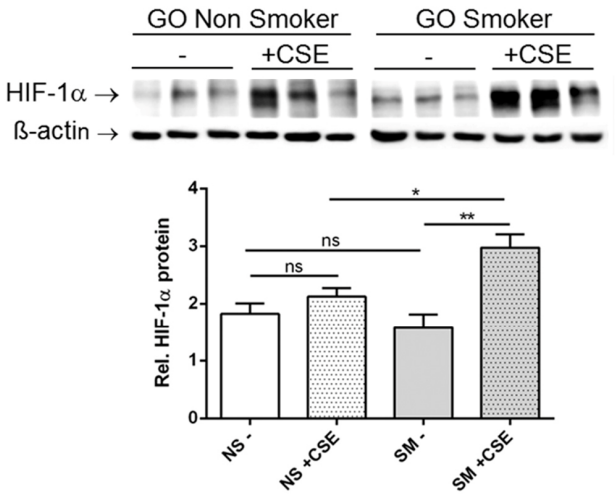

Figure 6. CSE elevates hypoxia-induced HIF-1α accumulation in OFs from GO smokers. OFs were obtained from surgical tissue explants of six GO nonsmokers (mean NOSPECS, 9.6; mean CAS, 4.8; mean age, 65 years; 83% female) and six GO smokers (mean NOSPECS, 9; mean CAS, 3.6; mean age, 49 years; 100% female). GO-OF from smokers (SM) and nonsmokers (NS) were incubated with 7.5% CSE or control extract (−) under hypoxic conditions for 4 hours. Whole-cell lysates were obtained and subjected to Western-blot analysis for detection of HIF-1α and β-actin as a loading control. Western-blot signals of GO-OF from six nonsmokers and six smokers were quantified using densitometry. The HIF-1α signal was normalized to the β-actin signal and expressed as relative HIF-1α protein. Representative immunoblots are shown. Data represent the mean ± SEM of an experiment representative of at least three separate experiments. $*P \leq .05$; $**P < .01$; ns = $P > .5$. ns, not significant.

genic differentiation (Figure 5) in agreement with a prior study demonstrating increased adiponectin gene expression in GO orbital fat (29, 34). These findings indicate that hypoxia can be a main factor promoting adipogenesis in GO, independently from other stimulating factors. Because TSHR expression is increased during adipogenesis (29), hypoxia-induced adipogenic differentiation will increase the target antigen for anti-TSHR antibodies in the orbit of GO patients and is likely an underlying mechanism triggering the autoantigen response in the orbita. In agreement with this, we could show that additional TSH stimulation of the TSHR increased adipogenesis of the GO-OF and induced adipogenesis of Ctrl-derived OFs under hypoxia (Figure 5). Moreover, because orbital adipogenesis is accompanied by increased hyaluronic acid production (35), HIF-1-dependent adipogenesis strongly promotes pathogenic processes that enhance tissue expansion in the orbita. Furthermore, hypoxia increases production of glycosaminoglycan in OFs derived from extraocular muscle (7), indicating that HIF-1 may also be directly involved in the overproduction of extracellular matrix in the orbita of GO patients. Furthermore, CSE has been shown to enhance adipocyte differentiation and hyaluronan production of GO-OF (36, 37). We showed that CSE, in addition to hypoxia, can induce HIF-1α in OFs derived from GO smokers (Figure 6). Considering that the detrimental influence of smoking on GO is caused by hypoxia combined with compounds in the cigarette smoke, overactivation of HIF-1 pathways could provide a molecular explanation as to why smokers more likely develop severe proptosis and/or myopathy than nonsmokers.

From the clinical point of view, our study supports the idea that the decision toward bony orbital decompression should be carefully evaluated in all GO patients with advanced disease states that are not responsive to inflammatory treatment. Drug-targeted inhibition of HIF-1/VEGF may provide a therapeutic strategy to control tissue expansion in GO. Poor control of thyroid function has been reported to increase the risk of a more severe course of GO (38, 39). Our data show a cumulative effect of hypoxia and TSH on adipogenesis and therefore provide the molecular explanation as to why, especially in patients with advanced stages of GO, thyroid treatment should be planned carefully to prevent hypothyroid disease stages that might increase TSH levels.

In conclusion, we propose that hypoxia and HIF-1-dependent pathways play a causal role in the tissue remodeling of GO and may provide new therapeutic targets to control tissue expansion in GO. Recently, we have established a GO mouse model (40) that will allow us to study the role of HIF-1 pathways and therapeutic targeting in vivo.

Acknowledgments

We gratefully acknowledge Christoph Jesenek (University Duisburg-Essen, Germany) for technical assistance. The authors thank all patients for their participation in this study.

Address all correspondence and requests for reprints to: Utta Berchner-Pfannschmidt, PhD, Molecular Ophthalmology, Medical Research Center, University Hospital Essen, 45147 Essen, Germany. E-mail: utta.berchner-pfannschmidt@uni-due.de.

The study was supported by Deutsche Forschungsgemeinschaft Grants BE 3177/2-1 (to U.B.-P.) and EC 379/3-1 (to A.E.) and by funding from Deutsche Ophthalmologische Gesellschaft (to U.B.-P. and A.E.).

Disclosure Summary: The authors have nothing to disclose.

References

1. **Wiersinga WM, Bartalena L.** Epidemiology and prevention of Graves' ophthalmopathy. *Thyroid*. 2002;12:855–860.
2. **Eckstein AK, Johnson KT, Thanos M, Esser J, Ludgate M.** Current insights into the pathogenesis of Graves' orbitopathy. *Horm Metab Res*. 2009;41:456–464.
3. **Bahn RS.** Graves' ophthalmopathy. *N Engl J Med*. 2010;362:726–738.

4. **Trayhurn P.** Hypoxia and adipose tissue function and dysfunction in obesity. *Physiol Rev*. 2013;93:1–21.
5. **Wiersinga WM.** Smoking and thyroid. *Clin Endocrinol (Oxf)*. 2013; 79:145–151.
6. **Bartalena L, Baldeschi L, Boboridis K, et al.** The 2016 European Thyroid Association/European Group on Graves' Orbitopathy guidelines for the management of Graves' orbitopathy. *Eur Thyroid J*. 2016;5:9–26.
7. **Metcalfe RA, Weetman AP.** Stimulation of extraocular muscle fibroblasts by cytokines and hypoxia: possible role in thyroid-associated ophthalmopathy. *Clin Endocrinol (Oxf)*. 1994;40:67–72.
8. **Chng CL, Lai OF, Chew CS, et al.** Hypoxia increases adipogenesis and affects adipocytokine production in orbital fibroblasts-a possible explanation of the link between smoking and Graves' ophthalmopathy. *Int J Ophthalmol*. 2014;7:403–407.
9. **Regensburg NI, Wiersinga WM, Berendschot TT, Saeed P, Mourits MP.** Effect of smoking on orbital fat and muscle volume in Graves' orbitopathy. *Thyroid*. 2011;21:177–181.
10. **Semenza GL.** Hypoxia-inducible factor 1: master regulator of O2 homeostasis. *Curr Opin Genet Dev*. 1998;8:588–594.
11. **Epstein AC, Gleadle JM, McNeill LA, et al.** *C. elegans* EGL-9 and mammalian homologs define a family of dioxygenases that regulate HIF by prolyl hydroxylation. *Cell*. 2001;107:43–54.
12. **Mahon PC, Hirota K, Semenza GL.** FIH-1: a novel protein that interacts with HIF-1α and VHL to mediate repression of HIF-1 transcriptional activity. *Genes Dev*. 2001;15:2675–2686.
13. **Zimna A, Kurpisz M.** Hypoxia-inducible factor-1 in physiological and pathophysiological angiogenesis: applications and therapies. *Biomed Res Int*. 2015;2015:549412.
14. **Wenger RH, Stiehl DP, Camenisch G.** Integration of oxygen signaling at the consensus HRE. *Sci STKE*. 2005;2005:re12.
15. **Meyer zu Hörste M, Ströher E, Berchner-Pfannschmidt U, et al.** A novel mechanism involved in the pathogenesis of Graves ophthalmopathy (GO): clathrin is a possible targeting molecule for inhibiting local immune response in the orbit. *J Clin Endocrinol Metab*. 2011;96:E1727–E1736.
16. **Maxwell PH, Wiesener MS, Chang GW, et al.** The tumour suppressor protein VHL targets hypoxia-inducible factors for oxygen-dependent proteolysis. *Nature*. 1999;399:271–275.
17. **Berchner-Pfannschmidt U, Yamac H, Trinidad B, Fandrey J.** Nitric oxide modulates oxygen sensing by hypoxia-inducible factor 1-dependent induction of prolyl hydroxylase 2. *J Biol Chem*. 2007;282: 1788–1796.
18. **Kumar S, Nadeem S, Stan MN, Coenen M, Bahn RS.** A stimulatory TSH receptor antibody enhances adipogenesis via phosphoinositide 3-kinase activation in orbital preadipocytes from patients with Graves' ophthalmopathy. *J Mol Endocrinol*. 2011;46:155–163.
19. **Ellinghaus P, Heisler I, Unterschemmann K, et al.** BAY 87–2243, a highly potent and selective inhibitor of hypoxia-induced gene activation has antitumor activities by inhibition of mitochondrial complex I. *Cancer Med*. 2013;2:611–624.
20. **Frede S, Stockmann C, Freitag P, Fandrey J.** Bacterial lipopolysaccharide induces HIF-1 activation in human monocytes via p44/42 MAPK and NF-κB. *Biochem J*. 2006;396:517–527.
21. **Rius J, Guma M, Schachtrup C, et al.** NF-κB links innate immunity to the hypoxic response through transcriptional regulation of HIF-1α. *Nature*. 2008;453:807–811.
22. **Choi YH, Back KO, Kim HJ, Lee SY, Kook KH.** Pirfenidone attenuates IL-1β-induced COX-2 and PGE2 production in orbital fibroblasts through suppression of NF-κB activity. *Exp Eye Res*. 2013; 113:1–8.
23. **Wang H, Zhu LS, Cheng JW, et al.** CD40 ligand induces expression of vascular cell adhesion molecule 1 and E-selectin in orbital fibroblasts from patients with Graves' orbitopathy. *Graefes Arch Clin Exp Ophthalmol*. 2015;253:573–582.
24. **Frede S, Berchner-Pfannschmidt U, Fandrey J.** Regulation of hypoxia-inducible factors during inflammation. *Methods Enzymol*. 2007;435:405–419.
25. **Cummins EP, Berra E, Comerford KM, et al.** Prolyl hydroxylase-1 negatively regulates IκB kinase-β, giving insight into hypoxia-induced NFκB activity. *Proc Natl Acad Sci USA*. 2006;103:18154–18159.
26. **Sene A, Chin-Yee D, Apte RS.** Seeing through VEGF: innate and adaptive immunity in pathological angiogenesis in the eye. *Trends Mol Med*. 2015;21:43–51.
27. **Penn JS, Madan A, Caldwell RB, Bartoli M, Caldwell RW, Hartnett ME.** Vascular endothelial growth factor in eye disease. *Prog Retin Eye Res*. 2008;27:331–371.
28. **DeNiro M, Alsmadi O, Al-Mohanna F.** Modulating the hypoxia-inducible factor signaling pathway as a therapeutic modality to regulate retinal angiogenesis. *Exp Eye Res*. 2009;89:700–717.
29. **Kumar S, Coenen MJ, Scherer PE, Bahn RS.** Evidence for enhanced adipogenesis in the orbits of patients with Graves' ophthalmopathy. *J Clin Endocrinol Metab*. 2004;89:930–935.
30. **Brandau S, Bruderek K, Hestermann K, et al.** Orbital fibroblasts from Graves' orbitopathy patients share functional and immunophenotypic properties with mesenchymal stem/stromal cells. *Invest Ophthalmol Vis Sci*. 2015;56:6549–6557.
31. **Cawood TJ, Moriarty P, O'Farrelly C, O'Shea D.** The effects of tumour necrosis factor-α and interleukin1 on an in vitro model of thyroid-associated ophthalmopathy; contrasting effects on adipogenesis. *Eur J Endocrinol*. 2006;155:395–403.
32. **Kumar S, Schiefer R, Coenen MJ, Bahn RS.** A stimulatory thyrotropin receptor antibody (M22) and thyrotropin increase interleukin-6 expression and secretion in Graves' orbital preadipocyte fibroblasts. *Thyroid*. 2010;20:59–65.
33. **Virakul S, Dalm VA, Paridaens D, et al.** Platelet-derived growth factor-BB enhances adipogenesis in orbital fibroblasts. *Invest Ophthalmol Vis Sci*. 2015;56:5457–5464.
34. **Marique L, Senou M, Craps J, et al.** Oxidative stress and upregulation of antioxidant proteins, including adiponectin, in extraocular muscular cells, orbital adipocytes, and thyrocytes in Graves' disease associated with orbitopathy. *Thyroid*. 2015;25:1033–1042.
35. **Zhang L, Grennan-Jones F, Lane C, Rees DA, Dayan CM, Ludgate M.** Adipose tissue depot-specific differences in the regulation of hyaluronan production of relevance to Graves' orbitopathy. *J Clin Endocrinol Metab*. 2012;97:653–662.
36. **Cawood TJ, Moriarty P, O'Farrelly C, O'Shea D.** Smoking and thyroid-associated ophthalmopathy: a novel explanation of the biological link. *J Clin Endocrinol Metab*. 2007;92:59–64.
37. **Yoon JS, Lee HJ, Chae MK, Lee SY, Lee EJ.** Cigarette smoke extract-induced adipogenesis in Graves' orbital fibroblasts is inhibited by quercetin via reduction in oxidative stress. *J Endocrinol*. 2013;216: 145–156.
38. **Prummel MF, Wiersinga WM, Mourits MP, Koornneef L, Berghout A, van der Gaag R.** Effect of abnormal thyroid function on the severity of Graves' ophthalmopathy. *Arch Intern Med*. 1990;150: 1098–1101.
39. **Tallstedt L, Lundell G, Blomgren H, Bring J.** Does early administration of thyroxine reduce the development of Graves' ophthalmopathy after radioiodine treatment? *Eur J Endocrinol*. 1994;130: 494–497.
40. **Berchner-Pfannschmidt U, Moshkelgosha S, Diaz-Cano S, et al.** Comparative assessment of female mouse model of Graves' orbitopathy under different environments, accompanied by proinflammatory cytokine and T-cell responses to thyrotropin hormone receptor antigen. *Endocrinology*. 2016;157:1673–1682.

Suppl. Figure 1 A: Ctrl person (no. 2)

Suppl. Figure 1 A: GO patient (no. 3)

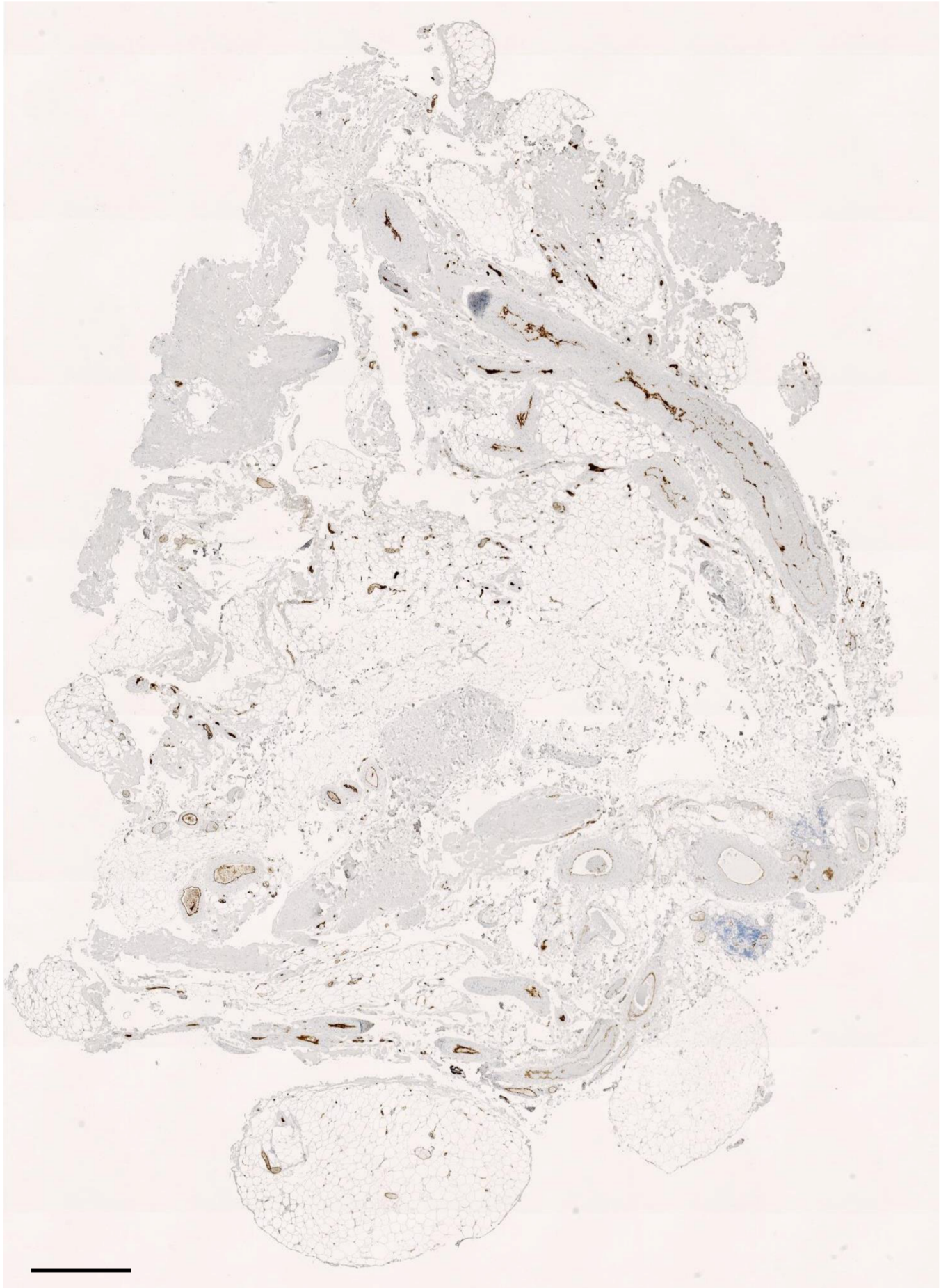

Suppl. Figure 1 B: Ctrl patients (no. 1-18)

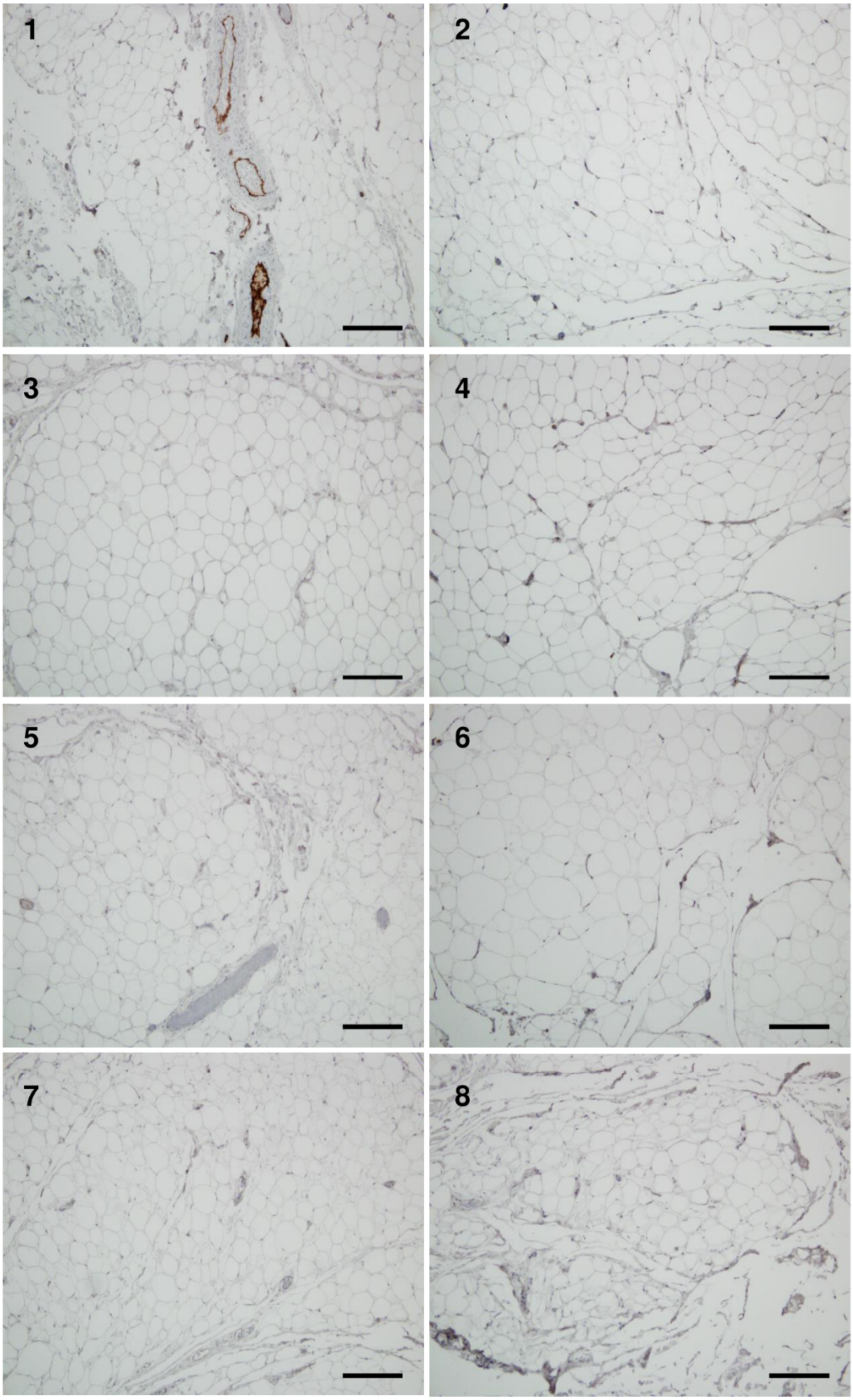

Ctrl (no. 9-16)

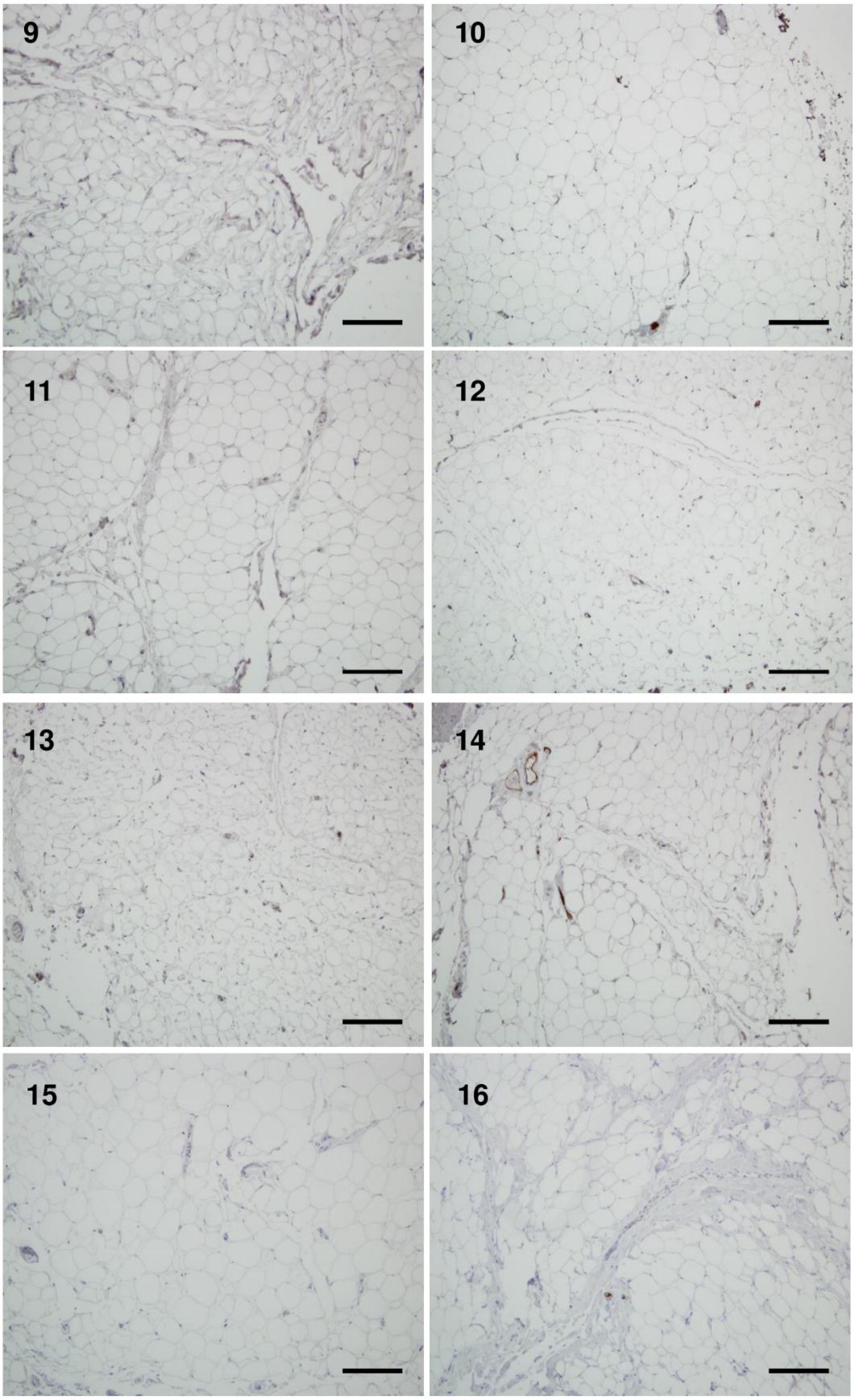

Ctrl (no. 17, 18)

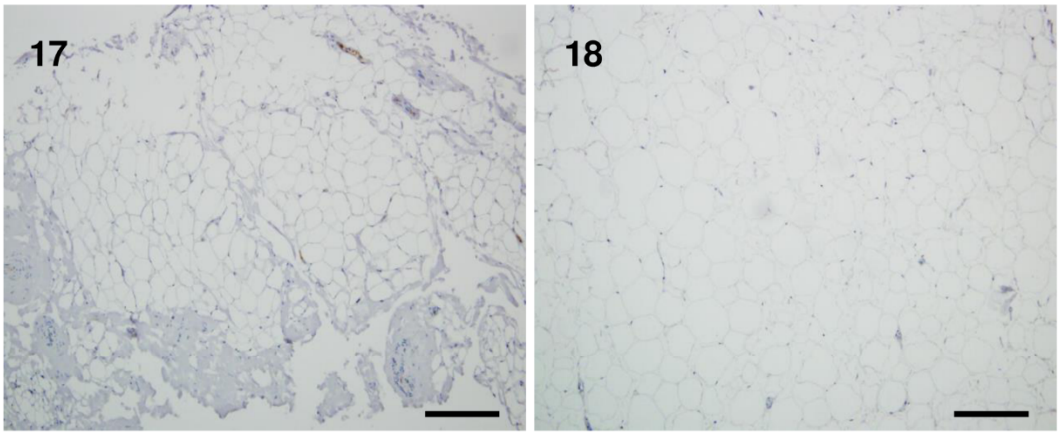

Suppl. Figure 1 B: GO patients (no. 1-21)

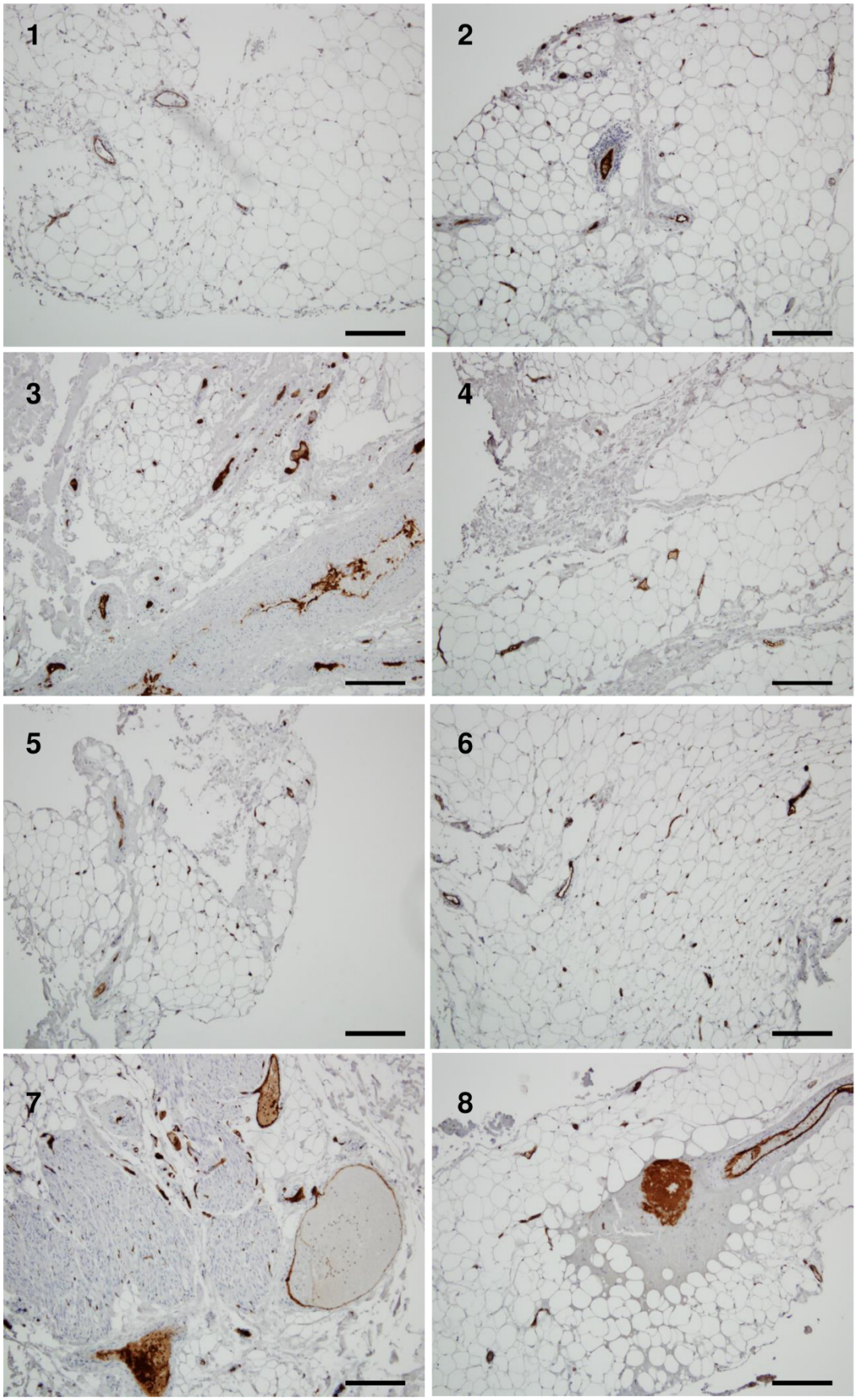

GO (no. 9-16)

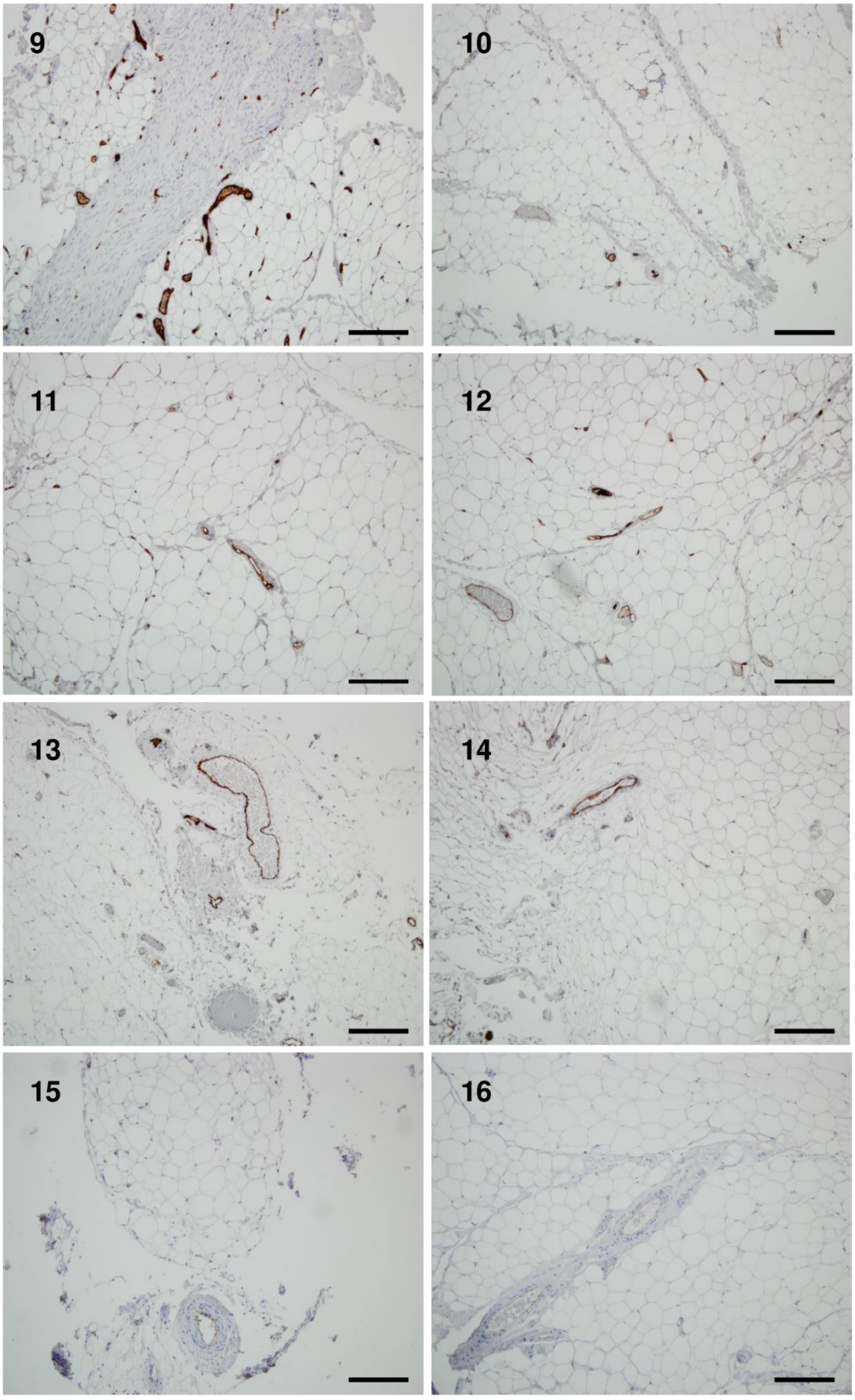

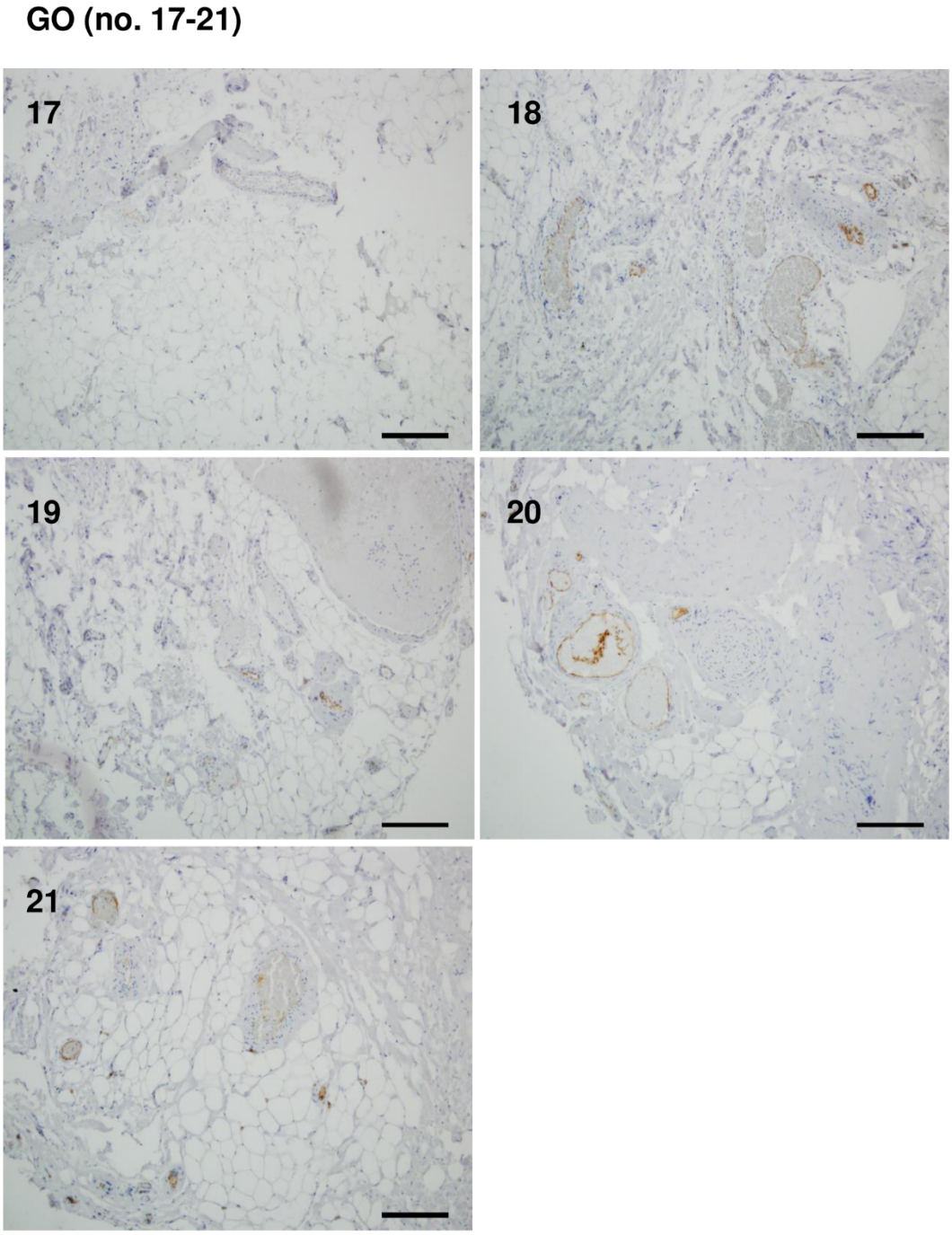
GO (no. 17-21)
17
18
19
20
21

Suppl. Figure 2

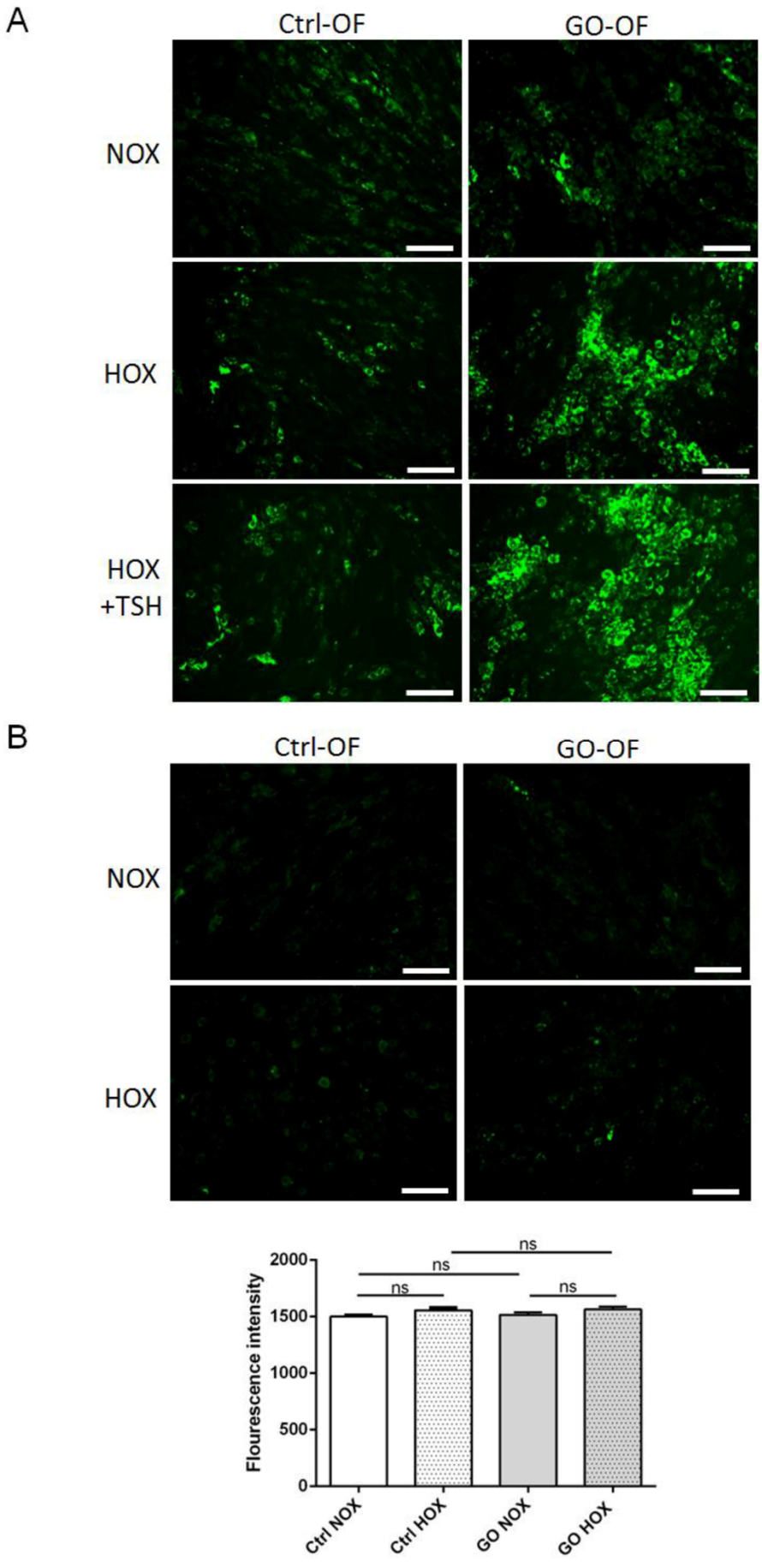

Publication 3

Comparative Assessment of female mouse of Graves' orbitopathy under different environments, accompanied by proinflammatory cytokine and T-cell response to thyrotropin hormone receptor antigen.

Berchner-Pfannschmidt U, Moshgelgosha S, Diaz-Cano S, Edelmann B, Görtz G-E, Horstmann M, Noble A, Hansen W, Eckstein A, Banga J. P.

Endocrinology. 2016, 157(4):1673-1682

Contribution

Herein, I was involved in immunization procedure of the mice with TSHR A-subunit and ß-galactosidase encoding plasmids. After scarification of the mice I contributed to preparation of orbital tissue and performed cell culture experiments. I was involved in discussing and analyzing data.

ORIGINAL RESEARCH

Comparative Assessment of Female Mouse Model of Graves' Orbitopathy Under Different Environments, Accompanied by Proinflammatory Cytokine and T-Cell Responses to Thyrotropin Hormone Receptor Antigen

Utta Berchner-Pfannschmidt,* Sajad Moshkelgosha,* Salvador Diaz-Cano, Bärbel Edelmann, Gina-Eva Görtz, Mareike Horstmann, Alistair Noble, Wiebke Hansen, Anja Eckstein, and J. Paul Banga

Molecular Ophthalmology (U.B.-P., S.M., G.-E.G., M.H., A.E., J.P.B.), Department of Ophthalmology; Department of Molecular Biology (B.E.); and Institute of Medical Microbiology (W.H.), University Hospital Essen/University of Duisburg-Essen, 45147 Essen, Germany; Faculty of Life Sciences and Medicine (S.M., A.N., J.P.B.), King's College London, London, SE5 9NU United Kingdom; and King's College Hospital NHS Foundation Trust (S.D.-C.), London, SE5 9RS United Kingdom

We recently described a preclinical model of Graves' orbitopathy (GO), induced by genetic immunization of eukaryotic expression plasmid encoding human TSH receptor (TSHR) A-subunit by muscle electroporation in female BALB/c mice. The onset of orbital pathology is characterized by muscle inflammation, adipogenesis, and fibrosis. Animal models of autoimmunity are influenced by their environmental exposures. This follow-up study was undertaken to investigate the development of experimental GO in 2 different locations, run in parallel under comparable housing conditions. Functional antibodies to TSHR were induced in TSHR A-subunit plasmid-immunized animals, and antibodies to IGF-1 receptor α-subunit were also present, whereas control animals were negative in both locations. Splenic T cells from TSHR A-subunit primed animals undergoing GO in both locations showed proliferative responses to purified TSHR antigen and secreted interferon-γ, IL-10, IL-6, and TNF-α cytokines. Histopathological evaluation showed orbital tissue damage in mice undergoing GO, manifest by adipogenesis, fibrosis, and muscle damage with classic signs of myopathy. Although no inflammatory infiltrate was observed in orbital tissue in either location, the appearances were consistent with a "hit-and-run" immune-mediated inflammatory event. A statistically significant increase of cumulative incidence of orbital pathology when compared with control animals was shown for both locations, confirming onset of orbital dysimmune myopathy. Our findings confirm expansion of the model in different environments, accompanied with increased prevalence of T cell-derived proinflammatory cytokines, with relevance for pathogenesis. Wider availability of the model makes it suitable for mechanistic studies into pathogenesis and undertaking of novel therapeutic approaches. **(*Endocrinology* 157: 1673–1682, 2016)**

Graves' disease is a common chronic autoimmune disease mediated by autoantibodies to the TSH receptor (TSHR), which stimulate the thyroid gland for overproduction of thyroid hormone (1). The TSHR also shows expression in extrathyroidal tissues, predominantly in the orbital tissue, where it has been shown to be functional by its ability to be activated by its cognate hormone TSH. Graves' orbitopathy (GO) or thyroid eye disease is an autoimmune condition closely associated with Graves' disease, characterized by remodeling of the orbital connective

ISSN Print 0013-7227 ISSN Online 1945-7170
Printed in USA

Received September 26, 2015. Accepted February 9, 2016.
First Published Online February 12, 2016

* U.B.-P. and S.M. share first authorship.

Abbreviations: GO, Graves' orbitopathy; hTSHR, human TSHR; IGF-1R, IGF-1 receptor; rhTSHR-E, recombinant hTSHR extracellular region protein; SPF, specific pathogen free; TBII, TSH-binding inhibitory immunoglobulin; TSAb, thyroid-stimulating antibody TSBAb, TSH-stimulating blocking antibody; TSHR, TSH receptor.

tissue as a result of lymphocyte infiltration, increased adipogenesis and excessive deposition of hyaluronan in the orbital muscle fibers (2). The pathophysiology of GO is complex and remains to be clarified. The orbital fibroblasts express TSHR, the target autoantigen in Graves' disease, and considered to be the primary pathogenic target of autoimmune attack in GO (3). Another receptor, the IGF-1 receptor (IGF-1R) is also expressed on the cell surface of orbital fibroblasts and considered to be the second target autoantigen in GO (2). Other than stimulation of TSHR on the orbital fibroblasts by functional anti-TSHR antibody subtype known as thyroid-stimulating antibodies (TSAbs), engagement of CD154 (CD40L) on inflammatory T cells infiltrating the orbital tissue with CD40 on orbital fibroblasts leads to fibroblast activation resulting in secretion of inflammatory cytokines, hyaluronan deposition, and differentiation into adipocytes. The disease is therefore largely TSHR antibody and T cell dependent, but the mechanisms involved in the initiation and perpetuation of the disease remain to be clarified (2, 4) (for antibodies, please see Table 1).

Animal models have contributed to the understanding of the pathophysiology and treatment modalities of autoimmune diseases and have led to successful translation of new therapeutics to the clinic in a number of inflammatory diseases (5). Experimental Graves' disease can be induced in mouse models by in vivo delivery via genetic immunization of human TSHR (hTSHR) or part of its extracellular region termed hTSHR A-subunit by a number of different protocols and exhibit many of the characteristics of hyperthyroidism present in patients (6–8). These include production of TSAbs, elevated serum T_4 levels and thyroid gland histology of hypertrophy and activated thyroid follicular cells. The most efficient and reproducible model relies on immunization with adenovirus encoding hTSHR A-subunit (9). Importantly, orbital pathology was rarely observed in these models of Graves' disease and thus the triggering events necessary for progression to orbital disease remain completely unknown. Recently, we described a novel, relevant preclinical model of GO based upon hTSHR A-subunit plasmid immunization in conjunction with highly efficient plasmid delivery by muscle electroporation in female BALB/c mice that shares many similarities with GO patients (10, 11). Thus, animals with induced anti-TSHR antibodies with either hyperthyroid or hypothyroid disease status progress to develop clinical signs of GO by 6–15 weeks after the last challenge. The characteristics of the GO model include a heterogeneous phenotype similar to GO patients, recapitulating orbital inflammation, adipogenesis, and proptosis of the eyeball, which manifest to variable degrees in different immune animals (11).

An important contributor to disease pathology in animal models of autoimmunity is the microbial environment in the housing conditions, because a variety of models including induced, spontaneous or genetically manipulated models are differently affected upon change of such conditions (12–14). However, for the adenovirus model of Graves' disease, different animal housing conditions ranging from specific pathogen-free (SPF) conditions to conventional housing do not appear to influence disease incidence (15). In order to better assess the new preclinical GO model for further studies on disease pathogenesis and novel therapeutic targets, we initiated comparative studies to evaluate the model in 2 independent locations, where the influence of housing conditions and environment on development of GO could be evaluated. In other experiments, induction of GO was studied in association with T lymphocyte responses to purified TSHR protein antigen. Our study reveals the GO model reproducibly resamples the clinical features of GO patients in different animal housing conditions in independent locations, accompanied by induction of TSHR-specific T cells primed for production of proinflammatory cytokines. The versatility of the preclinical model will allow mechanistic studies into disease pathogenesis and evaluation of novel therapeutic approaches.

Materials and Methods

Animal studies were conducted in parallel in 2 different locations, center 1 (King's College London) and center 2 (University of Duisburg-Essen). Female BALB/c mice of 6–8 weeks of age were purchased from commercial suppliers, center 1 animals from Harlan Ltd and center 2 animals from Harlan Laboratories BV and fed ad libitum on water and

Table 1. Antibody Table

Peptide/ Protein Target	Antigen Sequence (if Known)	Name of Antibody	Manufacturer, Catalog Number, and/or Name of Individual Providing the Antibody	Species Raised in; Monoclonal or Polyclonal	Dilution Used
CD4		Pacific blue rat antimouse CD4	BD Biosciences, 558107	Rat, monoclonal; clone RM4-5	1:1000
CD8		PE rat antimouse CD8a	BD Biosciences, 553032	Rat; monoclonal, clone 53-6.7	1:800
CD4		RM-4-5	eBioscience, 12-0042-81	Rat; IgG2a	1 μg/mL
CD8β		53-5.8	BioLegend, 140409	Rat; IgG1	1 μg/mL
IFN-γ		XMG1.2	BioLegend, 505825	Rat; IgG1	1 μg/mL

doi: 10.1210/en.2015-1829 press.endocrine.org/journal/endo 1675

commercial diet (Supplemental Table 1). The BALB/c mice in both the centers were the same subline (BALB/cOlaHsd) as used in our earlier study (11). Animals in center 1 were maintained in SPF conditions, and animals in center 2 were kept in individually ventilated cages under SPF conditions. Both center 1 and center 2 facilities instigate quarterly Health Screen Reports on viral, bacterial, mycoplasma, and parasite (including intestinal protozoa) screens in the units. Animal procedures in center 1 were reviewed and approved by the Ethical Committee of King's College London and conducted with Personal and Project licenses under United Kingdom Home Office regulations. Animal procedures in center 2 were reviewed and approved by North Rhine Westphalian State Agency for Nature, Environment and Consumer Protection, Germany.

The eukaryotic expression plasmid, pTriEx1.1Neo-hTSHR A-subunit (otherwise known as hTSHR289) and the control pTri1Ex1.1Neo-β-Gal plasmid were used and referred to as hTSHR A-subunit plasmid and β-Gal plasmid, respectively (11). Plasmid immunization by electroporation was performed as described (11) and in Supplemental Materials and Methods. In center 1, a total of 11 female BALB/c mice were challenged with hTSHR A-subunit plasmid and 4 mice with β-Gal plasmid; in center 2, a total of 10 mice were challenged with hTSHR A-subunit plasmid and 10 mice with β-Gal plasmid. All immune animals in center 1 and center 2 were killed 9 weeks after the end of last immunization, and serum determinations in individual mice for total T_4, anti-TSHR, and anti-IGF-1R antibodies were determined as described in Supplemental Materials and Methods.

Purified recombinant hTSHR extracellular region protein (rhTSHR-E) (amino acids 20 to 419) expressed in baculovirus system (16) was used as antigen in ex vivo stimulation assays and provided by Apitope International NV. Splenocyte proliferation assays were evaluated using either 5,6-carboxylfluorescein diacetate succinimidyl ester or eFlour670 dye-based assays in center 1 or center 2, respectively. The proliferation assay was first optimized in center 2 for dose of rhTSHR-E antigen and culture time and optimal conditions then used in both center 1 and center 2 for test samples, as described in Supplemental Materials and Methods. Cytokine response of T cells to rhTSHR-E antigen were measured by 2 different methods: intracellular interferon (IFN)-γ expression (center 1) and as cytokine secretion into culture media (center 1 and center 2) and assayed for the presence of IFN-γ, IL-17, IL-10, IL-6, and TNF-α using a Luminex Screening assay (R&D Systems) according to the manufacturer's recommendations, as described in Supplemental Materials and Methods. The assay was performed on a Luminex 200 instrument, and levels of cytokines were calculated with the Luminex IS software (Luminex Corp). Orbital histology and thyroid gland histology were conducted as described before (11, 17). Quantification of adipose tissue and orbital muscle atrophy in orbital sections of extraorbital inferior and medial rectus muscle was performed with ImageJ, as described in Supplemental Materials and Methods.

Full methods are available in Supplemental Materials and Methods.

Results

Comparative studies on the preclinical GO model in different locations

As a first step towards expanding the preclinical mouse model of GO, we evaluated the model in comparative studies, run in parallel in 2 different independent centers to determine its reproducibility. Identical strains of female BALB/c mice (BALB/cOlaHsd) maintained under SPF conditions were immunized by im injection of hTSHR A-subunit plasmid in conjunction with electroporation. To minimize any differences in injection procedure, which may influence the degree of induction of experimental disease, all immunization and electroporation steps in the both centers were completed by the same operator. During the course after the last immunization, 1 out of 11 animals injected with hTSHR A-subunit plasmid injected mice developed transient chemosis in center 1 and 1 out of 10 hTSHR A-subunit plasmid injected mice in center 2 developed transient chemosis (1 eye, respectively) (Supplemental Figure 1). Nine weeks after the end of immunization when the animals were killed, eyes of all mice appeared normal in appearance in both the centers. Immune serum was evaluated for antibodies to TSHR and showed hTSHR A-subunit-challenged animals to be significantly positive for TSH-binding inhibitory immunoglobulin (TBII) activity in both the centers, when compared with control β-Gal-immunized mice (Figure 1A). Measurement of anti-TSHR antibody subtypes in hTSHR A-subunit-challenged animals showed animals to be positive for TSAbs and TSH-stimulating blocking antibodies (TSBAbs), with higher levels in immune animals in center 2 (Figure 1B). Control animals challenged with β-Gal plasmid were negative for both these subtypes of anti-TSHR antibodies.

We have earlier shown the presence of antibodies to IGF-1R α-subunit in some animals immunized with hTSHR A-subunit plasmid (10, 11). In order to ascertain whether this was a unique phenomenon in our previous studies linked to the animals housed in center 1, we found in this study, anti-IGF-1R α-subunit antibody positivity in immune animals in both the centers. Thus, 8 out of 9 animals in center 1, and 4 out of 10 animals immunized with hTSHR A-subunit plasmid were significantly positive for anti-IGF-1R α-subunit antibodies (Figure 1C). Control animals challenged with β-Gal plasmid in center 1 and center 2 were all negative for anti-IGF-1R α-subunit antibodies, consistent with our earlier observations (Figure 1C) (10, 11). Interestingly the titers of IGF-1R α-subunit antibodies in hTSHR A-subunit plasmid-immunized animals were considerably higher in center 2 animals, with positivity in 1 animal showing OD

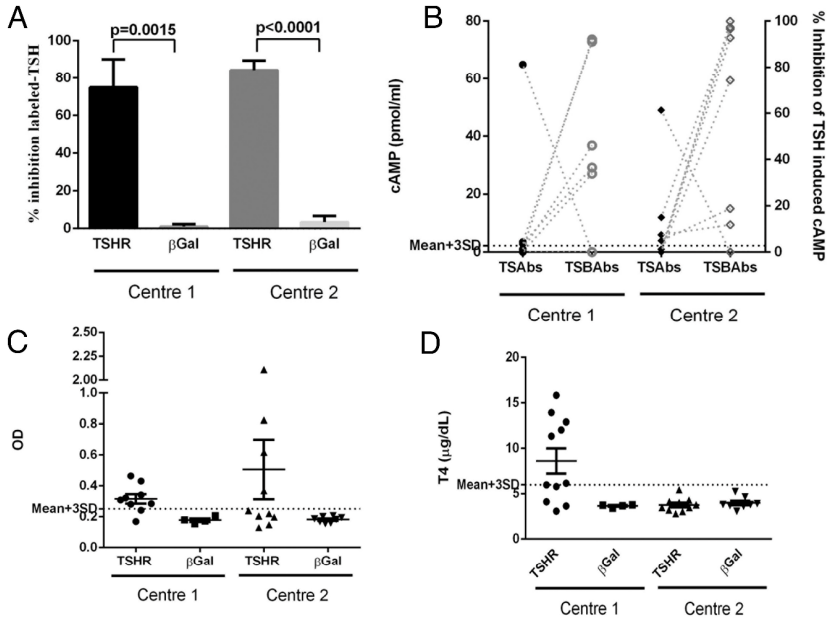

Figure 1. Evaluation of thyroid function and antibody in TSHR A-subunit plasmid and control β-Gal plasmid-immunized mice in center 1 and center 2. A, Measurement of total anti-TSHR antibodies in serum by TBII activity by competition with bTSH. B, Measurements of blocking TSBAbs and stimulating TSAbs in individual animals by bioassay. The ordinate shows percent blocking of TSH-mediated stimulation for TSBAbs (right axis) or cAMP generated for TSAbs (left axis). The dotted line indicates the mean ± 3 SD for TSAbs of the control β-Gal-immunized mice, the joined points in TSABs and TSBAbs indicate the respective measurements in the same animal. C, Antibodies to IGF-1R determined by ELISA. D, Total serum T_4 values in serum.

reading of more than 2.0, representing almost off-scale reading on the plate reader (Figure 1C).

In contrast to anti-TSHR and anti-IGF-1R α-subunit antibody induction, comparative assessment of thyroid hormone T_4 levels showed markedly different results in the 2 centers. High levels of serum T_4 and hence hyperthyroidism were induced in animals (5 mice out of 11) in center 1, but in contrast, animals in the other center lacked hyperthyroidism, as all the immune mice showed serum T_4 values in the normal range, as the β-Gal-immunized mice and hence were euthyroid (Figure 1D). Histological analyses of thyroid glands from immune animals in both centers were conducted blindly, with no information provided on the immunogen or the serum T_4 values as an indicator of thyroid function status. Examination of thyroid gland histology by hematoxylin and eosin (H&E) from animals housed in center 1 confirmed the thyroid hormone status of the animals, with all hyperthyroid mice with typical features of cuboidal/tall follicular thyroid epithelial cells in a microfollicular growth pattern, and euthyroid animals with thyroid glands showing typical normal thyroid histology; 1 thyroid showed focal infiltration of the gland (Supplemental Figure 2, A–C). In contrast, examination of thyroid gland histology from all immune animals in center 2 showed normal histological features (Supplemental Figure 2, D–F).

We next examined orbital histopathology of center 1 and center 2 immune animals immunized with hTSHR A-subunit plasmid or control β-Gal plasmid, conducted blindly without knowledge of tissue section for the examiner. All hTSHR A-subunit-immunized animals in center 1 and center 2 showed concordant orbital tissue abnormalities, with no inflammatory cells. The orbital muscle abnormalities showed 2 typical features: 1) expansion of fat cells (adipogenesis) extending into and partially replacing muscle tissue (Figure 2, B and F); or 2) atrophic muscle fibers in the periphery of the muscle fascicles featuring hyperchromatic nuclei and vacuolated cytoplasm, a characteristic pathological sign of muscle damage (Figure 2, D and H). These abnormalities were absent in control β-Gal plasmid-immunized mice (Figure 2, A, C, E, and G). Furthermore, there was no correlation between antibodies (TBII activity, TSAbs and TSBAbs) and adipogenesis or myopathy in any of the immune mice undergoing GO in either of the centers.

We quantified the orbital histological differences in animals undergoing GO compared with control β-Gal-immunized mice in both center 1 and center 2 animals (Supplemental Figure 3, A and B), with the quantifications shown in Supplemental Figure 3, C and D). The quantification data were individually normalized by Z-score method for adipogenesis and atrophy. We observed a statistically significant increase of cumulative incidence of orbital disease pathology when compared with control β-Gal-immunized mice in adipogenesis (center 1 [Figure 2I]) and atrophy (both centers [Figure 2J]). Moreover, when a combined Z-score for adipogenesis and atrophy was produced, the total orbital disease score for comparative evaluation of orbital pathology in hTSHR A-subunit plasmid-challenged mice reveals statistically significant disease onset compared with β-Gal-immunized animals in both center 1 and center 2 (Figure 2K). Importantly, quantification of the respective changes showed variable degrees of orbital changes in individual mice (Supplemental Figure 3, C and D). Taken together, the data supports findings that immune mice undergoing experimental GO in 2 independent centers show highly similar outcomes, in terms of robust and sustained anti-TSHR and anti-IGF-1R

doi: 10.1210/en.2015-1829 press.endocrine.org/journal/endo 1677

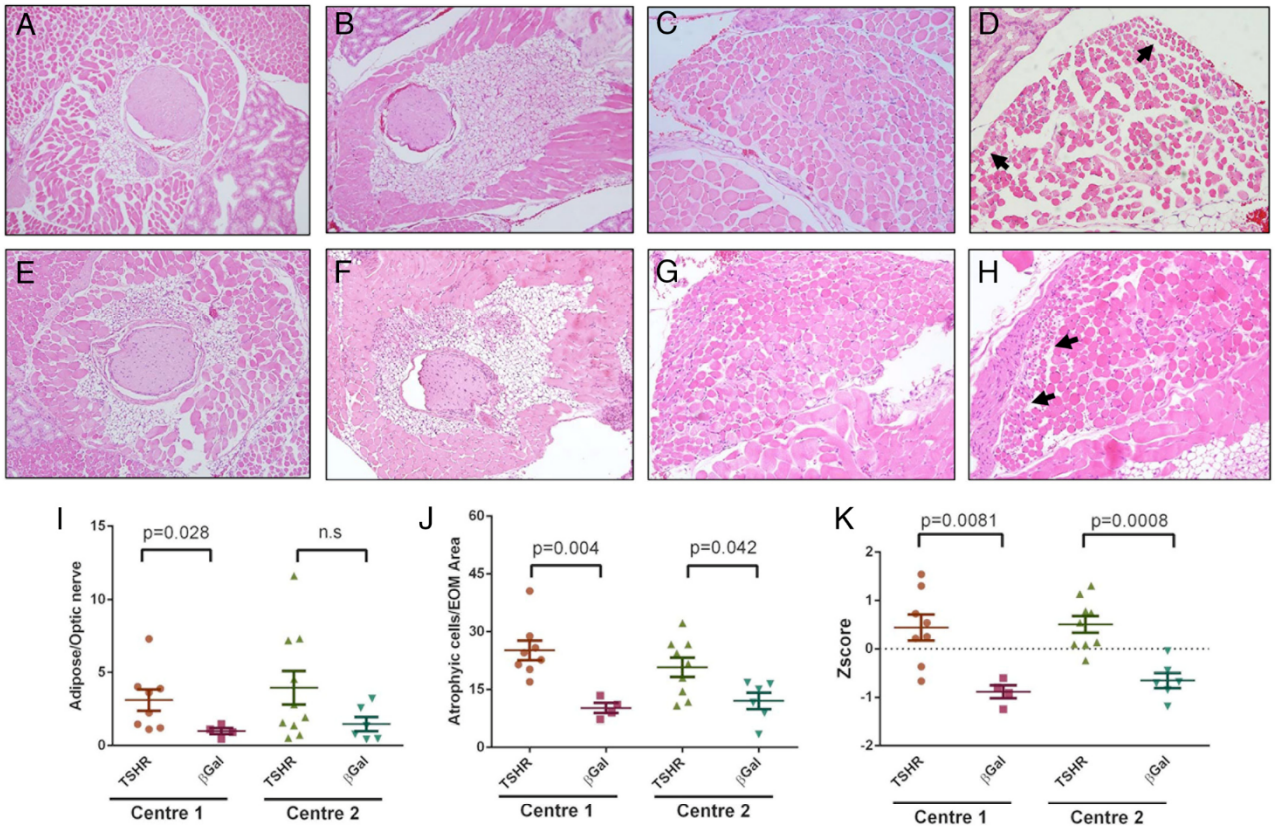

Figure 2. Orbital histology of mice undergoing GO in center 1 and center 2. H&E staining of orbital tissue, by orientating the paraffin block for sectioning with optic nerve as an anatomical landmark. Representative images from mouse orbital tissue are shown, with photomicrographs from center 1 animals (A–D) and center 2 animals (E–H). Expansion of adipose tissue in hTSHR A-subunit plasmid mice (B and F) compared with β-Gal plasmid-immunized control mice (A and E) (×100). hTSHR A-subunit plasmid-immunized mice show atrophy of extraocular muscles (D and H, arrows), whereas β-Gal control-immunized mice appeared normal (C and G) (×200). Quantification of fat expansion (I) and muscle atrophy (J), and normalizing and scoring of both showing the total orbital disease score (Z-score) (K) of individual mice.

α-subunit antibody responses and statistically significant similarity in orbital disease pathology.

Proliferation and expression of proinflammatory cytokines in antigen-specific T cells

We examined whether TSHR protein antigen induced T-cell responses in immune animals by ex vivo stimulation of unfractionated splenocytes with purified rhTSHR-E antigen using dye-based assays. As shown in Figure 3A, culture of total splenocytes from individual animals undergoing GO with 30-, 10-, and 3-μg/mL rhTSHR-E antigen for 5–6 days showed significant T-cell responses in most animals in both the centers; control animals immunized with β-Gal did not show any significant response, except for 1 immune control β-Gal plasmid injected animal in center 2, which showed a positive response to rhTSHR-E antigen at 30-μg/mL rhTSHR-E antigen (Figure 3A).

To further investigate the specific subset of CD4+ T cells activated by immunization with TSHR A-subunit plasmid in the GO model, we determined the cytokine profiles in T cell recall assays of primed T cells cultured in the presence of rhTSHR-E antigen. Cytokine responses were evaluated by 2 different protocols, including intracellular IFN-γ expression and as cytokine secretion into culture medium. Significantly increased frequencies of intracellular IFN-γ^+ T cells specific for rhTSHR-E antigen were present in animals undergoing GO compared with control β-Gal-immunized mice (Figure 3B). In addition, as shown in Figure 3, C–F, analysis of culture supernatants from splenocyte cultured with rhTSHR-E antigen showed high levels of cytokines including IFN-γ, IL-10, IL-6, and TNF-α into the culture medium in response to rhTSHR-E antigen. On the other hand, IL-17 secretory responses in center 1 and center 2 immune animals were detected at low levels in some immune animals, but most responses were below the threshold of detection in the system (data not shown). The increased cytokine secretion in immune animals responding to rhTSHR-E antigen compared with control β-Gal mice were above mean of the group for IFN-γ (40%–75%), IL-10 (40%–45%), IL-6 (20%–55%), and TNF-α (20%–75%) in both centers (Figure 3,

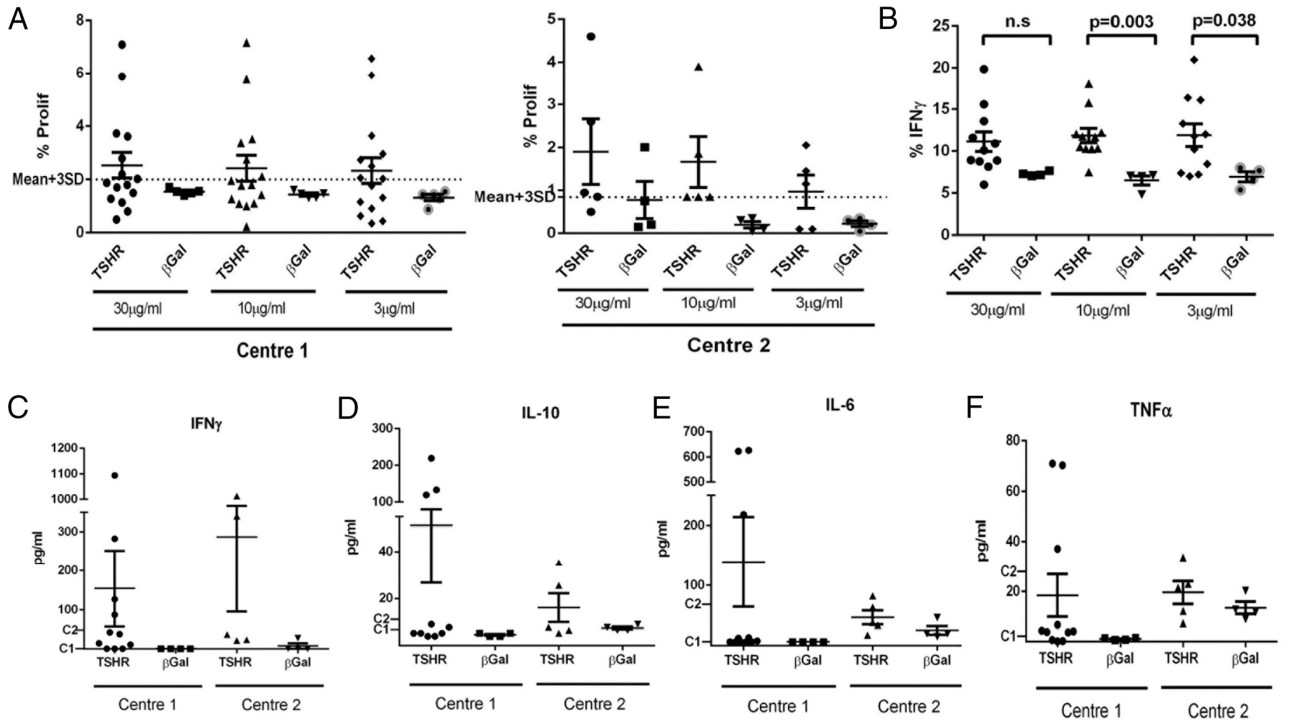

Figure 3. Proliferation and expression of proinflammatory cytokines in antigen-specific T cells. Culture of total splenocytes from individual immune animals undergoing GO were incubated with 30-, 10-, and 3-μg/mL rhTSHR-E antigen for 5–6 days. T-cell proliferation assay using either 5,6-carboxylfluorescein diacetate succinimidyl ester or eFlour670 dye-based assays in center 1 or center 2, respectively (A). The dotted line indicates the mean ± 3 SD for T proliferation of the control β-Gal-immunized mice (A). Frequencies of intracellular IFN-γ^+ T cells (B). Secretion of cytokines IFN-γ, IL-10, IL-6, and TNF-α into the culture medium incubated with 30-μg/mL rhTSHR-E antigen (C–F).

C–F). The strong cytokine response in IFN-γ, IL-10, IL-6, and TNF-α in animals undergoing GO suggests that T cells specific for TSHR antigen are likely to be involved in the pathogenesis of GO in the model.

Discussion

Studies of animal models of autoimmunity evaluated in multiple laboratories have shown that animal housing and environmental conditions to critically influence the development, disease incidence and severity of autoimmune conditions (12–14). Thus, studies on replicating the models in other laboratories have sometimes proved difficult. The major aim of the present study was to expand on our earlier observations on the development of a preclinical mouse model of experimental Graves' disease by evaluating the GO model in an independent laboratory. We ensured the same strain of animals used in our earlier study, BALB/cOlaHsd were immunized in the 2 centers (11). This issue was critically important, because inconsistent results have been reported in adenovirus-hTSHR A-subunit model of Graves' disease induced in other strains like BALB/cBy mice (18, 19). Moreover, in the studies reported here, we were unable to assess proptosis in the animals undergoing experimental GO. Proptosis is not observable by clinical examination, but only by small animal magnetic resonance imaging, as shown in our earlier study (11). Because small animal imaging facilities were not available in center 2, we did not conduct magnetic resonance imaging for comparative studies described in this report.

At the antibody level, sustained levels of antibodies to TSHR and pathogenic TSAbs and TSBAbs were induced in all the animals in both centers. Interestingly, center 2 animals showed higher levels of these antibodies, suggesting stronger immunization in this group. Although, we sought to use identical electroporation conditions in both locations, it is possible that stronger immunization may have occurred in center 2, equipped with the latest high tech digital electroporator. However, despite the presence of TSAbs in immune mice in center 1 and center 2, there was a marked difference in the induction of clinical hyperthyroidism as manifest by total serum T_4 levels, with animals in center 1 with significantly elevated levels of serum T_4 and characteristic microfollicular histology of hyperthyroidism, whereas all immune animals in center 2 remained euthyroid and normofollicular. The reasons for this discrepancy may arise from the stronger immuniza-

doi: 10.1210/en.2015-1829 press.endocrine.org/journal/endo 1679

tion in center 2 postulated above, which as shown by McLachlan et al does not lead to elevated levels of serum T_4 (6). As reported in our earlier studies, another consistent feature in the GO model described in this report for center 1 and center 2 animals has been the appearance of antibodies to IGF-1R α-subunit in some animals immunized with hTSHR A-subunit plasmid (10, 11). The finding that some hTSHR A-subunit plasmid-challenged animals in both center 1 and center 2 were positive for IGF-1R α-subunit antibodies provides further evidence that their induction was not restricted to a unique environmental or animal housing attribute present in center 1, where our earlier studies were conducted (10, 11).

Orbital pathology in preclinical model developed in the 2 locations

Examination of orbital tissue by H&E staining showed concordant pathology in mice undergoing GO in the 2 centers, manifest by expansion of the orbital adipose tissue. However, in contrast no inflammatory infiltrate was apparent in the orbital tissue in immune mice from either of the centers. Instead, all immune animals from both the centers revealed perifascicular atrophy of orbital muscles with appearances that are consistent with a dysimmune myopathy, pathologically similar to dermatomyositis (20, 21). The most obvious changes were seen in the inferior and medial rectus muscles of the mice, the 2 most often affected muscles in GO patients. The orbital pathology has the appearance of inflammatory lesion sequelae, but on this occasion with no inflammatory cells in the orbital muscle tissue. Perifascicular muscle atrophy is ischemic in origin, which in our case arises in a clear inflammatory background. In an effort to explain these results, we speculate that the orbital muscle myopathy is mediated by a "hit-and-run" immune-mediated inflammatory event (22), resulting from orbital tissue damage involving vascular structures from infiltrating T cells early in the onset of disease. Subsequently, when the animals were killed at 9 weeks after the end of immunization, the infiltrating cells may have died due to low affinity autoreactive T-cell receptor interactions, activation-induced cell death or poor costimulation; indeed they may also have also egressed from the orbital region, leaving an inflammatory footprint of orbital muscle damage as a sign of their activity. Interestingly, the role of myopathy as an element of the orbital damage have been highlighted in early histopathological studies on orbital muscle tissue from GO patients, and our studies on the preclinical model are consistent with these classical observations (23–26).

T-cell reactivity to hTSHR antigen and cytokine patterns

Although GO has been considered to be a T cell-mediated condition, the antigen specificity of the T cells in the disease has remained unknown (27, 28). To characterize the T-cell responses induced by hTSHR A-subunit plasmid immunization in the GO model, we examined the proliferative response of splenic cells from individual immune and control β-Gal plasmid-immunized mice to rhTSHR-E antigen. Antigen-specific proliferation to the receptor antigen in both center 1 and center 2 animals immunized with hTSHR A-subunit plasmid was demonstrated with the splenic T cells, which were absent in control β-Gal plasmid-immunized mice; however, 1 control β-Gal plasmid injected animal showed positive proliferative response to rhTSHR-E antigen in center 2. Otherwise, this animal did not show any visible signs of sickness or any other abnormal features which may relate to a heightened immune response. The proliferative responses differed in individual immune animals, possibly reflecting different degrees of immune stimulation or proportions of antigen-specific T cells induced in the model.

In numerous studies, examination of orbital infiltrating mononuclear cells in human GO have revealed regulation of multiple cytokines, particularly IFN-γ and TNF-α, which may be relevant for disease pathogenesis (29, 30). Stimulation with rhTSHR-E antigen induced secretion of a complex array of proinflammatory cytokines IFN-γ, IL-10, IL-6, and TNF-α, consistent with the view that Th1 type cells act as effectors in GO. Other studies on experimental Graves' disease in BALB/c mice have also implicated IFN-γ, IL-10, and TNF-α to be important cytokines in disease pathogenesis (19, 31, 32). However, the role of IFNγ in Graves' disease remains uncertain, because using *IFN-*$\gamma-/-$ gene knockout animals have given contradictory results. In 1 study, development of experimental Graves' disease in *IFN-*$\gamma-/-$ gene knockout animals in BALB/c background indicated successful induction of disease (33), whereas other studies showed refractoriness to the disease (34), suggesting a complex role for IFN-γ in the disease.

There has been recent debate on the contribution of subsets of Th1 helper cells, Th2 helper cells or Th17-type CD4+ T cells in pathogenesis of Graves' disease (35). Th17-type CD4+ T cells have been implicated to play important roles in autoimmune disease, but a number of studies have shown a redundant role for IL-17 in mouse models of Graves' disease (36, 37). Whether these findings can be extrapolated to our GO model remains uncertain. However, our studies show stimulation of splenocyte T cells from animals in both center 1 and center 2 undergoing GO with rhTSHR-E antigen resulted in production of

low levels of IL-17, but most the immune animals did not show any detectable IL-17 secretion, supporting findings of a redundant role for this cytokine in the GO model.

Our observations showing high IL-10 secretory responses in TSHR-specific T cells may indicate its important role in GO. A pathogenic role for T cell-derived IL-10 has been investigated in *IL-10−/−* mice in the BALB/c background resulting in reduction of disease activity (38, 39). However, contradictory data has been reported in other studies, where delivery of IL-10 with recombinant adenovirus in experimental Graves' disease model produced attenuation in disease activity, rather than exacerbation of the disease. Additional evidence for the role of IL-10 in human Graves' disease include reports on increased serum concentrations of IL-10 in patients with active disease, as well as genetic associations in IL-10 gene (40).

Our findings on TSHR antigen stimulated secretion of the proinflammatory cytokine IL-6 in immune animals undergoing GO are interesting, because this cytokine has been implicated in disease pathogenesis (2). The addition of IL-6 to in orbital fibroblast cultures has been shown to lead to increased expression of TSHR, which consequently could amplify the autoimmune response to the receptor in the pathogenesis of GO (41). Moreover, stimulation of orbital fibroblast cultures from active GO patients through CD40 engagement or with TSH or TSAb monoclonal antibody increases expression of IL-6 within the orbital tissue (42, 43). Serum from patients with Graves' disease, particularly those with active GO are known to have elevated levels of IL-6 (44). This, together with the local expression of IL-6 within the orbital tissues occurring by stimulation of orbital fibroblasts with TSAbs (45) may be sufficient for pathogenesis. Other recent studies have also investigated a pathogenic role for IL-6 in experimental Graves' disease, where a critical role for this proinflammatory cytokine was identified in a transgenic CD40-thyroid overexpression model (19). These findings have led to investigations to validate the role of anti-IL-6 humanized monoclonal, tocilizumab in treating GO, with encouraging results reported (46). More detailed analysis of the cytokine secretion patterns from individual immune animals evaluated in this study showed splenic T cells stimulated with rhTSHR-E antigen to be simultaneously secreting high levels of all the proinflammatory cytokines IFN-γ, IL-10, IL-6, and TNF-α. However, we were unable to find any correlation of cytokine secretion pattern with any feature of orbital pathology, nor with the multiplicity of cytokines secreted by the hTSHR-E antigen stimulated T cells, showing that the development of orbital pathology is more complex than merely the secretory cytokine patterns.

Comments on the preclinical GO model

Our experience in working with the preclinical mouse model of GO has shown that despite the successful induction of orbital pathogenesis, the model was also associated with differences in other aspects of induced experimental GO. These differences appear to arise when different groups of animals were immunized at different time points over the past 3 years in our laboratory (in center 1) and relate in particular to 2 features, namely the autoimmune induced endocrine status of the mice undergoing GO and the histological features of orbital pathology in hTSHR A-subunit-immunized mice. For example, in our earlier study (in center 1), 6 independent groups comprising of a total of 67 BALB/c mice immunized with hTSHR A-subunit or the control β-Gal plasmid by electroporation were established for studies on experimental GO (10, 11). In 1 study, all the hTSHR A-subunit plasmid-immunized animals showed a clear hyperthyroid status, both in terms of significant increase in serum T_4 levels and on activated thyroid follicular cell features of thyroid histology (10). However, subsequent groups of immune animals showed clear hypothyroid status using the same criteria to identify endocrine status of the mice (11). Because the experiments were conducted in the same animal housing unit (center 1), we inferred in those studies that the differences could be due to subtle differences in the leg muscle injection procedure of the plasmid during the immunization procedure (11). Moving to the studies described in this report, we find that in the new group of animals housed in center 1, a number of hTSHR A-subunit plasmid-immunized animals presented with clear hyperthyroidism. Thus, the data indicates undertaking of a complete circle in the model, where the autoimmune induced endocrine status has varied from hyper- to hypothyroid and, as reported in this study, back to hyperthyroid status. On this basis, we believe that the induction of stimulating or blocking antibodies responsible for the endocrine status in the model appear to be induced in a random fashion (10, 11). Similarly, our findings also show that it is difficult to predict the precise pattern of orbital pathology that may likely develop after immunization with hTSHR A-subunit plasmid, although all immune animals will ultimately progress to develop the orbital condition when left for number of weeks after the last immunization.

Other features in the GO model such as the induction of orbital inflammation, orbital fibrosis (10, 11), or the orbital myopathy reported here (in both center 1 and center 2) also appear to be variable in disease onset and difficult to predict, and it may be part of all aspects of common inflammatory damage and repair within the orbital tissue. The most likely target for that damage would be the blood vessels (endothelial cells resulting in ischemic

doi: 10.1210/en.2015-1829 press.endocrine.org/journal/endo 1681

changes for which the skeletal muscles as kinetically terminal cells would be particularly vulnerable) (20, 47) and mesenchymal stem cells (22). In support of this, we and others have recently identified mesenchymal stem cells in the retrobulbar fat and connective tissue (48, 49). Moreover, orbital fibroblasts shared functional and immunophenotypic properties with the orbital mesenchymal stem cells indicating that mesenchymal progenitors are effectively present in the orbital fibroblast population of GO patients (48, 49).

In summary, we show that the experimental model of GO induced by hTSHR A-subunit plasmid immunization of female BALB/c mice is a robust model in different environment exposures. The model faithfully reproduces pathogenic antibodies to TSHR and cell mediated T-cell responses to TSHR protein antigen accompanied by strong proinflammatory cytokine responses. A reproducible orbital feature present in animals undergoing experimental GO in different location and environment exposures is the onset of adipogenesis in all groups of immune animals examined to date. We report on a new additional feature of orbital muscle damage in the model by characteristic signs of muscle myopathy and postulate a hit-and-run immune-mediated inflammatory event involving blood vessels (endothelial cells) and mesenchymal stem cells. Within the orbital lesion of adipogenesis, we postulate that the kinetics of onset of orbital disease and the end stage result of orbital disease characterized by either orbital inflammation, fibrosis or myopathy are governed by unknown events during the chronic phase of induced hyper- or hypothyroidism, but all expressing a common pathway from the initial inflammatory injury. Future studies will need to identify the role of pathogenic antibodies to TSHR together with the engagement of receptor-specific T cells and their secreted cytokines and their effects on the orbital fibroblast populations within the orbital milieu in the disease process.

Acknowledgments

We thank Christoph Jesenek (University Duisburg-Essen, Germany) for technical assistance. We also thank Dr Andrea Jahraus, Apitope International NV, Belgium, for the gift of purified preparations of rhTSHR-E protein.

Address all correspondence and requests for reprints to: J. Paul Banga, PhD, Molecular Ophthalmology, Department of Ophthalmology, University Hospital Essen/University of Duisburg-Essen, 45147 Essen, Germany. E-mail: paul.banga@kcl.ac.uk; or Anja Eckstein, MD. E-mail: anja.eckstein@uk-essen.de.

This work was supported by internal King's College London funds (J.P.B.), Deutsche Forschungsgemeinschaft Grants BE 3177/3-1 (to U.B.-P., A.E., and J.P.B.) and BE3177/2-1 (to U.B.-P.), Bielschowsky Gesellschaft (U.B.-P. and A.E.) and Marie Sklodowska Curie Industry Industry-Academia Pathways and Partnerships (IAPP) action, GA number 612116 project INDIGO, to AE and others.

Disclosure Summary: The authors have nothing to disclose.

References

1. **Weetman AP.** Graves' disease. *N Engl J Med*. 2000;343:1236–1248.
2. **Bahn RS.** Graves' ophthalmopathy. *N Engl J Med*. 2010;362:726–738.
3. **Feliciello A, Porcellini A, Ciullo I, Bonavolontà G, Avvedimento EV, Fenzi G.** Expression of thyrotropin-receptor mRNA in healthy and Graves' disease retro-orbital tissue. *Lancet*. 1993;342:337–338.
4. **McLachlan SM, Prummel MF, Rapoport B.** Cell-mediated or humoral immunity in Graves' ophthalmopathy? Profiles of T-cell cytokines amplified by polymerase chain reaction from orbital tissue. *J Clin Endocrinol Metab*. 1994;78:1070–1074.
5. **Teng MW, Bowman EP, McElwee JJ, et al.** IL-12 and IL-23 cytokines: from discovery to targeted therapies for immune-mediated inflammatory diseases. *Nat Med*. 2015;21:719–729.
6. **McLachlan SM, Nagayama Y, Rapoport B.** Insight into Graves' hyperthyroidism from animal models. *Endocr Rev*. 2005;26:800–832.
7. **Wiesweg B, Johnson KT, Eckstein AK, Berchner-Pfannschmidt U.** Current insights into animal models of Graves' disease and orbitopathy. *Horm Metab Res*. 2013;45:549–555.
8. **Banga JP, Moshkelgosha S, Berchner-Pfannschmidt U, Eckstein A.** Modeling Graves' orbitopathy in experimental Graves' disease. *Horm Metab Res*. 2015;47:797–803.
9. **Chen CR, Pichurin P, Chazenbalk GD, et al.** Low-dose immunization with adenovirus expressing the thyroid-stimulating hormone receptor A-subunit deviates the antibody response toward that of autoantibodies in human Graves' disease. *Endocrinology*. 2004;145:228–233.
10. **Zhao SX, Tsui S, Cheung A, Douglas RS, Smith TJ, Banga JP.** Orbital fibrosis in a mouse model of Graves' disease induced by genetic immunization of thyrotropin receptor cDNA. *J Endocrinol*. 2011;210:369–377.
11. **Moshkelgosha S, So PW, Deasy N, Diaz-Cano S, Banga JP.** Cutting edge: retrobulbar inflammation, adipogenesis, and acute orbital congestion in a preclinical female mouse model of Graves' orbitopathy induced by thyrotropin receptor plasmid-in vivo electroporation. *Endocrinology*. 2013;154:3008–3015.
12. **Burek CL, Talor MV.** Environmental triggers of autoimmune thyroiditis. *J Autoimmun*. 2009;33:183–189.
13. **Pozzilli P, Signore A, Williams AJ, Beales PE.** NOD mouse colonies around the world–recent facts and figures. *Immunol Today*. 1993;14:193–196.
14. **Goverman J, Woods A, Larson L, Weiner LP, Hood L, Zaller DM.** Transgenic mice that express a myelin basic protein-specific T cell receptor develop spontaneous autoimmunity. *Cell*. 1993;72:551–560.
15. **Gilbert JA, Gianoukakis AG, Salehi S, et al.** Monoclonal pathogenic antibodies to the thyroid-stimulating hormone receptor in Graves' disease with potent thyroid-stimulating activity but differential blocking activity activate multiple signaling pathways. *J Immunol*. 2006;176:5084–5092.
16. **Inaba H, Moise L, Martin W, et al.** Epitope recognition in HLA-DR3

transgenic mice immunized to TSH-R protein or peptides. *Endocrinology*. 2013;154:2234–2243.
17. **Johnson KT, Wiesweg B, Schott M, et al.** Examination of orbital tissues in murine models of Graves' disease reveals expression of UCP-1 and the TSHR in retrobulbar adipose tissues. *Horm Metab Res*. 2013;45:401–407.
18. **Seetharamaiah GS, Land KJ.** Differential susceptibility of BALB/c and BALB/cBy mice to Graves' hyperthyroidism. *Thyroid*. 2006;16:651–658.
19. **Huber AK, Finkelman FD, Li CW, et al.** Genetically driven target tissue overexpression of CD40: a novel mechanism in autoimmune disease. *J Immunol*. 2012;189:3043–3053.
20. **Dalakas MC.** Progress in inflammatory myopathies: good but not good enough. *J Neurol Neurosurg Psychiatry*. 2001;70:569–573.
21. **Gherardi RK.** Pathogenic aspects of dermatomyositis, polymyositis and overlap myositis. *Presse Med*. 2011;40:e209–e218.
22. **Levy O, Zhao W, Mortensen LJ, et al.** mRNA-engineered mesenchymal stem cells for targeted delivery of interleukin-10 to sites of inflammation. *Blood*. 2013;122:e23–e32.
23. **Jacobson DH, Gorman CA.** Endocrine ophthalmopathy: current ideas concerning etiology, pathogenesis, and treatment. *Endocr Rev*. 1984;5:200–220.
24. **Hufnagel TJ, Hickey WF, Cobbs WH, Jakobiec FA, Iwamoto T, Eagle RC.** Immunohistochemical and ultrastructural studies on the exenterated orbital tissues of a patient with Graves' disease. *Ophthalmology*. 1984;91:1411–1419.
25. **Jensen SF.** Endocrine ophthalmoplegia. Is it due to myopathy or to mechanical immobilization? *Acta Ophthalmol (Copenh)*. 1971;49:679–684.
26. **Hermann JS.** Paretic thyroid myopathy. *Ophthalmology*. 1982;89:473–478.
27. **Bednarczuk T, Hiromatsu Y, Inoue Y, Yamamoto K, Wall JR, Nauman J.** T-cell-mediated immunity in thyroid-associated ophthalmopathy. *Thyroid*. 2002;12:209–215.
28. **Feldon SE, Park DJ, O'Loughlin CW, et al.** Autologous T-lymphocytes stimulate proliferation of orbital fibroblasts derived from patients with Graves' ophthalmopathy. *Invest Ophthalmol Vis Sci*. 2005;46:3913–3921.
29. **Heufelder AE, Bahn RS.** Detection and localization of cytokine immunoreactivity in retro-ocular connective tissue in Graves' ophthalmopathy. *Eur J Clin Invest*. 1993;23:10–17.
30. **Hiromatsu Y, Kaku H, Miyake I, Murayama S, Soejima E.** Role of cytokines in the pathogenesis of thyroid-associated ophthalmopathy. *Thyroid*. 2002;12:217–221.
31. **Pichurin P, Schwarz-Lauer L, Braley-Mullen H, et al.** Peptide scanning for thyrotropin receptor T-cell epitopes in mice vaccinated with naked DNA. *Thyroid*. 2002;12:755–764.
32. **Nagayama Y, Watanabe K, Niwa M, McLachlan SM, Rapoport B.** Schistosoma mansoni and α-galactosylceramide: prophylactic effect of Th1 immune suppression in a mouse model of Graves' hyperthyroidism. *J Immunol*. 2004;173:2167–2173.
33. **Dogan RN, Vasu C, Holterman MJ, Prabhakar BS.** Absence of IL-4, and not suppression of the Th2 response, prevents development of experimental autoimmune Graves' disease. *J Immunol*. 2003;170:2195–2204.
34. **Nagayama Y, Saitoh O, McLachlan SM, Rapoport B, Kano H, Kumazawa Y.** TSH receptor-adenovirus-induced Graves' hyperthyroidism is attenuated in both interferon-γ and interleukin-4 knockout mice; implications for the Th1/Th2 paradigm. *Clin Exp Immunol*. 2004;138:417–422.
35. **Rapoport B, McLachlan SM.** Graves' hyperthyroidism is antibody-mediated but is predominantly a Th1-type cytokine disease. *J Clin Endocrinol Metab*. 2014;99:4060–4061.
36. **Horie I, Abiru N, Saitoh O, et al.** Distinct role of T helper type 17 immune response for Graves' hyperthyroidism in mice with different genetic backgrounds. *Autoimmunity*. 2011;44:159–165.
37. **Zhou J, Bi M, Fan C, et al.** Regulatory T cells but not T helper 17 cells are modulated in an animal model of Graves' hyperthyroidism. *Clin Exp Med*. 2012;12:39–46.
38. **Ueki I, Abiru N, Kawagoe K, Nagayama Y.** Interleukin 10 deficiency attenuates induction of anti-TSH receptor antibodies and hyperthyroidism in a mouse Graves' model. *J Endocrinol*. 2011;209:353–357.
39. **Saitoh O, Mizutori Y, Takamura N, et al.** Adenovirus-mediated gene delivery of interleukin-10, but not transforming growth factor β, ameliorates the induction of Graves' hyperthyroidism in BALB/c mice. *Clin Exp Immunol*. 2005;141:405–411.
40. **Takeoka K, Watanabe M, Matsuzuka F, Miyauchi A, Iwatani Y.** Increase of serum interleukin-10 in intractable Graves' disease. *Thyroid*. 2004;14:201–205.
41. **Jyonouchi SC, Valyasevi RW, Harteneck DA, Dutton CM, Bahn RS.** Interleukin-6 stimulates thyrotropin receptor expression in human orbital preadipocyte fibroblasts from patients with Graves' ophthalmopathy. *Thyroid*. 2001;11:929–934.
42. **Sempowski GD, Rozenblit J, Smith TJ, Phipps RP.** Human orbital fibroblasts are activated through CD40 to induce proinflammatory cytokine production. *Am J Physiol*. 1998;274:C707–C714.
43. **Kumar S, Schiefer R, Coenen MJ, Bahn RS.** A stimulatory thyrotropin receptor antibody (M22) and thyrotropin increase interleukin-6 expression and secretion in Graves' orbital preadipocyte fibroblasts. *Thyroid*. 2010;20:59–65.
44. **Molnár I, Balázs C.** High circulating IL-6 level in Graves' ophthalmopathy. *Autoimmunity*. 1997;25:91–96.
45. **Wakelkamp IM, Bakker O, Baldeschi L, Wiersinga WM, Prummel MF.** TSH-R expression and cytokine profile in orbital tissue of active vs. inactive Graves' ophthalmopathy patients. *Clin Endocrinol*. 2003;58:280–287.
46. **Salvi M, Campi I.** Medical treatment of Graves' orbitopathy. *Horm Metab Res*. 2015;47:779–788.
47. **Choudhary MM, Hajj-Ali RA, Lowder CY.** Gender and ocular manifestations of connective tissue diseases and systemic vasculitides. *J Ophthalmol*. 2014;2014:403042.
48. **Brandau S, Bruderek K, Hestermann K, et al.** Orbital fibroblasts from Graves' orbitopathy patients share functional and immunophenotypic properties with mesenchymal stem/stromal cells. *Invest Ophthalmol Vis Sci*. 2015;56:6549–6557.
49. **Kozdon K, Fitchett C, Rose GE, Ezra DG, Bailly M.** Mesenchymal stem cell-like properties of orbital fibroblasts in Graves' orbitopathy. *Invest Ophthalmol Vis Sci*. 2015;56:5743–5750.

Materials and Methods

Animals and immunization with eukaryotic plasmid expressing hTSHR A-subunit and electroporation

Animals were fed *ad libitum* on water and commercial diet; the food pellets in centre 2 contained almost twice the levels of iodide compared to centre 1 diet pellets (Supplemental Table 1). The eukaryotic expression plasmid, pTriEx1.1Neo-hTSHR A-subunit (otherwise known as hTSHR289) and the control pTri1Ex1.1Neo-β-Gal plasmid have been described (1). All plasmids were purified from *E coli* extracts as a large single preparation using Qiagen Giga kits, the purified plasmids eluted from different columns, pooled and stored aliquoted at -80C. Subsequently, the aliquoted tubes were divided for immunizations in the two locations. Female BALB/c mice were anesthetized and injected with 50 µl (1mg/ml) into each biceps femoris muscle as described in detail before (1). Electroporations were performed in centre 1 using a BTX ECM830 square wave electroporator with 7-mm calliper electrodes at 112V/cm with current application in twelve-20 millisecond square wave pulses at 1 Hz (1); in centre 2, a BTX Gemini X^2 electroporation system was used with 7-mm calliper electrodes at 120V/cm with current application in two series of six-20 millisecond square wave pulses at 1 Hz. Injection and electroporation was performed 4 times at 3-week intervals. Thereafter the immune animals were left for 9 weeks after the end of immunization to allow development of chronic disease phase in hTSHR A-subunit plasmid challenged animals.

Antibody and serum thyroxine assays

All serum determinations were in individual mice for total T4, anti-TSHR antibodies, and their subtypes TSAbs and TSH binding blocking antibodies (TSBAbs), which were all evaluated together in single respective assays performed in centre 2 (1). TSH binding inhibitory imunoglobulins (TBII) were evaluated in TRAK assay

(ThermoFisher, BRAHMS, Germany) essentially according to the kit instructions. Briefly, 50µl test immune mouse serum was mixed with 50µl normal human serum (with negligible TRAK activity) and added to the appropriate tubes coated with captured recombinant hTSHR. All tubes, including standards were incubated for 2h with shaking at room temperature and after washing twice with 2ml wash buffer provided in the kit, 200µl of ^{125}I-TSH was added to each tube, incubation continued for 1hr with shaking at room temperature. Finally, the tubes were washed three times, each with 2ml wash buffer, dried and counted in a gamma counter. % inhibition of labeled TSH binding was calculated from the data, with 0% inhibition value derived from total ^{125}I-TSH binding to the tubes in the absence of any competitor serum.

Antibodies to IGF-1R were evaluated in single determination at 1:30 dilution by ELISA, using Nunc MaxiSorb plates coated with 100µl of 3.3µg/ml rIGF-R (R&D Systems, UK), and assay performed as described (1). In our laboratory, this assay has intra- and inter-assay coefficients of variation (CV) of <5% (1), we have previously shown that these anti-IGF-1R α-subunit antibodies also recognize hIGF-R in stably transfected CHO cells by flow cytometry (unpublished, Sajad Moshkelgosha, PhD thesis, University of London 2015). All serum samples from centre 1 and centre 2 animals were evaluated together in the same assay, which were all carried out in centre 2 laboratories.

Antigen specific splenocyte responses to TSHR protein antigen

Purified recombinant hTSHR extracellular region protein (amino acids 20 to 419) (rhTSHR-E) expressed in baculovirus system was provided by Apitope International NV (2). Splenocyte proliferation assays were evaluated using either CFSE (5,6-carboxylfluorescein diacetate succinimidly ester) or eFlour670 dye based assays in centre 1 or centre 2 respectively. The proliferation assay was first optimized in centre

2 for dose of rhTSHR-E antigen and culture time and optimal conditions then used in both centre 1 and centre 2 for test samples.

The CFSE proliferation assays in centre 1 were performed using spleens harvested at 9 weeks post immunization and analyzed in a blinded fashion. Single cell suspensions of splenocytes from individual animals were prepared, washed twice in PBS and labelled with 2.5μM CFSE (Invitrogen) for 10 minutes at 37C ($2.5x10^7$/ml in PBS). After washing, cells were cultured in XVIVO-15 serum-free medium (Lonza) at $5x10^6$/ml, in 200μl cultures at 37C 5% CO_2, with rhTSHR-E at 3, 10 or 30 μg/ml. After 6 days cells were washed and stained with fluorochrome-labelled antibodies for CD4 (RM-4-5, eBioscience) and CD8β (53-5.8, BioLegend), followed by analysis on a BD FACScalibur™ flow cytometer and CellQuest™ software (BD Biosciences). Cells were gated on viable $CD4^+$ lymphocytes and the proportion of these cells with low CFSE fluorescence was assessed as % proliferation. $CD8^+$ cells showed negligible responses.

In centre 2, in initial experiments, spleen cells from individual 5 immune mice challenged with hTSHR A-subunit plasmid and 4 β-Gal control mice were used for culture optimisation experiments. Thus, data shown from centre 2 are from remaining 5 immune hTSHR A-subunit plasmid challenged animals and 4 β-Gal control plasmid mice. Following the optimization of the assay, antigen specific proliferation was evaluated by using splenic mononuclear cells ($5x10^5$ cells) from individual hTSHR A-subunit or β-Gal plasmid immunized mice labelled with the dye, eFlour670 (eBioscience Frankfurt, Germany) and cultured with 3, 10 or 30μg/ml rhTSHR-E protein respectively for 5 days. Proliferation was assessed as loss of eFlour670 dye signal on gated T cells by flow cytometry (LSRII BD Biosciences, Heidelberg Germany).

Cytokine *assays*

Cytokine response of T cells to rhTSHR-E antigen were measured by intracellular IFN-γ expression (centre 1) and as cytokine secretion into culture media (centre 1 and centre 2). Spleen cells cultured as described above were washed on day 6 of culture and restimulated with PMA (20ng/ml), ionomycin (400ng/ml) and monensin (3μM) for 4 hours. Cells were then fixed in 4% formaldehyde, permeabilized with 0.1% saponin/1% FCS in PBS, and stained for IFN-γ (XMG1.2, BioLegend) in addition to CD4 and CD8, before flow cytometric analysis. %IFN-γ^+ cells within $CD4^+$ populations relative to negative controls were calculated.

For assessment of secreted cytokines, all culture supernatants from T cell proliferation assays from centre 1 and centre 2 collected after 5 or 6 days were measured simultaneously together in a single assay to ensure data is comparable. The culture supernatants were assayed for the presence of IFN-γ, IL-17, IL-10, IL-6 and TNF-α using a Luminex Screening assay (R&D Systems, Wiesbaden, Germany) according to the manufacturer's recommendations. The assay was performed on a Luminex 200 instrument, and levels of cytokines were calculated with the Luminex IS software (Luminex Corporation Austin, TX).

Orbital and thyroid tissue histopathology

Orbital histology and thyroid gland histology were conducted as described (1,3). Quantification of adipose tissue and orbital muscle atrophy in orbital sections of extraorbital nasal and inferior muscle was performed with Image J, where the area of adipose tissue was normalized to the optic nerve area. Cells undergoing atrophy were determined by diameter (<50μm) and round shape of muscle fibers. Immunohistochemistry for CD3+ve T cells infiltrating the orbital tissue was performed as described (1). Analysis of orbital infiltrating CD3+ T cells was conducted by quantifying number of positive cells in six different fields (region of interest, ROI, x200), including four fields in extraorbital muscles and two fields in adipose tissue in

each IHC section derived from individual mouse orbits. The average of infiltrating CD3+ T cells in all six ROI for each mouse orbital section was calculated.

Statistical analyses

Data from TBII activity, proliferation experiments were compared as mean +/- 3SD. Significant differences between the groups were compared by t-test. Two-way ANOVA was used for comparing TBII responses between control and immune mice. Analysis and Z-scoring was performed using Prism 6.01 (GraphPad Software). $p<0.05$ were considered statistically significant.

Supplemental Figureure Legends

Supplemental Figure 1

Appearance of eyes of animals undergoing transient chemosis

Head region of β-Gal plasmid or TSHR A-subunit plasmid immunized mouse undergoing transient chemosis in centre 1 and centre 2.

Supplemental Figure 2

Histological analysis of thyroid glands of animals undergoing GO in centre 1 and centre 2

The thyroid gland of centre 1 (panel A-C) mice revealed normo-microfollicular growth pattern and follicular structures lined by cuboidal-columnar cells (panel A, Hematoxylin-eosin HE-100x), focal inflammatory cell infiltrate (arrows) in immunized mouse (panel B, HE-100x; panel C, higher magnification of inset in panel B, HE-200x). Mouse immunized with control plasmid (panel D-F) show histologically normal pattern (panel D, HE-100x). Normal appearance of thyroid gland from a mouse

immunised with control plasmid (x100). TSHR-immunized euthyroid mice revealed normofollicular appearances (panel E and panel F, HE-100x).

Supplemental Figure 3

Quantification of histological analysis of orbital tissue from animals undergoing GO.

Panel A shows representative histological section of orbital tissue that has been used for pathological quantification. Two of the seven extraorbital muscles, mouse equivalent of the medial rectus muscles (black arrow) and inferior muscles (blue arrow), were selected for quantification (x40). Panel B shows higher magnification of medial rectus muscle (upper left panel) and inferior muscle (lower left panel) (x100) with their adjacent panels showing the result of ImageJ calculation on cells in less than 50μm diameter, which have been used for quantification of atrophic cells per muscle area. Panel C shows results of atrophic cell counts for centre 1 and centre 2 hTSHR A-subunit plasmid immunized mice, normalized against the area of extraorbital muscle fiber for each individual animal. Panel D shows the area of adipose tissue was quantified as displayed by green dotted line in panel (A) and normalized by the area of optic nerve (highlighted by yellow dotted line in panel A). As displayed in Figure 2, TSHR immunized mouse had significantly more atrophic muscle fibers and fat cells.

Supplemental Figure 4

Quantification of CD3+ve cells in orbital tissue by immunohistochemistry

Orbital sections were stained for CD3+ve cells infiltrating into orbital tissue by immunohistochemistry and counted. The scatter plot shows number of cells counted

in 'Region of Interest' (ROI) on the Y-axis. There were no significant (n.s) differences in CD3+ve cells infiltrating the orbital tissue in hTSHR A-subunit plasmid immunized animals versus the control B-Gal plasmid immunized mice in either centre 1 or centre 2 animals. Since orbital muscle damage was apparent in hTSHR A-subunit plasmid immunized animals in both centres, the data formed the basis of our hypothesis on 'hit and run' model in the manuscript.

Supplemental Table 1

Detail of commercial diet food pellets fed in Centre 1 and Centre 2 animals

References

1. Moshkelgosha S, So PW, Deasy N, Diaz-Cano S, Banga JP. Cutting Edge: Retrobulbar Inflammation, Adipogenesis, and Acute Orbital Congestion in a Preclinical Female Mouse Model of Graves' Orbitopathy Induced by Thyrotropin Receptor Plasmid-in Vivo Electroporation. Endocrinology 2013; 154:3008-3015.
2. Inaba H, Moise L, Martin W, De Groot AS, Desrosiers J, Tassone R, Buchman G, Akamizu T, De Groot LJ. Epitope recognition in HLA-DR3 transgenic mice immunized to TSH-R protein or peptides. Endocrinology 2013; 154:2234-2243.
3. Johnson KT, Wiesweg B, Schott M, Ehlers M, Muller M, Minich WB, Nagayama Y, Gulbins E, Eckstein AK, Berchner-Pfannschmidt U. Examination of orbital tissues in murine models of Graves' disease reveals expression of UCP-1 and the TSIIR in retrobulbar adipose tissues.

Hormone and metabolic research = Hormon- und Stoffwechselforschung = Hormones et metabolisme 2013; 45:401-40.

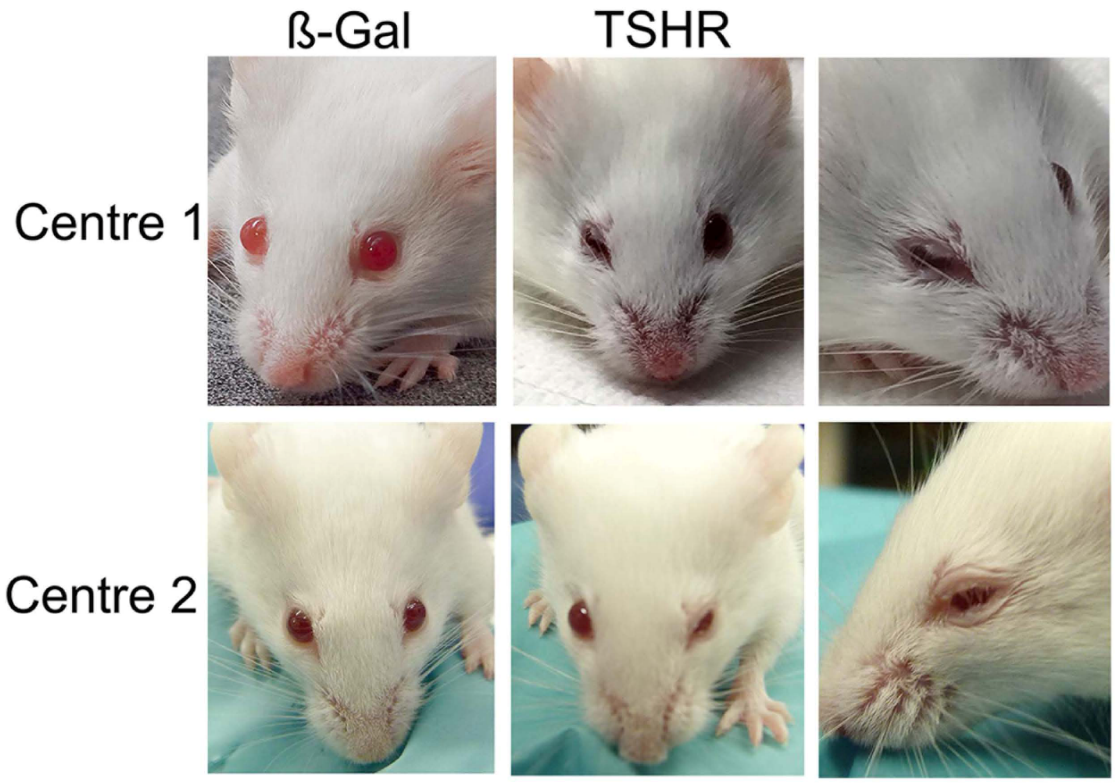

Supplementary Fig 1
Appearance of eyes of animals undergoing transient chemosis

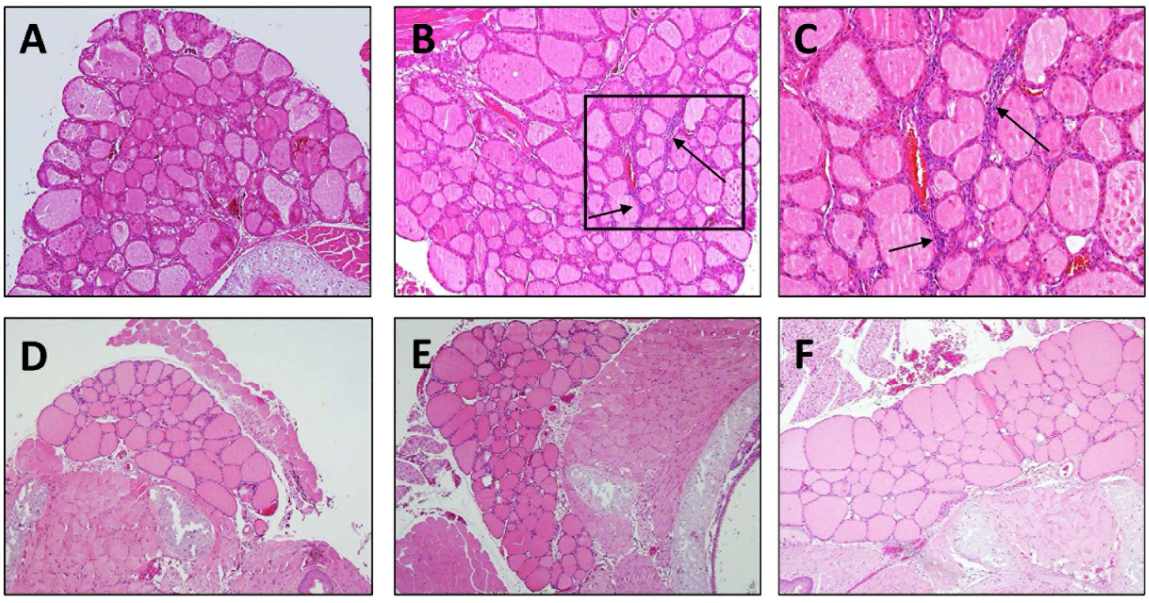

Supplementary Fig 2
Histological analysis of thyroid glands of animals undergoing GO in centre 1 and centre 2

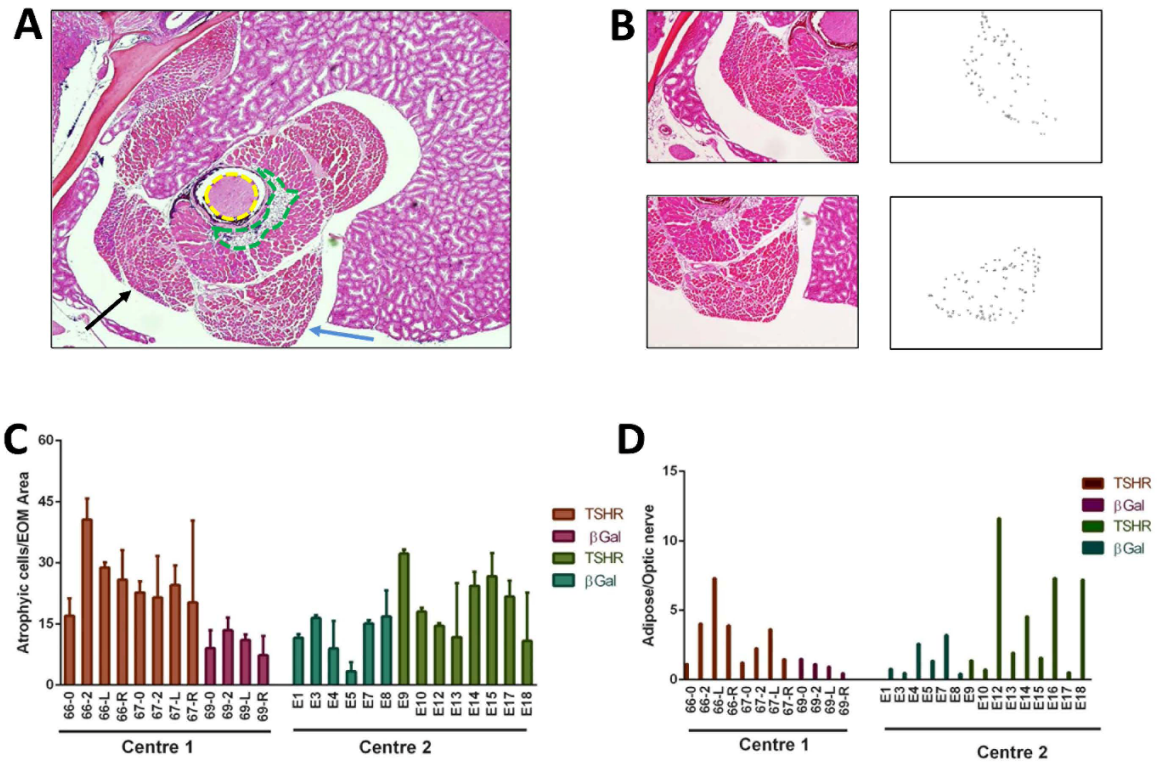

Supplementary Fig 3
Quantification of histological analysis of orbital tissue from animals undergoing GO

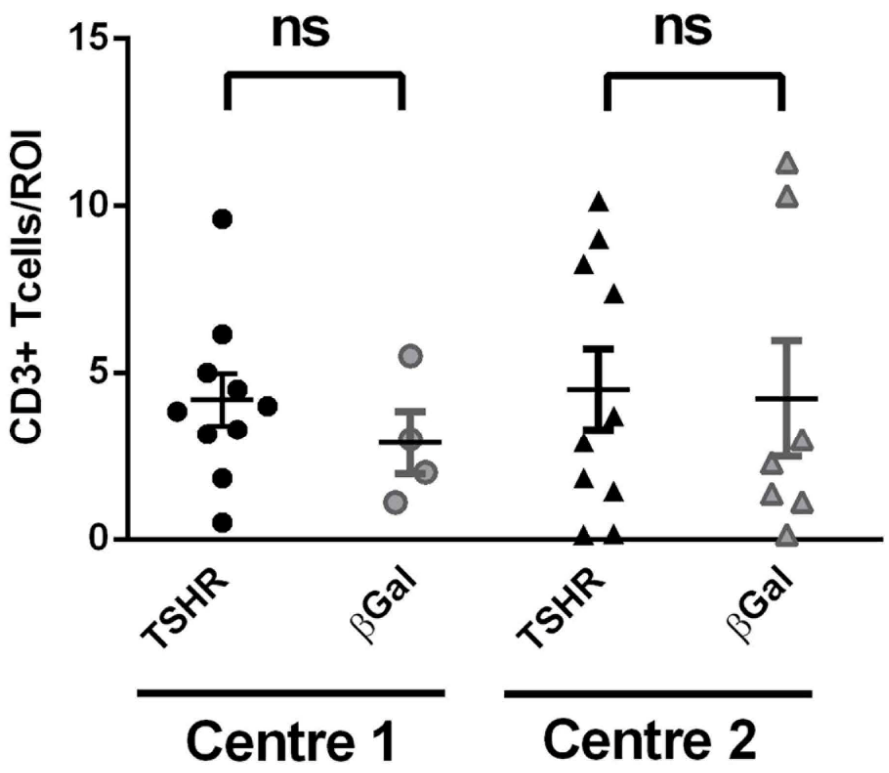

Supplementary Fig 4
Quantification of CD3+ve cells in orbital tissue by immunohistochemistry

		Centre 1	Centre 2
Food diet	Product name	Rat and Mouse No.1 Maintenance,	Rat/Mouse maintenance V1534-300
	Supplier	Special Diet Services, LBS Biotech, UK	Ssniff Spezialadiäten GmbH, Germany
	Protein	14.38%	19.00%
	Fat	2.71%	3.30%
	Fiber	4.65	4.90%
	Ca	0.73%	1.10%
	P	0.52%	0.70%
	Na	0.25%	0.24%
	I	1.2 mg/Kg	2.2 mg/Kg
	Gross Energy	14.74 MJ/Kg	16.3 MJ/Kg
	Metabolizable Energy	10.74 MJ/Kg	12.8 MJ/Kg

Supplementary Table 1
Detail of commercial diet food pellets fed to animals in centre 1 and centre 2

Publication 4

Pathogenic phenotype of adipogenesis and hyaluronan in orbital fibroblasts from female Graves' orbitopathy mouse model

Görtz G-E, Moshkelgosha S, Jesenek C, Horstmann M, Edelmann B, Banga JP, Eckstein A, Berchner-Pfannschmidt U

Endocrinology. 2016 Oct; 157(10):3771-3778

Contribution

In this study, I established cell culture of mouse OF and investigated growth and proliferation of the cells (Fig. 1). I was involved in detection of surface marker by flow cytometry and performed western-blot analysis of target antigens and proteins (Fig. 2, 4). I designed the experimental conditions and conducted adipogenic and myogenic differentiation assays (Fig. 3) and hyaluronan ELISA (Fig. 4). I designed all experiments, analyzed the obtained data and interpreted the results. I contributed to writing of abstract, introduction, methods, results and discussion of the publication.

BRIEF RESEARCH REPORT

Pathogenic Phenotype of Adipogenesis and Hyaluronan in Orbital Fibroblasts From Female Graves' Orbitopathy Mouse Model

Gina-Eva Görtz, Sajad Moshkelgosha, Christoph Jesenek, Bärbel Edelmann, Mareike Horstmann, J. Paul Banga, Anja Eckstein, and Utta Berchner-Pfannschmidt

[1]Molecular Ophthalmology (G.-E.G., S.M., C.J., M.H., J.P.B., A.E., U.B.-P.), Department of Ophthalmology, University Hospital Essen, University of Duisburg-Essen, 45147 Essen, Germany; and Department for Hematology and Oncology (B.E.), Otto-von-Guericke University, 39120 Magdeburg, Germany

A mouse model of Graves' orbitopathy (GO) induced by genetic immunization of human TSH receptor (TSHR) A-subunit encoding plasmid has recently been established. The orbital pathology was characterized by adipogenesis, myopathy and fibrosis. Human orbital fibroblasts (OFs) express TSHR and IGF-1 receptor (IGF-1R) and are considered to be pathogenic in GO. We established conditions for growing ex vivo cultures of mouse OFs (mOFs) from orbital tissue of animals undergoing GO and controls. Early passage mOFs showed characteristic fibroblast morphology and expressed mesenchymal stem cell markers including a strong expression of CD90.2 and CD40, whereas display of CD73 and all other leucocyte markers was uniformly absent. Importantly, OFs derived from GO mice expressed elevated levels of TSHR and IGF-1R and showed enhanced adipogensis compared with controls. Activation of TSHR in mOFs from GO animals with TSH, monoclonal thyroid-stimulating antibody M22, or stimulation of IGF-1R with IGF-1-induced hyaluronan secretion to significantly elevated levels compared with control animals. Hyaluronan synthase 2 was more abundant in OFs derived from GO mice. In conclusion, mOFs established from GO model recapitulate the pathogenicity of human OFs from GO patients by their increased propensity for adipogenesis and hyaluronan production leading to disease activity. To our knowledge, this is the first report to show mOFs from the preclinical GO model have pathogenic properties that will aid in understanding the molecular and genetic changes during progression to adipogenesis and hyaluronan deposition to provide new insights into GO pathogenesis. **(*Endocrinology* 157: 3771–3778, 2016)**

Graves' disease is an antibody mediated autoimmune condition of the thyroid gland, where stimulating antibodies to the TSH receptor (TSHR) activate the gland resulting in hyperthyroidism. One complication of Graves' disease is Graves' orbitopathy (GO), arising from inflammation of the orbital connective tissue in the eye, characterized by adipogenesis and deposition of glycosaminoglycan (1). The orbital fibroblasts (OFs) are the sentinel pathogenic cells in GO and respond to TSHR antibodies, inflammatory T cells, and cytokines in the orbit by undergoing differentiation to adipocytes and hyaluronan production (2). The ability to grow ex vivo human OFs as monolayer cultures from surgical specimens obtained from corrective surgery of GO patients have been instrumental in studying their interaction with the immune system in disease pathogenesis. OFs express functional molecules such as TSHR, IGF-1 receptor (IGF-1R), and CD40 and respond to their activation by differentiation into adipocytes together with secretion of inflammatory cytokines and production of hyaluronan (2, 3). Furthermore, 2 phe-

ISSN Print 0013-7227 ISSN Online 1945-7170
Printed in USA

Received May 10, 2016. Accepted August 19, 2016.
First Published Online August 23, 2016

Abbreviations: α-SMA, α-smooth muscle actin; Ctrl, control; GAPDH, glyceraldehyde 3-phosphate dehydrogenase; GO, Graves' orbitopathy; HAS, hyaluronan synthase; IGF-1R, IGF-1 receptor; mAb, monoclonal antibody; mOF, mouse OF; MSC, mesenchymal stem cell; OF, orbital fibroblast; TSHR, TSH receptor

Table 1. Antibody Table

Peptide/ Protein Target[a]	Name of Antibody	Manufacturer, Catalog Number, and/or Name of Individual Providing the Antibody	Species Raised in; Monoclonal or Polyclonal	Dilution Used
CD90.2	Antimouse CD90.2 (Thy-1.2)	eBioscience, 16-0903	Rat; IgG2b, clone 30-H1	0.1 μg/μL
Sca-1	Mouse Sca-1/Ly6 antibody	R&D Systems, MAB1226	Rat; monoclonal, clone 1777228	0.1 μg/μL
CD106	Mouse VCAM-1/CD106 antibody	R&D Systems, MAB6432	Rat; monoclonal, clone 112734	0.1 μg/μL
CD105	Mouse endoglin/CD105 antibody	R&D Systems, MAB13201	Rat; monoclonal, clone 209721	0.1 μg/μL
CD73	Mouse 5′-nucleotidase/CD73 antibody	R&D Systems, MAB44881	Rat; monoclonal, clone 496424	0.1 μg/μL
CD29	Mouse integrin β1/CD29 antibody	R&D Systems , MAB2405	Rat; monoclonal, clone 265917	0.1 μg/μL
CD11b	Mouse integrin αM/CD11b antibody	R&D Systems, MAB1124	Rat; monoclonal, clone M1/70	0.1 μg/μL
CD45	Mouse CD45 antibody	R&D Systems, MAB114	Rat; monoclonal, clone 30-F11	0.1 μg/μL
CD44	Mouse/rat/porcine/equine CD44 antibody	R&D Systems, AF6127	Sheep; polyclonal, IgG	0.1 μg/μL
M22	RSR-TSHR hmAb M22	RSR limited, M22/FD/0.04	Human; monoclonal, IgG	0.1 μg/mL
TSHR	TSHR (N-19)	Santa Cruz Biotechnology, sc-7816	Goat; polyclonal, IgG	1:200
TSHR	TSHR (4C1)	Santa Cruz Biotechnology, sc-32262	Mouse; monoclonal, IgG2a	0.4 μg/μL
IGF-1R	IGF-1R antibody (Ab-1161)	GenScript, A00380	Rabbit; polyclonal, IgG	1:500
α-SMA	Anti-α-SMA	Sigma-Aldrich, A2547	Mouse; monoclonal, IgG	1:500
HAS2	HAS2 (S-15)	Santa Cruz Biotechnology, sc-34067	Goat; polyclonal, IgG	1:200
CD40	CD40/TNFRSF5 antibody	NOVUS Biologicals, NB100-56127	Rabbit; polyclonal, IgG	1:1000
GAPDH	GAPDH (14C10) rabbit mAb	Cell Signaling, 2118	Rabbit; monoclonal, IgG	1:1000
IgG	Antigoat IgG (whole molecule)-peroxidase	Sigma-Aldrich, A5420	Rabbit; IgG	1:5000
IgG	Antimouse IgG (Fab specific)-peroxidase	Sigma-Aldrich, A2304	Goat; IgG	1:5000
IgG	Antirabbit IgG (whole molecule)-peroxidase	Sigma-Aldrich, A0545	Goat; IgG	1:5000
IgG	Rat F(ab)2 IgG (H + L) fluorescein-conjugated antibody	R&D Systems, F0104B	Rat; polyclonal, IgG	10 μL/10^6 cells
IgG	Sheep IgG (H + L) fluorescein-conjugated antibody	R&D Systems, F0125	Donkey; polyclonal, IgG	10 μL/10^6 cells
IgG	Goat antimouse IgG (H + L) fluorescein-conjugated	Thermo Scientific, F-2761	Mouse; polyclonal, IgG	5 μg/mL
IgG	Rat IgG2A isotype control	R&D Systems, MAB006	Rat; monoclonal, clone 54447	0.5 μg/μL
IgG	Rat IgG2B isotype control	R&D Systems, MAB0061	Rat; monoclonal, clone 141945	0.5 μg/μL
IgG	Purified sheep IgG	R&D Systems, 5-001-A	Normal sheep serum	0.5 μg/μL
IgG	Purified mouse IgG1	BioLegend, 400101	Mouse (BALB/c); IgG1	0.1 μg/mL
IgG	Normal mouse IgG2a	Santa Cruz Biotechnology, sc-3878	Mouse; IgG2a	1:5

[a] Antigen sequences not known.

notypic subpopulations of human OF distinguished by stable expression of CD90 (Thy1) has been identified, with CD90 negative population of OF responsible for adipogenesis and CD90-positive cells with myogenic differentiation ability. Moreover, the CD90-positive fibroblasts appear to be heterogeneously distributed in orbital connective tissue in different disease subtypes, implicating these cells to be pivotal in pathogenesis of GO (4–6). In

doi: 10.1210/en.2016-1304 press.endocrine.org/journal/endo 3773

other recent studies, we and others have demonstrated human OFs derived from GO patients show additional characteristic properties of mesenchymal stem cells (MSCs) (7, 8).

Recently, we developed an induced experimental model of GO by genetic immunization of BALB/c mice with plasmid encoding the A subunit of human TSHR (termed hTSHR A-subunit) (9, 10). Although genetic immunization with hTSHR A-subunit plasmid is effective in inducing experimental GO, similar immunization with human IGF-1R α-subunit coding region plasmid does not lead to any manifestation of disease, providing compelling evidence on the role of TSHR as a primary antigen in GO pathogenesis (9, 11). All GO mice were serum positive for TSHR antibodies and some of the GO mice showed elevated levels of anti-IGF-1R antibodies (10). The orbital pathology in GO mice was reminiscent of human GO showing adipogensis and myopathy (10). Moreover, antigen specific T cells from GO mice show robust responses to TSHR protein antigen by secretion of a cocktail of proinflammatory cytokines, which in the orbital tissue may lead to onset of inflammation and GO (10). In GO patients, OFs are considered to be pathogenic by mediating inflammatory and remodeling processes in the orbital tissue (2). In this study, our aim was to identify the pathologic cell type in the mouse orbital tissue from animals undergoing experimental GO and to determine whether they showed similar properties to those derived from human GO patients. Here, we demonstrate the ex vivo cultivation and characterization of OFs from GO mice and controls and show their inherent ability for adipocyte differentiation and hyaluronan production when activated by a variety of ligands, including TSH and IGF-1. Our study suggests mouse OFs (mOFs) as a pathogenic cell type responsible for tissue expansion in the orbital region of GO mice. The availability of ex vivo mOF cultures from GO mice at different stages of disease will provide novel genetic and molecular signatures associated with GO pathogenesis to provide new intervention targets for the disease.

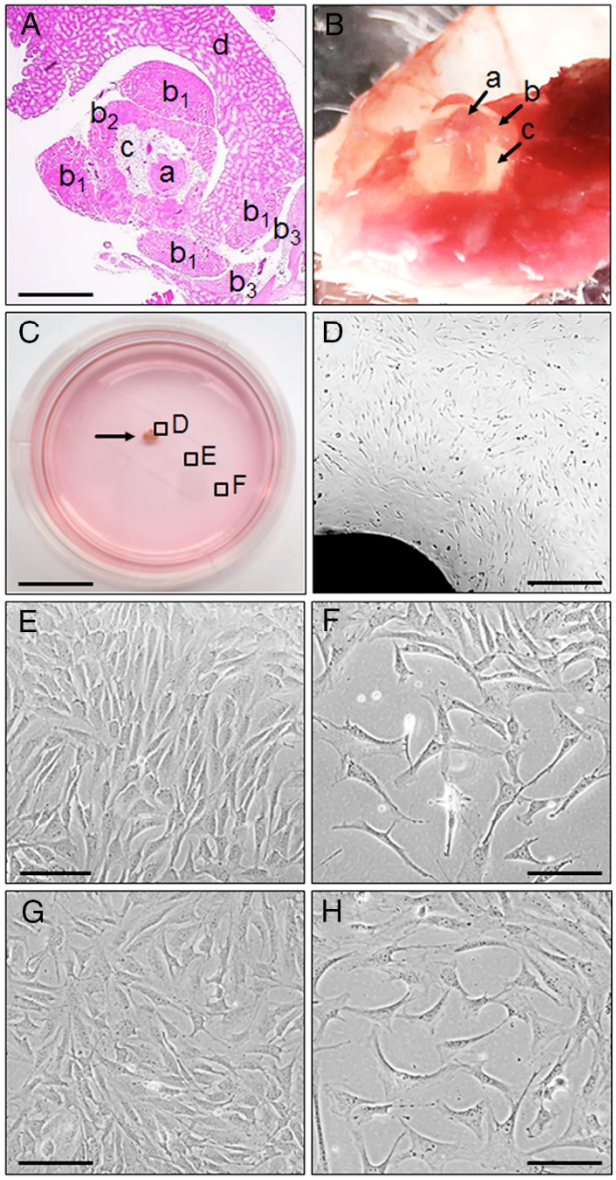

Figure 1. Ex vivo cultivation of mOFs. A, H&E staining of a control mouse orbita section. Optic nerve (a). Seven extraocular muscles: 4 rectus muscle (b_1), 1 retractor bulbi muscle (b_2), and 2 oblique/tear muscles (b_3). For a schematic overview of mouse eye with attached muscles refer to LifeMap Discovery (35). Connective/fat tissue (c), harderian gland (d), ×40, bar represents 200 μm. B, Preparation of mouse bulbar tissue including optic nerve (a), extraocular muscle (rectus muscle is shown, retractor bulbi muscle, and connective/fat tissue is not visible) eye bulbus (b), and harderian gland and oblique/tear muscles (c) were excised and discarded. C, Bulbar tissue from a Ctrl mouse was placed into cell culture dish (arrow), bar represents 10 mm. D, mOFs grow out the bulbar tissue derived from a Ctrl mouse, ×40, bar represents 200 μm. E, Confluent OFs at passage 0, ×100, bar represents 100 μm. F, OFs at low density at passage 0, ×100, bar represents 100 μm. Representative images from a Ctrl mouse are shown. G, Confluent OFs derived from a GO mouse at passage 0, ×100, bar represents 100 μm. H, OFs derived from a GO mouse at low density at passage 0, ×100, bar represents 100 μm. Plastic adherent orbital cells with morphological appearance of fibroblasts were cultured to passage 6–8 from control and GO mice.

Materials and Methods

Cell culture

All the orbital cultures were established from female BALB/c mice immunized with hTSHR A-subunit plasmid (GO mice, n = 10) or control β-galactosidase plasmid (Ctrl mice, n = 8) and killed 9 weeks after the last immunization, derived from center 2 (University of Duisburg-Essen) described in our recent study (10). After killing, for each mouse one orbit was excised in sterile hood under aseptic conditions, and the bulbar tissue was dissected by careful removal of the harderian gland, and the oblique/

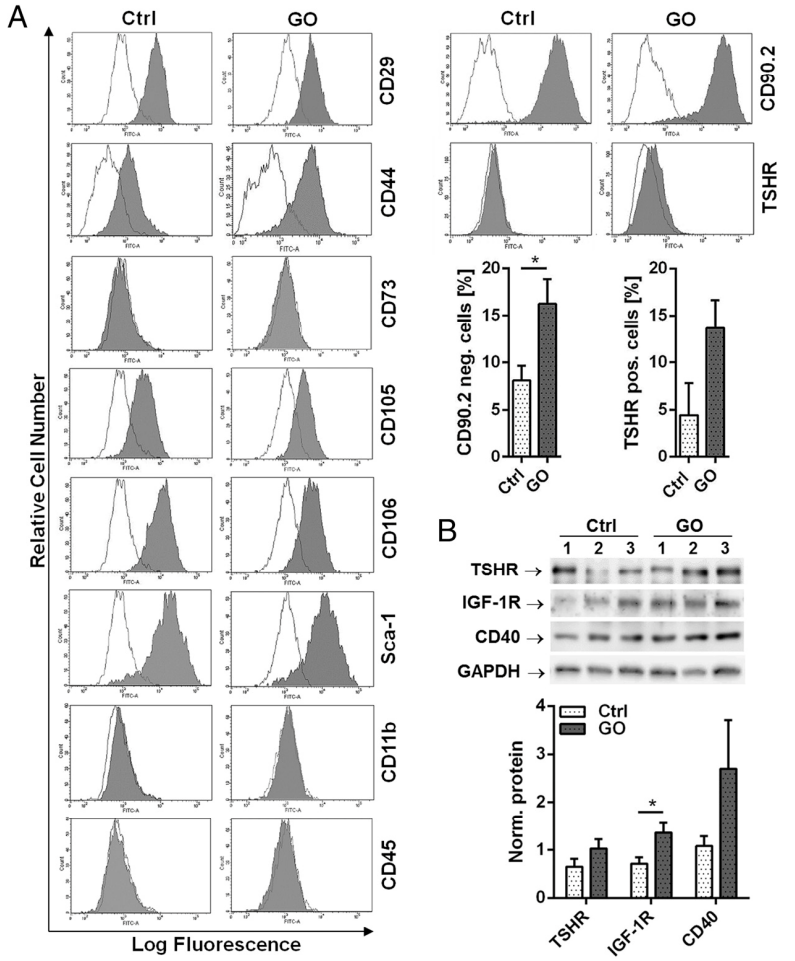

Figure 2. Phenotyping of surface markers and receptors present on mOFs. A, OFs (passage 2–4) from individual Ctrl (n = 8) and GO mice (n = 10) were labeled with antibodies against the indicated antigens and analyzed by flow cytometry. Representative histograms are shown (gray), and the respective isotype control is shown in gray line. CD90.2 negative/low and TSHR positive/high expressing cells were quantified from individual 8 Ctrl and 10 GO mice cell cultures. The staining pattern of surface markers from Ctrl and GO mice derived OFs was highly similar and indicates a mesenchymal cell/fibroblast immune phenotype. GO mice derived OF population show elevated levels of CD90.2 low expressing and TSHR high expressing cells. B, Whole-cell lysates from OFs derived from Ctrl or GO mice were analyzed for TSHR, IGF-1R, and CD40 expression by Western blot analysis. GAPDH expression served as an internal control. Representative staining patterns of mOFs derived from 3 individual Ctrl and GO mice are shown. Western blotting signals from mOFs derived from individual Ctrl mice (n = 8) or GO mice (n = 10) were quantified by densitometry using ImageJ software. TSHR, IGF-1R, and CD40 signals were normalized to GAPDH signals and are shown as normalized protein expression. A representative experiment of at least 3 independent experiments is shown. OFs derived from GO mice expressed elevated levels TSHR and IGF-1R protein compared with Ctrl mice derived OFs. CD40 was expressed to high levels by mOFs derived from GO mice.

tear muscles and transferred directly into 35-mm culture dish containing standard medium: DMEM (Invitrogen) supplemented with 10% fetal calf serum, 10mM HEPES (pH 7.4), 2mM L-glutamine, 1mM sodium pyruvate, 100mM nonessential amino acids, 100-U/mL penicillin, and 100-μg/mL streptomycin. The other orbit was processed for histology as described earlier (10, 12). The mouse OFs were obtained from the bulbar tissue by out-grow protocol as described earlier for human OFs (8, 13, 14). After 3–4 weeks, the orbital tissue and nonadherent cells were removed by washing with PBS. Once cells grew in adherent monolayers, they were transferred to a 75-mL flask, serially passaged, and maintained in medium described above. All experiments were performed with orbital cells between passages 2 and 8 after culture initiation.

Flow cytometry

Cells (9×10^4) were incubated with a panel of nonconjugated mouse bone marrow stem cell markers (UK018; R&D Systems), CD90.2 (Thy1.2), and TSHR or respective isotype controls, for 30 minutes at room temperature, followed by 2 washing steps with cell staining buffer (contains bovine calf serum, metabolic inhibitor, and sodium azide; BioLegend) and incubation with secondary antirat IgG or antisheep IgG conjugated to fluorescein for 30 minutes at room temperature. After washing, cells were resuspended in cell staining buffer, and 1×10^4 cells were analyzed by BD FACS Aria III. Data were analyzed using BD Diva. Quantification of CD90.2 low expressing cells and TSHR high expressing cells were conducted with FlowJo V.10.1 software. For detailed antibody description see Table 1.

Western blot analysis

Cells were grown in 6-well dishes at 5×10^5 cells overnight, lysed in 50-μL extraction buffer (300mM NaCl, 10nM Tris/HCl [pH7.9], 1mM EDTA, 0.1% Nonidet P-40, and protease inhibitors [Roche Applied Science]) for 20 minutes on ice. After centrifugation at 3600*g* at 4°C for 5 minutes to remove cellular debris, supernatants were subjected to Western blotting (50-μg protein per lane) using antibodies for detection of TSHR, IGF-1R, CD40, hyaluronan synthase 2 (HAS2), and GAPDH as described in Table 1. Western blot analysis was carried out as described earlier (15). Quantification of Western blotting signals was conducted with ImageJ software.

Differentiation assays and microscopy

Cells were seeded at a density of 1×10^5 cells per well on coverslips in 24-well dishes and grown in standard culture medium until reaching 90% confluence. For myogenic differentiation, cells were cultured on coverslips and seeded at a density of 1×10^4 in 96-well plates. Cells were incubated with or without 500-ng/mL TGF-β (Peprotech) for 48 hours and immunostained for α-smooth muscle actin (α-SMA) as described before (8). Im-

doi: 10.1210/en.2016-1304 press.endocrine.org/journal/endo 3775

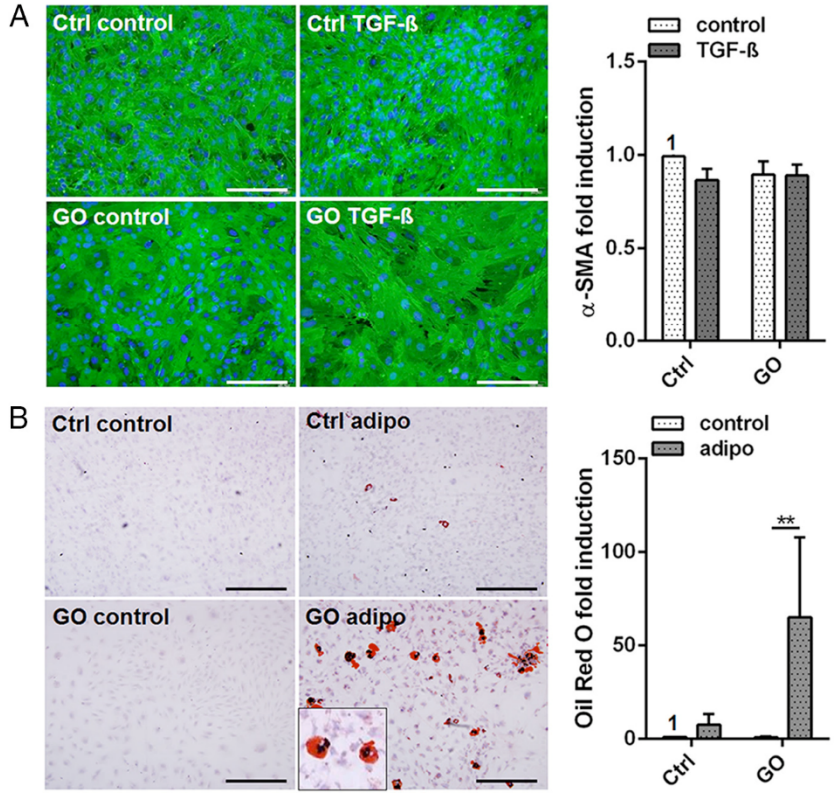

Figure 3. Myocyte and adipocyte differentiation of mOFs. Mouse OF (passage 2–4) from Ctrl (n = 8) and GO mice (n = 10) were subjected to differentiation assays. Induction of differentiation is shown in relation to nondifferentiated OF derived from Ctrl mice. A, To induce myocyte differentiation, cells were incubated with TGF-β (or without as nondifferentiated control) for 48 hours and immunostained for α-smooth muscle actin (α-SMA) (green). Cell nuclei were counterstained with DAPI (blue). Representative images are shown, ×200, bar represents 100 μm. Fluorescence intensity of α-SMA stained cells was quantified with a fluorescence plate reader in parallel experiments. Fluorescence intensity of α-SMA stained cells is shown as fold induction of fluorescence intensity of nondifferentiated Ctrl cells (Ctrl control). Both OFs derived from Ctrl or GO mice expressed basically high amounts of α-SMA indicating constitutive myogenic differentiation. B, To induce adipocyte differentiation cells were cultivated with adipocyte differentiation medium (adipo, or without as a nondifferentiated control) for 21 days, and oil vacuoles were stained with Oil Red O. Representative images are shown, ×100, bar represents 100 μm; inset, ×200. Quantification of Oil Red O staining (red color) was conducted in 4 field views of each of individual Ctrl (n = 8) or GO-derived mOF (n = 10) at ×40 using ImageJ software. Oil Red O staining of lipid vacuoles in cells is shown as fold induction of nondifferentiated Ctrl cells (Ctrl control). Mouse OF derived from GO mice were substantially capable of adipocyte differentiation.

ages were generated using an Olympus BX51 microscope. Fluorescence intensity of stained cells was quantified with a fluorescence plate reader (FLUOstar Omega; BMG LABTECH) using an excitation at 485 nm and an emission at 520 nm. Adipogenic differentiation was induced with mouse adipogenic stimulatory supplement diluted 1:5 in mouse Mesencult MSC Basal medium (both Stemcell Technologies). The medium does not contain antibiotics and is specifically formulated for the in vitro differentiation of mouse MSCs into cells of the adipogenic lineage (16). The medium was exchanged every 3–4 days during the 21-day differentiation period. To analyze the accumulation of lipid droplets in the cytoplasm after differentiation, cells were fixed with 10% paraformaldehyde, rinsed with 60% isopropanol solution, and stained with Oil Red O solution (Sigma). Cells were counterstained with Mayers hematoxylin solution (Sigma). Images were generated using an Olympus BX51 microscope. Quantification of Oil Red O staining was conducted in 4 field views of each of individual GO- or Ctrl-derived mOF at ×40 and analyzed using ImageJ software. The microscopic images were segmented by thresholding to detect and to quantify the red stained particles from the background noise.

Hyaluronan ELISA

Cells were seeded at a density of 1×10^4 cells per well on 96-well dishes and grown in standard culture medium. After 1 day, the medium was exchanged with low serum medium (1%). The cells were pretreated for 1h hour by 37°C with hyaluronidase (1 U/mL; Sigma) and stimulated with TSHR mAb M22 (0.1 μg/mL), bovine TSH (100 mU/mL; Sigma), IGF-1 (0.1 μg/mL; R&D Systems), or control IgG (0.1 μg/mL) for 5 days. Hyaluronan levels in the supernatants were measured using an ELISA kit (R&D Systems) according to the manufacturer's instructions. Samples were diluted 1:50 before analysis. Viability/density of cells was measured with (3-(4,5-Dimethylthiazol-2-yl)-2,5-diphenyltetrazoliumbromid) assay as described earlier (14).

Statistical analysis

Statistical analyses were performed with 2-tailed Student's *t* tests with a confidence level greater than 95%. Data are presented as arithmetic mean ± SEM. Statistical significance was set at the level of $P \leq .05$ with * $P < .05$ and ** $P < .01$.

Results and Discussion

For the establishment of mouse OF model, all GO and Ctrl mice were derived from our recently described study, where orbital tissue from one eye was used for histological analysis and the orbital tissue of the second eye was excised under aseptic conditions for the cultures (10). Histological analysis revealed that the excised mouse orbital tissue contained the optic nerve with connective/fat tissue, extraocular muscles, and harderian gland (Figure 1A). For in vitro studies of OFs from GO patients, the tissue has frequently been obtained from either fat/connective tissue or extraorbital muscles (13, 17). To excise the orbital tissues from mice orbits, the harderian gland and the oblique/tear muscles was carefully removed from the mice orbits. The remaining bulbar tissue including the

optic nerve, connective fat/tissue, and extraocular muscles (rectus and retractor bulbi muscles) was placed in a cell culture dish (Figure 1, B and C). At 1 week of initial culture, fibroblast-like cells migrated out from the orbital tissue and adhere to the dish (Figure 1D). A confluent monolayer was obtained after 3–4 weeks (Figure 1, E and G), and cells were passaged and cultivated like human OFs up to maximum 6–8 passages. Similarly, mouse orbital cells from Ctrl mice grow equally well as those derived from GO mice with highly similar fibroblast-like appearance and proliferation (Figure 1, F and H). Having established cell culture of mOFs, we characterized the cells by phenotyping several surface marker and receptors (Figure 2) as well as by analyzing their myocyte and adipocyte differentiation ability (Figure 3). Furthermore, we measured hyaluronan secretion of the cells in response to TSHR and IGF-1R stimulation (Figure 4).

The immune phenotype of GO- and Ctrl animals-derived mOFs were highly similar (Figure 2A). They were positive for MSC marker CD29, CD44, CD90.2, CD105, CD106, Sca-1, and negative for leukocyte marker CD11.b and CD45, which indicates their mesenchymal cell immune phenotype akin both to mouse bone marrow stem cells or embryonic fibroblasts (18, 19) and human OFs (7, 8, 14). However, the mOFs were negative for MSC marker CD73, indicating that the cells were similar but not identical to OFs or orbital MSCs derived from GO patients orbital fat tissue (8, 14). CD73 functions as an ecto-enzyme to produce adenosine that exerts immune suppressive properties by negatively regulating Th1 immune responses. Consequently, CD73 inhibition or deficiency leads to increased susceptibility to autoimmune conditions like arthritis in mice (20). However, the role of CD73 in GO still awaits further investigation. Human OFs can be separated into 2 populations based on expression of CD90 (Thy1), and different proportions of CD90 positive/negative cells have been observed in GO patients dependent on orbital localization with CD90-positive cells more abundant in extraocular muscles (21). In our study, the mOFs express high levels of mouse strain specific Thy1 allele CD90.2. Interestingly, mOF derived from GO mice showed a statistically significant increase in low expressing cells compared with Ctrl mOF (Figure 2A). However, we do not find subdivision of 2 distinct populations based on Thy1 expression as we and others have observed in OF derived from GO patients (4, 8). Because the main body of mouse orbital tissue was extraocular muscle, high CD90.2 expression of derived mOFs most likely reflects rather their muscle than fat tissue origin. This notion is confirmed by the finding that mOFs expressed basically high amounts of α-SMA that was not further increased in response to TGF-β stimulation (Figure 3A), indicating constitutive myogenic differentiation of the cells (5, 8, 22).

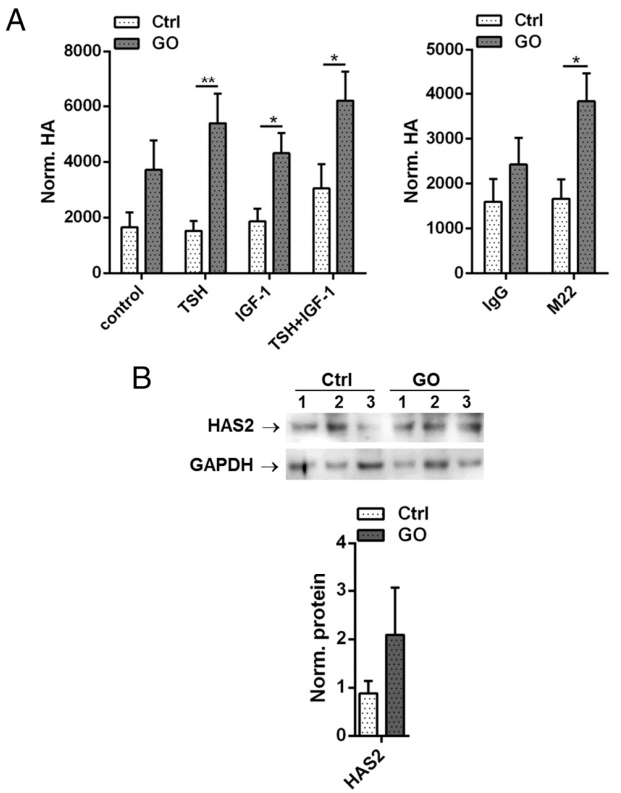

Figure 4. Hyaluronan (HA) secretion of mOFs. A, Mouse OF from Ctrl (n = 8) and GO (n = 10) mice were incubated with bTSH and/or IGF-1 or without (control) or incubated with stimulating TSHR mAb M22 or control IgG for 5 days. HA production was normalized to cell viability and expressed as normalized HA in arbitrary units. GO-derived mOFs increased HA production upon stimulation of the TSHRs or/and IGF-1Rs, whereas Ctrl-derived mOFs remained less responsive. B, Western blot analysis for HAS2 expression and GAPDH as an internal control. Representative signals derived from 3 Ctrl and GO mice are shown. Signals of Ctrl (n = 8) and GO-derived mOFs (n = 10) were quantified. HAS2 signals were normalized to GAPDH signals and are shown as normalized protein expression. GO mice derived OFs expressed elevates levels of HAS2 compared with control mOFs.

The main target antigens involved in GO pathology are TSHR and IGF-1R, which are expressed to highest levels in orbital tissues of GO patients and derived OFs (23–25). Previously, we have shown high expression of TSHR in the retroorbital tissue in several mice strains (12, 26) and concordantly the OFs derived from both GO and Ctrl mice expressed TSHR and also IGF-1R (Figure 2, A and B). However, unlike of the mesenchymal marker these antigens were expressed to higher levels on OFs derived from GO mice compared with Ctrl mice derived fibroblasts (Figure 2, A and B). Further significant differences between GO- and Ctrl-derived mOFs were obtained when adipogenesis and hyaluronan production of the cells was investigated (Figures 3 and 4). Mouse OFs derived from GO mice readily differentiated into adipocytes when in-

doi: 10.1210/en.2016-1304 press.endocrine.org/journal/endo 3777

cubated with mouse adipocyte differentiation medium, whereas Ctrl mice-derived mOFs remained less responsive (Figure 3B). The data indicate that the mOFs population derived from GO mice contained substantially preadipocytes capable of differentiating into adipocytes just like OF population derived from GO patients (8, 27). However, it remains to be investigated whether the CD90.2 low expressing cells were responsible for elevated adipocyte differentiation of mOF derived from GO mice. It was shown that either TSHR or IGF-1R activation of human orbital preadipocytes/fibroblasts does increase hyaluronan production (28–31). Likewise, GO-derived mOFs secreted elevated levels hyaluronan compared with Ctrl-derived mOFs, and statistically significant differences occurred after stimulation of TSHRs and/or IGF-1Rs (Figure 4). Hyaluronan production of GO-derived mOFs was significantly induced in response to TSH and/or IGF-1 or stimulating TSHR mAb M22 when compared with hyaluronan production of Ctrl-derived mOFs (Figure 4A). Three HASs (HAS1–HAS3) control hyaluronan abundance, but HAS2 is considered to represent the major contributor of hyaluronan overproduction in the human orbit (29, 32). We found high constitutive HAS2 protein expression in OFs derived from GO mice (Figure 4B). Thus, overexpression of TSHR, IGF-1R, and HAS2 most likely contributed to the stimulatory effect of TSH and/or IGF-1 or M22 on hyaluronan production of mOF in GO-derived mice. Furthermore, human OFs are prime targets of T-cell response in GO, and it has been shown that T cells also stimulate adipogenic differentiation and hyaluronan production (33, 34). Just like human OFs, the OFs derived from GO mice expressed CD40 to high levels (Figure 2B), and CD40-CD154 ligation with T cells could be another potential pathway by which OFs were activated in GO mice. Finally, in this study, we have investigated mOFs populations derived from the orbital tissue of mice undergoing experimental GO or Ctrl mice immunized with β-galactosidase plasmid. However, studies in human GO patients using fibroblast populations from other anatomical sites such as dermal fibroblasts from normal individuals have provided compelling evidence that they are distinct in their hyperresponsive phenotype from the OFs derived from the orbital region (28). In this context, human dermal fibroblasts from GO patients or in the GO model, mouse fibroblast derived from other anatomical sites remain to be evaluated.

To our knowledge, this is the first report on ex vivo cultures of mouse OFs. Our data provide evidence that mOFs are substantially affected in response to systemic hTSHR A-subunit immunization and recapitulate the main features of human OF derived from GO patients and are therefore to be considered as pathogenic cell type responsible for tissue expansion in the orbit of GO mice. Whether TSHR and IGF-1R antibodies present in the GO mice (10) are the main cause or TSHR primed T cells and/or inflammatory cytokines present in the GO mice (10) were the main activating factors is open question and subject of further investigations. The study opens the way to investigate phenotypic and molecular changes in stimulated OF cultures from immune mice at different stages of disease to evaluate their progression to disease pathogenesis, which are not possible with human OFs.

Acknowledgments

We thank the Imaging Core Facility Essen IMCES.

Address all correspondence and requests for reprints to: Utta Berchner-Pfannschmidt, PhD, Molecular Ophthalmology, Medical Research Center, University Hospital Essen, 45147 Essen, Germany. E-mail: utta.berchner-pfannschmidt@uni-due.de.

This work was supported by Deutsche Forschungsgemeinschaft Grants BE 3177/2-1 (to U.B.-P.) and EC 379/3-1 (to A.E.) and by Marie Sklodowska Curie Industry-Academia Pathways and Partnerships Action, GAN (grant agreement number) 612116 Project INDIGO (Investigation of Novel biomarkers and Definition of the role of the microbiome In Graves' Orbitopathy) (to A.E. and others).

Disclosure Summary: The authors have nothing to disclose.

References

1. **Eckstein AK, Johnson KT, Thanos M, Esser J, Ludgate M.** Current insights into the pathogenesis of Graves' orbitopathy. *Horm Metab Res*. 2009;41(6):456–464.
2. **Dik WA, Virakul S, van Steensel L.** Current perspectives on the role of orbital fibroblasts in the pathogenesis of Graves' ophthalmopathy. *Exp Eye Res*. 2016;142:83–91.
3. **Heufelder AE, Bahn RS.** Modulation of Graves' orbital fibroblast proliferation by cytokines and glucocorticoid receptor agonists. *Invest Ophthalmol Vis Sci*. 1994;35(1):120–127.
4. **Smith TJ, Sempowski GD, Wang HS, Del Vecchio PJ, Lippe SD, Phipps RP.** Evidence for cellular heterogeneity in primary cultures of human orbital fibroblasts. *J Clin Endocrinol Metab*. 1995;80(9):2620–2625.
5. **Koumas L, Smith TJ, Feldon S, Blumberg N, Phipps RP.** Thy-1 expression in human fibroblast subsets defines myofibroblastic or lipofibroblastic phenotypes. *Am J Pathol*. 2003;163(4):1291–1300.
6. **Kuriyan AE, Woeller CF, O'Loughlin CW, Phipps RP, Feldon SE.** Orbital fibroblasts from thyroid eye disease patients differ in proliferative and adipogenic responses depending on disease subtype. *Invest Ophthalmol Vis Sci*. 2013;54(12):7370–7377.
7. **Kozdon K, Fitchett C, Rose GE, Ezra DG, Bailly M.** Mesenchymal stem cell-like properties of orbital fibroblasts in Graves' orbitopathy. *Invest Ophthalmol Vis Sci*. 2015;56(10):5743–5750.
8. **Brandau S, Bruderek K, Hestermann K, et al.** Orbital fibroblasts from Graves' orbitopathy patients share functional and immunophenotypic properties with mesenchymal stem/stromal cells. *Invest Ophthalmol Vis Sci*. 2015;56(11):6549–6557.
9. **Moshkelgosha S, So PW, Deasy N, Diaz-Cano S, Banga JP.** Cutting

doi: 10.1210/en.2016-1304 press.endocrine.org/journal/endo 3777

cubated with mouse adipocyte differentiation medium, whereas Ctrl mice-derived mOFs remained less responsive (Figure 3B). The data indicate that the mOFs population derived from GO mice contained substantially preadipocytes capable of differentiating into adipocytes just like OF population derived from GO patients (8, 27). However, it remains to be investigated whether the CD90.2 low expressing cells were responsible for elevated adipocyte differentiation of mOF derived from GO mice. It was shown that either TSHR or IGF-1R activation of human orbital preadipocytes/fibroblasts does increase hyaluronan production (28–31). Likewise, GO-derived mOFs secreted elevated levels hyaluronan compared with Ctrl-derived mOFs, and statistically significant differences occurred after stimulation of TSHRs and/or IGF-1Rs (Figure 4). Hyaluronan production of GO-derived mOFs was significantly induced in response to TSH and/or IGF-1 or stimulating TSHR mAb M22 when compared with hyaluronan production of Ctrl-derived mOFs (Figure 4A). Three HASs (HAS1–HAS3) control hyaluronan abundance, but HAS2 is considered to represent the major contributor of hyaluronan overproduction in the human orbit (29, 32). We found high constitutive HAS2 protein expression in OFs derived from GO mice (Figure 4B). Thus, overexpression of TSHR, IGF-1R, and HAS2 most likely contributed to the stimulatory effect of TSH and/or IGF-1 or M22 on hyaluronan production of mOF in GO-derived mice. Furthermore, human OFs are prime targets of T-cell response in GO, and it has been shown that T cells also stimulate adipogenic differentiation and hyaluronan production (33, 34). Just like human OFs, the OFs derived from GO mice expressed CD40 to high levels (Figure 2B), and CD40-CD154 ligation with T cells could be another potential pathway by which OFs were activated in GO mice. Finally, in this study, we have investigated mOFs populations derived from the orbital tissue of mice undergoing experimental GO or Ctrl mice immunized with β-galactosidase plasmid. However, studies in human GO patients using fibroblast populations from other anatomical sites such as dermal fibroblasts from normal individuals have provided compelling evidence that they are distinct in their hyperresponsive phenotype from the OFs derived from the orbital region (28). In this context, human dermal fibroblasts from GO patients or in the GO model, mouse fibroblast derived from other anatomical sites remain to be evaluated.

To our knowledge, this is the first report on ex vivo cultures of mouse OFs. Our data provide evidence that mOFs are substantially affected in response to systemic hTSHR A-subunit immunization and recapitulate the main features of human OF derived from GO patients and are therefore to be considered as pathogenic cell type responsible for tissue expansion in the orbit of GO mice. Whether TSHR and IGF-1R antibodies present in the GO mice (10) are the main cause or TSHR primed T cells and/or inflammatory cytokines present in the GO mice (10) were the main activating factors is open question and subject of further investigations. The study opens the way to investigate phenotypic and molecular changes in stimulated OF cultures from immune mice at different stages of disease to evaluate their progression to disease pathogenesis, which are not possible with human OFs.

Acknowledgments

We thank the Imaging Core Facility Essen IMCES.

Address all correspondence and requests for reprints to: Utta Berchner-Pfannschmidt, PhD, Molecular Ophthalmology, Medical Research Center, University Hospital Essen, 45147 Essen, Germany. E-mail: utta.berchner-pfannschmidt@uni-due.de.

This work was supported by Deutsche Forschungsgemeinschaft Grants BE 3177/2-1 (to U.B.-P.) and EC 379/3-1 (to A.E.) and by Marie Sklodowska Curie Industry-Academia Pathways and Partnerships Action, GAN (grant agreement number) 612116 Project INDIGO (Investigation of Novel biomarkers and Definition of the role of the microbiome In Graves' Orbitopathy) (to A.E. and others).

Disclosure Summary: The authors have nothing to disclose.

References

1. **Eckstein AK, Johnson KT, Thanos M, Esser J, Ludgate M.** Current insights into the pathogenesis of Graves' orbitopathy. *Horm Metab Res*. 2009;41(6):456–464.
2. **Dik WA, Virakul S, van Steensel L.** Current perspectives on the role of orbital fibroblasts in the pathogenesis of Graves' ophthalmopathy. *Exp Eye Res*. 2016;142:83–91.
3. **Heufelder AE, Bahn RS.** Modulation of Graves' orbital fibroblast proliferation by cytokines and glucocorticoid receptor agonists. *Invest Ophthalmol Vis Sci*. 1994;35(1):120–127.
4. **Smith TJ, Sempowski GD, Wang HS, Del Vecchio PJ, Lippe SD, Phipps RP.** Evidence for cellular heterogeneity in primary cultures of human orbital fibroblasts. *J Clin Endocrinol Metab*. 1995;80(9):2620–2625.
5. **Koumas L, Smith TJ, Feldon S, Blumberg N, Phipps RP.** Thy-1 expression in human fibroblast subsets defines myofibroblastic or lipofibroblastic phenotypes. *Am J Pathol*. 2003;163(4):1291–1300.
6. **Kuriyan AE, Woeller CF, O'Loughlin CW, Phipps RP, Feldon SE.** Orbital fibroblasts from thyroid eye disease patients differ in proliferative and adipogenic responses depending on disease subtype. *Invest Ophthalmol Vis Sci*. 2013;54(12):7370–7377.
7. **Kozdon K, Fitchett C, Rose GE, Ezra DG, Bailly M.** Mesenchymal stem cell-like properties of orbital fibroblasts in Graves' orbitopathy. *Invest Ophthalmol Vis Sci*. 2015;56(10):5743–5750.
8. **Brandau S, Bruderek K, Hestermann K, et al.** Orbital fibroblasts from Graves' orbitopathy patients share functional and immunophenotypic properties with mesenchymal stem/stromal cells. *Invest Ophthalmol Vis Sci*. 2015;56(11):6549–6557.
9. **Moshkelgosha S, So PW, Deasy N, Diaz-Cano S, Banga JP.** Cutting

edge: retrobulbar inflammation, adipogenesis, and acute orbital congestion in a preclinical female mouse model of Graves' orbitopathy induced by thyrotropin receptor plasmid-in vivo electroporation. *Endocrinology*. 2013;154(9):3008–3015.

10. **Berchner-Pfannschmidt U, Moshkelgosha S, Diaz-Cano S, et al.** Comparative assessment of female mouse model of Graves' orbitopathy under different environments, accompanied by pro-inflammatory cytokine and T cell responses to thyrotropin hormone receptor antigen. *Endocrinology*. 2016;157(4):1673–1682.
11. **Banga JP, Moshkelgosha S, Berchner-Pfannschmidt U, Eckstein A.** An animal model of Graves' orbitopathy. In Chan CC, ed. *Animal Models of Ophthalmic Diseases*. Basel, Switzerland: Springer; 2016: 117–126.
12. **Johnson KT, Wiesweg B, Schott M, et al.** Examination of orbital tissues in murine models of Graves' disease reveals expression of UCP-1 and the TSHR in retrobulbar adipose tissues. *Horm Metab Res*. 2013;45(6):401–407.
13. **Bahn RS, Gorman CA, Woloschak GE, David CS, Johnson PM, Johnson CM.** Human retroocular fibroblasts in vitro: a model for the study of Graves' ophthalmopathy. *J Clin Endocrinol Metab*. 1987;65(4):665–670.
14. **Meyer zu Hörste M, Ströher E, Berchner-Pfannschmidt U, Schmitz-Spanke S, et al.** A novel mechanism involved in the pathogenesis of Graves ophthalmopathy (GO): clathrin is a possible targeting molecule for inhibiting local immune response in the orbit. *J Clin Endocrinol Metab*. 2011;96(11):E1727–E1736.
15. **Niecknig H, Tug S, Reyes BD, Kirsch M, Fandrey J, Berchner-Pfannschmidt U.** Role of reactive oxygen species in the regulation of HIF-1 by prolyl hydroxylase 2 under mild hypoxia. *Free Radic Res*. 2012;46(6):705–717.
16. **Swart JF, de Roock S, Hofhuis FM, et al.** Mesenchymal stem cell therapy in proteoglycan induced arthritis. *Ann Rheum Dis*. 2015; 74(4):769–777.
17. **Metcalfe RA, Weetman AP.** Stimulation of extraocular muscle fibroblasts by cytokines and hypoxia: possible role in thyroid-associated ophthalmopathy. *Clin Endocrinol*. 1994;40(1):67–72.
18. **Saeed H, Taipaleenmäki H, Aldahmash AM, Abdallah BM, Kassem M.** Mouse embryonic fibroblasts (MEF) exhibit a similar but not identical phenotype to bone marrow stromal stem cells (BMSC). *Stem Cell Rev*. 2012;8(2):318–328.
19. **Lei J, Hui D, Huang W, et al.** Heterogeneity of the biological properties and gene expression profiles of murine bone marrow stromal cells. *Int J Biochem Cell Biol*. 2013;45(11):2431–2443.
20. **Chrobak P, Charlebois R, Rejtar P, El Bikai R, Allard B, Stagg J.** CD73 plays a protective role in collagen-induced arthritis. *J Immunol*. 2015;194(6):2487–2492.
21. **Smith TJ, Koumas L, Gagnon A, et al.** Orbital fibroblast heterogeneity may determine the clinical presentation of thyroid-associated ophthalmopathy. *J Clin Endocrinol Metab*. 2002;87(1):385–392.
22. **Darby IA, Laverdet B, Bonté F, Desmoulière A.** Fibroblasts and myofibroblasts in wound healing. *Clin Cosmet Investig Dermatol*. 2014;7:301–311.
23. **Starkey KJ, Janezic A, Jones G, Jordan N, Baker G, Ludgate M.** Adipose thyrotrophin receptor expression is elevated in Graves' and thyroid eye diseases ex vivo and indicates adipogenesis in progress in vivo. *J Mol Endocrinol*. 2003;30(3):369–380.
24. **Wakelkamp IM, Bakker O, Baldeschi L, Wiersinga WM, Prummel MF.** TSH-R expression and cytokine profile in orbital tissue of active vs. inactive Graves' ophthalmopathy patients. *Clin Endocrinol*. 2003;58(3):280–287.
25. **Smith TJ.** The putative role of fibroblasts in the pathogenesis of Graves' disease: evidence for the involvement of the insulin-like growth factor-1 receptor in fibroblast activation. *Autoimmunity*. 2003;36(6–7):409–415.
26. **Wiesweg B, Johnson KT, Eckstein AK, Berchner-Pfannschmidt U.** Current insights into animal models of Graves' disease and orbitopathy. *Horm Metab Res*. 2013;45(8):549–555.
27. **Kumar S, Coenen MJ, Scherer PE, Bahn RS.** Evidence for enhanced adipogenesis in the orbits of patients with Graves' ophthalmopathy. *J Clin Endocrinol Metab*. 2004;89(2):930–935.
28. **Smith TJ, Hoa N.** Immunoglobulins from patients with Graves' disease induce hyaluronan synthesis in their orbital fibroblasts through the self-antigen, insulin-like growth factor-I receptor. *J Clin Endocrinol Metab*. 2004;89(10):5076–5080.
29. **Zhang L, Bowen T, Grennan-Jones F, et al.** Thyrotropin receptor activation increases hyaluronan production in preadipocyte fibroblasts: contributory role in hyaluronan accumulation in thyroid dysfunction. *J Biol Chem*. 2009;284(39):26447–26455.
30. **Zhang L, Grennan-Jones F, Lane C, Rees DA, Dayan CM, Ludgate M.** Adipose tissue depot-specific differences in the regulation of hyaluronan production of relevance to Graves' orbitopathy. *J Clin Endocrinol Metab*. 2012;97(2):653–662.
31. **Krieger CC, Neumann S, Place RF, Marcus-Samuels B, Gershengorn MC.** Bidirectional TSH and IGF-1 receptor cross talk mediates stimulation of hyaluronan secretion by Graves' disease immunoglobins. *J Clin Endocrinol Metab*. 2015;100(3):1071–1077.
32. **Kaback LA, Smith TJ.** Expression of hyaluronan synthase messenger ribonucleic acids and their induction by interleukin-1β in human orbital fibroblasts: potential insight into the molecular pathogenesis of thyroid-associated ophthalmopathy. *J Clin Endocrinol Metab*. 1999;84(11):4079–4084.
33. **Cao HJ, Wang HS, Zhang Y, Lin HY, Phipps RP, Smith TJ.** Activation of human orbital fibroblasts through CD40 engagement results in a dramatic induction of hyaluronan synthesis and prostaglandin endoperoxide H synthase-2 expression. Insights into potential pathogenic mechanisms of thyroid-associated ophthalmopathy. *J Biol Chem*. 1998;273(45):29615–29625.
34. **Feldon SE, O'loughlin CW, Ray DM, Landskroner-Eiger S, Seweryniak KE, Phipps RP.** Activated human T lymphocytes express cyclooxygenase-2 and produce proadipogenic prostaglandins that drive human orbital fibroblast differentiation to adipocytes. *Am J Pathol*. 2006;169(4):1183–1193.
35. **LifeMap Discovery.** Version 1.8. 2015. Available at http://discovery.lifemapsc.com/library/images/extraocular-skeletal-muscle-anatomy. LifeMapSciences, Inc.

4 Discussion

The pathogenesis of Graves' orbitopathy (GO) is very complex and molecular processes are not fully understood. The physical and mental burdens of GO patients are high and the development of new treatments and therapies must be encouraged. It is known that orbital fibroblasts (OF) fulfill a central role in the pathophysiology of GO and activated OF enhance tissue remodeling and inflammatory processes in the orbit (Bahn, 2010). The causal roles of pathophysiological processes in GO need more insight in OF activation as well as signal cascades and this may provide new therapeutic targets. In this thesis, the orbital cell populations were isolated, investigated and characterized. Further the causal role of hypoxia and HIF-1 dependent pathways for tissue remodeling in GO was discovered. Furthermore, the implementation of a new GO mouse model and the isolation and characterization of mouse OF (mOF) complete this work.

4.1 Characteristics of human orbital cell population - orbital fibroblasts and mesenchymal stem cells

Since orbital fibroblasts (OF) cell cultivation derived from fat biopsies of GO patients has been established in 1987 (Bahn et al., 1987) various *in vitro* studies identified the OF as the key players in GO pathology. Previous studies indicated that OF may share some characteristics with mesenchymal stem cells (MSCs) like expression of CD90 and potential to differentiate into adipocytes and myocytes (Koumas et al., 2002; Smith et al., 2002; Meyer zu Horste et al., 2011). Mesenchymal stem cells (MSC) are undifferentiated fibroblastic like non hematopoietic progenitor cells which are able to differentiate into mesenchymal (fat, bone, cartilage and muscle) and non-mesenchymal lineages (neuron) (Le Blanc and Mougiakakos, 2012). This suggests that MSC are an important component in tissue remodeling as well as immune response (Uccelli et al., 2008). Furthermore, MSC are characterized by regenerative and immunoregulatory properties, indicating MSC as an interesting cellular treatment tool for inflammation and autoimmunity. Little has been known so far about tissue-resident mesenchymal progenitor cells in the retrobulbar connective/fat tissue of GO patients and about the interrelation of fibroblasts and MSC in this tissue.

Therefore, in our study we derived GO-MSC and GO-OF simultaneously from the orbital adipose tissue of GO patients. Our results show that GO-OF exhibit similar morphological features, surface marker sets and differentiation potentials like GO-MSCs (Publication 1, Fig. 1-3). In addition, loss of CD31 and CD146 in early passages (Publication 1, Fig. 2 and Supplementary Fig. S1) was described as a characteristic of mesenchymal progenitor cells from orbital fat tissue (Chen et al., 2014). This suggesting that both GO-OF and GO-MSC have characteristics of fat derived stem cells. Interestingly, we found that GO-MSC and GO-OF are able to differentiate in adiogenic, osteogenic, chondrogenic, myogenic and neurogenic lineages (Publication 1, Fig. 3). The ability of GO-OF to differentiate in adipocytes and myocytes (Valyasevi et al., 1999; Lin et al., 2013; Chen et al., 2014) has been known but we could also show their ability to differentiate along the osteogenic, chondrogenic, and neuronal lineages. However, GO-MSC showed a better differentiation potential than the GO-OF in relation to adipogenesis, osteogenesis and myogenesis. This suggests that OF from retrobulbar adipose tissue from GO patients contain lesser mesenchymal stem cells and more mature differentiated cells. In contrasts, potential MSC isolated from ethmoid of the same GO patients (GO-EthC) showed any multilinage differentiation capacity and constitutively expressed α-SMA indicating that these cells are myofibroblasts with an absence of MSC populations. In addition, fibroblast isolated from eyelid skin during blepharoplastic have similar cell surface marker as orbital fat-derived stem cells but did not show the same differentiation characteristics (Lin et al., 2013). The cells did not differentiate to the adipogenic or osteogenic lineage and have a less powerful ability of chondrogenic differentiation (Martins et al., 2014). The multilineage differentiation potential of MSC populations of bone marrow cells from different species and the ability to differentiate in multilineages is well discovered. It has been also reported that MSC are heterogenous regarding of their multilineages differentiation potential. The MSC pool in bone marrow comprised subpopulations at various differentiation states (Baksh et al., 2004). Likewise orbital fibroblast population may contain also subpopulations and many differentiation states. The function and heterogeneous character of the cell subpopulations within the orbital fat tissue is not fully enlightened and need further investigations.

Another aspect of heterogeneity within the orbital population is a different degree of CD90 (Thy-1) expression on the cell surface. It is known that the presence of CD90 influences the differentiation ability (Koumas et al., 2002; Douglas et al., 2010; Smith, 2010). CD90 positive subtypes have a higher capacity to differentiate into myocytes

and CD90 negative subtypes differentiate into adipocytes (Koumas et al., 2002; Koumas et al., 2003). We found that GO-MSC and GO-OF were merely CD90 positive but OF from some GO patients (two out of nine patients) showed indeed a CD90 negative subpopulation (Publication 1, Fig. 2). As described earlier, GO-MSC demonstrated a higher adipogenic and myogenic differentiation potential than GO-OF (Publication 1, Fig. 3), but the CD90 expression in both populations was very similar (Publication 1, Fig. 2). This suggests that other factors than CD90 expression are also considered to impact differentiation capacity of orbital subpopulations. Adipogenic differentiation can also be induced by stress under pressure shown in a three-dimensional culture model as might occur in the diseases orbit (Li et al., 2014). Therefore, it is necessary to investigate the orbital cells in terms of adipogenic/myogenic differentiation capacity as well as proliferation and hyaluronan production (Publication 1, Fig. 1) under inflammatory conditions which are present in the diseased orbit. The role of osteogenic, chondrogenic and neuronal differentiation pathways is completely unknown in context of GO pathology. In our study we investigated characteristics of MSC and OF derived from GO patients but studies with MSC and OF derived from healthy control persons are needed to fully understand the role of stems cells for remodeling and expansion of the retrobulbar fat tissue.

Additional to the self-renewal potential and differentiation capacity MSC also have an immunoregulatory ability (Baksh et al., 2004). This immunoregulatory abilities include immunosuppressive and proinflammatory properties and can act as switchers of inflammation. MSC can influence the adaptive and the innate immune cells and are an underestimated player in local immune regulation (Bernardo and Fibbe, 2013). In contrast, GO-OF are important as regulators of immune cell recruitment and activation (Bahn et al., 1998; Cao et al., 1998; Hwang et al., 2009). Because GO-MSC are involved in local immune regulation we investigated the potential role of GO-MSC in orbital immunology. We tested key features of immunologic cell-cell interactions such as suppression of T-cell proliferation and secretion of inflammatory cytokines and compared the results with results of GO-OF. The results demonstrated that GO-MSC were more effective in suppression of T-cell proliferation (Publication 1, Fig. 4) and a higher secretion of IL-6 cytokine (Publication 1, Fig. 5). The constitutively secreted IL-6 by MSC assists in polarization of monocytes into pro-inflammatory M2 macrophages. In absence of IL-6 MSC help monocytes by polarization into proinflammatory M1 macrophages and this stimulates the T-cell activation (Bernardo and Fibbe, 2013). Our study

gives first evidence that GO-MSC represent an anti-inflammatory cell type with the result of inflammation inhibition. Interestingly, it was shown already during cornea injury orbital fat-derived stem cells could dampen inflammation (Lin et al., 2013). Studies of the immunological potential of GO-MSC and control-MSC could give a further insight in orbital pathology and can help to find promising therapeutic approaches for GO.

With our study we could show the first time that mesenchymal progenitor cells (GO-MSC) are present in the orbital fat tissue of GO patients. However, we also showed the GO-OF have the same biological characteristics like GO-MSC but the differentiation potential, T-cell suppression and cytokine release reported some functional differences. Important is to investigate the function and population properties of orbital MSC from healthy control persons to better understand the pathological processes of GO.

A further important cell type involved in GO pathogenesis are fibrocytes which are bone-marrow derived MSC (Smith, 2015). Fibrocytes play a role in wound healing, tissue remodeling and immune function. They are extremely rare present in blood circulation of healthy persons but their presence is dramatically increased in pathological states like tissue injury (Douglas et al., 2010). Likewise, Smith and colleagues found increased fibrocytes levels in the peripheral blood and in the orbital tissue of GO patients (Smith, 2010; Douglas et al., 2010). Fibrocytes just like OF expressed the target antigen TSHR and IGF-1R, showed CD90 heterogeneity and were able to differentiate in adipocytes and myocytes. The role of fibrocytes for pathogenesis of GO and their potential relation to OF or MSC is currently unknown.

Hypoxia is a well-known factor driving MSC development, maturation and differentiation (Ejtehadifar et al., 2015). The natural microenvironment in bone-marrow are drawn by a low oxygen content and the cells are able to deal with the conditions or adapt themselves. Through the inflammation and tissue expansion in the orbit it is also possible that some patients develop hypoxic conditions in the orbit where present GO-MSC and GO-OF have to adapt. Tissue hypoxia triggers the activation of many cellular pathways trough the stimulation of many genes and proteins involved in angiogenesis and adipogenesis. This suggests that hypoxic signaling in orbital fibroblasts populations could play an important role during tissue expansion and differentiation processes.

4.2 Orbital fibroblasts under influence of hypoxia - role of hypoxia for tissue remodeling

Hypoxia plays a role in tissue augmentation and differentiation processes of many tissue types, e.g. in adipogenesis of MSC (Ejtehadifar et al., 2015). Increasing tissue expansion and inflammation processes as well as swelling of the tissue in the limited space of the bony orbit, leads to local chronic hypoxic conditions. Key regulator of hypoxia is the transcription complex hypoxia-inducible factor 1 (HIF-1), which regulations the expression of genes which are involved in the clinical manifestation in the GO pathogenesis. The pathogenesis of GO is determined by many factors. One of these factors is the consumption of cigarette smoke. Cigarette smoke is a strong risk factor for the course and severity of the GO. The establishment of GO and smoking is associated with a 1-3 fold increase in overall incidence of symptomatic and an 2-6 fold as well as 3-1 fold increase in the incidence of proptosis and diplopia (Pfeilschifter and Ziegler, 1996; Vestergaard, 2002).

Therefore, we investigated how hypoxia-dependent and hypoxia-independent HIF-1 signaling may contribute to tissue remodeling in GO. Orbital fibroblasts are considered as the central cell type in inflammation and tissue remodeling in GO. We could show that orbital fibroblast derived from GO patients responded more sensitively toward hypoxia than orbital fibroblasts from control persons. This was shown by increased induction of HIF-1α (Publication 2, Fig. 1) as well as enhanced HIF-1 transcriptional action (Publication 2, Fig. 2, 3, 5) which leads to enhanced angiogenesis (Publication 2, Fig. 3, 4) and adipogenesis (Publication 2, Fig. 5). Furthermore, we could show that cigarette smoke extract elevates hypoxic-induced HIF-1α accumulation in OF from GO smoker (Publication 2, Fig. 6).

Angiogenesis, in pathological sense is a critical mediator of neovascularization in disorders like eye diseases, cancer formation, chronic inflammatory disorders such as rheumatoid arthritis (RA), proriasis and periodontitis (Penn et al., 2008; Sene et al., 2015). We found that in GO derived fat/connective tissue CD31 positive vessels were dramatically increased compared to control fat tissue (Publication 2, Fig. 4 and Supplementary Fig. 1). Since CD31 is a marker of newly developing vessels (Wang et al., 2008) it appeared that during adipose tissue expansion in the orbit neovascularization occurred most likely to overcome low oxygen concentration in the tissue. This is re-

flected by increased HIF-1α in cells of the fat/connective tissue of GO patients (Publication 2, Fig. 4). The results indicate that hypoxia was present in the tissue of GO patients. HIF-1 induced by hypoxic conditions can stimulate production of genes e.g. VEGF and PDFG driving the angiogenic processes. The tissue enlargement especially by adipogenesis, which is one of the most present processes in the pathology of GO, require a continuous remodeling of the vasculature to survive.

The increased adipose tissue in GO patients can be caused by de novo adipogenesis of OF also called preadipocytes (Kumar et al., 2005) or by adipose tissue derived mesenchymal stromal/stem cells (Publication 1). The adipogenic differentiation stimulated by activating anti-TSHR antibodies, TSH or various growth factors and cytokines like IL-1β and IL-6 is known (Cawood et al., 2006; Kumar et al., 2010; Kumar et al., 2011; Virakul et al., 2015). In the present study we could show that hypoxia induced adipogenic differentiation in an HIF-1 dependent manner in OF derived from GO patients whereas Ctrl-OF were mainly unaffected (Publication 2, Fig. 5). The adiponectin release of GO-OF during adipogenic differentiation (Publication 2, Fig. 5) was increased in agreement with the enhanced adiponectin gene expression found in GO orbital fat of previous studies (Kumar et al., 2005; Marique et al., 2015). These findings indicate that hypoxia is an important factor for the induction and stimulation of adipogenesis of the orbital tissue independently from other stimulating factors. The contribution of orbital MSC population to adipogenesis in GO remains to be investigated. However, in other studies adipogenic differentiation of MSC was depended on the severity and duration of hypoxic conditions. Whereas short duration leads to adipogenic differentiation long time exposure towards hypoxia inhibited adipogenesis (Buravkova et al., 2014).

The adipose tissue and OF from GO patients expressed TSHR to higher levels than control persons (Bahn et al., 1998; Bahn, 2010). Our result show that additional to hypoxia the stimulation of the TSHR using TSH leads to augmented adipogenesis of GO-OF and also to a low induction of adipogenic differentiation of Ctrl-OF (Publication 2, Fig. 5). The combination of hypoxia and TSHR stimulation increased adipogenesis to highest levels. This result is especially important for the clinical treatment of these patients. Poor control of thyroid function – long period of hypothyroidism with increased levels of TSH will foster adipogenesis and set up a circulus vitiosus in the volume limited bony orbit. In this context, hypoxia turned out to be an important factor which determines the extent of orbital fat expansion. The occurrence or degree of hypoxia depending of the configuration of the bony orbit in the orbital tissue of individual patients

could be an explanation why some patients develop fat tissue to high levels whereas other patients only show low or moderate fat expansion. Another main feature of GO pathogenesis is the overproduction of hyaluronan in the orbit. OF are known to produce hyaluronan in response to TSHR and IGF-1R stimulation (Smith et al., 1991; Smith et al., 1995). Moreover orbital adipogenesis is associated with increased hyaluronan production (Zhang et al., 2012). Thus hypoxia by stimulating adipogenesis can also contribute to hyaluronan overproduction in the orbit. In this respect it was shown earlier that hypoxia enhanced glycosaminoglycan production in OF derived from EOM of GO patients (Metcalfe and Weetman, 1994). These findings imply that hypoxia dependent pathways are involved in enhanced adipogenesis as well as overproduction of extracellular matrix both of which contributes to the excessive tissue expansion within the limited bony orbit of GO patients.

4.2.1 Hypoxia-inducible factor 1 dependent pathways in orbital fibroblasts

Cells respond to hypoxia by adapting gene expression trough the activation of hypoxia-inducible factor 1 (HIF-1). HIF-1 has been recognized as the master regulator of oxygen homeostasis both in physiology and pathophysiology (Semenza, 1998). HIF-1 coordinates the hypoxia-inducible expression of angiogenic factors such as vascular endothelial growth factor (VEGF) and thus finally coordinates tissue vascularization. Hypoxia induced the expression of glucose transporters (GLUT), and many HIF-1 dependent genes promote excessive proliferation, matrix formation, differentiation and adipogenesis (e.g. adiponectin) (Publication 2, Fig. 5). As described above, OF represent the key cell type in tissue activity and remodeling processes in the dysregulated orbital tissue of GO patients. These cells react more sensitively towards hypoxia and showed an increased HIF-1α accumulation than Ctrl-OF (Publication 2, Fig. 1). The increased HIF-1α induction was positively correlated with the clinical activity score of GO patients, indicating a relationship between inflammatory/immunological degree and hypoxic reaction (Publication 2, Fig. 1). The OF derived from GO patients showed also enhanced basal expression of HIF-1α mRNA, independently from oxygen concentration applied indicating that the other factor than hypoxia promote HIF-1 expression in OF of GO patients. (Publication 2, Fig. 2). Inflammation and immunity can activate several signaling pathways which are involved in stimulation of HIF-1α synthesis (Frede et al., 2006; Rius et al., 2008). It is also known that NF-κB and MAPK pathways,

inducible by inflammatory mediators like IL-1β or CD40 ligand, impacts on HIF-1α up-regulation. On the other site HIF-1 can also activate NF-κB (Jung et al., 2003; Frede et al., 2007; Choi et al., 2013; Wang et al., 2015). Thus NF-κB and HIF-1 can occur in a cross-talk and hypoxia can activate both transcription factors resulting in an HIF-1/NF-κB loop during inflammatory hypoxia (Cummins et al., 2006; van Uden et al., 2008). The exact role of NF-κB/HIF-1 pathway and the cross-talk between both transcription factors needs further investigation in context of GO pathogenesis.

VEGF is well known as a target gene of HIF-1 and is the main growth factor of angiogenesis. As described above our results show increased new vessel development in fat tissue and enhanced HIF-1α accumulation in fat tissue and OF from GO patients (Publication 2, Fig. 1, 4). Additional, we found an induction in VEGF production by OF as a direct consequence of HIF-1 action (Publication 2, Fig. 3). This increased VEGF secretion could also be responsible for the increased vascularization, which can promote tissue remodeling (Thesis Fig. 10). In addition, the elevated adipogenesis of OF derived from GO patients in response to hypoxia was inhibited by HIF-1 activation inhibitor BAY 87-2243 (Publication 2, Fig. 5) suggesting that HIF-1 action also is involved in adipogenic differentiation.

Smoking is one of the strongest risk factor of GO and it has been shown that cigarette smoke extract (CSE) increased adipogenic differentiation and hyaluronan acid production in GO-OF (Cawood et al., 2007; Yoon et al., 2013). To investigate, whether HIF-1α is affected by smoking we treated OF from GO smoker and non-smoker with CSE under hypoxic conditions. We found that HIF-1α was elevated in response to CSE in OF derived from GO smoker whereas HIF-1α in OF derived from non-smoker remains unaffected (Publication 2, Fig. 6). Smoking GO patients show stronger eye symptoms than non-smoking GO patients. The average incidence of smokers is four times higher than of non-smokers (Vestergaard, 2002) and the cessation of cigarette consumptions alleviated symptoms (Pfeilschifter and Ziegler, 1996). One reason could be the combination of hypoxia and compounds of the cigarette smoke, which lead to an over-activation of HIF-1 pathways and thus development of sever proptosis and/or myopathy in smokers.

In conclusion hypoxia and HIF-1 dependent pathways can play a causal role in the tissue remodeling of GO by induction of important factors like VEGF and adiponectin, which stimulate the neovascularization and adipogenic differentiation (Thesis Fig. 10).

Both processes are involved in the tissue expansion in the orbit. Hypoxia is also known to favor inflammatory processes and plays a role by recruitment of inflammatory cells and immune cells in tissues (Haddad and Harb, 2005; Kiers et al., 2016). The role of hypoxia for inflammation or immunity of the orbital tissue in GO is subject of further studies.

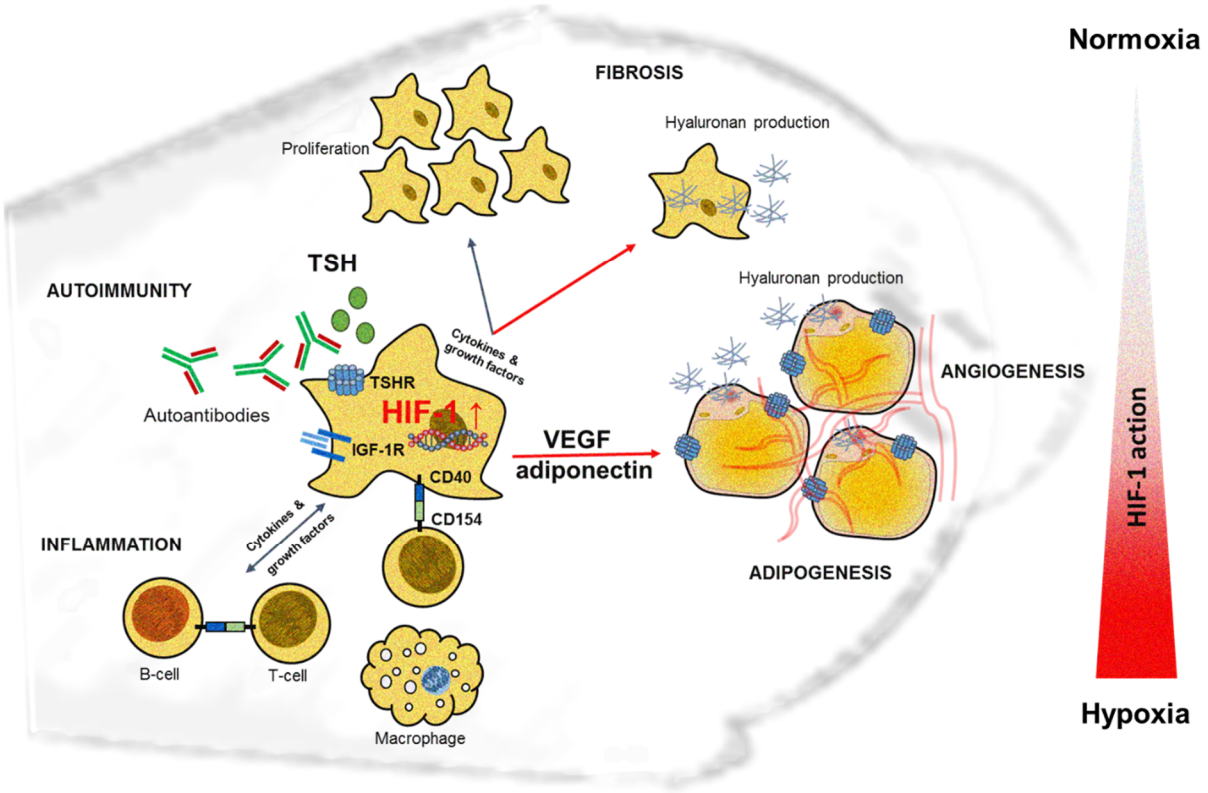

Figure 10. Involvement of HIF-1 dependent pathways in the pathological processes of GO. Under hypoxic conditions OF produce HIF-1α. Increased HIF-1α levels lead to stimulation of adipogenic differentiation of OF and increase hyaluronan production both of which are associated with volume entlargment of the orbital tissue. Additionally, stimulation of the TSHR by TSH or autoantibodies leads to an augmented adipogenesis. Furthermore, increased HIF-1a levels lead to elevated VEGF secretion of OF promoting neovascularisation during tissue enlagement. Thus HIF-1 dependent pathways contribute to expansion of orbital tissue. The role of HIF-1 in orbital inflammation and autoimmunity processes remains to be investigated.

4.2.2 Clinical relevance of hypoxia in Graves' orbitopathy

From today's point of view the main treatment for moderate-to-severe and sight-threatening GO is the medication of immunosuppressive corticosteroids and orbital decompression surgery. Bony orbital decompression is predominantly applied to GO patients with sight-threatening symptoms or when the anti-inflammatory treatment failed

(Bartalena et al., 2008; Salvi and Campi, 2015). Our results give first evidence that the control of HIF-1 pathway is important to control tissue expansion in GO. From clinical observations it is known that poor control of thyroid function, promotes a more severe course of GO (Prummel et al., 1990; Tallstedt et al., 1994). The observed cumulative effect of hypoxia and TSH on adipogenesis could explain why the thyroid gland treatment should be carefully planned especially in GO patients with advanced stages to prevent long periods of elevated TSH levels due to hypothyroidism. The development of treatments which prevent uncontrolled stimulation of the TSHR in response to TSAb binding is equally or even more important at this background. The recently established GO mouse model (Publication 3) will allow us to study the role of HIF-1 pathways and new therapeutic targets *in vivo*.

4.3 Establishment of GO mouse model and derived orbital fibroblasts

Graves' disease (GD) is the most common autoimmune disorder, affecting approximately 2-5% of the Caucasian population. In which, Graves' orbitopathy represents with 25-50% of Graves' patients the most frequent extrathyroidal manifestation (Wiersinga and Bartalena, 2002; McLachlan et al., 2005). There are no reports that animals spontaneously develop a GD. However, since Graves' disease is known to be due to an autoimmune mechanism, various approaches have been developed for the immunological induction of disease in animals. These approaches included injection of TSHR transfected fibroblasts or injection of plasmids or adenovirus encoding for the extracellular subunit of the human TSHR (Banga et al., 2015; Moshkelgosha et al., 2015; Banga et al., 2016). Most of these models were successful in induction of GD. However, some of these models were only for short time period or were self-limiting and showed almost no eye symptomatic or eye symptoms where not reproducible. The first preclinical GD mouse model including full blown GO pathology was developed by Banga and co-worker in 2013 (Moshkelgosha et al., 2013). We initiated a collaboration and conducted a comparative study in which we established the GO mouse model in our laboratory. During the course of the GO mouse study we demonstrated the *ex vivo* cultivation and characterization of orbital fibroblast from GO mice and controls. We investigated the pathologic cell type by discovering the adipogenic differentiation ability, hyaluronan production and expression of receptors involved in GO pathology.

4.3.1 Establishment of GO mouse model

Animal housing and environmental factors can critically influence the development, disease incidence and severity of autoimmune conditions of animal models. To evaluate the outcome of GO in the GD mouse model in our laboratory compared to the outcome of the model in Banga's laboratory we conducted a parallel study in which we used the same mouse strain (BALB/cOlaHs) and performed the immunization protocol of the mice as described before (Moshkelgosha et al., 2013). The outcome of the GO mouse model was similar in both laboratories. All mice develop TSHR autoantibodies (TRAbs) to high levels with different levels of stimulating (TSAbs) and blocking (TSBAbs) antibodies (Publication 3, Fig. 1). Additionally, some mice developed anti-IGF-1R antibodies (Publication 3, Fig. 1). The mice developed hyperthyroidism but remained mainly euthyroid in our laboratory (Publication 3, Fig. 1) which was confirmed by histology of the thyroids (Publication 3, Supplementary Fig. 2). Hyperthyroidism or euthyroidism is most likely the result of the action of the respective mixture of stimulating and blocking antibodies either activating or blocking the TSHR of the thyroids. However, the outcome of GO pathology was very similar in the mice of both of the laboratories. Some of the mice showed chemosis (sterile inflammation) of the eye lids but proptosis or diplopia was not evident. However, examination of the retroorbital tissue revealed expansion of the adipose tissue and atrophic EOM (Publication 3, Fig. 2). Since the mice behaved like GO patients by developing either more fat expansion or myopathy we normalized and combined both features by Z scoring to obtain a total eye disease score (Publication 3, Figure 2). The total eye disease score revealed that the overall outcome of GO was very similar in the mice of both laboratories. To confirm a TSHR antigen specific T cell response in the immune mice, we investigated proliferation and cytokine release of splenic T cells in response to recombinant TSHR antigen. We found a significant splenic T-cells response under recombinant TSHR antigen stimulation and high levels of cytokine (IFN-γ, IL-10, IL-6 and TNF-α) secretion (Publication 3, Fig. 3). However, we could not show any correlation between cytokine secretion and orbital pathology indicating that the orbital pathology is more complex than merely the secretory cytokine pattern.

In conclusion, we could show that the preclinical mouse model induced by hTSHR-A-subunit immunization is a well-functioning animal model and reproducible in different environment exposures. Orbital pathology was reproducible and present in 80% of

mice undergoing GO. To investigate the role of orbital fibroblast for pathology of experimental GO in the mice we established *ex vivo* cultivation of OF from mice orbits undergoing GO in our laboratory.

4.3.2 Characterization of orbital fibroblasts derived from GO mouse model and comparison to human orbital fibroblast

Herein, we demonstrated *ex vivo* cultivation and characterization of OF derived from GO mice and control mice. Additionally, we show mouse OF (mOF) inherent ability for adipocyte differentiation and hyaluronan production when activated by a variety of ligands, including TSH and IGF-1. The aim was to identify the pathological cell type in orbital tissue from mice undergoing experimental GO and to investigate whether there showed similar properties to those derived from human GO patients.

For establishment of mOF cell culture we used the orbital tissue from one eye of the respective immune mice from the recently described study (see 4.3.1). In *in vitro* studies of OF from GO patients the cells were derived either from fat/connective tissue or EOM (Bahn et al., 1987; Metcalfe and Weetman, 1994). Therefore we subjected mouse orbital tissue consisting of mainly EOM and partly connective/fat tissue to cell culture (Publication 4, Fig. 1). For examination of tissue components we used histological analysis of the other eye of the respective mouse (Publication 4, Fig. 1). We could show that fibroblast like cells migrated out from the orbital tissue and adhered to a confluent monolayer (Publication 4, Fig. 1). We found no morphological and growth-related differences between cells from GO mice and control mice (Publication 4, Fig. 1). For characterization of the obtained cells we analyzed several surface marker, receptors and differentiation ability (Publication 4, Fig. 2, 3).

The immune phenotype of mOF derived from GO and control mice were highly similar (Publication 4, Fig. 2). They were positive for MSC marker and negative for leukocyte marker indicating their mesenchymal cell immune phenotype akin both to mouse bone marrow stem cells or embryonic fibroblasts as well as human OF (Meyer zu Horste et al., 2011; Saeed et al., 2012; Kozdon et al., 2015). In contrast mOF were negative for the MSC marker CD73 showing that the cells derived from mouse orbits are similar but not identical to cells derived from GO orbital fat tissue (Publication 1; (Meyer zu Horste et al., 2011). CD73 is a catabolic enzyme leading to the generation of immunosuppressive, pro-angiogenic and negatively regulating Th1 adenosine (Chrobak et al., 2015;

Antonioli et al., 2016). An inhibition or deficiency favored autoimmune conditions like arthritis in mice (Chrobak et al., 2015). The role of CD73 in GO still requires extensive investigations. Further, mOF expressed mainly high levels of CD90.2, the BALB/c specific Thy 1 allele (Publication 4, Fig. 2). Interestingly, mOF derived from GO mice expressed CD90.2 more frequently to low levels compared to Ctrl mOF (Publication 4, Fig. 2). But unlike to findings in human OF derived from GO patients, the mOF derived from GO mice did not present distinct CD90 positive and CD90 negative populations (Smith et al., 1995); Publication 1). In humans the portion of these subpopulations are dependent on the derived orbital region. CD90 negative cells were more abundant in orbital adipose tissue and CD90 positive cells were predominantly found in EOM (Smith et al., 2002). In our study the main body of investigated orbital tissue was EOM suggesting that the high CD90.2 expression of mOF reflects their EOM origin. To investigate myogenic differentiation we analyzed expression of α-smooth muscle actin (α-SMA). We could show that mOF constitutively expressed high levels of α-SMA which was not further elevated in response to TGF-β stimulation (Publication 4, Fig. 3). The high expression of α-smooth muscle actin characterize the mOF as myofibroblastic cell type and could be a further indication for the EOM origin of the cells (Koumas et al., 2003). In contrast, human OF were frequently isolated from orbital connective/fat tissue of GO patients (for comparison see Thesis Table 1) and only a few studies using OF derived from EOM of GO patients exist (Metcalfe and Weetman, 1994). Furthermore, these studies did not phenotypically characterize OF derived from EOM to clarify similarities and differences compared to OF derived from fat tissue. Whereas biopsies from fat tissues are obtained during decompression surgery of GO patients in active stage, biopsies from EOM of GO patients can be obtained during surgery of diplopia. However, surgery of diplopia takes place after treatment of inflammation using steroids driving the eye disease in an inactive stage. Nevertheless we obtained OF from an EOM biopsy of a diplopia patient (without GO) and could show constitutively α-SMA expression of the cells as observed for mOF (Thesis Supplementary Fig. 1). This initial result indicates that indeed myofibroblast-like cells can be also derived from human EOM tissue. Further studies are needed to characterize different fibroblast populations in fat or EOM and their contribution to GO subtype with either more fat expansion or myopathy.

The main target genes of GO pathology are the TSHR and IGF-1R, both are highly expressed in GO orbital tissue and OF (Starkey et al., 2003; Wakelkamp et al., 2003;

Smith, 2009). In previously studies, it could be shown that TSHR is highly expressed in retro-orbital tissue of different mice strains (Johnson et al., 2013; Wiesweg et al., 2013). In our study we found also TSHR and IGF1R expression in mOF derived from GO and control mice (Publication 4, Fig. 2). Additionally, we could show that mOF from GO mice expressed higher levels of TSHR and IGF-1R compared to control mOF (Publication 4, Fig. 2). Further, we investigated the expression of CD40 and found high expression in mOF derived from GO mice (Publication 4, Fig. 2). High expression of CD40 is also known in human OF and the interaction between OF and T cells via CD40-CD154 and various cytokines increase the proliferation rate, adipogenic differentiation and hyaluronan production of OF (Heufelder and Bahn, 1994; Cao et al., 1998; Feldon et al., 2005; Feldon et al., 2006). The ligation of CD40-154 with T-cells could be another pathway which plays a role in the pathogenic processes of GO in mice and needs further investigations.

The investigation of adipogenic differentiation potential and hyaluronan production revealed a significant difference between GO and control derived mOF (Publication 4, Fig. 3, 4). The GO mice derived mOF showed stronger adipogenic differentiation potential than control mOF which remained less responsive (Publication 4, Fig. 3). This suggest that mOF derived from GO mice contained more substantially preadipocyte like cells which are capable to differentiate in mature adipocytes just like human OF or MSC populations from GO patients (Publication 1; (Kumar et al., 2004). It is known that CD90 negative human OF have a high capacity to differentiate into adipocytes (Smith et al., 2002). Therefore, it is tempting to speculate that the CD90.2 low expressing mOF were responsible for the higher adipogenic differentiation ability of mOF derived from GO mice. Increased hyaluronan production can be caused by activated OF/preadipocytes through stimulation of TSHR or IGF-1R (Smith and Hoa, 2004; Zhang et al., 2009; Zhang et al., 2012; Krieger et al., 2015). Treatment of human OF with TSH or IGF-1 stimulated hyaluronan secretion and simultaneous treatment with TSH and IGF-1 acted synergistically (Krieger et al., 2015). In agreement with these findings, the mOF derived from GO mice secreted elevated levels of hyaluronan compared to control mOF in response to TSH and/or IGF-1 as well as in response to stimulating anti-TSHR antibody M22 (Publication 4, Fig. 4). The hyaluronan production is controled by three hyaluronan synthases (HAS1-3), in which HAS 2 represents the main contributor of hyaluronan overproduction in the human orbit (Publication 4, Fig. 4). Altogether, the overexpression of TSHR, IGF1R and HAS2 in connection with TSH and/or IGF-1 or

M22 stimulation contributed to an increased hyaluronan secretion of OF derived from GO mice just like in GO patients.

Earlier we found a role of Hypoxia-inducible factor 1α (HIF-1α) for tissue remodeling in GO patients (Publication 2). OF from GO patients expressed increased HIF-1α accumulation compared to OF derived from control patients (Publication 2, Fig. 1). Likewise we found that mOF derived from GO mice showed significantly increased HIF-1α levels under hypoxic conditions compared to mOF from control mice (Thesis Supplementary Fig. 2). This result represents the findings in human OF and studies are underway to confirm the role of HIF-1 action for tissue remodeling in GO mice. Moreover the role of HIF-1 can be proven in mice model by using HIF-1 -/- (knock out) mice. It is also possible to study the course of hypoxic effects and smoking in individual stages of the disease in the GO mouse model.

In summary, our data give first evidences that mouse OF substantially affected in response to hTSHR A-subunit immunization and recapitulate the main features of OF derived from GO patients (Thesis Table 1). Therefore, the mouse OF can be considered as pathogenic target cell type responsible for tissue expansion in the orbit of GO mice. One important question raised is why and when OF were activated and/or changed into a pathologic phenotype in response to autoimmunity during the course of the disease. In immunized mice OF will be derived from all stages of GO and changes will be investigated in response to various kinds of treatments. This will lead to a better insight of disease pathogenesis and is fundamental to develop potential novel therapeutic targets.

Table 1. Comparison of fibroblastic cells involved in GO. Comparison of orbital fibroblastic cells derived from GO patients and GO mice. The table shows some properties of orbital cells from GO patients and GO mice. Results obtained from Publication 1, 2, 4, and from *Thesis Supplementary Fig. 2, 3. **Already fully myogenic differentiated; nd, not determined; MSC, mesenchymal stem cells; EOM, extraocular muscle.

	GO patients	**GO mice**
Tissue origin	Connective/fat tissue	Mainly EOM, partly fat
Cell type	Fibroblasts/Preadipocytes/MSC	Myofibroblasts
MSC marker	CD29+, CD44+, CD105+, CD73+, CD90-/+	CD29+, CD44+, CD105+, CD73-, CD90 low/high
Leucocyte marker	CD45-, CD11b-	CD45-, CD11b-
Target antigen	TSHR+, IGF-1R+	TSHR+, IGF-1R+
T-cell interaction	CD40+	CD40+
Adipogenesis	+	+
Myogenesis	+	-**
Osteogenesis	+	+*
Chondrogenesis	+	nd
Neurogenesis	+	nd
Hyaluronan production	+	+
Hypoxia	HIF-1α induction	HIF-1α induction*

5 References

Allelein, S., M. Ehlers, S. Goretzki, D. Hermsen, J. Feldkamp, M. Haase, T. Dringenberg, C. Schmid, H. Hautzel, and M. Schott. 2016. Clinical Evaluation of the First Automated Assay for the Detection of Stimulating TSH Receptor Autoantibodies. *Hormone and metabolic research = Hormon- und Stoffwechselforschung = Hormones et metabolisme* 48(12):795–801. doi:10.1055/s-0042-121012.

Antonioli, L., C. Blandizzi, F. Malavasi, D. Ferrari, and G. Hasko. 2016. Anti-CD73 immunotherapy: A viable way to reprogram the tumor microenvironment. *Oncoimmunology* 5(9):e1216292. doi:10.1080/2162402X.2016.1216292.

Arjamaa, O., and M. Nikinmaa. 2006. Oxygen-dependent diseases in the retina: role of hypoxia-inducible factors. *Experimental eye research* 83(3):473–483. doi:10.1016/j.exer.2006.01.016.

Bahn, R. S. 2010. Graves' ophthalmopathy. *The New England journal of medicine* 362(8):726–738. doi:10.1056/NEJMra0905750.

Bahn, R. S. 2015. Current Insights into the Pathogenesis of Graves' Ophthalmopathy. *Hormone and metabolic research = Hormon- und Stoffwechselforschung = Hormones et metabolisme* 47(10):773–778. doi:10.1055/s-0035-1555762.

Bahn, R. S., C. M. Dutton, N. Natt, W. Joba, C. Spitzweg, and A. E. Heufelder. 1998. Thyrotropin receptor expression in Graves' orbital adipose/connective tissues: potential autoantigen in Graves' ophthalmopathy. *The Journal of clinical endocrinology and metabolism* 83(3):998–1002. doi:10.1210/jcem.83.3.4676.

Bahn, R. S., C. A. Gorman, G. E. Woloschak, C. S. David, P. M. Johnson, and C. M. Johnson. 1987. Human retroocular fibroblasts in vitro: a model for the study of Graves' ophthalmopathy. *The Journal of clinical endocrinology and metabolism* 65(4):665–670. doi:10.1210/jcem-65-4-665.

Baksh, D., L. Song, and R. S. Tuan. 2004. Adult mesenchymal stem cells: Characterization, differentiation, and application in cell and gene therapy. *J Cellular Mol Med* 8(3):301–316. doi:10.1111/j.1582-4934.2004.tb00320.x.

Banga, J. P., S. Moshkelgosha, U. Berchner-Pfannschmidt, and A. Eckstein. 2015. Modeling Graves' Orbitopathy in Experimental Graves' Disease. *Hormone and metabolic research = Hormon- und Stoffwechselforschung = Hormones et metabolisme* 47(10):797–803. doi:10.1055/s-0035-1555956.

Banga, J. P., S. Moshkelgosha, U. Berchner-Pfannschmidt, and A. Eckstein. 2016. An Animal Model of Graves' Orbitopathy. In Animal Models of Ophthalmic Diseases. C.-C. Chan, editor. Springer International Publishing, Cham. 117–126.

Bartalena, L., L. Baldeschi, K. Boboridis, A. Eckstein, G. J. Kahaly, C. Marcocci, P. Perros, M. Salvi, and W. M. Wiersinga. 2016. The 2016 European Thyroid Association/European Group on Graves' Orbitopathy Guidelines for the Management of Graves' Orbitopathy. *European thyroid journal* 5(1):9–26. doi:10.1159/000443828.

Bartalena, L., L. Baldeschi, A. J. Dickinson, A. Eckstein, P. Kendall-Taylor, C. Marcocci, M. P. Mourits, P. Perros, K. Boboridis, A. Boschi, N. Curro, C. Daumerie, G. J. Kahaly, G. Krassas, C. M. Lane, J. H. Lazarus, M. Marino, M. Nardi, C. Neoh, J. Orgiazzi, S. Pearce, A. Pinchera, S. Pitz, M. Salvi, P. Sivelli, M. Stahl, G. von Arx, and W. M. Wiersinga. 2008. Consensus statement of the European group on Graves' orbitopathy (EUGOGO) on management of Graves' orbitopathy. *Thyroid*

official journal of the American Thyroid Association 18(3):333–346. doi:10.1089/thy.2007.0315.

Berchner-Pfannschmidt, U., S. Tug, M. Kirsch, and J. Fandrey. 2010. Oxygen-sensing under the influence of nitric oxide. *Cellular signalling* 22(3):349–356. doi:10.1016/j.cellsig.2009.10.004.

Berchner-Pfannschmidt, U., H. Yamac, B. Trinidad, and J. Fandrey. 2007. Nitric oxide modulates oxygen sensing by hypoxia-inducible factor 1-dependent induction of prolyl hydroxylase 2. *The Journal of biological chemistry* 282(3):1788–1796. doi:10.1074/jbc.M607065200.

Bernardo, M. E., and W. E. Fibbe. 2013. Mesenchymal stromal cells: sensors and switchers of inflammation. *Cell stem cell* 13(4):392–402. doi:10.1016/j.stem.2013.09.006.

Buravkova, L. B., E. R. Andreeva, V. Gogvadze, and B. Zhivotovsky. 2014. Mesenchymal stem cells and hypoxia: where are we? *Mitochondrion* 19 Pt A:105–112. doi:10.1016/j.mito.2014.07.005.

Burch, H. B., and D. S. Cooper. 2015. Management of Graves Disease: A Review. *JAMA* 314(23):2544–2554. doi:10.1001/jama.2015.16535.

Cao, H. J., H. S. Wang, Y. Zhang, H. Y. Lin, R. P. Phipps, and T. J. Smith. 1998. Activation of human orbital fibroblasts through CD40 engagement results in a dramatic induction of hyaluronan synthesis and prostaglandin endoperoxide H synthase-2 expression. Insights into potential pathogenic mechanisms of thyroid-associated ophthalmopathy. *The Journal of biological chemistry* 273(45):29615–29625.

Carroll, V. A., and M. Ashcroft. 2006. Role of hypoxia-inducible factor (HIF)-1alpha versus HIF-2alpha in the regulation of HIF target genes in response to hypoxia, insulin-like growth factor-I, or loss of von Hippel-Lindau function: implications for targeting the HIF pathway. *Cancer research* 66(12):6264–6270. doi:10.1158/0008-5472.CAN-05-2519.

Cawood, T., P. Moriarty, and D. O'Shea. 2004. Recent developments in thyroid eye disease. *BMJ (Clinical research ed.)* 329(7462):385–390. doi:10.1136/bmj.329.7462.385.

Cawood, T. J., P. Moriarty, C. O'Farrelly, and D. O'Shea. 2006. The effects of tumour necrosis factor-alpha and interleukin1 on an in vitro model of thyroid-associated ophthalmopathy; contrasting effects on adipogenesis. *European journal of endocrinology* 155(3):395–403. doi:10.1530/eje.1.02242.

Cawood, T. J., P. Moriarty, C. O'Farrelly, and D. O'Shea. 2007. Smoking and thyroid-associated ophthalmopathy: A novel explanation of the biological link. *The Journal of clinical endocrinology and metabolism* 92(1):59–64. doi:10.1210/jc.2006-1824.

Chen, C., N. Pore, A. Behrooz, F. Ismail-Beigi, and A. Maity. 2001. Regulation of glut1 mRNA by hypoxia-inducible factor-1. Interaction between H-ras and hypoxia. *The Journal of biological chemistry* 276(12):9519–9525. doi:10.1074/jbc.M010144200.

Chen, S.-Y., M. Mahabole, E. Horesh, S. Wester, J. L. Goldberg, and S. C. G. Tseng. 2014. Isolation and characterization of mesenchymal progenitor cells from human orbital adipose tissue. *Investigative ophthalmology & visual science* 55(8):4842–4852. doi:10.1167/iovs.14-14441.

Choi, Y.-H., K. O. Back, H. J. Kim, S. Y. Lee, and K. H. Kook. 2013. Pirfenidone attenuates IL-1beta-induced COX-2 and PGE2 production in orbital fibroblasts through

suppression of NF-kappaB activity. *Experimental eye research* 113:1–8. doi:10.1016/j.exer.2013.05.001.

Chrobak, P., R. Charlebois, P. Rejtar, R. El Bikai, B. Allard, and J. Stagg. 2015. CD73 plays a protective role in collagen-induced arthritis. *Journal of immunology (Baltimore, Md. 1950)* 194(6):2487–2492. doi:10.4049/jimmunol.1401416.

Costagliola, S., N. G. Morgenthaler, R. Hoermann, K. Badenhoop, J. Struck, D. Freitag, S. Poertl, W. Weglohner, J. M. Hollidt, B. Quadbeck, J. E. Dumont, P. M. Schumm-Draeger, A. Bergmann, K. Mann, G. Vassart, and K. H. Usadel. 1999. Second generation assay for thyrotropin receptor antibodies has superior diagnostic sensitivity for Graves' disease. *The Journal of clinical endocrinology and metabolism* 84(1):90–97. doi:10.1210/jcem.84.1.5415.

Cummins, E. P., E. Berra, K. M. Comerford, A. Ginouves, K. T. Fitzgerald, F. Seeballuck, C. Godson, J. E. Nielsen, P. Moynagh, J. Pouyssegur, and C. T. Taylor. 2006. Prolyl hydroxylase-1 negatively regulates IkappaB kinase-beta, giving insight into hypoxia-induced NFkappaB activity. *Proceedings of the National Academy of Sciences of the United States of America* 103(48):18154–18159. doi:10.1073/pnas.0602235103.

Davies, T. F., T. Ando, R.-Y. Lin, Y. Tomer, and R. Latif. 2005. Thyrotropin receptor-associated diseases: from adenomata to Graves disease. *The Journal of clinical investigation* 115(8):1972–1983. doi:10.1172/JCI26031.

Diana, T., M. Kanitz, M. Lehmann, Y. Li, P. D. Olivo, and G. J. Kahaly. 2015. Standardization of a bioassay for thyrotropin receptor stimulating autoantibodies. *Thyroid official journal of the American Thyroid Association* 25(2):169–175. doi:10.1089/thy.2014.0346.

Douglas, R. S., N. F. Afifiyan, C. J. Hwang, K. Chong, U. Haider, P. Richards, A. G. Gianoukakis, and T. J. Smith. 2010. Increased generation of fibrocytes in thyroid-associated ophthalmopathy. *The Journal of clinical endocrinology and metabolism* 95(1):430–438. doi:10.1210/jc.2009-1614.

Eckstein, A., J. Esser, S. Mattheis, and U. Berchner-Pfannschmidt. 2016. Endokrine Orbitopathie. *Klinische Monatsblatter fur Augenheilkunde* 233(12):1385–1407. doi:10.1055/s-0042-118040.

Eckstein, A. K., K. T. M. Johnson, M. Thanos, J. Esser, and M. Ludgate. 2009. Current insights into the pathogenesis of Graves' orbitopathy. *Hormone and metabolic research = Hormon- und Stoffwechselforschung = Hormones et metabolisme* 41(6):456–464.

Eckstein, A. K., H. Lax, C. Losch, D. Glowacka, M. Plicht, K. Mann, J. Esser, and N. G. Morgenthaler. 2007. Patients with severe Graves' ophthalmopathy have a higher risk of relapsing hyperthyroidism and are unlikely to remain in remission. *Clinical endocrinology* 67(4):607–612. doi:10.1111/j.1365-2265.2007.02933.x.

Eckstein, A. K., M. Plicht, H. Lax, H. Hirche, B. Quadbeck, K. Mann, K. P. Steuhl, J. Esser, and N. G. Morgenthaler. 2004. Clinical results of anti-inflammatory therapy in Graves' ophthalmopathy and association with thyroidal autoantibodies. *Clinical endocrinology* 61(5):612–618. doi:10.1111/j.1365-2265.2004.02143.x.

Eckstein, A. K., M. Plicht, H. Lax, M. Neuhauser, K. Mann, S. Lederbogen, C. Heckmann, J. Esser, and N. G. Morgenthaler. 2006. Thyrotropin receptor autoantibodies are independent risk factors for Graves' ophthalmopathy and help to predict severity

and outcome of the disease. *The Journal of clinical endocrinology and metabolism* 91(9):3464–3470. doi:10.1210/jc.2005-2813.

Ejtehadifar, M., K. Shamsasenjan, A. Movassaghpour, P. Akbarzadehlaleh, N. Dehdilani, P. Abbasi, Z. Molaeipour, and M. Saleh. 2015. The Effect of Hypoxia on Mesenchymal Stem Cell Biology. *Advanced pharmaceutical bulletin* 5(2):141–149. doi:10.15171/apb.2015.021.

Evans, M., J. Sanders, T. Tagami, P. Sanders, S. Young, E. Roberts, J. Wilmot, X. Hu, K. Kabelis, J. Clark, S. Holl, T. Richards, A. Collyer, J. Furmaniak, and B. R. Smith. 2010. Monoclonal autoantibodies to the TSH receptor, one with stimulating activity and one with blocking activity, obtained from the same blood sample. *Clinical endocrinology* 73(3):404–412. doi:10.1111/j.1365-2265.2010.03831.x.

Feldon, S. E., C. W. O'Loughlin, D. M. Ray, S. Landskroner-Eiger, K. E. Seweryniak, and R. P. Phipps. 2006. Activated human T lymphocytes express cyclooxygenase-2 and produce proadipogenic prostaglandins that drive human orbital fibroblast differentiation to adipocytes. *The American journal of pathology* 169(4):1183–1193. doi:10.2353/ajpath.2006.060434.

Feldon, S. E., D. J. J. Park, C. W. O'Loughlin, V. T. Nguyen, S. Landskroner-Eiger, D. Chang, T. H. Thatcher, and R. P. Phipps. 2005. Autologous T-lymphocytes stimulate proliferation of orbital fibroblasts derived from patients with Graves' ophthalmopathy. *Investigative ophthalmology & visual science* 46(11):3913–3921. doi:10.1167/iovs.05-0605.

Frede, S., U. Berchner-Pfannschmidt, and J. Fandrey. 2007. Regulation of hypoxia-inducible factors during inflammation. *Methods in enzymology* 435:405–419. doi:10.1016/S0076-6879(07)35021-0.

Frede, S., C. Stockmann, P. Freitag, and J. Fandrey. 2006. Bacterial lipopolysaccharide induces HIF-1 activation in human monocytes via p44/42 MAPK and NF-kappaB. *The Biochemical journal* 396(3):517–527. doi:10.1042/BJ20051839.

Garrity, J. A., and R. S. Bahn. 2006. Pathogenesis of graves ophthalmopathy: implications for prediction, prevention, and treatment. *American journal of ophthalmology* 142(1):147–153. doi:10.1016/j.ajo.2006.02.047.

Gerding, M. N., J. W. van der Meer, M. Broenink, O. Bakker, W. M. Wiersinga, and M. F. Prummel. 2000. Association of thyrotrophin receptor antibodies with the clinical features of Graves' ophthalmopathy. *Clinical endocrinology* 52(3):267–271.

Ginsberg, J. 2003. Diagnosis and management of Graves' disease. *CMAJ Canadian Medical Association journal = journal de l'Association medicale canadienne* 168(5):575–585.

Grimm, C., A. Wenzel, M. Groszer, H. Mayser, M. Seeliger, M. Samardzija, C. Bauer, M. Gassmann, and C. E. Reme. 2002. HIF-1-induced erythropoietin in the hypoxic retina protects against light-induced retinal degeneration. *Nature medicine* 8(7):718–724. doi:10.1038/nm723.

Haddad, J. J., and H. L. Harb. 2005. Cytokines and the regulation of hypoxia-inducible factor (HIF)-1alpha. *International immunopharmacology* 5(3):461–483. doi:10.1016/j.intimp.2004.11.009.

Hagg, E., and K. Asplund. 1987. Is endocrine ophthalmopathy related to smoking? *British medical journal (Clinical research ed.)* 295(6599):634–635.

Hegedius, L., T. H. Brix, and P. Vestergaard. 2004. Relationship between cigarette smoking and Graves' ophthalmopathy. *Journal of endocrinological investigation* 27(3):265–271.

Heufelder, A. E., and R. S. Bahn. 1994. Modulation of Graves' orbital fibroblast proliferation by cytokines and glucocorticoid receptor agonists. *Investigative ophthalmology & visual science* 35(1):120–127.

Hiromatsu, Y., D. Yang, T. Bednarczuk, I. Miyake, K. Nonaka, and Y. Inoue. 2000. Cytokine profiles in eye muscle tissue and orbital fat tissue from patients with thyroid-associated ophthalmopathy. *The Journal of clinical endocrinology and metabolism* 85(3):1194–1199. doi:10.1210/jcem.85.3.6433.

Hwang, C. J., N. Afifiyan, D. Sand, V. Naik, J. Said, S. J. Pollock, B. Chen, R. P. Phipps, R. A. Goldberg, T. J. Smith, and R. S. Douglas. 2009. Orbital fibroblasts from patients with thyroid-associated ophthalmopathy overexpress CD40: CD154 hyperinduces IL-6, IL-8, and MCP-1. *Investigative ophthalmology & visual science* 50(5):2262–2268. doi:10.1167/iovs.08-2328.

Iyer, S., and R. Bahn. 2012. Immunopathogenesis of Graves' ophthalmopathy: the role of the TSH receptor. *Best practice & research. Clinical endocrinology & metabolism* 26(3):281–289. doi:10.1016/j.beem.2011.10.003.

Jaume, J. C., A. Kakinuma, G. D. Chazenbalk, B. Rapoport, and S. M. McLachlan. 1997. Thyrotropin receptor autoantibodies in serum are present at much lower levels than thyroid peroxidase autoantibodies: analysis by flow cytometry. *The Journal of clinical endocrinology and metabolism* 82(2):500–507. doi:10.1210/jcem.82.2.3740.

Johnson, K. T. M., B. Wiesweg, M. Schott, M. Ehlers, M. Muller, W. B. Minich, Y. Nagayama, E. Gulbins, A. K. Eckstein, and U. Berchner-Pfannschmidt. 2013. Examination of orbital tissues in murine models of Graves' disease reveals expression of UCP-1 and the TSHR in retrobulbar adipose tissues. *Hormone and metabolic research = Hormon- und Stoffwechselforschung = Hormones et metabolisme* 45(6):401–407. doi:10.1055/s-0032-1333224.

Jung, Y.-J., J. S. Isaacs, S. Lee, J. Trepel, and L. Neckers. 2003. IL-1beta-mediated up-regulation of HIF-1alpha via an NFkappaB/COX-2 pathway identifies HIF-1 as a critical link between inflammation and oncogenesis. *FASEB journal official publication of the Federation of American Societies for Experimental Biology* 17(14):2115–2117. doi:10.1096/fj.03-0329fje.

Kaback, L. A., and T. J. Smith. 1999. Expression of hyaluronan synthase messenger ribonucleic acids and their induction by interleukin-1beta in human orbital fibroblasts: potential insight into the molecular pathogenesis of thyroid-associated ophthalmopathy. *The Journal of clinical endocrinology and metabolism* 84(11):4079–4084. doi:10.1210/jcem.84.11.6111.

Kavran, J. M., J. M. McCabe, P. O. Byrne, M. K. Connacher, Z. Wang, A. Ramek, S. Sarabipour, Y. Shan, D. E. Shaw, K. Hristova, P. A. Cole, and D. J. Leahy. 2014. How IGF-1 activates its receptor. *eLife* 3. doi:10.7554/eLife.03772.

Ke, Q., and M. Costa. 2006. Hypoxia-inducible factor-1 (HIF-1). *Molecular pharmacology* 70(5):1469–1480. doi:10.1124/mol.106.027029.

Khoo, D. H., S. C. Ho, L. L. Seah, K. S. Fong, E. S. Tai, S. P. Chee, P. H. Eng, S. E. Aw, and A. C. Fok. 1999. The combination of absent thyroid peroxidase antibodies and high thyroid-stimulating immunoglobulin levels in Graves' disease identifies a

group at markedly increased risk of ophthalmopathy. *Thyroid official journal of the American Thyroid Association* 9(12):1175–1180. doi:10.1089/thy.1999.9.1175.

Khoo, T. K., and R. S. Bahn. 2007. Pathogenesis of Graves' ophthalmopathy: the role of autoantibodies. *Thyroid official journal of the American Thyroid Association* 17(10):1013–1018. doi:10.1089/thy.2007.0185.

Khoo, T. K., M. J. Coenen, A. R. Schiefer, S. Kumar, and R. S. Bahn. 2008. Evidence for enhanced Thy-1 (CD90) expression in orbital fibroblasts of patients with Graves' ophthalmopathy. *Thyroid official journal of the American Thyroid Association* 18(12):1291–1296. doi:10.1089/thy.2008.0255.

Kiers, H. D., G.-J. Scheffer, J. G. van der Hoeven, H. K. Eltzschig, P. Pickkers, and M. Kox. 2016. Immunologic Consequences of Hypoxia during Critical Illness. *Anesthesiology* 125(1):237–249. doi:10.1097/ALN.0000000000001163.

Kita, M., L. Ahmad, R. C. Marians, H. Vlase, P. Unger, P. N. Graves, and T. F. Davies. 1999. Regulation and transfer of a murine model of thyrotropin receptor antibody mediated Graves' disease. *Endocrinology* 140(3):1392–1398. doi:10.1210/endo.140.3.6599.

Koumas, L., T. J. Smith, S. Feldon, N. Blumberg, and R. P. Phipps. 2003. Thy-1 expression in human fibroblast subsets defines myofibroblastic or lipofibroblastic phenotypes. *The American journal of pathology* 163(4):1291–1300. doi:10.1016/S0002-9440(10)63488-8.

Koumas, L., T. J. Smith, and R. P. Phipps. 2002. Fibroblast subsets in the human orbit: Thy-1+ and Thy-1- subpopulations exhibit distinct phenotypes. *European journal of immunology* 32(2):477–485. doi:10.1002/1521-4141(200202)32:2<477:AID-IMMU477>3.0.CO;2-U.

Kozdon, K., C. Fitchett, G. E. Rose, D. G. Ezra, and M. Bailly. 2015. Mesenchymal Stem Cell-Like Properties of Orbital Fibroblasts in Graves' Orbitopathy. *Investigative ophthalmology & visual science* 56(10):5743–5750. doi:10.1167/iovs.15-16580.

Krieger, C. C., S. Neumann, R. F. Place, B. Marcus-Samuels, and M. C. Gershengorn. 2015. Bidirectional TSH and IGF-1 receptor cross talk mediates stimulation of hyaluronan secretion by Graves' disease immunoglobins. *The Journal of clinical endocrinology and metabolism* 100(3):1071–1077. doi:10.1210/jc.2014-3566.

Krieger, C. C., R. F. Place, C. Bevilacqua, B. Marcus-Samuels, B. S. Abel, M. C. Skarulis, G. J. Kahaly, S. Neumann, and M. C. Gershengorn. 2016. TSH/IGF-1 Receptor Cross Talk in Graves' Ophthalmopathy Pathogenesis. *The Journal of clinical endocrinology and metabolism* 101(6):2340–2347. doi:10.1210/jc.2016-1315.

Kumar, S., M. J. Coenen, P. E. Scherer, and R. S. Bahn. 2004. Evidence for enhanced adipogenesis in the orbits of patients with Graves' ophthalmopathy. *The Journal of clinical endocrinology and metabolism* 89(2):930–935. doi:10.1210/jc.2003-031427.

Kumar, S., A. Leontovich, M. J. Coenen, and R. S. Bahn. 2005. Gene expression profiling of orbital adipose tissue from patients with Graves' ophthalmopathy: a potential role for secreted frizzled-related protein-1 in orbital adipogenesis. *The Journal of clinical endocrinology and metabolism* 90(8):4730–4735. doi:10.1210/jc.2004-2239.

Kumar, S., S. Nadeem, M. N. Stan, M. Coenen, and R. S. Bahn. 2011. A stimulatory TSH receptor antibody enhances adipogenesis via phosphoinositide 3-kinase activation in orbital preadipocytes from patients with Graves' ophthalmopathy. *Journal of molecular endocrinology* 46(3):155–163. doi:10.1530/JME-11-0006.

Kumar, S., R. Schiefer, M. J. Coenen, and R. S. Bahn. 2010. A stimulatory thyrotropin receptor antibody (M22) and thyrotropin increase interleukin-6 expression and secretion in Graves' orbital preadipocyte fibroblasts. *Thyroid official journal of the American Thyroid Association* 20(1):59–65. doi:10.1089/thy.2009.0278.

Kuriyan, A. E., C. F. Woeller, C. W. O'Loughlin, R. P. Phipps, and S. E. Feldon. 2013. Orbital fibroblasts from thyroid eye disease patients differ in proliferative and adipogenic responses depending on disease subtype. *Investigative ophthalmology & visual science* 54(12):7370–7377. doi:10.1167/iovs.13-12741.

Lantz, M., T. Vondrichova, H. Parikh, C. Frenander, M. Ridderstrale, P. Asman, M. Aberg, L. Groop, and B. Hallengren. 2005. Overexpression of immediate early genes in active Graves' ophthalmopathy. *The Journal of clinical endocrinology and metabolism* 90(8):4784–4791. doi:10.1210/jc.2004-2275.

Le Blanc, K., and D. Mougiakakos. 2012. Multipotent mesenchymal stromal cells and the innate immune system. *Nature reviews. Immunology* 12(5):383–396. doi:10.1038/nri3209.

Li, H., C. Fitchett, K. Kozdon, H. Jayaram, G. E. Rose, M. Bailly, and D. G. Ezra. 2014. Independent adipogenic and contractile properties of fibroblasts in Graves' orbitopathy: an in vitro model for the evaluation of treatments. *PloS one* 9(4):e95586. doi:10.1371/journal.pone.0095586.

Lin, K.-J., M.-X. Loi, G.-S. Lien, C.-F. Cheng, H.-Y. Pao, Y.-C. Chang, A. T.-Q. Ji, and J. H.-C. Ho. 2013. Topical administration of orbital fat-derived stem cells promotes corneal tissue regeneration. *Stem cell research & therapy* 4(3):72. doi:10.1186/scrt223.

Lisy, K., and D. J. Peet. 2008. Turn me on: regulating HIF transcriptional activity. *Cell death and differentiation* 15(4):642–649. doi:10.1038/sj.cdd.4402315.

Lu, H., R. A. Forbes, and A. Verma. 2002. Hypoxia-inducible factor 1 activation by aerobic glycolysis implicates the Warburg effect in carcinogenesis. *The Journal of biological chemistry* 277(26):23111–23115. doi:10.1074/jbc.M202487200.

Ludgate, M. 2000. Animal models of Graves' disease. *European journal of endocrinology* 142(1):1–8.

Marique, L., M. Senou, J. Craps, A. Delaigle, E. van Regemorter, A. Werion, V. van Regemorter, M. Mourad, C. Nyssen-Behets, B. Lengele, L. Baldeschi, A. Boschi, S. Brichard, C. Daumerie, and M.-C. Many. 2015. Oxidative Stress and Upregulation of Antioxidant Proteins, Including Adiponectin, in Extraocular Muscular Cells, Orbital Adipocytes, and Thyrocytes in Graves' Disease Associated with Orbitopathy. *Thyroid official journal of the American Thyroid Association* 25(9):1033–1042. doi:10.1089/thy.2015.0087.

Martins, T. M. d. M., A. C. C. de Paula, D. A. Gomes, and A. M. Goes. 2014. Alkaline phosphatase expression/activity and multilineage differentiation potential are the differences between fibroblasts and orbital fat-derived stem cells--a study in animal serum-free culture conditions. *Stem cell reviews* 10(5):697–711. doi:10.1007/s12015-014-9529-9.

McLachlan, S. M., Y. Nagayama, and B. Rapoport. 2005. Insight into Graves' hyperthyroidism from animal models. *Endocrine reviews* 26(6):800–832. doi:10.1210/er.2004-0023.

McLachlan, S. M., and B. Rapoport. 2004. Thyroid stimulating monoclonal antibodies: overcoming the road blocks and the way forward. *Clinical endocrinology* 61(1):10–18. doi:10.1111/j.1365-2265.2004.02028.x.

McLeod, D. S. A., and D. S. Cooper. 2012. The incidence and prevalence of thyroid autoimmunity. *Endocrine* 42(2):252–265. doi:10.1007/s12020-012-9703-2.

Metcalfe, R. A., and A. P. Weetman. 1994. Stimulation of extraocular muscle fibroblasts by cytokines and hypoxia: possible role in thyroid-associated ophthalmopathy. *Clinical endocrinology* 40(1):67–72.

Meyer zu Horste, M., E. Stroher, U. Berchner-Pfannschmidt, S. Schmitz-Spanke, M. Pink, J. R. Gothert, J. W. Fischer, E. Gulbins, and A. K. Eckstein. 2011. A novel mechanism involved in the pathogenesis of Graves ophthalmopathy (GO): clathrin is a possible targeting molecule for inhibiting local immune response in the orbit. *The Journal of clinical endocrinology and metabolism* 96(11):E1727-36. doi:10.1210/jc.2011-1156.

Minich, W. B., N. Dehina, T. Welsink, C. Schwiebert, N. G. Morgenthaler, J. Kohrle, A. Eckstein, and L. Schomburg. 2013. Autoantibodies to the IGF1 receptor in Graves' orbitopathy. *The Journal of clinical endocrinology and metabolism* 98(2):752–760. doi:10.1210/jc.2012-1771.

Morshed, S. A., T. Ando, R. Latif, and T. F. Davies. 2010. Neutral antibodies to the TSH receptor are present in Graves' disease and regulate selective signaling cascades. *Endocrinology* 151(11):5537–5549. doi:10.1210/en.2010-0424.

Morshed, S. A., and T. F. Davies. 2015. Graves' Disease Mechanisms: The Role of Stimulating, Blocking, and Cleavage Region TSH Receptor Antibodies. *Hormone and metabolic research = Hormon- und Stoffwechselforschung = Hormones et metabolisme* 47(10):727–734. doi:10.1055/s-0035-1559633.

Morshed, S. A., R. Ma, R. Latif, and T. F. Davies. 2013. How one TSH receptor antibody induces thyrocyte proliferation while another induces apoptosis. *Journal of autoimmunity* 47:17–24. doi:10.1016/j.jaut.2013.07.009.

Moshkelgosha, S., P.-W. So, N. Deasy, S. Diaz-Cano, and J. P. Banga. 2013. Cutting edge: retrobulbar inflammation, adipogenesis, and acute orbital congestion in a preclinical female mouse model of Graves' orbitopathy induced by thyrotropin receptor plasmid-in vivo electroporation. *Endocrinology* 154(9):3008–3015. doi:10.1210/en.2013-1576.

Moshkelgosha, S., P.-W. So, S. Diaz-Cano, and J. P. Banga. 2015. Preclinical models of Graves' disease and associated secondary complications. *Current pharmaceutical design* 21(18):2414–2421.

Mourits, M. P., M. F. Prummel, W. M. Wiersinga, and L. Koornneef. 1997. Clinical activity score as a guide in the management of patients with Graves' ophthalmopathy. *Clinical endocrinology* 47(1):9–14.

Neumann, S., E. Eliseeva, J. G. McCoy, G. Napolitano, C. Giuliani, F. Monaco, W. Huang, and M. C. Gershengorn. 2011. A new small-molecule antagonist inhibits Graves' disease antibody activation of the TSH receptor. *The Journal of clinical endocrinology and metabolism* 96(2):548–554. doi:10.1210/jc.2010-1935.

Neumann, S., R. F. Place, C. C. Krieger, and M. C. Gershengorn. 2015. Future Prospects for the Treatment of Graves' Hyperthyroidism and Eye Disease. *Hormone and metabolic research = Hormon- und Stoffwechselforschung = Hormones et metabolisme* 47(10):789–796. doi:10.1055/s-0035-1555901.

Park, J.-W., Y.-S. Chun, and M.-S. Kim. 2004. Hypoxia-inducible factor 1-related diseases and prospective therapeutic tools. *Journal of pharmacological sciences* 94(3):221–232.

Penn, J. S., A. Madan, R. B. Caldwell, M. Bartoli, R. W. Caldwell, and M. E. Hartnett. 2008. Vascular endothelial growth factor in eye disease. *Progress in retinal and eye research* 27(4):331–371. doi:10.1016/j.preteyeres.2008.05.001.

Pfeilschifter, J., and R. Ziegler. 1996. Smoking and endocrine ophthalmopathy: Impact of smoking severity and current vs lifetime cigarette consumption. *Clin Endocrinol* 45(4):477–481. doi:10.1046/j.1365-2265.1996.8220832.x.

Place, R. F., C. C. Krieger, S. Neumann, and M. C. Gershengorn. 2016. Inhibiting thyrotropin/insulin-like growth factor 1 receptor crosstalk to treat Graves' ophthalmopathy: studies in orbital fibroblasts in vitro. *British journal of pharmacology*. doi:10.1111/bph.13693.

Pritchard, J., R. Han, N. Horst, W. W. Cruikshank, and T. J. Smith. 2003. Immunoglobulin activation of T cell chemoattractant expression in fibroblasts from patients with Graves' disease is mediated through the insulin-like growth factor I receptor pathway. *Journal of immunology (Baltimore, Md. 1950)* 170(12):6348–6354.

Prummel, M. F., W. M. Wiersinga, M. P. Mourits, L. Koornneef, A. Berghout, and R. van der Gaag. 1990. Effect of abnormal thyroid function on the severity of Graves' ophthalmopathy. *Archives of internal medicine* 150(5):1098–1101.

Rapoport, B., H. A. Aliesky, B. Banuelos, C.-R. Chen, and S. M. McLachlan. 2015. A unique mouse strain that develops spontaneous, iodine-accelerated, pathogenic antibodies to the human thyrotrophin receptor. *Journal of immunology (Baltimore, Md. 1950)* 194(9):4154–4161. doi:10.4049/jimmunol.1500126.

Rapoport, B., B. Banuelos, H. A. Aliesky, N. Hartwig Trier, and S. M. McLachlan. 2016. Critical Differences between Induced and Spontaneous Mouse Models of Graves' Disease with Implications for Antigen-Specific Immunotherapy in Humans. *Journal of immunology (Baltimore, Md. 1950)* 197(12):4560–4568. doi:10.4049/jimmunol.1601393.

Rapoport, B., and S. M. McLachlan. 2016. TSH Receptor Cleavage Into Subunits and Shedding of the A-Subunit; A Molecular and Clinical Perspective. *Endocrine reviews* 37(2):114–134. doi:10.1210/er.2015-1098.

Ratcliffe, P. J. 2007. HIF-1 and HIF-2: working alone or together in hypoxia? *The Journal of clinical investigation* 117(4):862–865. doi:10.1172/JCI31750.

Rees Smith, B., S. M. McLachlan, and J. Furmaniak. 1988. Autoantibodies to the thyrotropin receptor. *Endocrine reviews* 9(1):106–121. doi:10.1210/edrv-9-1-106.

Rege, T. A., and J. S. Hagood. 2006. Thy-1, a versatile modulator of signaling affecting cellular adhesion, proliferation, survival, and cytokine/growth factor responses. *Biochimica et biophysica acta* 1763(10):991–999. doi:10.1016/j.bbamcr.2006.08.008.

Rius, J., M. Guma, C. Schachtrup, K. Akassoglou, A. S. Zinkernagel, V. Nizet, R. S. Johnson, G. G. Haddad, and M. Karin. 2008. NF-kappaB links innate immunity to

the hypoxic response through transcriptional regulation of HIF-1alpha. *Nature* 453(7196):807–811. doi:10.1038/nature06905.

Rosenblum, M. D., K. A. Remedios, and A. K. Abbas. 2015. Mechanisms of human autoimmunity. *The Journal of clinical investigation* 125(6):2228–2233. doi:10.1172/JCI78088.

Saeed, H., H. Taipaleenmaki, A. M. Aldahmash, B. M. Abdallah, and M. Kassem. 2012. Mouse embryonic fibroblasts (MEF) exhibit a similar but not identical phenotype to bone marrow stromal stem cells (BMSC). *Stem cell reviews* 8(2):318–328. doi:10.1007/s12015-011-9315-x.

Salvi, M., and I. Campi. 2015. Medical Treatment of Graves' Orbitopathy. *Hormone and metabolic research = Hormon- und Stoffwechselforschung = Hormones et metabolisme* 47(10):779–788. doi:10.1055/s-0035-1554721.

Salvi, M., G. Vannucchi, N. Curro, I. Campi, D. Covelli, D. Dazzi, S. Simonetta, C. Guastella, L. Pignataro, S. Avignone, and P. Beck-Peccoz. 2015. Efficacy of B-cell targeted therapy with rituximab in patients with active moderate to severe Graves' orbitopathy: a randomized controlled study. *The Journal of clinical endocrinology and metabolism* 100(2):422–431. doi:10.1210/jc.2014-3014.

Sanders, J., R. N. Miguel, J. Furmaniak, and B. R. Smith. 2010. TSH receptor monoclonal antibodies with agonist, antagonist, and inverse agonist activities. *Methods in enzymology* 485:393–420. doi:10.1016/B978-0-12-381296-4.00022-1.

Schott, M., D. Hermsen, M. Broecker-Preuss, M. Casati, J. C. Mas, A. Eckstein, D. Gassner, R. Golla, C. Graeber, J. van Helden, K. Inomata, J. Jarausch, J. Kratzsch, N. Miyazaki, M. A. N. Moreno, T. Murakami, H. J. Roth, W. Stock, J. Y. Noh, W. A. Scherbaum, and K. Mann. 2009. Clinical value of the first automated TSH receptor autoantibody assay for the diagnosis of Graves' disease (GD): an international multicentre trial. *Clinical endocrinology* 71(4):566–573. doi:10.1111/j.1365-2265.2008.03512.x.

Semenza, G. L. 1998. Hypoxia-inducible factor 1: master regulator of O2 homeostasis. *Current opinion in genetics & development* 8(5):588–594.

Sene, A., D. Chin-Yee, and R. S. Apte. 2015. Seeing through VEGF: innate and adaptive immunity in pathological angiogenesis in the eye. *Trends in molecular medicine* 21(1):43–51. doi:10.1016/j.molmed.2014.10.005.

Shimojo, N., Y. Kohno, K. Yamaguchi, S. Kikuoka, A. Hoshioka, H. Niimi, A. Hirai, Y. Tamura, Y. Saito, L. D. Kohn, and K. Tahara. 1996. Induction of Graves-like disease in mice by immunization with fibroblasts transfected with the thyrotropin receptor and a class II molecule. *Proceedings of the National Academy of Sciences of the United States of America* 93(20):11074–11079.

Smith, T. J. 2009. The Putative Role of Fibroblasts in the Pathogenesis of Graves' Disease: Evidence for the Involvement of the Insulin-like Growth Factor-1 Receptor in Fibroblast Activation. *Autoimmunity* 36(6-7):409–415. doi:10.1080/08916930310001603000.

Smith, T. J. 2010. Potential role for bone marrow-derived fibrocytes in the orbital fibroblast heterogeneity associated with thyroid-associated ophthalmopathy. *Clinical and experimental immunology* 162(1):24–31. doi:10.1111/j.1365-2249.2010.04219.x.

Smith, T. J. 2015. TSH-receptor-expressing fibrocytes and thyroid-associated ophthalmopathy. *Nature reviews. Endocrinology* 11(3):171–181. doi:10.1038/nrendo.2014.226.

Smith, T. J., R. S. Bahn, C. A. Gorman, and M. Cheavens. 1991. Stimulation of glycosaminoglycan accumulation by interferon gamma in cultured human retroocular fibroblasts. *The Journal of clinical endocrinology and metabolism* 72(5):1169–1171. doi:10.1210/jcem-72-5-1169.

Smith, T. J., and L. Hegedus. 2017. Graves' Disease. *The New England journal of medicine* 376(2):185. doi:10.1056/NEJMc1614624.

Smith, T. J., and N. Hoa. 2004. Immunoglobulins from patients with Graves' disease induce hyaluronan synthesis in their orbital fibroblasts through the self-antigen, insulin-like growth factor-I receptor. *The Journal of clinical endocrinology and metabolism* 89(10):5076–5080. doi:10.1210/jc.2004-0716.

Smith, T. J., L. Koumas, A. Gagnon, A. Bell, G. D. Sempowski, R. P. Phipps, and A. Sorisky. 2002. Orbital fibroblast heterogeneity may determine the clinical presentation of thyroid-associated ophthalmopathy. *The Journal of clinical endocrinology and metabolism* 87(1):385–392. doi:10.1210/jcem.87.1.8164.

Smith, T. J., and S. J. Parikh. 1999. HMC-1 mast cells activate human orbital fibroblasts in coculture: evidence for up-regulation of prostaglandin E2 and hyaluronan synthesis. *Endocrinology* 140(8):3518–3525. doi:10.1210/endo.140.8.6881.

Smith, T. J., H. S. Wang, and C. H. Evans. 1995. Leukoregulin is a potent inducer of hyaluronan synthesis in cultured human orbital fibroblasts. *The American journal of physiology* 268(2 Pt 1):C382-8.

Stan, M. N., J. A. Garrity, B. G. Carranza Leon, T. Prabin, E. A. Bradley, and R. S. Bahn. 2015. Randomized controlled trial of rituximab in patients with Graves' orbitopathy. *The Journal of clinical endocrinology and metabolism* 100(2):432–441. doi:10.1210/jc.2014-2572.

Starkey, K. J., A. Janezic, G. Jones, N. Jordan, G. Baker, and M. Ludgate. 2003. Adipose thyrotrophin receptor expression is elevated in Graves' and thyroid eye diseases ex vivo and indicates adipogenesis in progress in vivo. *Journal of molecular endocrinology* 30(3):369–380.

Stolze, I., U. Berchner-Pfannschmidt, P. Freitag, C. Wotzlaw, J. Rossler, S. Frede, H. Acker, and J. Fandrey. 2002. Hypoxia-inducible erythropoietin gene expression in human neuroblastoma cells. *Blood* 100(7):2623–2628. doi:10.1182/blood-2001-12-0169.

Tallstedt, L., G. Lundell, H. Blomgren, and J. Bring. 1994. Does early administration of thyroxine reduce the development of Graves' ophthalmopathy after radioiodine treatment? *European journal of endocrinology* 130(5):494–497.

Tomer, Y., and T. F. Davies. 2003. Searching for the autoimmune thyroid disease susceptibility genes: from gene mapping to gene function. *Endocrine reviews* 24(5):694–717. doi:10.1210/er.2002-0030.

Trayhurn, P. 2013. Hypoxia and adipose tissue function and dysfunction in obesity. *Physiological reviews* 93(1):1–21. doi:10.1152/physrev.00017.2012.

Turcu, A. F., S. Kumar, S. Neumann, M. Coenen, S. Iyer, P. Chiriboga, M. C. Gershengorn, and R. S. Bahn. 2013. A small molecule antagonist inhibits thyrotropin receptor antibody-induced orbital fibroblast functions involved in the pathogenesis of

Graves ophthalmopathy. *The Journal of clinical endocrinology and metabolism* 98(5):2153–2159. doi:10.1210/jc.2013-1149.

Uccelli, A., L. Moretta, and V. Pistoia. 2008. Mesenchymal stem cells in health and disease. *Nature reviews. Immunology* 8(9):726–736. doi:10.1038/nri2395.

Ungerer, M., J. Fassbender, Z. Li, G. Munch, and H.-P. Holthoff. 2016. Review of Mouse Models of Graves' Disease and Orbitopathy-Novel Treatment by Induction of Tolerance. *Clinical reviews in allergy & immunology*. doi:10.1007/s12016-016-8562-7.

Valyasevi, R. W., D. Z. Erickson, D. A. Harteneck, C. M. Dutton, A. E. Heufelder, S. C. Jyonouchi, and R. S. Bahn. 1999. Differentiation of human orbital preadipocyte fibroblasts induces expression of functional thyrotropin receptor. *The Journal of clinical endocrinology and metabolism* 84(7):2557–2562. doi:10.1210/jcem.84.7.5838.

van Uden, P., N. S. Kenneth, and S. Rocha. 2008. Regulation of hypoxia-inducible factor-1alpha by NF-kappaB. *The Biochemical journal* 412(3):477–484. doi:10.1042/BJ20080476.

van Zeijl, C. J. J., E. Fliers, C. J. van Koppen, O. V. Surovtseva, M. E. de Gooyer, M. P. Mourits, W. M. Wiersinga, A. M. M. Miltenburg, and A. Boelen. 2011. Thyrotropin receptor-stimulating Graves' disease immunoglobulins induce hyaluronan synthesis by differentiated orbital fibroblasts from patients with Graves' ophthalmopathy not only via cyclic adenosine monophosphate signaling pathways. *Thyroid official journal of the American Thyroid Association* 21(2):169–176. doi:10.1089/thy.2010.0123.

Vestergaard, P. 2002. Smoking and thyroid disorders--a meta-analysis. *European journal of endocrinology* 146(2):153–161.

Virakul, S., V. A. S. H. Dalm, D. Paridaens, W. A. van den Bosch, M. T. Mulder, N. Hirankarn, P. M. van Hagen, and W. A. Dik. 2015. Platelet-Derived Growth Factor-BB Enhances Adipogenesis in Orbital Fibroblasts. *Investigative ophthalmology & visual science* 56(9):5457–5464. doi:10.1167/iovs.15-17001.

Wakelkamp, I. M. M. J., O. Bakker, L. Baldeschi, W. M. Wiersinga, and M. F. Prummel. 2003. TSH-R expression and cytokine profile in orbital tissue of active vs. inactive Graves' ophthalmopathy patients. *Clinical endocrinology* 58(3):280–287.

Wang, D., C. R. Stockard, L. Harkins, P. Lott, C. Salih, K. Yuan, D. Buchsbaum, A. Hashim, M. Zayzafoon, R. W. Hardy, O. Hameed, W. Grizzle, and G. P. Siegal. 2008. Immunohistochemistry in the evaluation of neovascularization in tumor xenografts. *Biotechnic & histochemistry official publication of the Biological Stain Commission* 83(3-4):179–189. doi:10.1080/10520290802451085.

Wang, H., L.-S. Zhu, J.-W. Cheng, J.-P. Cai, Y. Li, X.-Y. Ma, and R.-L. Wei. 2015. CD40 ligand induces expression of vascular cell adhesion molecule 1 and E-selectin in orbital fibroblasts from patients with Graves' orbitopathy. *Graefe's archive for clinical and experimental ophthalmology = Albrecht von Graefes Archiv fur klinische und experimentelle Ophthalmologie* 253(4):573–582. doi:10.1007/s00417-014-2902-1.

Wang, Y., and T. J. Smith. 2014. Current concepts in the molecular pathogenesis of thyroid-associated ophthalmopathy. *Investigative ophthalmology & visual science* 55(3):1735–1748. doi:10.1167/iovs.14-14002.

Weetman, A. P. 2000. Graves' disease. *The New England journal of medicine* 343(17):1236–1248. doi:10.1056/NEJM200010263431707.

Weidemann, A., and R. S. Johnson. 2008. Biology of HIF-1alpha. *Cell death and differentiation* 15(4):621–627. doi:10.1038/cdd.2008.12.

Wiersinga, W. M., and L. Bartalena. 2002. Epidemiology and prevention of Graves' ophthalmopathy. *Thyroid official journal of the American Thyroid Association* 12(10):855–860. doi:10.1089/105072502761016476.

Wiesweg, B., K. T. M. Johnson, A. K. Eckstein, and U. Berchner-Pfannschmidt. 2013. Current insights into animal models of Graves' disease and orbitopathy. *Hormone and metabolic research = Hormon- und Stoffwechselforschung = Hormones et metabolisme* 45(8):549–555. doi:10.1055/s-0033-1343451.

Yoon, J. S., H. J. Lee, M. K. Chae, S. Y. Lee, and E. J. Lee. 2013. Cigarette smoke extract-induced adipogenesis in Graves' orbital fibroblasts is inhibited by quercetin via reduction in oxidative stress. *The Journal of endocrinology* 216(2):145–156. doi:10.1530/JOE-12-0257.

Zhang, L., T. Bowen, F. Grennan-Jones, C. Paddon, P. Giles, J. Webber, R. Steadman, and M. Ludgate. 2009. Thyrotropin receptor activation increases hyaluronan production in preadipocyte fibroblasts: contributory role in hyaluronan accumulation in thyroid dysfunction. *The Journal of biological chemistry* 284(39):26447–26455. doi:10.1074/jbc.M109.003616.

Zhang, L., F. Grennan-Jones, C. Lane, D. A. Rees, C. M. Dayan, and M. Ludgate. 2012. Adipose tissue depot-specific differences in the regulation of hyaluronan production of relevance to Graves' orbitopathy. *The Journal of clinical endocrinology and metabolism* 97(2):653–662. doi:10.1210/jc.2011-1299.

Ziello, J. E., I. S. Jovin, and Y. Huang. 2007. Hypoxia-Inducible Factor (HIF)-1 regulatory pathway and its potential for therapeutic intervention in malignancy and ischemia. *The Yale journal of biology and medicine* 80(2):51–60.

6 Appendix

6.1 Supplementary Figures

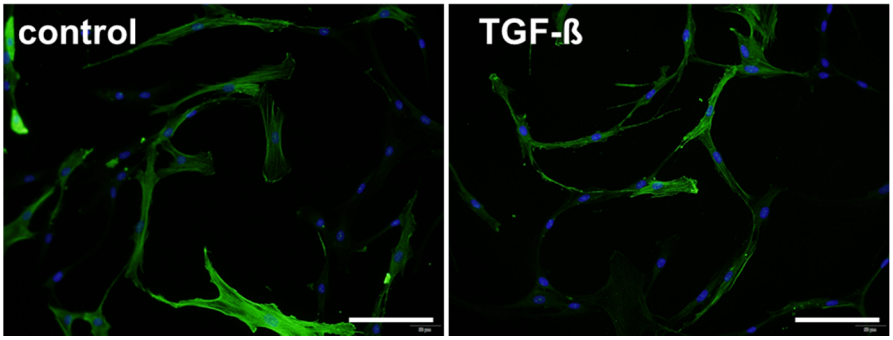

Supplementary Figure 1. Myocyte differentiation of human OF derived from EOM. Human OF were derived from EOM biopsy of a diplopia patient (no GO). Cells of passage 1 were incubated with or without 500ng/ml TGF-ß for 48h to induce myogenic differentiation and immunostained for α-smooth muscle actin (α-SMA) (green). Cell nuclei were counterstained with DAPI (blue). Representative images are shown, x200, bar represents 100µm. Human OF derived from EOM expressed basically α-SMA indicating constitutive myogenic differentiation.

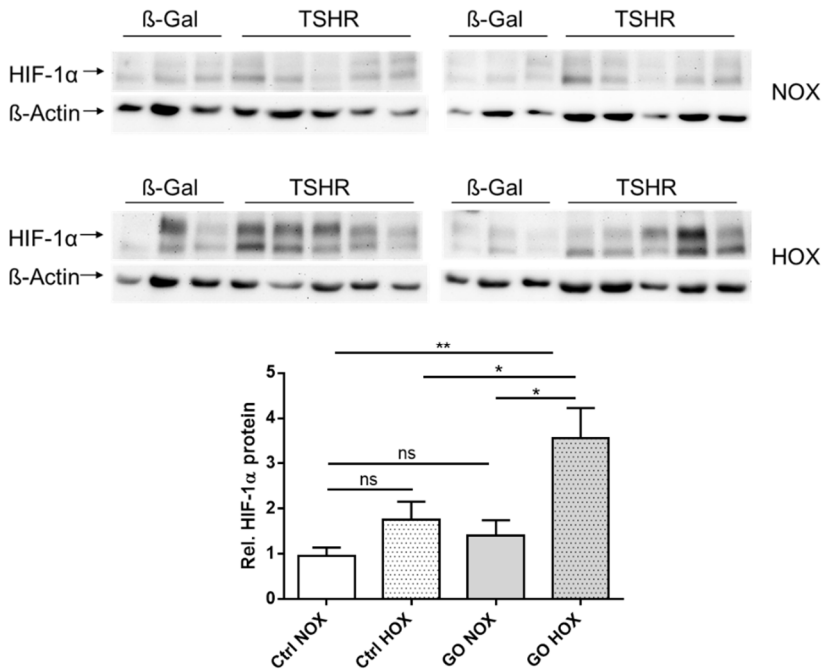

Supplementary Figure 2. HIF-1α accumulation in mouse OF. Mouse OF were subjected to normoxic (NOX) or hypoxic (HOX) conditions for 24 h. Whole cell lysates were subjected to Western-blot analysis for detection HIF-1α and β-actin as a loading control. Western-Blot signals of 10 GO-mOF and 6 Ctrl-mOF were quantified by densitometry of immunoblots. The HIF-1α signal was normalized to the β-actin signal and expressed as relative HIF-1α protein. *P≤0.05, **P<0.01. Mouse OF derived from GO mice (GO) express more HIF-1α under hypoxia (HOX) than control mOF (Ctrl). No differences in HIF-1α expression were found under-normoxia.

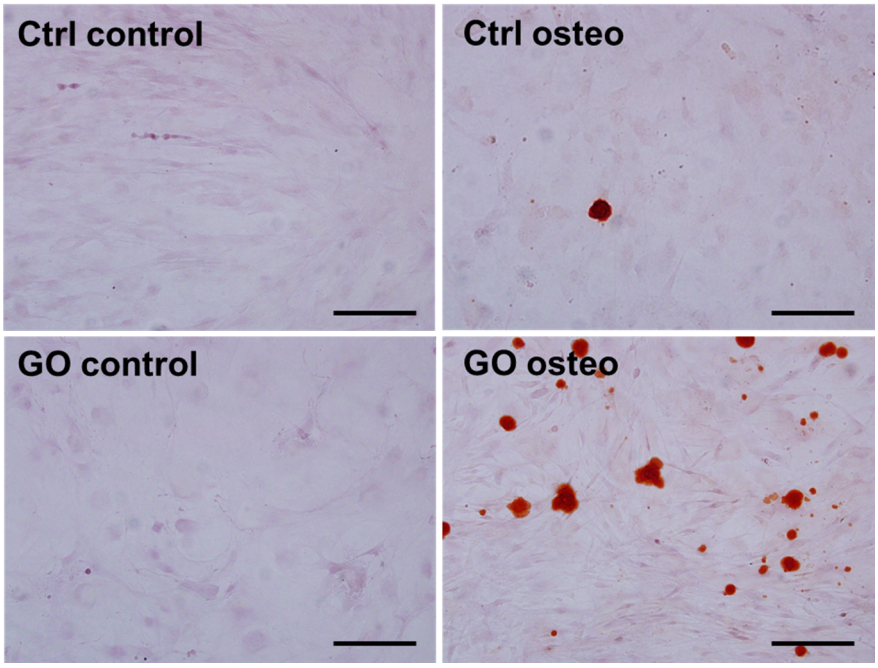

Supplementary Figure 3. Osteogenic differentiation of mouse OF. Mouse OF (passage 2-4) from control (n= 8) and GO mice (n= 10) were subjected to differentiation assay. To induce ostegenic differentiation cells were cultivated with (GO osteo) or without (GO control) osteogenic differentiation medium for 21 days and stained with Alzian red as described earlier (Publication1). Representative images are shown x200, bar represent 100 µm. Mice OF derived from GO mice were substantially capable to osteocyte differentiation.

6.2 Abbreviations

%	percent
AdiQ	adiponectin
Akt	protein kinase B
bHLH	basic-helix-loop helix
cAMP	cyclic adenosine monophosphate
CAS	clinical activity score
CBP	CREB binding protein
CD	cluster of differentiation
COLAGN	collagen
CREB	cAMP response element-binding protein
CSE	cigarette smoke extract
C-TAD	C-terminal transactivation domain
CTLA-4	cytotoxic T-lymphocyte-associated Protein 4
Ctrl	control
EOM	extraocular muscles
EPO	erythropoietin
ERK	extracellular signal-regulated kinases
Fig.	Figure
GAGs	glycosaminglycans
GAPDH	glyceraldehyde 3-phoshatedehydrogenase
GD	Graves' disease
GLUT	glucose transporter
GO	Graves' orbitopathy
HAS	hyaluronansynthase
HIF	hypoxia-inducible-factor
HLA	human leucocyte antigen
HRE	hypoxia response element
hTSHR	human thyrotropin stimulating hormone receptor
ICAM	intracellular adhesions molecule
IGF-1R	insulin growth factor 1 receptor
IL	interleukin
LRRs	leucine rich repeats
mOF	mouse orbital fibroblast

MSC	mesenchymal stem cell
NF-κB	nuclear factor-kappa B
N-TAD	N-terminal transactivation domain
ODDD	oxygen-dependent degradation domain
OF	orbital fibroblast
PAS	period/ARNT/single minded domain
PHD	prolyl hydroxylases
PI3	phosphatidyl inositol 3
PKA	protein kinase A
PPAR	peroxisome proliferator-activated receptor
PTPN22	protein tyrosine phosphatase, non-receptor type 22
pVHL	von Hippel-Lindau tumor suppressor protein
Raf	rapidly accelerated fibrosarcoma
RCT	randomized controlled trial
rhTSHR-E	recombinant hTSHR extracellular region protein
ROS	reactive oxygen species
siRNA	small interfering RNA
SPF	specific pathogen free
TBII	TSH-binding inhibitory immunoglobulin
TGF-ß	transforming growth factor-ß
TRAbs	thyrotropin-receptor autoantibodies
TSAbs	TSH-stimulating antibodies
TSBAbs	TSH-stimulating blocking antibodies
TSH	thyrotropin stimulating hormone
TSHR	thyrotropin stimulating hormone receptor
VEGF	vascular endothelial growth factor
α-SMA	α-smooth muscle actin

6.3 List of figures

2 Introduction

3 Publication

Publication 1

Publication 2

Publication 3

Publication 4

4 Discussion

5 Appendix

6.4 List of Tables

3 Publications

Publication 3

Publication 4

4 Discussion

6.5 Bestätigung Betreuerin

Bestätigung:

Hiermit bestätige ich die Darstellung zu den Anteilen von Frau Görtz an Konzeption, Durchführung und Abfassung jeder Publikation (Publication 1-4, 26-88) gem. der Promotionsordnung der Fakultät für Biologie zur Erlangung des Dr. rer. nat.

Essen, den _____ _____
Unterschrift der Betreuerin

6.6 Eidesstattliche Erklärungen

Erklärung:

Hiermit erkläre ich, gem. § 7 Abs. (2) d) + f) der Promotionsordnung der Fakultät für Biologie zur Erlangung des Dr. rer. nat., dass ich die vorliegende Dissertation selbständig verfasst und mich keiner anderen als der angegebenen Hilfsmittel bedient, bei der Abfassung der Dissertation nur die angegeben Hilfsmittel benutzt und alle wörtlich oder inhaltlich übernommenen Stellen als solche gekennzeichnet habe.

Essen, den _____ _____
Unterschrift des Doktoranden

Erklärung:

Hiermit erkläre ich, gem. § 7 Abs. (2) e) + g) der Promotionsordnung der Fakultät für Biologie zur Erlangung des Dr. rer. nat., dass ich keine anderen Promotionen bzw. Promotionsversuche in der Vergangenheit durchgeführt habe und dass diese Arbeit von keiner anderen Fakultät/Fachbereich abgelehnt worden ist.

Essen, den _____ _____
Unterschrift des Doktoranden

Erklärung:

Hiermit erkläre ich, gem. § 6 Abs. (2) g) der Promotionsordnung der Fakultät für Biologie zur Erlangung der Dr. rer. nat., dass ich das Arbeitsgebiet, dem das Thema „The role of Hypoxia-inducible factor 1 dependent gene expression fort he pathogenesis of Graves‘ orbitopathy“ zuzuordnen ist, in Forschung und Lehre vertrete und den Antrag von (Gina-Eva Görtz) befürworte und die Betreuung auch im Falle eines Weggangs, wenn nicht wichtige Gründe dem entgegenstehen, weiterführen werde.

Essen, den _____ _____
Unterschrift eines Mitglieds der Universität Duisburg Essen

Curriculum vitae

Der Lebenslauf ist in der Online-Version aus Gründen des Datenschutzes nicht enthalten.

The CV is not included in the online version for reasons of data protection.

Acknowledgement

Die Danksagung ist in der Online-Version aus Gründen des Datenschutzes nicht enthalten.

The acknowledgement is not included in the online version for reasons of data protection.